UNIVERSITY OF OKLAHOMA

GRADUATE COLLEGE

ACTIVATION OF FUNGAL SILENT BIOSYTHETIC PATHWAYS BY EPIGENETIC MODIFICATION

A DISSERTATION

SUBMITTED TO THE GRADUATE FACULTY

in partial fulfillment of the requirements for the

Degree of

DOCTOR OF PHILOSOPHY

By

XIAORU WANG
Norman, Oklahoma
2011

ACTIVATION OF FUNGAL SILENT BIOSYTHETIC PATHWAYS BY EPIGENETIC MODIFICATION

A DISSERTATION APPROVED FOR THE
DEPARTMENT OF CHEMISTRY AND BIOCHEMISTRY

BY

Dr. Robert Cichewicz, Chair

Dr. Susan Schroeder

Dr. Richard Taylor

Dr. Bradley Stevenson

Dr. Robert White

Acknowledgements

I would never have been able to finish my dissertation without the guidance of my committee members, help from friends, and support from my family.

I would like to express my deepest gratitude to my advisor, Dr. Cichewicz, for his excellent guidance, caring, patience, support and supervision in all the time of research.

I would also like to thank Dr. Blank, Dr. White, Dr. Stevenson, and Dr. Schroeder for guiding my research and providing precious advices as my committee members for the past six years. Special thanks go to Dr. Taylor, who was willing to participate in my final defense committee at the last moment.

I would like to thank University of Oklahoma, Department of Chemistry and Biochemistry for financial support as a teaching assistant.

I would like to thank Drs. Russell Williams and Trevor Ellis for teaching me basic experimental techniques and providing their best suggestions when they stayed in the lab as postdocs. Special thanks go to Dr. Nimmo for training me and helping with all NMR experiments. Many thanks to my lab members: Naiyun, Lin, Jianguo, Jianlan, Katie, Alexandra, Amanda, Jon, Matt, Christine, and Jarrod and other workers in the laboratory. My research would not have been possible without their helps. I would also like to thank my parents and my parents in law. They were always supporting me and encouraging me with their best wishes. Finally, I would like to thank my husband, Weifeng and my two lovely kids, Annabella and Evan, they were always there cheering me up and stood by me through the good times and bad.

Table of Contents

List of tables

List of Figures

List of Schemes

Abstract

Natural products have played an important role as drug leads for different diseases. They provide unique structural cores with diverse biological activities. Because of the overuse of antibiotics many pathogens have developed antibiotic-resistance; there is an urgent and continuing need for new antibiotics.

Fungi are a great source for new natural products with diverse biological activities; fungal genomic sequence data have shown that there are more secondary metabolite pathways than known metabolites. To obtain new natural products, an efficient way is needed to access these silent biosynthetic pathways (SBPs). Currently, different strategies have been used to access silent biosynthetic pathways including culture dependent methods like One Strain Many Compound (OSMAC) and co-culture, and genomic-based methods including heterologous expression and promoter activation. All of the above methods have their limitations, which prohibit their broad usage. In our group we have proposed a simple and feasible method for this purpose. Epigenetic regulation is a process commonly used by fungi to regulate biosynthesis. Epigenetic processes may silence/downregulate some secondary metabolite biosynthetic pathways. Small molecular epigenetic modifiers can inhibit epigenetic targets and upregulate gene expression. In this dissertation I have applied this strategy on two fungi and demonstrated that some secondary metabolite pathways can be activated/upregulated by epigenetic modifiers. Chapter 3 and chapter 4 will focus on the description of using small molecules epigenetic modifier (5-azacytidine) to access SBPs. Chapter 3 reports a significant change in the secondary metabolites excreted by an Atlantic-forest-soil-derived *Penicillium citreonigrum*, which is a rich source of secondary metabolites. Two

new metabolites, atlantinones A and B accompanied by eight known compounds were isolated from the guttates. Chapter 4 describes the application of different culture methods let to the production of different secondary metabolites. Waikialoids A and B were isolated from static culture whereas asperonol A and B were from shaking culture. Chapter 5 is different from above chapters and it mainly focuses on the hybrid NRPS-PKS gene coded metabolites, mutanobactin B-D, which are the signal regulators with other microorganisms.

Chapter 1. Activation of silent biosynthetic pathway by epigenetic modification – an approach to combat multi-drug resistance

This chapter has been adapted from portions of a previously published chapter.[1]

1.1 The importance of natural products

Natural products, also called secondary metabolites, are produced by living organisms and they play a variety of specific roles such as antifeedant, sex attractants, antibiotic agents and others[2]. Natural products have been the source of most of the active studied ingredients of medicines[3]. By 1990 about 80% of drugs were either from natural products or their analogs[4]. In 1991, almost half of the best-selling drugs were from natural products or their derivatives [5]. Between 1991 and 2006, 34% of all small-molecule drugs were from natural products or their direct semisynthetic derivatives[6], >75% of approved antibacterials are natural products or their semisynthetic derivatives[6]; furthermore, almost 50% of new anticancer drugs were natural products or their derivatives between 2000 and 2006[7].

1.2 The need and resources for new antibiotics

Since penicillin was discovered and used as an effective antibiotic in 1940 more and more antibiotics have been discovered[8]. However, because of the overuse of antibiotics, pathogens have developed drug resistance. There are different resistances developed in bacteria such as methicillin-resistant *Staphylococcus aureus* (MRSA), vancomycin-resistant *Enterococcus faecium* [9] and fluoroquinolone-resistant *Pseudomonas aeruginosa*[10]. Antibiotics resistances are rapidly increasing in US hospitals and the development of new treatments is rather slow[11].

The situation even gets worse because big pharmaceutical companies have withdrawn their interest in natural product antibiotics research. The need for new antibiotics is urgent to combat new multi-drug resistant bacteria. Microorganisms are ideal natural products providers because they live in complex ecosystems where they compete and communicate with other organisms[12]. Among them fungi will be a major natural products provider because their ability to produce prolific drug candidates. A total of 1,500 fungal metabolites were examined between 1993 and 2001 and more than half of them showed antibacterial, antifungal or antitumour activity.[13] Furthermore, only a small portion of fungi have been cultured in the laboratory[14]. As a result fungal secondary metabolites are underexplored and will be a great source for finding new antibiotics.

1.3 Triggering silent biosynthetic pathway in fungi

Whole genome sequence data for fungi have shown that fungal secondary metabolite genes far outnumber the known metabolites[15], the concept of silent of biosynthetic pathways (SBPs) was used to describe this situation that many microorganisms express only a fraction of their secondary-metabolite-encoding pathways under typical laboratory culture conditions. To access silent biosynthetic pathways (SBP), different methods are needed.

1.3.1 Manipulation of culture condition

One of the traditional, but effective methods is manipulating culture conditions. This method has been used for decades but was first systemically proposed by Bode in 2002 as the OSMAC approach (**O**ne **S**train–**MA**ny **C**ompounds) [16]. It has been demonstrated that changing the carbon source, pH, medium, and culture conditions can

significantly alter secondary metabolite production. Some successful examples of varying this technique are summarized in Table 1.1

Table 1.1. Examples of culture manipulation techniques.

Organisms	Elicitation	Compounds	Reference
Aspergillus ochraceus	Variation of media composition, vessel, and oxygenation	Total of 15 compounds produced including seven new pentaketides	17
Chaetomium chiversii	Switch from solid to liquid medium	Chaetochromin A (liquid) radicicol (solid)	18
Gymnascella dankaliensis	Carbon source of media varied	Dankasterones A and B; gymnasterones A , B ,C , and D	19
Paraphaeosphaeria quadriseptata	Changing from tap H_2O to distilled H_2O	Cytosporones F-I, quadriseptin A, and 5′-hydroxymonocillin III	18
Phomopsis asparagi	Addition of jasplakinolide (F-actin inhibitor)	Chaetoglobosins 510, 540, and 542	20
Sphaeropsidales sp. F-24'707	Variation of culture conditions	Cladospirones B-I	21
Sphaeropsidales sp. F-24'707	Addition of tricyclazole (inhibitor of 1,8-dihydroxynaphthalene pathway)	Sphaerolone and dihydrosphaerolone	22
Spicaria elegans	10 media types with and without shaking	Spicochalasin A and aspochalasins M–Q	23

One prime example of OSMAC is the fungus *Sphaeropsidales* sp. F-24'707 which altered its metabolite profile in response to changes in media, cultivation vessels, solid versus liquid fermentation technique, and enzyme inhibitors. Nineteen new and known spirobisnaphthalene, bisnaphthalene, naphthoquinone, and macrolide metabolites were isolated from this single strain (Figure 1.1).

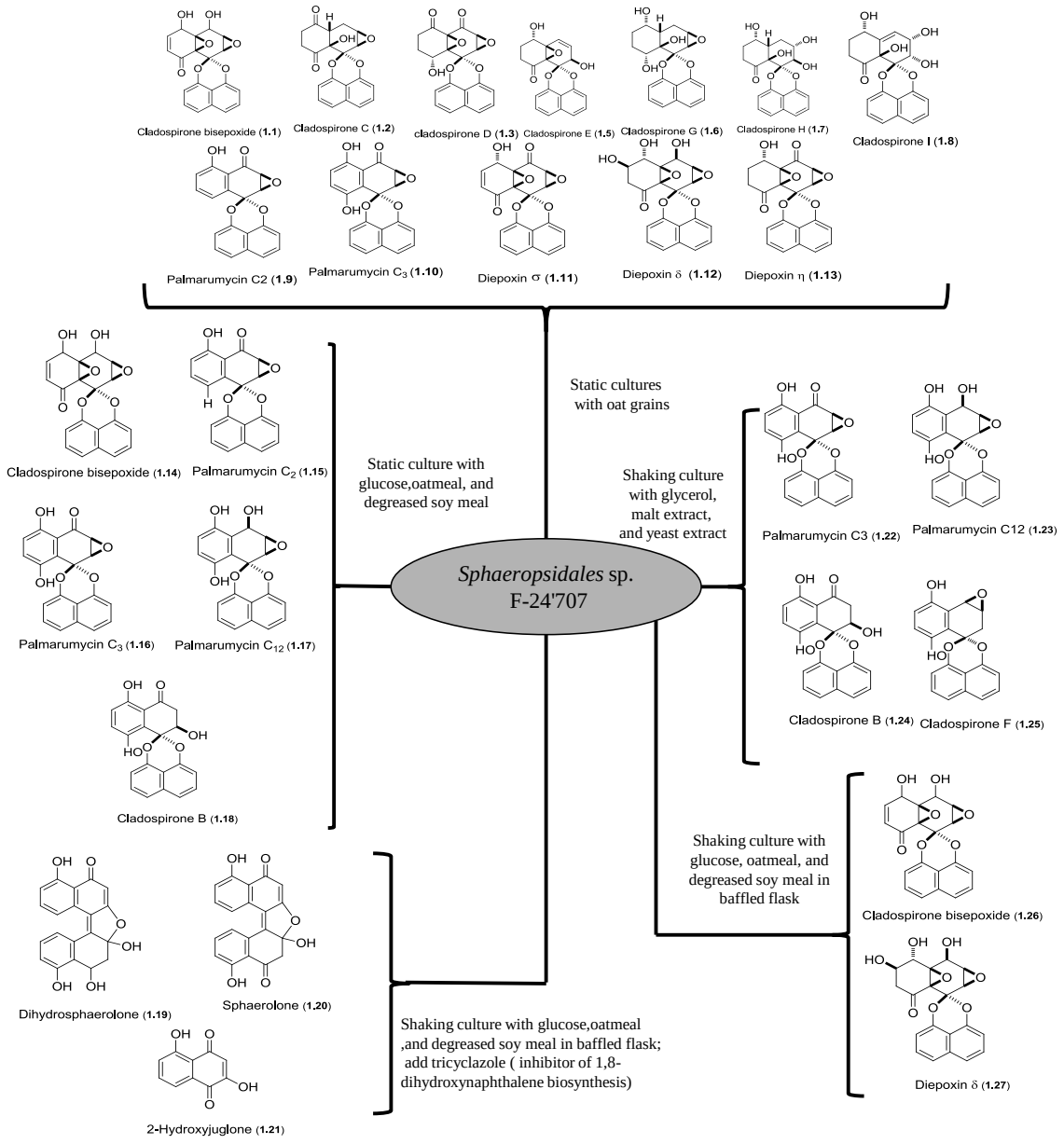

Figure 1.1 Compounds obtained from *Spha eropsidales* sp. F-24'707 using culture manipulation.

Other typical examples of OSMAC are cytosporones F−I from *Paraphaeosphaeria quadriseptata* [18], daldinin A-C from *Daldinia concentric* [24]; ascospiroketals A and B from *Ascochyta salicorniae* [25]; chaetoglobosins 510, 540, and 542 from *Phomopsis asparagi* [20]; and dankasterones A and B from *Gymnacella dankaliensis* [26], all of which responded to culture manipulation strategies by providing higher yields or inducing the expression of new natural products (Figure 1.2).

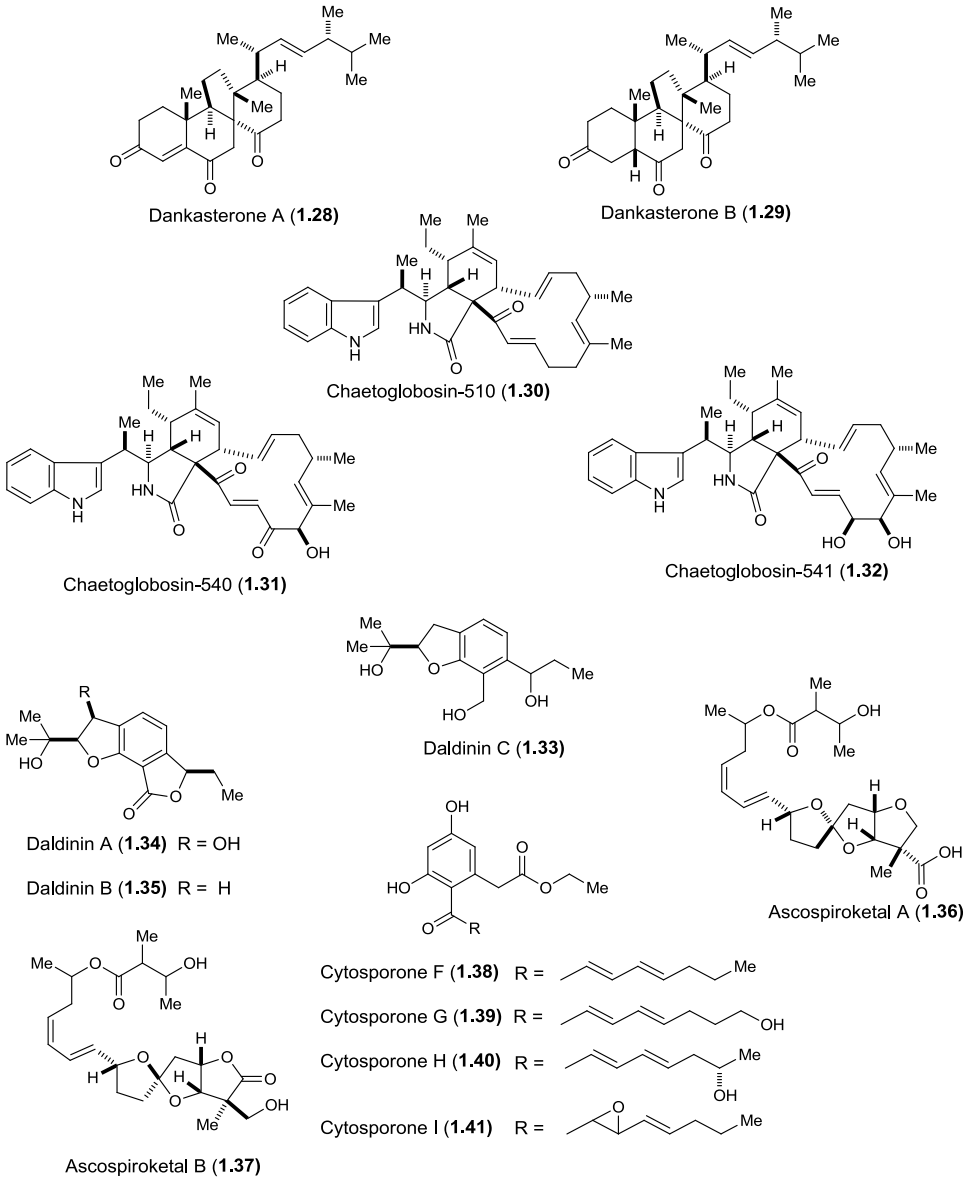

Figure 1.2 Examples of natural products obtained by manipulating microbial culture conditions

Besides culture manipulation another strategy is the co-culture method. The rationale behind this method is that microbes live in complex communities with close relationships such as competitive, symbiotic interactions, etc. and mimicking those kinds of interactions in the laboratory might serve as eliciting agents for the production of natural products [27]. Based on this strategy, some agents may able to trigger SBP making co-culture a promising approach for natural product production[28].

For example, pestalone, a unique chlorinated benzophenone, which was isolated from a marine-derived *Pestalotia* sp. in 2001[29], possesses potent antimicrobial activity against several bacterial strains. However, the yield of this compound was very low, when live bacteria cells (an unidentified Gram-negative bacterium strain CNJ-328) were added to the growing fungus the yield of this compound was significantly increased (Figure 1.3). Later, co-culture was applied to another fungus *Libertella* sp. fermented with CNJ-328 and the fungus *Emericella* sp. grown in combination with a marine actinomycete (*Salinispora arenicola*) to be able to produced libertellenones A-D[30] and emericellamides A-B[31] respectively (Figure 1.3). Recently, the production of pyocyanin was described from mixed fermentations of marine-sediment-derived *Pseudomonas aeruginosa* and *Enterobacter* sp (Figure 1.3).[32] They observed mixed cultures can produce a blue metabolite pyocyanin but neither of single isolates alone were found capable of generating it. They designed a series of Boyden chamber experiments, the authors were able to demonstrate that a small-molecule membrane-diffusible factor(s) was generated by *Enterobacter* sp. leading to the induction of pyocyanin production in *Pseudomonas aeruginosa*.

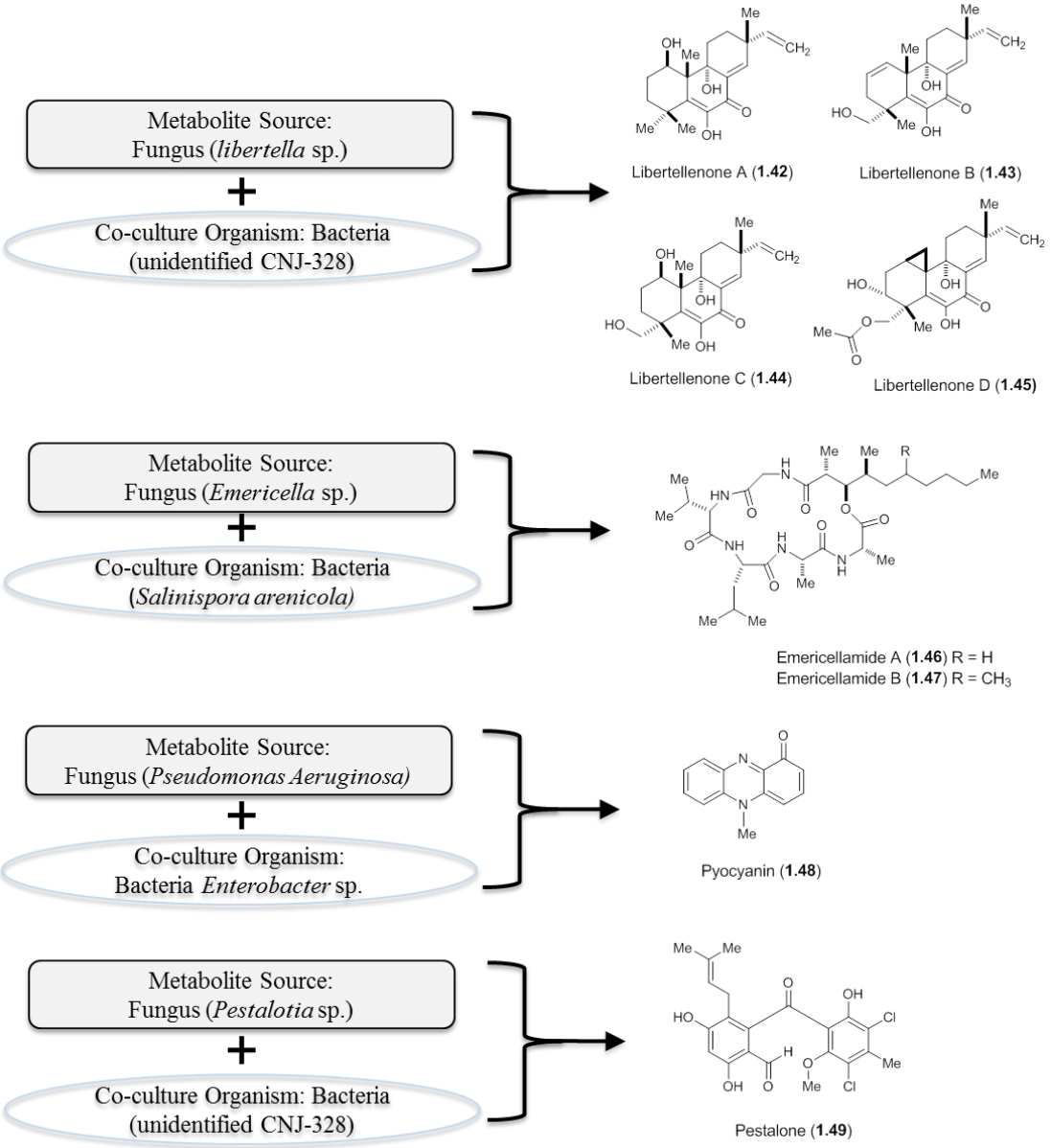

Figure 1.3 Examples demonstrating the use of co-culture technique to induce the production of microbial natural products.

1.3.2 Using genetic-manipulation to access the silent biosynthetic pathway

The rapid development of new microbiological techniques and the availability of whole genome sequences allow activating the SBPs by heterologous expression and promoter exchange[33]. Heterologous expression allows silent biosynthetic genes to be expressed in a suitable host that contain enzymes to generate the metabolite. This

method was used by some groups to successfully transfer specific secondary metabolite genes to express the metabolite. In 2006, Muller and colleagues scanned the myxobacterium *Sorangium cellulosum* genome and found a type III PKS for which no corresponding secondary metabolite could be identified [34]. In that paper, they cloned and transferred the type III PKS into *Escherichia coli* and *Pseudomonas* sp. They found that only the pseudomonad was suitable as a host for gene expression. The transfected *Pseudomonas* sp. culture turned visibly red and HPLC profiling confirmed the presence of a new metabolite. The structure of the compound was determined to be the naphthoquinone flaviolin which is readily generated from the oxidation of its biosynthetic precursor product, 1, 3, 6, 8-tetrahydroxynaphthalene (Figure 1.4).

Other groups have also employed heterologous expression for natural product discovery. Palmu et al. have taken the idea of silent biosynthetic pathway manipulation for the production of new angucycline analogs[35]. They observed that both *Streptomyces* sp. PGA64 and *Streptomyces* sp. H021 shared a high homology of PKS gene cluster [36]. Heterologous expression of varying portions of the gene clusters in *Streptomyces lividans* TK24 resulted in the generation of natural products gaudimycin A and B (Figure 1.4). More and more examples demonstrated that using heterologous expression systems to manipulate SBPs is an effective way to access SBPs.

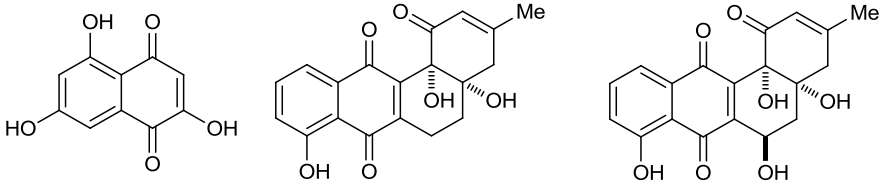

Flaviolin (**1.50**) Gaudimycin A (**1.51**) Gaudimycin B (**1.52**)

Figure 1.4. Examples of SBP-derived natural products that were identified using heterologous expression techniques

Promoter activation is another genetic based technology to access SBPs. One example is the enhanced production of β-lactam by using promoter activation[37]. One of the key enzymes during penicillin biosynthesis, δ-(L-R-aminoadipyl)-L-cysteinyl-D-valine synthetase, is encoded by the *Aspergillus nidulans* gene acvA. Replacement of the native promoter by an inducible alcohol dehydrogenase promoter (p)alcA resulted in increased penicillin yield about 30-fold. More recently, Chiang and colleagues discovered two silent PKS gene clusters adjacent to one another in the *Aspergillus nidulans* genome [38]. By closely exam the *A. nidulans* genome sequence, they found that a gene cluster has high homology to a citrinin biosynthesis transcriptional activator. They replaced the putative promoter with an inducible *alcA*p, resulting in the accumulation of two new (one major and one minor) metabolites. Purification of the major metabolite yielded the new polyketide asperfuranone, which is structurally reminiscent of the azaphilones.

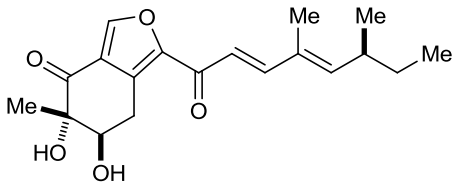

Asperfuranone (**1.53**)

1.4 New directions and conclusions

Current methods for accessing silent biosynthetic pathways have their limitations. OSMAC is time consuming and labor intensive. For heterologous expression, the specific gene for transfection and expression must be determined. Recently, the genomisotopic method and chemical epigenetics have been proposed and

examined for accessing the SBPs. The genomisotopic method was described by Gerwick et al.[39], they used a structure prediction approach and isotopic labeling to detect a targeted natural product (Figure 1.5). *Pseudomonas fluorescens* Pf-5 is known to contain a large NRPS cluster encoding a decapeptide product. Four of the non-ribosomal peptides synthetase's modules exhibit highly conserved domains that are presumably responsible for the addition of leucine residues to metabolite. Using ^{1}H-^{15}N HMBC NMR, researchers were able to track the incorporation of ^{15}N-labeled leucine residues into a group of related secondary metabolites, which led to the isolation of orfamide A (**1.56**) and its related congeners. This technique explores the idea of accessing the SBPs and also provides an important new tool for microbial secondary metabolite investigation.

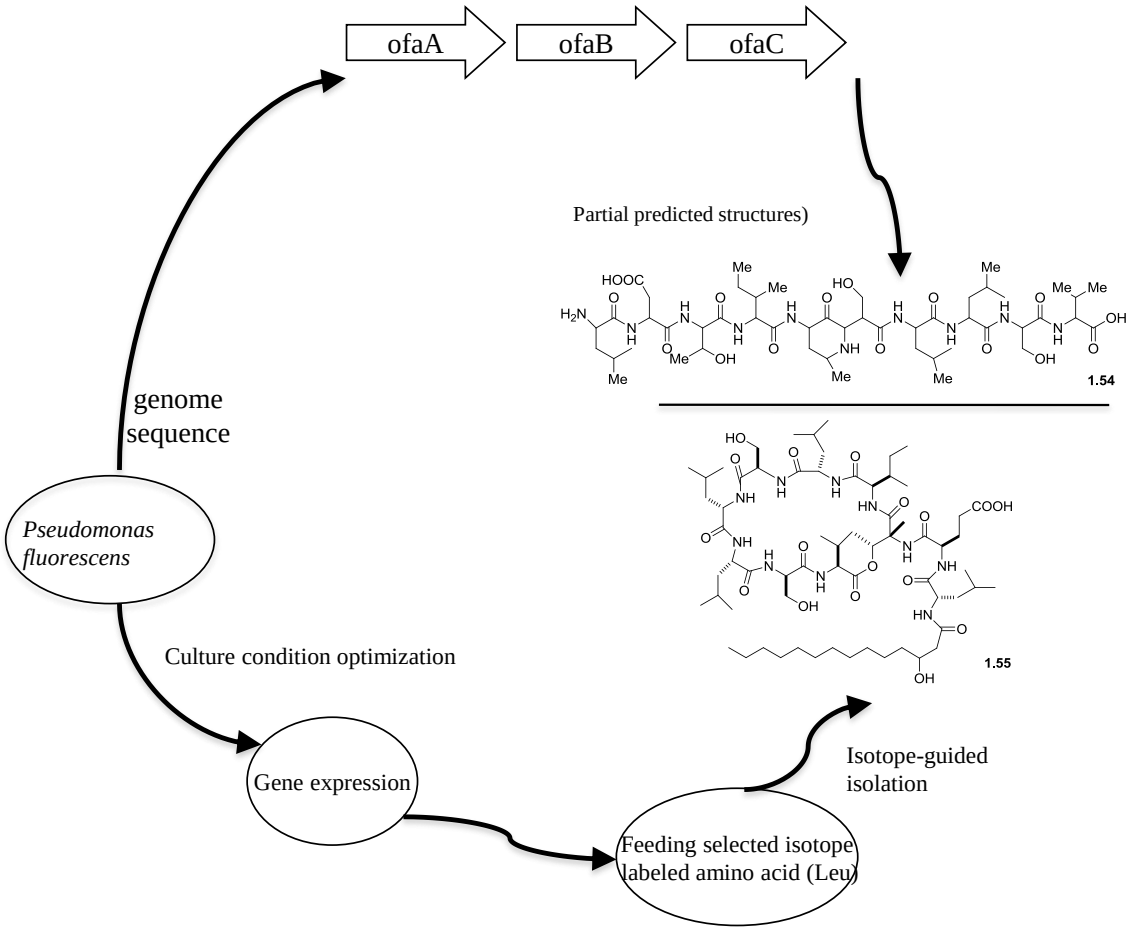

Figure 1.5 Overview of the genomisotopic method and its application to the study of the orfamide gene cluster in *P. fluorescens* Pf-5.

Another method was proposed by our group which uses epigenetic modification to access the SBP. Several epigenetic processes occur naturally in fungi[40]. This process involves the modification of DNA, DNA-binding proteins and histones and leads to changes in chromatin structure without changing the DNA sequence[41]. Two common epigenetic modifications are DNA methylation and histone deactylation[41b]. Other epigenetic alternatives have demonstrated important functions in fungi including altering gene transcription[42] and modulating transcript elongation[43]. DNA methylation and histone deactylation can change in chromatin status and gene expression

or silencing in fungi and other organisms[44]. The inhibition of DNA methylation and histone deactylation might activate/upregulate the silent biosynthetic pathways by using epigenetic modifying agents to induce changes in fungal secondary metabolism. Based on this idea we have demonstrated that treating *Aspergillus niger* with suberoylanilide hydroxamic acid (SAHA) and 5-azacytidine (5-Aza), an inhibitor for histone deacetylases and DNA methyltransferases, will cause the upregulation of many secondary metabolite genes[45]. It has provided an easy and effective tool for accessing the silent biosynthetic pathway. We have successfully isolated the lunalides A and B from *Diatrype disciformis* [46]. Significant changes of secondary metabolites have been observed in the fungus *Penicillium* with two new compounds, atlantinones A and B[47]. For the natural product research, new methods and strategies must be devised for producing new and bioactive secondary metabolites from microorganisms. In this dissertation, I describe that epigenetic modification was applied for the production of new antimicrobial secondary metabolites from fungi.

Chapter 2. Hypothesis and chapter overviews

2.1 Hypothesis

Fungal genomic sequence information showed that there are more undiscovered secondary metabolites in fungi than known compounds. Epigenetic modifications are proposed to be an effective tool for activating silent biosynthetic pathways, leading to the proposal of the hypothesis: **Small molecular epigenetic modifiers (suberoylanilide hydroxamic acid and 5-azacytidine) activate or upregulate silent biosynthetic pathways in fungi.** This hypothesis was tested via the following specific aims:

1. Isolation of new antimicrobial natural products from *Penicillium citreonigrum* collected from the Brazilian Atlantic Forest
2. Isolation of new antimicrobial natural products from an *Aspergillus.* sp collected in Hawaii

Chapter 3 and 4 describes the result of using epigenetic modifiers on two different fungi along with the discovery of new natural products. Chapter 5 is a description of hybrid polyketide-non-ribosomal-peptide natural products from a human oral pathogen *Streptococcus mutans*. The point of view was the same as other two projects: trying to find new antimicrobial drugs by using unique strategy.

2.2 Chapter 3. Chemical Epigenetics Alters the Secondary Metabolite Composition of Guttate Excreted by an Atlantic-Forest-Soil-Derived *Penicillium citreonigrum*

In this project we applied the epigenetic modifier 5-azacytidine to an Atlantic-forest-soil-derived *Penicillium citreonigrum* for activating biosynthetic pathway. We observed profound changes in the secondary metabolite profile of its guttates which are

fungal exudates. While guttate from control cultures exhibited a relatively simple assemblage of secondary metabolites, the guttate collected from cultures treated with 50 μM 5-azacytidine (a DNA methyltransferase inhibitor) were highly enriched in compounds representing at least three distinct biosynthetic families. The metabolites obtained from the fungus included six azaphilones (sclerotiorin, sclerotioramine, ochrephilone, dechloroisochromophilone III, dechloroisochromophilone IV, and 6-((3*E*,5*E*)-5,7-dimethyl-2-methylenenona-3,5-dienyl)-2,4-dihydroxy-3-methylbenzaldehyde), pencolide, and two new meroditerpenes (atlantinones A and B). While pencolide was detected in the exudates of both control and 5-azacytidine-treated cultures, all of the other natural products were found exclusively in the guttates of the epigenetically modified fungus.

2.3 Chapter 4. Novel dimeric isoprenylated indole alkaloids isolated from Aspergillus sp. by manipulating the culture conditions

This chapter mainly focuses on the isolation of new natural products by manipulating the culture conditions. We applied epigenetic modifiers 5-azacytidine (5-Aza) and suberoylanilide hydroxamic acid (SAHA) to a Hawaii-soil-derived fungus. However, we did not observe significant secondary metabolite profile changes compared to that of untreated culture. We did observe a significant difference of secondary metabolite profiles of static cultures compared to liquid culture. Two novel dimeric isoprenylated indole alkaloids, waikialoid A (**4.7**) and B (**4.8**), with a unique bicyclo[2.2.2]diazaoctane ring, and two new metabolites, asperonol A and B, were isolated from static and liquid condition, respectively. These structures were identified

on the basis of spectroscopic data. The isolated compounds were evaluated for their anticancer and antibiofilm activity.

2.4 Chapter 5. New hybrid NRPS-PKS encoded cyclopeptides mutanobactins B-D from the human oral pathogen *Streptococcus mutans*.

Streptococcus mutans is a Gram-positive pathogen that is a primary inhabitant of the human oral biofilm and responsible for the development of dental caries.[48] The deletion of a gene cluster encoding a putative hybrid polyketide synthase-nonribosomal peptide synthetase (PKS-NRPS) derived metabolite in *Streptococcus mutans* UA159 caused a loss of several resistance traits associated with oxygen and hydrogen peroxide tolerance, as well as biofilm formation.[49] We have isolated the NRPS-PKS coded metabolites mutanobactin A-D and their structures have been identified on the basis of spectroscopic data.

Chapter 3. Chemical Epigenetics Alters the Secondary Metabolite Composition of Guttate Excreted by an Atlantic-Forest-soil-derived *Penicillium citreonigrum*

This chapter is adapted from a publication in the Journal of Natural Products [50]

3.1 Introduction

Our research group has been actively pursuing the development of chemical epigenetic methods for procuring secondary metabolites from fungi.[51] We have demonstrated that this is an effective technique for promoting the transcription of silent biosynthetic pathways involved in the formation of polyketide, non-ribosomal peptide, and hybrid polyketide-non-ribosomal-peptide natural products.[52] Moreover, we have shown that a chemical epigenetics approach is well suited for the generation of structurally unique secondary metabolites with promising drug discovery applications.[53] In order to maximize the opportunity for detecting novel secondary metabolites, we have begun using chemical epigenetic induction as a routine part of our screening program involving the exploration of fungi obtained from minimally explored environments/ecological niches (*e.g.*, insects and littoral zones[53b]).

Our investigation of fungi from ecologically diverse environments has recently expanded to include soil from the Brazilian Atlantic Forest. The Atlantic Forest is regarded as one of the most species-rich habitats in the world, but unfortunately, it is also an exceedingly endangered habitat with < 8% of its original 1.3×10^6 km^2 still intact.[54] The secondary metabolite profile (observed by HPLC) for one of the solid-state fungal cultures exhibited an exceptionally dramatic response to chemical epigenetic manipulation: in the presence of 5-azacytidine (a DNA methyltransferase inhibitor)[51],

the fungus produced rust-red-colored droplets of exudate on its mycelial surface, whereas untreated (control) cultures produced colorless exudates.

Fungal exudates, which are more formally known as guttates, are observed with considerable frequency in solid-state fungal cultures. Despite the widespread occurrence of this phenomenon, a surprisingly small number of accounts have been published exploring the composition of fungal guttates. The few studies that do exist suggest that these droplets are a rich source of primary and secondary metabolites, inorganic elements, and proteins/enzymes.[55] For example, strains of *Penicillium nordicum* and *Penicillium verrucosum* grown for 14 days on Petri plates containing Czapek yeast agar were reported to have accumulated substantial amounts of guttate, which was enriched in ochratoxins A and B (on average, approximately 1-8 μg/mL).[55e] Similarly, cultures of *Metarhizium anisopliae* that were reared on several different media accumulated destruxins A, B, and E in their exudates at levels averaging between 2-6 μg/mL.[55a] The ecological significance of guttation remains uncertain although several possible functions have been proposed. These roles include facilitating active hyphal expansion under conditions of unfavorable water potential,[56] providing a mechanism for transporting enzymes that are involved in host invasion and/or liberation of essential nutrients from substrates,[55d, 57] and creation of unique microhabitats capable of supporting symbiotic bacterial communities.[58] In light of the striking guttate coloration induced in the Atlantic Forest fungal isolate, we initiated this project to discern what changes occurred to the chemical diversity of the fungal guttate upon treatment of the organism with 5-azacytidine which is a DNA methyltransferase inhibitor. In this report, we demonstrate that chemical epigenetic manipulation led to a substantial restructuring

of secondary metabolite pools in the guttate produced by an Atlantic-Forest-derived fungal isolate.

3.2 Result and Discussion

The sequence of a 321 base-pair portion of the large ribosomal subunit 28S rRNA gene from the Atlantic-Forest-soil-derived isolate shared 100% homology with the sequence reported in the NCBI database for *Penicillium citreonigrum* Dierckx (syn. *Eupenicillium hirayamae* D. B. Scott & Stolk). Growth of the fungus on a vermiculite-based solid-state medium containing 0, 10, 50, 100, or 200 μM 5-azacytidine showed that cultures exposed to ≥50 μM of the epigenetic modifier developed dark red guttates, which stood in vivid contrast to the colorless guttates produced by control cultures (Figure 3.1A and 3.1B). Gradient HPLC was used to compare the guttates from 20-day old control cultures versus fungal colonies treated with 50 μM 5-azacytidine. Whereas the control guttates were relatively devoid of small molecules, the HPLC profiles of guttates from 5-azacytidine-treated cultures were highly enriched in secondary metabolites (Figure 3.1C and 3.1D).

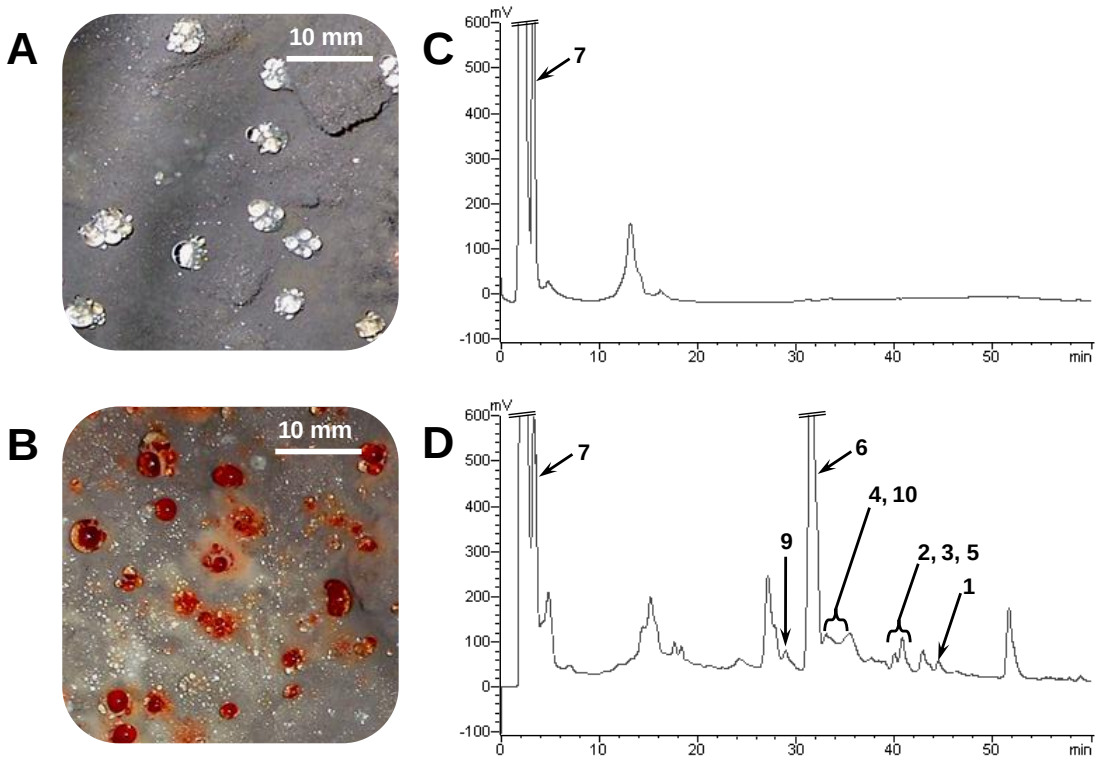

Figure 3.1. Guttates of solid-state *P. citreonigrum* cultures grown under control conditions (**A**) or in the presence of 50 µM 5-azacytidine (**B**). HPLC chromatograms (C_{18} column using a gradient of 5-100% methanol in water and recorded at 210 nm) illustrating the differences between the metabolite profiles of the control (**C**) and 5-azacytidine-treated (**D**) *P. citreonigrum* guttates. Metabolites identified in scale-up isolation studies were used as authentic references to verify the identities of compounds **3.1**-**7** and **3.9** and **3.10** in the guttates.

Scale-up solid-state cultures of *P. citreonigrum* treated with 50 µM 5-azacytidine were prepared and after 20 days, the resulting guttate-covered mycelia were washed with ethyl acetate. The ethyl acetate was removed under vacuum and the remaining solid residue was resuspended in methanol prior to defatting with hexane. The methanol-soluble material was subjected to repeated C_{18} gradient HPLC, which yielded six pigmented compounds that ranged in color from yellow-orange to dark red. A combination of ^{1}H and ^{13}C NMR, optical rotation, and high resolution electron spray

ionization mass spectra (HRESIMS) data facilitated the rapid dereplication of five azaphilones.[59] These compounds were determined to be sclerotiorin (**3.1**),[60] ochrephilone (**3.2**),[61] dechloroisochromophilone III (**3.3**),[62] dechloroisochromophilone IV (8-acetyldechloroisochromophilone III) (**3.4**),[62] and 6-((3*E*,5*E*)-5,7-dimethyl-2-methylenenona-3,5-dienyl)-2,4-dihydroxy-3-methylbenzaldehyde (**3.5**).[62]

A sixth highly colored substance (red solid) was obtained that exhibited ^{1}H and ^{13}C NMR data that were remarkably similar to the chemical shifts observed for **3.1**-**5**. Interpretation of the HRESIMS (*m/z* of 412.1290 $[M+Na]^{+}$ calcd for $C_{21}H_{24}NO_4ClNa$, 412.1292) and NMR data for **3.6** revealed that our metabolite matched the structure reported for the sclerotioramine (**3.6**), which had been previously obtained as a semisynthetic derivative of **3.1**.[63] Unfortunately, we were unable to find any NMR data published for this substance so we performed a thorough analysis of **3.6** using $^{2\text{-}3}J_{\text{H-C}}$ HMBC NMR spectroscopy to facilitate the assignment of its proton and carbon resonances. An important step in our investigation was confirming the location of the amine nitrogen in ring B. This was achieved by comparing the upfield changes in the chemical shifts for the C-1 and C-3 resonances (δ_C 138.4 and 146.6, respectively) in **3.6** to the corresponding C-1 and C-3 chemical shifts surrounding the oxygen atom in compound **3.1** (δ_C 152.6 and 158.1, respectively).

The installment of a nitrogen atom at the 2-position of compound **3.6** is quite remarkable since the biosynthesis of the azaphilones has been proposed to arise from a strictly polyketide-based pathway and feeding experiments utilizing both singly and doubly labeled ^{13}C and ^{14}C sodium acetate have leant strong support for this hypothesis.[61, 64] Moreover, the recent report of a two-part polyketide synthase gene

cluster complex that is responsible for generating an azaphilone metabolite in *Aspergillus nidulans* has provided convincing support for the polyketide origins of this metabolite family.[65] Although **3.6** has not been previously described as a natural product, other nitrogen-containing azaphilones have been reported from fungal sources.[66] All of these vinylogous γ-pyridone metabolites are thought to arise from the substitution of a primary amine/ammonia for the azaphilone's pyranyl oxygen atom in a process that is initiated by the nucleophilic attack of the nitrogen at the C-1 position.[66a] Therefore, we can reasonably surmise that **3.6** is formed as a consequence of **3.1** reacting with endogenous ammonia from *P. citreonigrum* during the culture process.[67]

Compound **3.7** was obtained as a colorless solid that exhibited a *m/z* of 218.0432 $[M+Na]^+$ by HRESIMS. This established a molecular formula of $C_9H_9NO_4$ for **3.7** (calcd for $C_9H_9NO_4Na$, 218.0429), which required six units of unsaturation. Analysis of the NMR data for the metabolite (^1H, ^{13}C, $^1J_{H\text{-}C}$ HSQC, and $^{2\text{-}3}J_{H\text{-}C}$ HMBC) led us to determine that the structure of **3.7** was the same as the structure that had been previously proposed for pencolide.[68] Although this metabolite had been encountered on at least two prior occasions from *Penicillium* species,[68-69] no detailed investigation concerning both its ^1H and ^{13}C NMR resonances had been reported. Moreover, debate that had arisen concerning the C-2, C-3 double bond configuration of **3.7** had not yet been fully resolved.[70] Therefore, we investigated the double bond configuration of **3.7** by treating it with thionyl chloride in methanol, which yielded the methyl ester derivative **3.8**. Using one-dimensional nuclear Overhauser effect difference correlation (1D difference NOE) spectroscopy, we observe reciprocal NOEs between the olefinic H-3 proton (δ_H 7.30) and the protons of the C-1 methyl ester (δ_H 3.73). In contrast,

irradiation of the C-4 methyl protons (δ_H 1.77) only provided enhancement of the H-3 resonance. These findings strongly support a *Z* configuration for the C-2, C-3 double bond in 3.**7**.

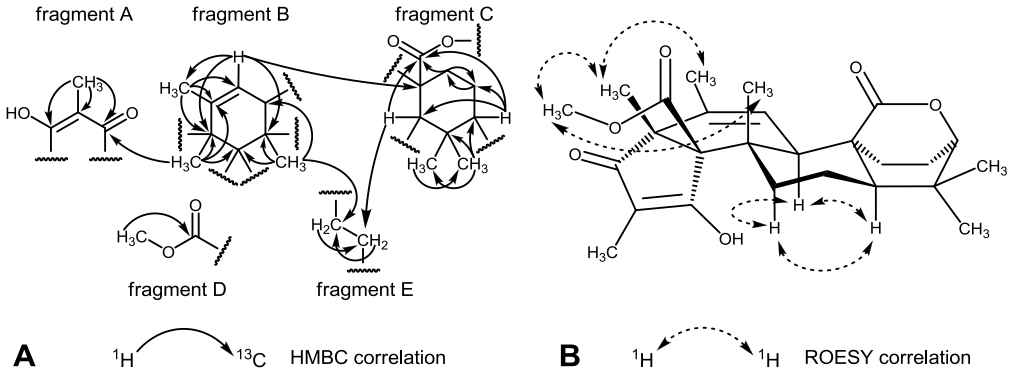

Figure 3.2. Correlations obtained from $^{2\text{-}3}J_{H\text{-}C}$ HMBC experiment that were used to generate fragments A-F, which were critical for deducing the structure of **3.9a** (**A**). Key ^{1}H-^{1}H ROESY correlations that were used to help assign the relative configuration of **3.9a** (**B**).

HRESIMS analysis of compound **3.9** provided a pseudomolecular ion with a *m*/*z* of 465.2256 $[M + Na]^+$ that was consistent with a molecular formula of $C_{26}H_{34}O_6$ (calcd for $C_{26}H_{34}O_6Na$, 465.2253). This required 10 degrees of unsaturation in the metabolite. A survey of the ^{13}C NMR data for **3.9** collected in $CDCl_3$ (Table 3.1) confirmed the presence of 26 unique carbon atoms including two ketone (δ_C 209.6 and 211.3), two ester (δ_C 168.3 and 174.8), and two vinylic carbon (δ_C 127.4 and 132.0) resonances. This accounted for five of the 10 double-bond equivalents in **3.9**, which meant that the remaining units of unsaturation were derived from five rings. Examination of the ^{1}H NMR data (Table 3.1) revealed six methyl singlets (δ_H 1.02, 1.07, 1.32 (×2), 1.69, and 3.54; each integrated for 3H), a methyl doublet (δ_H 1.19, J = 6.8 Hz, 3H), a vinylic hydrogen singlet (δ_H 5.67, 1H), a doublet (δ_H 4.07, J = 3.9, 1H), a quartet (δ_H 3.20, J = 6.8, 1H), and a series of overlapping multiplets spanning the region from δ_H 1.0 – 2.4.

The congestion caused by multiple resonances overlapping in the upfield region of the ^{1}H NMR spectrum prompted us to explore other solvents for performing NMR experiments with **3.9**. Turning to CD_3OD, we were surprised by two significant qualitative changes in the ^{1}H NMR spectrum (Table 3.1): the methyl doublet previously at δ_H 1.19 now appeared as a singlet (δ_H 1.57, 3H) and the quartet at δ_H 3.20 was missing. Upon reexamination of the $^{1}J_{H\text{-}C}$ HSQC data for **3.9** collected in $CDCl_3$ we observed that the missing hydrogen had been bonded to a carbon resonating at δ_C 51.4. The ^{13}C NMR data for **3.9** collected in CD_3OD (Table 3.1) exhibited other substantial changes that included both the loss of a ketone resonance (δ_C 211.3) and the carbon at δ_C 51.4. In place of the missing carbon spins, we observed two new vinylic carbon resonances appearing at δ_C 113.7 and 192.1. The substantial downfield shift of the vinylic carbon at δ_C 192.1 suggested that it was attached to an oxygen atom. The $^{2\text{-}3}J_{H\text{-}C}$ HMBC data for **3.9** in CD_3OD revealed that the protons of the methyl singlet at δ_H 1.57 coupled not only with both of the vinylic carbons, but also exhibited a correlation to a ketone resonance at δ_C 201.8 (Figure 3.2A, fragment A). This led us to deduce that compound **3.9** possessed a tautomerizable substructure that existed in its keto-enol form in CD_3OD (**3.9a**) and rearranged into a β-diketone in $CDCl_3$ (**3.9b**) (Figure 3.3). We confirmed this by removing **3.9** from the CD_3OD and resuspending the compound in $CDCl_3$. This provided ^{1}H and ^{13}C NMR and HRESIMS data for the metabolite that were identical to those we had previously observed for **3.9b**.

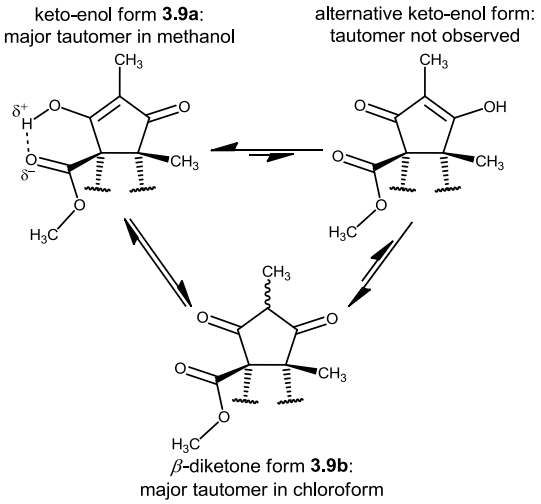

Figure 3.3. Possible tautomers proposed for compound **3.9**. The enol-keto structure **3.9a** (upper left) was the only tautomer observed in methanol; while the β-diketone compound **3.9b** (lower center) was exclusively seen in chloroform. The alternative enol-keto form of **3.9** (upper right) was not detected by NMR under these experimental conditions.

Having established the tautomeric portion of the new metabolite (Figure 3.2A, fragment A), we focused our attention on determining the remaining structural elements of **3.9a**/**9b**. We noted that the ^{1}H and ^{13}C NMR resonances associated with the rest of the metabolite in **3.9a** and **3.9b** appeared very similar to one another (Table 3.1). Therefore, we concentrated on using the 2D NMR dataset collected for **3.9a** as the basis for resolving the rest of this compound's structure. Examination of the $^{2\text{-}3}J_{\text{H-C}}$ HMBC data for **3.9a** enabled us to construct four additional substructures for the metabolite (Figure 3.2A, fragments B-E).

The development of fragment B (Figure 3.2A) was largely facilitated by the fortuitous proximity of three methyl groups and one olefinic proton, which provided a nearly exhaustive set of overlapping $^{2\text{-}3}J_{\text{H-C}}$ HMBC correlations among the substructure's nine carbon atoms. The first methyl singlet (δ_{H} 1.36) exhibited a series of three couplings with carbon resonances at δ_{C} 43.0, 47.6, 69.8. The second methyl singlet (δ_{H} 1.22) was also correlated to the carbon at δ_{C} 69.8, as well as carbons at δ_{C} 57.5 and 134.7. The third methyl singlet (δ_{H} 1.82) shared two of the same correlations (δ_{C} 57.5 and 134.7), as well as an additional coupling to a carbon at δ_{C} 126.3. Finally,

the olefinic singlet proton (δ_H 5.44) was coupled to a methyl carbon (δ_C 20.3) and carbons at δ_C 43.0 and 57.5. The combination of these overlapping $^{2\text{-}3}J_{H\text{-}C}$ couplings enabled us to deduce that fragment B constituted a highly substituted cyclohexene system (Figure 3.2A, fragment B).

Initially, the array $^{2\text{-}3}J_{H\text{-}C}$ couplings in CD_3OD for fragment C appeared perplexing and structurally uninformative; however, by expanding our assessment of this portion of **3.9** to include additional HMBC coupling detected in $CDCl_3$, we were able to derive three sets of $^1H \rightarrow {}^{13}C$ correlations that were useful for revealing the composition of this substructure. The first set consisted of correlations from a doublet proton at δ_H 4.12 (J = 3.7 Hz, 1H) to carbons at δ_C 22.8, 22.9, 52.9, and 178.1. Upon considering the chemical shifts of these carbons and their respective numbers of attached protons (determined by $^1J_{H\text{-}C}$ HSQC), we were able to deduce that they represented two aliphatic methyl groups, a methylene, and a quaternary carbon, respectively. We also noted a strong $^1H\text{-}^1H$ COSY correlation from the proton at δ_H 4.12 to geminal protons attached to the carbon δ_C 22.9 [based on $^1J_{H\text{-}C}$ HSQC; δ_H 1.88 (m, 1H) and 2.17 (m, 1H)]. These protons in turn coupled with a second set of geminal protons (δ_H 1.48, m, 1H and δ_H 2.04, m, 1H) that were attached to a carbon at δ_C 33.5 (based on $^1J_{H\text{-}C}$ HSQC). Additional $^{2\text{-}3}J_{H\text{-}C}$ couplings were found that originated from a methyl singlet at δ_H 1.03 and extended out to carbons at δ_C 28.3, 38.4, 52.9, and 86.1, as well as from a proton triplet at δ_H 1.50 (J = 3.4 Hz, 1H) to carbon resonances at δ_C 23.2, 28.3, 38.4, and 178.1. The abundance of carbons shared among at least two of the three sets of $^{2\text{-}3}J_{H\text{-}C}$ couplings enabled us to construct a cyclohexane substructure with an ester and geminal methyl groups at the 1- and 3-positions, respectively (Figure 3.2A,

fragment C). Further consideration of the downfield shift observed for the carbon at δ_C 86.1 and the $^{3}J_{H\text{-}C}$ coupling exhibited by its attached proton to the ester carbonyl resonance (δ_C 178.1) led us to deduce the presence of a second fused ring in fragment C. Thus, fragment C was proposed to consist of a 7,7-dimethyl-2-oxabicyclo[2.2.2]octan-3-one system (Figure 3.2A).

With the establishment of fragments A-C, only a handful of atoms remained to be assigned ($C_4H_7O_2$). Three of the remaining protons belonged to a methyl singlet (δ_H 3.58, 3H) that was judged by its chemical shift and $^{3}J_{H\text{-}C}$ HMBC coupling to be associated with an ester carbonyl (δ_C 172.7). Since no other correlations were observed from the other fragments to any of the atoms in fragment D (Figure 3.2A), we waited to assign its position in the metabolite until other evidence was secured. Fragment E (Figure 3.2A) was determined to be composed of two methylenes based on ^{1}H-^{1}H COSY data showing the coupling of their attached protons (geminal protons at δ_H 1.60 and 1.37 coupled to a second set of geminal protons at δ_H 2.10 and 2.08).

With all of the atoms accounted for in **3.9**, the final task was to determine the linkages among fragments A-E. Reexamination of the $^{2\text{-}3}J_{H\text{-}C}$ HMBC data showed that the methyl protons at δ_H 1.22 in fragment B exhibited a $^{3}J_{H\text{-}C}$ coupling with the ketone resonance (δ_C 201.8) in fragment A. With no other $^{2\text{-}3}J_{H\text{-}C}$ couplings apparent, we considered the fact that one of the quaternary carbons in fragment B (δ_C 69.8) was still lacking two of its four required bonding groups. We deduced that the enol carbon (δ_C 192.1) in fragment A was joined to this quaternary carbon in fragment B, which resulted in a five-membered 3-hydroxy-2-methylcyclopent-2-enone system. A series of three additional $^{2\text{-}3}J_{H\text{-}C}$ HMBC couplings were detected that allowed us to link fragments B, C,

and E (fragment B δ_H 1.36 → fragment E δ_C 32.9, fragment B δ_H 5.44 → fragment C δ_C 46.7, and fragment C δ_H 1.50 → fragment E δ_C 23.2) and this enabled us to establish the final ring system required for **3.9**. With only two unbonded carbon atoms left, we concluded that the ester comprising fragment D must be attached to the remaining quaternary carbon (δ_C 69.8) in fragment B.

With the planar structure of **3.9a** established, the assignment of the relative configuration for each of the compound's asymmetric centers was addressed by a 2D ^{1}H-^{1}H ROESY experiment. We observed a set of reciprocal correlations among several of the cyclohexene's substituents including H-22 ↔ H-11 and H-23, H-23 ↔ H-26 and H-21, and H-26 ↔ H-21 (Figure 3.2B). These data supported a *cis* fusion between the five-membered 3-hydroxy-2-methylcyclopent-2-enone and the cyclohexene ring systems. In addition, we detected reciprocal ^{1}H-^{1}H ROESY correlations among three of the four axial protons of the cycloalkane (H-7$_{axial}$ ↔ H-9$_{axial}$ ↔ H-5$_{axial}$) (Figure 3.2B). This enabled us to establish the relative configuration of **3.9a** as 3*R**, 5*R**, 8*S**, 9*R**, 10*S**, 13*R**, 14*R**. During the process of characterizing the structure of **3.9a**, we were able to secure a crystal of the metabolite from methanol that was suitable for X-ray crystallography. An ORTEP drawing of **3.9a** derived from the X-ray diffraction analysis is illustrated in Figure 3.4. In addition to verifying the proposed relative atom configuration for **3.9a**, we were also able to confirm the compound's absolute configuration as 3*R*, 5*R*, 8*S*, 9*R*, 10*S*, 13*R*, 14*R*. Considering the unique Atlantic Forest habitat from which the *P. citreonigrum* strain was obtained, we have given **3.9** the name atlaninone A.

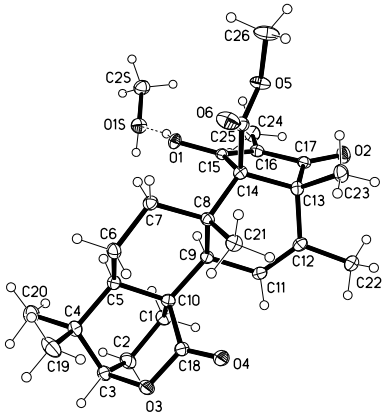

Figure 3.4. ORTEP structure for **3.9a** generated from the X-ray diffraction data.

At this point in the investigation, we returned our attention to the occurrence and population distribution of the three potential tautomers of **3.9** (Figure 3.3). Whereas the keto-enol tautomer **3.9a** (Figure 3.3) was readily apparent in methanol (C-17 ketone and C-15 enol carbon), we were not able to detect any traces of the complementary keto-enol tautomer (C-15 ketone and C-17 enol carbon) in solution. We suspect this may be due to the stabilizing influence of intramolecular hydrogen bonding between the C-15 enol hydroxyl group and the C-25 carbonyl oxygen atom. However, it is interesting to note that neither the andrastins[71] or citreohybridonol,[72] which share similar *cis*-fused cyclohexene and 3-hydroxy-2-methylcyclopent-2-enone substructures with **3.9**, are reported to exhibit a preference in methanol or chloroform for a single tautomeric species. Instead both sets of compounds undergo rapid transitions between their keto-enol and *β*-diketone forms in solution. We also noted that the corresponding *β*-diketone **3.9b** was the only form of the metabolite observed in chloroform. Examination of ^{1}H-^{1}H ROESY data for **3.9b** in $CDCl_3$ showed that both 16*R* and 16*S* configurations were present in solution (correlations between H-24 ↔ H-9 and H-24 ↔ H-26 were observed).

A related metabolite (**3.10**) was detected in one of the HPLC fractions that eluted just after 3.**9**. HRESIMS showed that **3.10** varied from the latter by the addition of an oxygen atom (*m*/*z* 481.2203 $[M + Na]^+$ consistent with a molecular formula of $C_{26}H_{34}O_6$; calcd for $C_{26}H_{34}O_7Na$, 481.2202). The ^1H and ^{13}C NMR data for **3.10** collected in $CDCl_3$ (Table 3.1) showed remarkable similarity to **3.9b** with one exception: C-16 was shifted substantially downfield (δ_C 72.5 in **3.10** versus δ_C 51.4 in **3.9b**) and its attached proton was missing (based on $^1J_{H\text{-}C}$ HSQC). This suggested that **3.10** was the C-16 hydroxy analog of **3.9b** and it was given the name atlantinone B. The remaining structural similarity between **3.10** and **3.9b** was quickly confirmed via analysis of the new metabolite's $^{2\text{-}3}J_{H\text{-}C}$ HMBC data (Table 3.1). Inspection of the 2D ^1H-^1H ROESY spectrum for **3.10** revealed a correlation between the H-24 methyl protons and the H-26 methyl ester, which suggested an *R* configuration for C-16. In light of the these data and considering that compounds **3.9** and **3.10** have a shared biogenic origin, we propose that the absolute configuration of **3.10** is 3*R*,5*R*,8*S*,9*R*,10*S*,13*R*,14*R*,16*R*.

A substantial portion of the atlantinones' structures are similar to other fungal-derived meroterpenoids such as citreohybriddiones A and B.[72] This group of compounds is proposed to arise from the *C*-alkylation of 3,5-dimethylorsellinate with farnesyl pyrophosphate, which is subjected to cyclization and further functionalization, yielding a diverse assemblage of products.[73] Geris and Simpson[73] recently hypothesized that the biosynthetic machinery responsible for generating a wide range of homologous meroterpenoids from *Aspergillus* and *Penicillium* (*e.g.*, andrastins, berkeleyones, penisimplicin, and territonin) is likely achieved by means of structural elaboration upon an shared scaffold. We propose that the atlantinones, which incorporate a unique 7, 7-

dimethyl-2-oxabicyclo[2.2.2]octan-3-one bridged-bicyclic-ring system, constitute a new branch of unusual structural diversification within this metabolite family.

The preponderance of secondary metabolites in the guttate of epigenetically modified *P. citreonigrum* (Figure 3.1C and 1D) suggests that fungal exudates warrant further exploration as a resource for natural product exploration. Considering the proposed role that guttates might play as nutrient sources for symbiotic microbial species, we rationalized that fungal hosts could incorporate bioactive compounds into exudates to influence the composition of the developing microbial community's structure. Accordingly, we tested **3.1**-**7**, **3.9**, and **3.10** against a panel of bacteria and fungi to ascertain if these compounds exhibited antimicrobial activities. Out of the nine compounds, only **3.1** and **3.6** exhibited modest zones of inhibition in a disk diffusion assay at a concentration of 30 μg/6mm paper disk. Both **3.1** and **3.6** inhibited *Staphylococcus epidermidis* (both produced 8 mm zones of inhibition), whereas only **3.6** inhibited *Candida albicans*, *Candida parapsilosis*, *Candida tropicalis*, and *Candida krusei* (8, 7, 8, and 8 mm zones of inhibition, respectively). In contrast, gentamicin (15 μg/6mm paper disk) exhibited more substantial zones of inhibition that averaged 8-16 mm against a range of bacteria, while ketoconazole (15 μg/6 mm paper disks) produced zones of inhibition that averaged 15-26 mm against a panel of yeast. The modest antimicrobial activities of the azaphilones were not surprising given the similar results that have been reported for other members of this secondary metabolite family.[74] However, we did find that our data stood in disagreement with results that had been recently reported for **3.7**. Whereas Lucas and colleagues observed modest activity for **3.7** against *Streptococcus pyogenese*, *Staphylococcus aureus*, *Salmonella typhimurium*,

Escherichia coli, and *Candida albicans* (13-16 mm zones of inhibition using 100 μg/disk),[69b] we observed no activity for this metabolite against 10 Gram-negative and Gram-positive bacteria and five fungi at concentrations ranging up to 135 μg/disk. Further studies of the secondary metabolites found in fungal guttates are required to critically assess their drug discovery potential and to understand their biological functions.

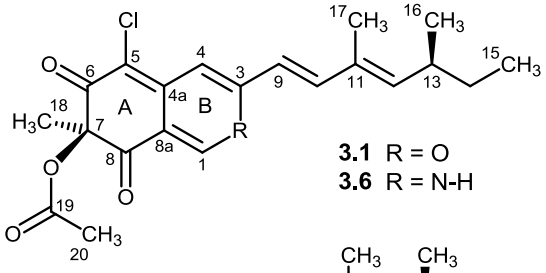

3.1 R = O
3.6 R = N-H

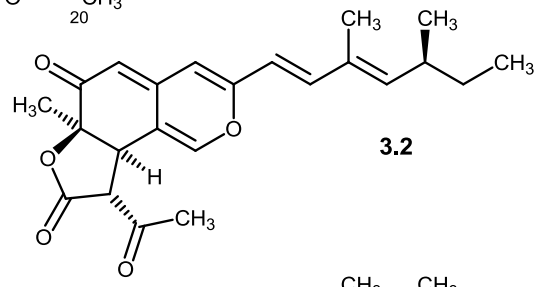

3.2

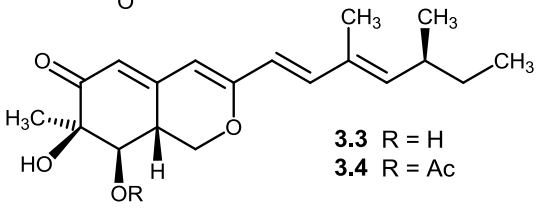

3.3 R = H
3.4 R = Ac

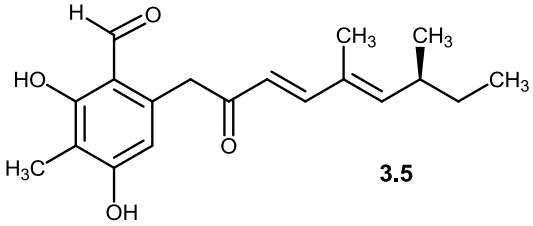

3.5

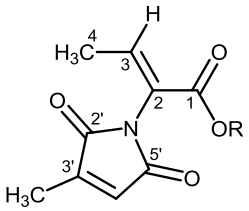

3.7 R = H
3.8 R = CH_3

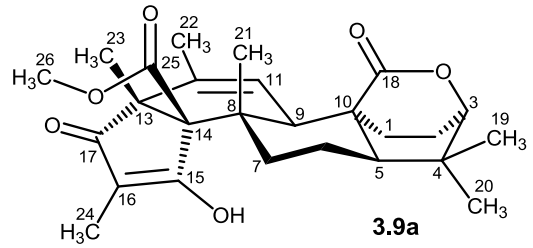

3.9a

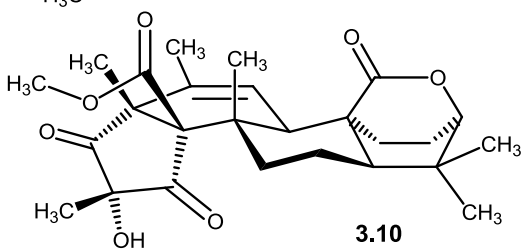

3.10

Table 3.1. ^{1}H (500 MHz) and ^{13}C (125 MHz) NMR data for **3.9a** (CD_3OD), **3.9b** ($CDCl_3$), and **3.10** ($CDCl_3$)

atlantinone A (**3.9a**)				atlantinone A (**3.9b**)			atlantinone B (**3.10**)		
Position	δ_C	δ_H, mult (*J* in Hz)	HMBC	δ_C	δ_H, mult (*J* in Hz)	HMBC	δ_C,	δ_H, mult (*J* in Hz)	HMBC
1	33.5	1.48 (1H, m)	3, 5, 10	32.6	1.39 (1H, m)	18	32.6	1.43 (1H, m)	3, 10
		2.04 (1H, m)	6		2.05 (1H, m)			2.09 (1H, m)	
2	22.9	2.17 (1H, m)	5, 18	21.8	2.07 (1H, m)	5	21.8	2.13 (1H, m)	1
		1.88 (1H, m)	3		1.89 (1H, m)	3		1.95 (1H, m)	3
3	86.1	4.12 (1H, d, 3.7)	2, 5, 18	84.4	4.07 (1H, d, 3.6)	1, 5, 18, 19	84.4	4.11 (1H, d, 4.0)	1, 2, 5, 18
4	38.4			37.4			37.4		
5	52.9	1.50 (1H, t, 3.7)	6, 18, 20	51.3	1.44 (1H, m)	4, 20	51.2	1.49 (1H, m)	1, 4, 18
6	23.2	1.60 (1H, m)	5	21.9	1.56 (1H, m)	8, 10	21.8	1.50 (1H, m)	
		1.37 (1H, m)	5		1.42 (1H, m)	5, 10		1.60 (1H, m)	
7	32.9	2.10 (1H, m)	5, 9	30.1	2.39 (1H, m)	8	30.0	2.58 (1H, td, 4.5, 13.0)	5, 8, 9
		2.08 (1H, m)	5, 9		2.28 (1H, dt, 13.7, 3.5)	5		2.25 (1H, m)	14
8	43.0			39.7			38.8		
9	47.6	1.90 (1H, m)	18, 21	47.2	1.82 (1H, m)	11, 12	46.6	1.96 (1H, t, 3.0)	8, 11, 18
10	46.7			45.0			45.0		
11	126.3	5.44 (1H, s)	8, 10, 13, 22	127.4	5.67 (1H, s)	9, 10, 13, 22	129.4	5.82 (1H, s)	8, 9, 13, 22
12	134.7			132.0			131.0		
13	57.5			61.1			61.3		
14	69.8			73.3			71.7		
15	192.1			211.3			211.5		
16	113.7			51.4	3.20 (1H, q, 6.7)	15, 17, 24	72.5		
17	201.8			209.6			207.5		
18	178.1			174.8			174.9		
19	22.8	1.03 (3H, s)	4, 20	22.6	1.02 (3H, s)	3, 4, 5, 20	22.6	1.06 (3H, s)	3, 4, 5, 20
20	28.3	1.14 (3H, s)	4, 19	28.1	1.07 (3H, s)	3, 4, 5, 19	28.0	1.12 (3H, s)	3, 4, 5, 19
21	17.6	1.36 (3H, s)	7, 8, 9, 14	16.5	1.32 (3H, s)	7, 8, 10	16.9	1.35 (3H, s)	7, 8, 9, 14
22	20.3	1.82 (3H, s)	11, 12, 13	19.2	1.69 (3H, s)	11, 12, 13, 14	19.1	1.76 (3H, s)	11, 13
23	16.7	1.22 (3H, s)	12, 13, 14, 17	16.5	1.32 (3H, s)	12, 13, 14, 17	17.7	1.41 (3H, s)	12, 13, 14, 17
24	6.7	1.57 (3H, s)	15, 16, 17	9.6	1.19 (3H, d, 6.8)	15, 16, 17	19.9	1.38 (3H, s)	15, 16, 17
25	172.7			168.3			167.6		
26	52.0	3.58 (3H, s)	25	52.0	3.54 (3H, s)	25	52.1	3.61 (3H, s)	25
OH								2.22 (1H, brs)	15, 16, 17, 24

3.3 Materials and Methods

3.3.1 General Methods

NMR data were obtained on Varian VNMR spectrometers (400 and 500 MHz for ^{1}H, 100 and 125 MHz for ^{13}C) with broad band and triple resonance probes at 20 ± 0.5 °C. Electrospray-ionization mass spectrometry data was performed on a LCT Premier (Waters Corp.) time-of-flight instrument. Optical rotations were measured on a Rudolph Research Autopol III automatic polarimeter. HPLC separations were performed on a Shimadzu system using a SCL-10A VP system controller and Gemini 5µm C_{18} column, (110Å, 250 x 21.2 mm) with flow rates of 1 to 10 mL/min. X-ray diffraction data were collected on a Bruker-AXS with an APEX CCD area detector with a Cu X-ray source. All solvents were of ACS grade or better.

3.3.2 Organism Collection, Identification, and Culture Methods

A soil sample (~100 g taken from about 20 cm below the soil surface) was collected in a small patch of remnant forest near the coast of Joao Pessoa, State of Para ba, Brazil in January of 2006. Samples (1 g) were placed in autoclaved H_2O (10 mL) and diluted 10- and 100-fold. Aliquots (300 uL) of the diluted soil suspensions were lawned onto the surfaces of 10 cm diameter Petri plates containing potato-dextrose agar with chloramphenicol (100 mg/L) and cycloheximide (100 mg/L). Plates were maintained at 20 ℃ for four weeks and emerging colonies were picked from the plates and transferred to fresh Petri plates containing potato-dextrose agar with chloramphenicol (100 mg/L). This process was repeated for each isolate until a uniform fungal colony was established. Fungi were transferred to new Petri plates containing potato-dextrose agar and after 2-3 weeks of incubation at 20 ℃, pieces of the agar containing mycelia (~0.5 cm^2) were cut and placed in cryogenic storage tubes with

sterile glycerol-H_2O (15:85). The tubes were then stored at -80 ℃ until the fungus was needed for scale-up studies. The fungus was identified based on sequence analysis of a 321 base-pair portion of its large ribosomal subunit 28S rRNA gene using a previously published method.[53b] The sequence of the isolate was compared by BLAST analysis to sequences publically available through the NCBI database.

For the preparative-scale grow-up, fungal mycelia and spores were inoculated into 50 mL potato-dextrose media and grown for one week with shaking (125 rpm). The cellular material was placed in a sterile Falcon tube and mixed by vortexing for several minutes to create a uniform fungal cell/spore suspension. Aliquots (500 µL) of the fungal suspension were used to inoculate 110 Erlenmeyer flasks (1 L) containing autoclaved media (0.1 g rice, 0.1 g oatmeal, 0.1 g cornmeal, 0.32 g nutrient broth, ~0.5 g vermiculite, and 50 mL of deionized H_2O). Epigenetically modified cultures were treated with 50 µM 5-azacytidine, while the control cultures were treated with vehicle only (filter-sterilized H_2O). Culture vessels were maintained on the bench-top at 25 ℃ for 20 days.

3.3.3 Extraction and Isolation

The guttate-covered mycelia mats were washed by adding 100 mL of EtOAc to each flask and gently swirling the contents. The liquid was decanted from the flasks, pooled, and placed in a separatory funnel. The organic layer was recovered and the solvent was removed under vacuum. The resulting organic extract was resolubilized in MeOH and partitioned three times against an equal volume of hexane. Solvent from the defatted MeOH extract was removed under vacuum, which yielded a rust-colored crude extract (0.8 g). The extract was subjected to gradient C_{18} HPLC (mobile phase 20% to 100% MeOH in H_2O), which yielded three fractions containing secondary metabolites:

fraction A (40 mg of **7**), fraction B (160 mg mixture of **3.9** and **3.10**), and fraction C (182 mg mixture of azaphilones **3.1**-**3.6**). Fraction B was subjected to repeated semi-preparative C_{18} HPLC (mobile phase 75% to 100% MeOH in H_2O), which provided **3.9** (7 mg) and **3.10** (3 mg). The azaphilones in fraction C were purified in two additional steps. The first step consisted of passing the mixture over silica gel in a step gradient fashion with hexane and increasing amounts (10% increments) of acetone. The second step involved applying a portion of the fractions containing the azaphilones to semi-preparative C_{18} HPLC (mobile phase 80% to 100% MeOH in H_2O) to give purified **3.1**-**3.6**.

3.3.4 Sclerotioramine (3.6)

Red solid; ^{1}H NMR (400 MHz, $CDCl_3$) δ_H 7.80 (1H, s, H-1), 6.79 (1H ,s ,H-4), 6.10 (1H, d, J = 16.0 Hz, H-9), 6.95 (1H, d, J = 16.0 Hz, H-10), 5.68 (1H, d, J = 9.8 Hz, H-12), 2.47 (1H, m, H-13), 1.44 (1H, m, H-14), 1.34 (1H, m, H-14), 0.88 (3H, t, J = 7.4 Hz, H-15), 1.04 (3H, d, J = 6.7 Hz, H-16), 1.85 (3H, s, H-17), 1.58 (3H, s, H-18), 2.23 (3H, s, H-20); ^{13}C NMR (100 MHz, $CDCl_3$) δ_C 138.4 (CH, C-1), 146.1 (C, C-3), 110.5 (CH, C-4) , 146.6 (C, C-4a), 102.1 (C, C-5), 183.1 (C, C-6), 85.6 (C, C-7), 193.4 (C, C-8), 114.2 (C, C-8a), 116.3 (CH, C-9), 143.0 (CH, C-10), 132.1 (C, C-11), 149.1 (CH, C-12), 35.3 (CH, C-13), 30.2 (CH_2, 14), 12.2 (CH_3, C-15), 20.3 (CH_3,C-16), 12.6 (CH_3, C-17), 23.7 (CH_3, C-18), 171.4 (C, C-19), 20.8 (CH_3, C-20); HRESIMS *m/z*: $[M+Na]^+$ 412.1290 (calcd for $C_{21}H_{24}NO_4ClNa$, 412.1292).

3.3.5 Pencolide (3.7)

White solid; ^{1}H NMR(500 MHz, $CDCl_3$), δ_H 7.40 (1H, q, J = 7.0 Hz, H-3), 1.81 (3H, d, J = 7.0 Hz, H-4), 6.46 (1H, q, J = 2.0 Hz, H-4'), 2.13 (3H, d, J = 2.0 Hz, H-6'); ^{13}C NMR (125 MHz, $CDCl_3$) δ_C 167.3 (C, C-1), 123.0 (C, C-2), 145.3 (CH, C-3), 14.7

(CH_3, C-4), 170.2 (C, C-2'), 146.7 (C, C-3'), 128.3 (CH, C-4'), 169.1 (C, C-5'), 11.7 (CH_3, C-6'); HRESIMS *m/z*: $[M+Na]^+$ 218.0432 (calcd for $C_9H_9NO_4Na$, 218.0429).

3.3.6 Preparation of Pencolide Methyl Ester (3.8)

Thionyl chloride (0.10 mmol) was slowly added to a solution of dry MeOH (1 mL) and pencolide (**7**, 0.051 mmol) under a N_2 atmosphere at 0^o C. The mixture was allowed to slowly warm to room temperature with stirring. After 12 hours, the excess MeOH was removed under high vacuum and the crude material was subjected to partitioning with EtOAc and H_2O. The organic layer was collected, dried by passing over magnesium sulfate, filtered, and the solvent was removed under vacuum. The sample was then subjected to HPLC (C18, 5% to 15% MeOH in H_2O) providing pencolide methyl ester (**8**) in 58% yield (6.2 mg, 0.030 mmol). ^{1}H NMR (400 MHZ, $CDCl_3$), δ_H 7.30 (1H, q, *J* = 7.2 Hz, H-3), 1.77 (3H, d, *J* = 7.2 Hz, H-4), 6.44 (1H, q, *J* = 2.0 Hz, H-4'), 2.13 (3H, d, *J* = 2.0 Hz, H-6'), 3.73 (3H, s, $COOCH_3$); ^{13}C NMR (100 MHZ, $CDCl_3$), δ_C 163.3 (C-1), 123.3 (C-2), 143.5 (C-3), 14.5 (C-4), 170.3 (C-2'), 146.7 (C-3'), 128.3 (C-4'), 170.3 (C-5'), 11.5 (C-6'), 52.8 (COO<u>C</u>H3)

3.3.7 Atlantinone A (3.9)

Colorless, crystalline solid; $[\alpha]^{21}_D$ –102.1 (*c* 0.023, MeOH); ^{1}H and ^{13}C NMR data, see Table 3.1; *m/z* 465.2256 $[M + Na]^+$ (calcd for $C_{26}H_{34}O_6Na$, 465.2253).

3.3.8 X-ray Crystallographic Analysis of Atlantinone A (3.9)

$C_{26}H_{34}O_6 \cdot CH_4O$, FW = 474.57, orthorhombic, $P2_12_12_1$, *a* = 12.0199(6), *b* = 13.7713(6), *c* = 14.8276(8) Å, Volume = 2454.4Å^3, Z = 4, ρ_{calc} = 1.284 Mg/m^3, Cu *K*α radiation, λ = 1.54178 Å. Intensity data were collected on a Bruker instrument with an APEX detector, and a graphite-monochromated sealed tube source at a temperature of

100 K. A total of 26,979 data points were collected using ω and ϕ oscillation frames to give 4,555 unique data out to 67° θ with a R_{int} = 0.0476 and 100.0% coverage. All data were included in the refinement of F^2 values. Hydrogens bonded to carbons were included with assumed geometries and refined with a riding model. Hydrogens bonded to oxygens were located on a difference map, and their positions were refined independently. Final wR2 = 0.0802, R1 = 0.327, S = 1.001.

3.3.9 Atlantinone B (3.10)

Colorless, crystalline solid; [α] (sample degraded before optical rotation data were obtained); ^{1}H and ^{13}C NMR data, see Table 3.1; *m*/*z* 481.2203 $[M + Na]^+$ (calcd for $C_{26}H_{34}O_7Na$, 481.2202).

3.3.10 Analysis of Guttate Metabolites

Cultures treated with 50 μM 5-azacytidine and vehicle controls were prepared in triplicate using the method described for the scale-up metabolite isolation studies (*vide supra*). The cultures were incubated for 20 days and the guttates were sampled by pinching them off at their bases from the mycelia surface using a pair of fine-tip forceps. We initially experimented with employing a syringe to aspirate the guttate, but were not able to use this approach since both the control and treatment group guttates were quite resinous in consistency. Instead, a total of 25 equal-sized guttate droplets were freed from the mycelia in control and treated cultures and were placed in separate Eppendorf tubes. Control and treated guttates were washed three times with 500 μL of MeOH and the organic extracts were centrifuged to remove solids. The MeOH soluble materials were passed over a C_{18} SPE cartridge and subjected to C_{18} HPLC (mobile phase 20% to 100% acetonitrile in H_2O) with parallel ESIMS analysis. Standards consisting of

purified **3.1**-**3.7** and **3.9** and **3.10** were used to authenticate components in the treated and control samples.

3.3.11 Antimicrobial Assay

Compounds were tested for antimicrobial activity using a disk-diffusion assay. Seed cultures of eight bacteria (*Staphylococcus aureus* ATCC 700787, *Staphylococcus epidermidis* ATCC 12228, *Burkholderia cepacia* ATCC 25608, *Klebsiella pneumoniae* ATCC 33495, *Actinobacter baumannii* ATCC 19606, *Pseudomonas aeruginosa* ATCC 10145, *Escherichia coli* ATCC 11775, and *Enterobacter cloacae* ATCC 13047,) and five fungi (*Candida albicans* ATCC 12983, *Candida parapsilosis* ATCC 12969, *Candida glabrata* NRRL Y-65, *Candida tropicalis* ATCC 12968, and *Candida krusei* ATCC 27803) were prepared by incubating the organisms for 10 h at 30 ℃ (fungi) or 37 ℃ (bacteria). Aliquots of the overnight cultures (80 µL) were lawned onto the surfaces of nutrient agar (bacteria) or yeast extract agar with 2% (w/v) glucose (fungi). Sterile filter disks (6 mm diameter) infused with 3 µL of test solution (10 µg/µL DMSO), positive control (5 µg/µL DMSO gentamicin for bacteria or 5 µg/µL DMSO ketoconazole for fungi), or vehicle only (DMSO) were added to the plates. The plates were left upright for 30 minutes at room temperature before being placed in an incubator at 30 ℃ (fungi) or 37 ℃ (bacteria). After 10 h, the diameters of the zones of growth inhibition around each disk were recorded.

Chapter 4 Novel dimeric isoprenylated indole alkaloids isolated from Aspergillus sp. by manipulating the culture conditions

This chapter is adapted from publication that is currently under preparation.

4.1 Introduction

During our continuing study of new fungal metabolites a fungus *Aspergillus* sp. from Hawaii was investigated. In our group we have continually applied the chemical epigenetic method for producing secondary metabolites from fungi.[51] This method has been demonstrated as an effective tool for promoting the transcription of silent biosynthetic pathways involved in the formation of polyketide, non-ribosomal peptide, and hybrid polyketide-non-ribosomal-peptide natural products. [75] In this study, we have applied different epigenetic modifiers on this fungus and compared its secondary metabolites production by LC-MS respectively. In the meantime, we also compared the secondary metabolite production by growing this fungus in the liquid and static medium.

4.2 Results and Discussion

LC-MS has been used to analyze the secondary metabolite production in each culture condition. Fungi treated with suberoylanilide hydroxamic acid (SAHA) or 5-Azacytidine (5-Aza) showed increasing yield of secondary metabolite which demonstrated epigenetic modification can upregulate the fungal secondary metabolites gene expression. Based on LC-MS guided separation we have focused on those compounds with a mass higher than 400 amu under the static condition. A series of compounds had been isolated and quickly dereplicated based on their ^{1}H NMR and HRESIMS. They possess a unique structural core of bicyclo[2.2.2]diazaoctane and

were identified as notoamide B (**4.1**)[120], sclerotiamide (**4.2**)[76], notoamide F(**4.3**) [77], notoamide R (**4.4**)[78], stephacidin A (**4.5**)[79] and CJ-17665 (**4.6**) [80].

Compound **4.7**, a yellow plate (MeOH), HRESIMS analysis provided a pseudomolecular ion with a *m/z* of 875.4119 $[M+H]^-$ that was consistent with a molecular formula of $C_{52}H_{54}N_6O_7$ (calcd for $C_{52}H_{55}N_6O_7$, 875.4132), indicating 29 degrees of unsaturation. ^{1}H-NMR suggested that this compound maybe a mixture of two alkaloids. However, the single peak in the HPLC profile and the HRESIMS data confirmed this was only one compound belonging to a class of prenylated indole alkaloids. Analysis of HSQC and ^{1}H-NMR (table 4.1) revealed 8 singlet methyl signals at δ_H 1.02 (s, 3 H), 1.15 (s, 3 H), 1.26 (s, 3 H), 1.28 (s, 3 H), 1.37 (s, 3 H), 1.39 (s, 3 H), 1.68 (s, 3 H), and 1.83 (s, 3 H), 10 methylene signals in a range of δ_H 1.8 -2.8, 8 doublet olefinic signals at δ_H 5.52 (d, J = 10.5 Hz), 7.56 (d, J = 10.5 Hz), 6.44 (d, J = 8.3 Hz), 6.89 (d, J = 8.3 Hz), 6.64 (d, J = 8.3 Hz), 7.14 (d, J = 8.8 Hz), 5.58 (d, J = 9.8 Hz), and 6.40 (d, J = 9.3 Hz). 4 methine at δ_H 5.55 (s), 5.14 (s,) 3.08 (dd, J = 10.3, 6.7 Hz), and 3.00 (m, 1H), and two exchangeable protons at δ 7.58 (s, 1 H) and 7.44 (s, 1 H). ^{13}C NMR signals at δ_C 174.3, 174.2, 168.8, and 167.1 implied the presence of four carbonyl functional groups. By performing the literature search, the ^{1}H and ^{13}C NMR spectra of compound **4.7** are similar to those of stephacidin B which is a dimer of CJ-17665 (avrainvillamide)[81]. The molecular weight difference of *m/z* 16 between **4.7** and stephacidin B indicated the absence of one less oxygen atom in **4.7**. Extensive 2D-NMR studies including COSY, HMBC and NOESY have been used to establish all structural fragments. To characterize its structure we started from each methylene signal of –C^1H_2-C^2H_2-C^3H_2- which was revealed through the analysis of the ^{1}H-^{1}H COSY. The

chemical shifts of C-1 and C-4 indicated a 5-membered ring having nitrogen between them. The methylene protons H-5 and H-6, vicinally connected with H-5, were coupled to the C-4 and the amide carbonyl group (C-23); the 5-H and 3-Ha showed long range couplings to the remaining amide carbonyl group at C-26, which resulted in the formation of amide bridge between C-22 and C-4 to produce diketopiperazine substructure. Two singlet methyl protons H-27 and H-28 were coupled to C-7 and C-8 and H-6 was coupled to C-5, C-7. Furthermore, a singlet methine proton at H-21 was coupled to C-20, C-22 and C-23.Those described correlations enabled us to propose the partial structure A (Fig. 4.1A) Similarly, the partial structure B was determined based on HMBC and COSY correlations (Figure 4.1A). ^{1}H-^{1}H COSY correlations showed two connectivities (-C^{17}H=C^{18}H-, -C^{12}H=C^{13}H-) which have HMBC correlations from H-12 to C-10, C-14 and C-16, from H-13 to C-11, C-14; from H-17 to C-11, C-16 and an C-19, from H-18 to C-10,C-11 and C-16. Two singlet non-equivalent methyl groups were, in addition, coupled to C-13 and C-14. The position of O-15 was deduced by the oxygenated features of chemical shifts C-14 and C-16. All above correlations enable us to establish the partial structure (B). Based on the chemical shifts of C-8 (δ_C 151.3) and C-10 (δ_C 140.0) we postulated that nitrogen was present between C-8 and C-10, furthermore, a key HMBC correlation from H-21 to C-19 was observed. Finally, partial structure A and B was linked from C-10 to N-9 and from C-19 to C-20 to give substructure which was identified as CJ17665 (**4.6**). HMBC correlations from an exchangeable proton at δ_H 7.58 to C-38 and 50 connected fragment A1 and B1 to give the planar structure that was identified as stephacidin A (**4.5**). The HMBC correlations from H-51 to C-19 and C-20 were used to determine the linkage between C-20 and C-

51 and a correlation from H-21 to C-52 confirmed the linkage between C-21 and N-55. Thus heterodimer (**4.7**) is originated from CJ-17665 (**4.6**) and stephacidin A (**4.5**). We named it as waikialoid A. A crystal grew from 100% MeOH under room temperature was obtained and its structure was confirmed by single-crystal X-ray analysis (Figure 4.4). X-ray analysis provided the absolute configuration of **4.7** as 4*S*,6*S*,20*S*,21*S*,22*R*, 34*S*,36*S*,51*R*,52*R*.

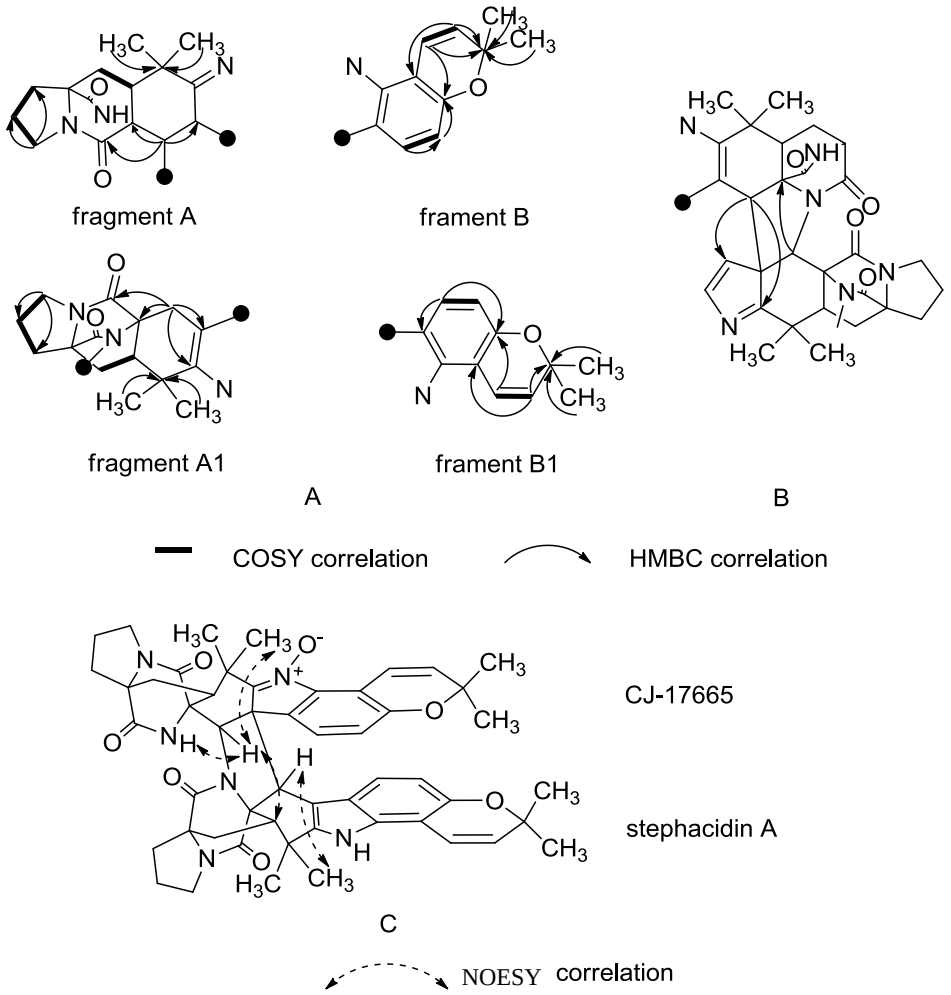

Figure 4.1. Correlations obtained from $^{2\text{-}3}J_{\text{H-C}}$ HMBC and ^{1}H-^{1}H COSY experiment that were used to generate fragments A-B which were critical for deducing the structure of **4.7** (A) Key $^{2\text{-}3}J_{\text{H-C}}$ HMBC correlations that were used to assign the linkage between two monomers **4.7** (B) Key ^{1}H-^{1}H NOESY correlations that were used to help assign the relative configuration of **4.7** (C).

HRESIMS analysis of compound **4.8** provided a pseudomolecular ion with a *m/z* of 905.3827 $[M-H]^-$ that was consistent with a molecular formula of $C_{52}H_{54}N_6O_9$ (calcd for $C_{52}H_{53}N_6O_9$, 905.3874), indicating 29 degrees of unsaturation. Based on the HMBC and HSQC we were able to assign chemical shifts to all carbon atoms although we did not obtain a well resolved carbon signal. By carefully analyzing the NMR data (table 4.1), compound **4.8** showed a similar ^{1}H NMR spectrum as that of compound **4.7** (table 4.1) indicating a third natural occurring dimer of prenylated indole alkaloid type compound. The molecular weight difference of *m/z* 32 between **4.8** and **4.7** indicated the presence of two more oxygen atoms in **4.8.** The IR spectrum showed a distinguished absorption band at 3380 indicating an OH group in **4.8**. The HMBC correlations from OH-62 to C-49, 50 and 51 were used to confirm the position of OH group at C-50. By carefully analyzing the HMBC and HSQC data we did not see any significant chemical shift changes, so two other oxygen atoms must attach to the N-9 and N-39. Thus compound **4.8** is a heterodimeric metabolite derived from CJ-17665 and aspergamide A [162]. The linkages between these two compounds were identified at the same way as that of **4.7** by HMBC correlations from H-51 to C-8 and C-20, and H-21 to C-51 and C-52. The relative configuration of compound **4.8** was determined by 2D ^{1}H-^{1}H ROESY experiment. We observed a set of reciprocal correlations including H-51 ↔ H-48, OH-62, H-6, H-28, H-36 ↔ H-17, H-35b and H-58, H-21↔ H-25, H-17, H51, H-6, OH-62 ↔H27, H51 and H-57. This enabled us to establish the relative configuration of **4.8** as 4*S**,6*S**,20*S**,21*S**,22*R**,34*S**,36*S**,50*R**,51*R**,52*R**. The CD spectra of compound **4.8** and **4.7** showed very similar cotton effects (Appendix pg. 138, 144)

which indicated that they had the same absolute configuration. So we determined the absolute configuration of compound **4.8** as 4*S*,6*S*,20*S*,21*S*,22*R*,34*S*,36*S*,50*R*,51*R*,52*R*.

Besides compounds **4.1-8**, six other known compounds were isolated and identified as circumdatin F (**4.9**) [82], circumdatin C (**4.10**) [83], two diketopiperazines (**4.11-12**)[84], flavacol (**4.13**)[85] and 3-isobutyl-6-(1-hydroxyl-2-methylpropyl)-2(1H)-pyrazinone (**4.14**) [86] from the static culture.

Liquid culture provides less secondary metabolites and we did not observe any of the above compounds except circumdatin F and circumdatin C from this fungus. Compound **4.15** and **4.16** are exclusively isolated from liquid culture.

Compound **4.15** has a molecular formula $C_{14}H_{20}O_2Na$ based on HRESIMS *m/z* 243.1378 (Calcd: 243.1360), indicating 5 degrees of unsaturation. Based on the HSQC and ^{1}H-NMR there are 2 singlet methyl signals at δ_H 0.93, 1.78, 6 olefinic signals at δ_H 5.73, 6.13 (×4), and 5.55, 3 methine at δ_H 1.95, 2.25, 3.78 (oxygenated), and a series of overlapping multiplets spanning the region δ_H 1.6-2.7. By analysis of the ^{13}C NMR it showed there were 6 olefinic carbons at δ_C 130.5, 133.2, 133.6, 131.7, 133.0, 136.4 and a carbonyl at δ_C 211.7 which indicated **4.15** must be a monocyclic compound. The connectivity of -C^8-C^9-C^{10}- was revealed by the $^{2\text{-}3}J_{H\text{-}C}$ HMBC correlations from H-10 to C-8 and C-9 , in addition, the $^{2\text{-}3}J_{H\text{-}C}$ HMBC correlations from H-11b to C-9, C-10, C-12 and C-13 indicated the connectivity -C^9-C^{10}-C^{11}-C^{12}-C^{13}-. Thus the partial structure A was proposed as cyclohexanone ring moiety (Figure 4.2). The COSY correlations between a methyl group δ_H 1.78 and an olefinic proton δ_H 5.73 connected C-1 with C-2. HMBC correlations from overlapped δ_H 6.13 to δ_C 130.5, 131.7 and 133.0 connected the six olefinic carbons and δ_H 5.55 with δ_C 46 connected C-7 with C-8. By

incorporation of the assignments together compound **4.15** was determined as 3-((1E, 3E, 5E)-hepta-1, 3, 5-trien-1-yl)-5-hydroxy-2-methylcyclohexanone. The relative configuration was determined using *J*-based coupling constant analysis and NOESY experiments. The sp3 methine proton H-8 showed NOE correlations with H-10 and H-13; In addition, the large coupling constant ($J_{13,\,8}$ = 13.0 Hz) indicated that they should be axial and axial oriented. The H-10 showed axial-axial coupling to H-9a (d, *J* = 11.3Hz) and H-11a (d, *J* = 11.4Hz). These couplings enabled us to deduce its relative configuration as 8*S**, 10*R**, and 13*R**. Considering the origin of compound **4.15** from the *Aspergillus* sp. with hydroxyl group in the structure we have given **4.15** the name asperonol A. A crystal grew from 100% MeOH under room temperature was obtained and its structure was confirmed by single-crystal X-ray analysis (Figure A1).

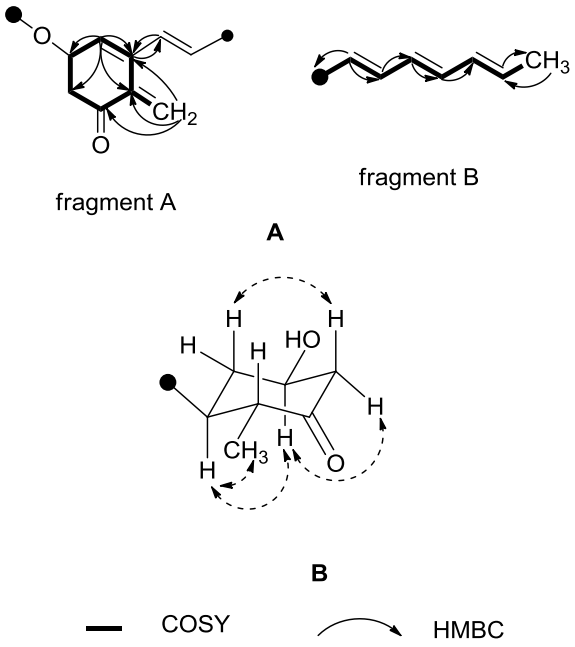

Figure 4.2. (A) Correlations obtained from $^{2-3}J_{H-C}$ HMBC experiment that were used to generate fragments A-B, which were critical for deducing the structure of **4.15.** (B) Key ^{1}H-^{1}H NOESY correlations that were used to help assign the relative configuration of **4.15.**

The absolute configuration of the tertiary alcohol at C-10 was determined by the Mosher ester method[87]. Comparing the ^{1}H NMR showed a slight difference of δ_H caused by the diamagnetic effect of the α-methoxy-α-(trifluoromethyl)phenylacetic acid (MTPA) benzene ring (Figure 4.3). The absolute configuration of C-10 was determined as 10*R* as calculation of the $\Delta\delta_{SR} = \delta_H(S) - \delta_H(R)$. We also used CD spectrum to confirm the absolute configuration. Compound **4.15** showed a negative Cotton effect resulting from n- π * transition at 290 nm indicative of a 13*R* configuration based on the octant rule.[15] The absolute configuration from CD was agreed with the assignment from Mosher ester method. So the absolute configuration was determined as (8*S*,10*R*,13*R*) - 3-((1E, 3E, 5E)-hepta-1, 3, 5-trien-1-yl)-5-hydroxy-2-methylcyclohexanone.

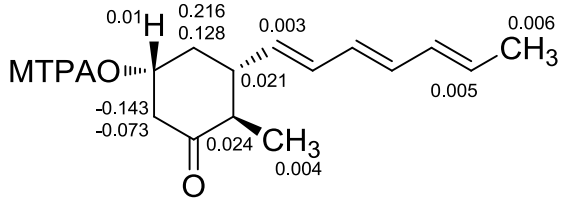

Figure 4.3. Values of δ_S-δ_R of the MTPA esters of **4.15**

Compound **4.16** has a molecular formula $C_{14}H_{22}O_2$ based on HRESIMS 221.1543 $[M-H]^-$ (Calcd: 221.1542) indicating 4 degree unsaturation. The ^{1}H NMR showed compound **4.16** is structurally close to compound **4.15**. Carbon NMR revealed a new carbon at δ_C 72.8 accompanying with a loss of a carbonyl group compared to those of compound **4.15**. This change also made H-11 and H-13 shift more upfield in compound **4.16**. All evidences supported that the structural change at C-12 from a carbonyl to an oxygenated methine. Based on the HMBC and COSY correlations compound **4.16** is a C-12 hydroxyl analog of **4.15** and it was named asperonol B. The relative configuration was determined by NOESY experiment. We observed the

reciprocal correlation including H-8 ↔ H-11a, H-6, H-12 ↔ H-8, H-13, H14, H-13 ↔ H-7, H-12 and H-14, H-10 ↔ H- 9b which helped us to determine the relative configuration as 8*S**, 10*R**, 12*R** and 13*R**. Because compound **4.16** and **4.15** had close planar structure and positive specific rotation we proposed the absolute configuration of compound **4.16** as 8*S*, 10*R*, 12*R* and 13*R*.

The effects of compounds **4.1-10, 4.13-16** on *C. albicans* growth and biofilm formation were evaluated in 96-well polystyrene microplates. *C. albicans* cells were treated with various concentrations (6.25–200 μM) of test compounds or DMSO as negative control at 37 ℃ for 48 h. The growth and biofilm formation of *C. albicans* were measured using XTT assay. The samples were compared to the negative controls to determine any reduction in the total amount of growth or biofilm. Test compounds did not inhibit the growth of *C. albicans* at 200 μM while eight of them showed the biofilm inhibition activity (Table 4.3). In the bioassays of the isolated metabolites, compound **4.1, 4.2**, **4.4**, and **4.16** showed low activity (IC_{50} >80 μM). Compound **4.5**, **4.6** and **4.8** exhibited a similar moderate activity, while **4.7** and **4.15** were the most potent compounds, with IC_{50} of 32.36 μM and 1.40 μM, respectively. And the effects of compounds **4.7** and **4.15** on *C. albicans* hyphae formation were observed under a phase contrast microscope. **7** and **15** inhibited the hyphae formation in a dose dependent manner. *C. albicans* cells treated with DMSO formed germ tubes at 2.5 h, hyphae at 6 h, biofilms at 24 h, while the cells treated with **4.7** or **4.15** did not form germ tubes and hyphae, and even at 24 h few cells formed short hyphae. It suggested that compound **4.7** and **4.15** inhibited biofilm formation through inhibiting the hyphae formation in *C. albicans*.

To evaluate whether **4.7** inhibited the biofilm formation in a time dependent manner, compound **4.7** (from 100 μM to 0.2 μM) was added before or at 0, 2, 4, 6, 8 and 24 h after *C. albicans* cells have been seeded. At 48 h after seeding, the amount of biofilm formation in the wells was determined using XTT assay and the IC_{50} were calculated (Figure 4.6). The effect of **7** on biofilm development was time dependent and it inhibited the biofilm formation at different stages. When **4.7** was added before seeding the cell, the IC_{50} was low. It suggested that **4.7** inhibited the adherence of *C. albicans*. And it even could inhibit the biofilm formation after the hyphae had formed, but **4.7** could not destroy pre-formed biofilms. Once hyphal formation had been initiated farnesol was not able to inhibit the biofilm formation[88].

Compounds **4.1-10, 4.13-16** were evaluated for their anticancer activity against MIA PACA-2 pancreatic cancer cells. Compound **4.8** and **4.6** exhibited weak anticancer activity with IC_{50} values of 8.21, 11.30 μ M respectively.

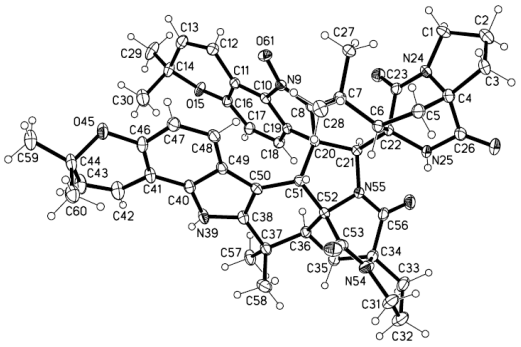

Figure 4.4. ORTEP structure for **4.7** generated from the X-ray diffraction data

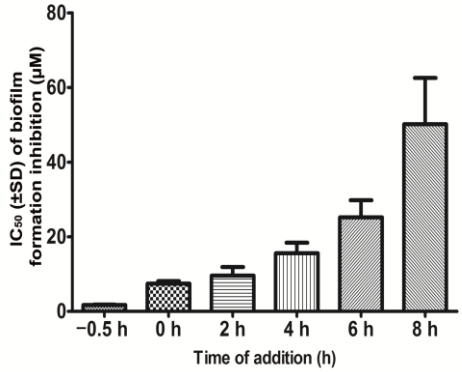

Figure 4.5. Time of addition study of compound **4.7**. **4.7** (from 100 μM to 0.2 μM) was added before (-0.5 h) or after (0, 2, 4, 6, 8 and 24 h) inoculation *C. albicans* DAY185 into 96-well microplates. At 48 h after seeding, the wells were washed by PBS twice and the amount of biofilm formation in the wells was determined by XTT assay. The 50% inhibitory concentration (IC_{50}) value for biofilm inhibition was calculated using GraphPad Prism software (GraphPad, La Jolla, CA, USA). All experiments were performed in triplicate on three replicate experiments in separate dose.

Table 4.1. ^{1}H (500 MHz) and ^{13}C (100 MHz) NMR data for **4.7** and **4.8**

	waikialoid A (4.7)		waikialoid B (4.8)	
position	**δ_C, mult.**	**δ_H (*J* in Hz)**	**δ_C, mult.**	**δ_H (*J* in Hz)**
1a	44.2, CH_2	3.29, td (7.2, 11.6)	43.8, CH_2	3.19, m
1b		3.47, m		3.41, m
2	24.8, CH_2	2.00, m	24.6, CH_2	1.98, m
				2.22, m
3a	29.4, CH_2	1.83, m	29.1, CH_2	1.81, m
3b		2.76, td (6.5, 12.8)		2.75, m
4	65.8, qC		65.5, qC	
5	28.6, CH_2	2.16, m	28.7, CH_2	2.12, m
				2.20, m
6	43.6, CH	3.00, m	43.0, CH	2.74, m
7	38.1, qC		38.0, qC	
8	151.3, qC		148.5, qC	
10	140.0, qC		140.9, qC	
11	113.0, qC		112.6, qC	
12	116.7, CH	7.56, d (10.5)	116.9, CH	7.34, d (10.3)
13	131.7, CH	5.52, d (10.5)	131.8, CH	5.54, d (10.2)
14	76.4, qC		76.3, qC	
16	153.6, qC		154.6, qC	
17	115.0, CH	6.44, d (8.3)	115.4, CH	6.98, d (8.4)
18	120.7, CH	6.89, d (8.3)	120.6, CH	6.70, d (8.3)
19	129.7, qC		124.0, qC	
20	61.8, qC		58.7, qC	
21	58.2, CH	5.55, s	59.7, CH	5.25, s
22	64.6, qC		64.8, qC	
23	167.1, qC		166.2, qC	
25-NH		7.44, s		7.78, s
26	174.2, qC		173.7, qC	
27	17.0, CH_3	1.68, s	18.2, CH_3	1.60, s
28	26.6, CH_3	1.83, s	27.5, CH_3	1.76, s
29	27.4, CH_3	1.15, s	27.6, CH_3	1.26, s
30	27.4, CH_3	1.28, s	28.9, CH_3	1.47, s
31a	44.6, CH_2	3.62, m	45.0, CH_2	3.73, m
31b		3.47, m		
32	25.0, CH_2	2.11, m	28.7, CH_2	2.12, m
				2.20, m
33a	29.9, CH_2	1.99, m	29.5, CH_2	2.09, m
33b		2.94, m		2.95, m
34	68.8, qC		68.5, qC	
35a	30.9, CH_2	2.02, m	31.7, CH_2	1.99
35b		2.42, dd (10.5, 12.5)		2.44, dd (12.8, 9.8)
36	46.9, CH	3.08, dd (10.3, 6.7)	51.2, CH	3.12, dd (17.5, 8.5)
37	34.2, qC		37.0, qC	
38	141.4, qC		146.8, qC	
39		7.58, s		
40	132.7, qC		139.1, qC	
41	104.6, qC		112.6, qC	
42	117.0, CH	6.40, d (9.3)	116.9, CH	7.48, d (10.3)
43	129.7, CH	5.58, d (9.8)	131.4, CH	5.61, d (10.3)
44	75.6, qC		76.3, qC	
46	148.8, qC		154.9, qC	
47	111.0, CH	6.64, d (8.3)	118.4, CH	6.78, d (8.3)
48	120.1, CH	7.14, d (8.8)	122.8, CH	7.06, d (8.3)
49	120.4, qC		124.0, qC	
50	103.5, qC		76.9, qC	
51	43.4, CH	5.14, s	52.2, CH	4.46, s
52	70.4, qC		71.1, qC	
53	168.8, qC		169.5, qC	
56	174.3, qC		174.0, qC	
57	22.4, CH_3	1.02, s	27.4, CH_3	1.22, s
58	27.5, CH_3	1.26, s	26.4, CH_3	1.74, s
59	27.4, CH_3	1.37, s	19.5, CH_3	1.25, s
60	27.4, CH_3	1.39, s	28.8, CH_3	1.47, s
62-OH				6.46, s

Table 4.2. ^{1}H (400 MHz) and ^{13}C (100 MHz) NMR data for **4.15** and **4.16** (CD_3OD)

	asperonol A (4.15)		**asperonol B (4.16)**	
position	**δ_C, mult.**	**δ_H (*J* in Hz)**	**δ_C mult.**	**δ_H (*J* in Hz)**
1	18.5, CH_3	1.78, d (6.8)	18.6, CH_3	1.77, d (6.7)
2	130.5, CH	5.73, qd (14.3, 6.8)	129.8, CH	5.66, m
3	133.2, CH	6.13, m	131.8, CH	6.06, m
4	133.6, CH	6.13, m	131.8, CH	6.06, m
5	131.7, CH	6.13, m	132.6, CH	6.06, m
6	133.0, CH	6.13, m	133.3, CH	6.06, m
7	136.4, CH	5.55, dd (13.7, 9.0)	138.8, CH	5.46, dd (13.7, 9.0)
8	46.0, CH	1.95, dddd (9.0, 11.3, 13.0, 3.8)	42.2, CH	2.11, m
9a	42.9, CH_2	1.67, ddd (11.3, 11.3, 11.6)	43.4, CH_2	1.16, ddd (11.6, 10, 11.6)
9b		2.08, ddddd (11.3, 3.8, 3.9, 2.2, 2.2)		1.88, dddd (12.1, 2.0, 3.5, 4.0)
10	69.7, CH	3.78, dddd (11.6, 3.9, 4.2, 11.4)	66.3, CH	3.95, m
11a	52.0, CH_2	2.45, ddd (11.2, 11.4, 2.5)	43.5, CH_2	1.39, ddd (12.0, 11.7, 2.7)
11b		2.65, ddd (11.2, 4.8, 2.5)		2.16, m
12	211.7, qC		72.8, CH	3.90, m
13	49.5, CH	2.25, dq (13.0, 6.5)	41.8, CH	1.28, m
14	12.6, CH_3	0.93, d (6.7)	16.8, CH_3	0.91, d (7.0)

Table 4.3. *Candida albicans* biofilm and growth inhibition by test compounds and farnesol

Compound	The IC_{50}[a] of biofilm inhibition (μM)	The MIC[b] of growth inhibition (μM)
	108.58 ±3.73	>200
4.2	93.49 ±3.62	>200
4.4	97.34 ±5.46	>200
4.5	55.24 ±2.43	>200
4.6	43.30 ±3.53	>200
4.7	1.40 ±0.24	>200
4.8	46.27 ±1.57	>200
4.15	32.36 ±1.98	>200
4.16	96.94 ±2.10	>200
farnesol	128.60 ±2.60	>200

[a]IC_{50} expressed as the concentration corresponding to 50% reduction of *candida* biofilm formation.
[b]MIC were defined as the lowest concentration causing prominent growth reduction (in ≥80% reduction in the metabolic activity).

4.3 Method and material

4.3.1 General Methods.

The melting points were obtained on a Mel-Temp capillary melting point apparatus. Optical rotations were measured on a Rudolph Research Autopol III automatic polarimeter. UV were measured on Hewlett Packard 8452A diode array spectrometer, CD spectra were measured on AVIV circular dichroism spectrometer model 202-01. IR was measured on A2 technology nano FTIR and Bruker vector 22 FTIR spectrometer respectively. NMR data were obtained on Varian VNMR spectrometers (400 and 500 MHz for ^{1}H, 100 and 125 MHz for ^{13}C) with broad band and triple resonance probes at $20 \pm 0.5\ ^{\circ}C$. Electrospray-ionization mass spectrometry data was performed on an Agilent 6538 high-mass-resolution QTOF mass spectrometer. Crude extract was separated on prepacked silica cartridges using Biotage Isolera chromatography system. HPLC separations were performed on a Shimadzu system using a SCL-10A VP system controller and Gemini 5 μm C_{18} column, (110 Å, 250 x 21.2 mm) with flow rates of 1 to 10 mL/min. X-ray diffraction data (**4.7**) were collected on a Bruker APEX II CCD system equipped with a Cu ImuS micro-focus source with Quazar MX optics (λ = 1.54178 Å), X-ray data (**4.15**) were collected using a diffractometer with a Bruker APEX ccd area detector and graphite-monochromated Mo K radiation (λ = 0.71073 Å). All solvents were of ACS grade or better.

4.3.2 Organism Collection, Identification, and Culture Methods.

A ~1 g portion of a soil sample collected near Waikiki Beach (Honolulu, Hawaii) in July, 2010 was placed in autoclaved H_2O (10 mL) and diluted 10- and 100-fold. Aliquots (300 μL) of the soil suspensions were spread over the surfaces of 10 cm diameter Petri plates containing czapek agar with chloramphenicol (50 mg/L). Plates

were maintained at 25 ℃ for four weeks. Colonies were selected from the plates and transferred to fresh Petri plates containing czapek agar with chloramphenicol (50 mg/L). This process was repeated for each isolate until pure fungal cultures were established. Pure isolates were transferred to new Petri plates containing czapek agar (without chloramphenicol) and after 2-3 weeks of incubation at 25 ℃, pieces of the agar with mycelia (~0.5 cm^2) were cut and placed in cryogenic storage tubes with sterile glycerol-H_2O (15:85). The tubes were then stored at -80 ℃ until the fungus was needed for scale-up studies. The fungus was identified as *Aspergillus* sp. based on sequence analysis of its large-ribosomal-subunit ITS1 region of the rDNA gene.

For the static preparative-scale grow-up, fungal mycelia and spores were inoculated into 50 mL potato-dextrose media and grown for one week with shaking (125 rpm). The cellular material was placed in a sterile Falcon tube and mixed by vortexing for several minutes to create a uniform fungal cell/spore suspension. Aliquots (500 µL) of the fungal suspension were used to inoculate 110 Erlenmeyer flasks (1 L) containing autoclaved media (0.1 g rice, 0.1 g oatmeal, 0.1 g cornmeal, 0.32 g nutrient broth, ~0.5 g vermiculite, and 50 mL of deionized H_2O). Culture vessels were maintained on the bench-top at 25 ℃ for 20 days.

For the shaking preparative-scale grow-up, aliquots (500 µL) of the fungal suspension were used to inoculate 12 L autoclaved media (potato-dextrose) in 20 L fermentator. The culture was fermented at 25 ℃ for 14 days.

4.3.3 Extraction and Isolation.

The static scale up culture was extracted by ethyl acetate overnight and the organic layer was removed under vacuum. The crude was separated by silica gel (mobile phase

50% to 100% hexane in methylene chloride for 8 min then 100% methylene chloride for 8 min. 0% to 20% methylene chloride in MeOH for 20 min gradient) and yielded four fractions. The fractions Fr.2 (500 mg) eluted under 18% methylene chloride in MeOH was subjected to preparative HPLC (mobile phase 40% to 100% MeOH in H_2O). Subfraction Fr. 11-14 were eluted under 80% MeOH and further purified by semi-prep HPLC provided compound **4.1** (1 mg), **4.2** (1.8 mg), **4.3** (20 mg), **4.4** (1 mg), **4.5** (1 mg), **4.6** (1 mg), **4.7** (4 mg) and compound **4.8** (1 mg), **4.11** (2 mg), **4.12** (0.3 mg), **4.13** (13 mg) and **4.14** (2.2 mg)

The liquid scale up culture was extracted with ethyl acetate with 1:1 ratio. The organic layer was recovered and the solvent was removed under vacuum. The resulting organic extract was separated by silica gel (mobile phase 50% to 100% hexane in methylene chloride for 8 min then 100% methylene chloride for 8 min, 0% to 20% methylene chloride in MeOH for 20 min gradient) using Isolera. Then the 15% methylene chloride in MeOH fraction (660 mg) was subjected to the silica gel separation under 0% to 50% methylene chloride in MeOH gradient and a fraction (320 mg) under 12% methylene chloride in MeOH was subjected to prep-HPLC (mobile phase 30% to 100% MeOH) yielded compound **4.9** (12 mg), **4.10** (10 mg), **4.15** (9.5 mg) and **16** (61.8 mg)

4.3.4 Waikialoid A (4.7)

Yellow, crystalline solid; mp: 174-176 ℃, $[\alpha]^{21}_{D}$ –12.0 (c 0. 15, MeOH); UV (MeOH) λ_{max} (log ε) 206 (4.99), 264 (4.75), 302 (4.39) nm; CD (MeOH; $\Delta\varepsilon$) 231(+29.2), 254 (-82.7), 311 (-14.4); IR ν_{max} 1680, 2980, 3120, 3320, 3490 cm^{-1}; ^{1}H and ^{13}C NMR data, see Table 4.1; HRESIMS *m/z* 875.4119 $[M+H]^+$ (calcd for $C_{52}H_{55}N_6O_7$, 875.4132).

4.3.5 Waikialoid B (4.8)

Yellow, amorphous solid; $[\alpha]^{21}_{D}$ 28.5 (c 0.035, MeOH); UV (MeOH) λ_{max} (log ε) 206 (4.74), 264 (4.29) nm; CD (MeOH; $\Delta\varepsilon$) 226 (+16.3), 243 (-18.2), 320 (-8.7); IR ν_{max} 1590, 2920, 2980, 3390 cm^{-1}; ^{1}H and ^{13}C NMR data, see Table 4.1; HRESIMS *m/z* 905.3827 $[M-H]^-$(calcd for $C_{52}H_{53}N_6O_9$, 905.3874).

4.3.6 Asperonol A (4.15)

White, crystalline solid; mp: 115-117 °C, $[\alpha]^{21}_{D}$ 11.4 (*c* 0.035, MeOH); UV (MeOH) λ_{max} (log ε) 202 (4.38), 266 (4.81) nm; CD (MeOH; $\Delta\varepsilon$) 266 (10.9), 293(-9.9) ; IR ν_{max} 1690, 2910, 2920, 2950, 2980, 3000, 3430 cm^{-1}; ^{1}H and ^{13}C NMR data, see Table 4.2; HRESIMS *m/z* 243.1378 (calcd for $C_{14}H_{20}O_2Na$, 243.1361).

4.3.7 Asperonol B (4.16)

White, amorphous solid; $[\alpha]^{21}_{D}$ 97.1 (*c* 0.175, MeOH); UV (MeOH) λ_{max} (log ε) 202 (4.43), 268 (3.93) nm; IR (KBr) ν_{max} 3400, 2910 cm^{-1}; ^{1}H and ^{13}C NMR data, see Table 4.2; HRESIMS *m/z* 221.1543 $[M-H]^-$ (calcd for $C_{14}H_{21}O_2$, 221.1542).

4.3.8 Preparation of Mosher Ester Derivatives 4.15a and 4.15b.

Compound **4.15** was transferred into two NMR tubes (0.25 mg each, 0.0011 mmol) and totally dried under vacuum then treated with dry pyridine (0.4 mL each) and 0.5uL (0.00267 mmol) of (*S*)-(+)-*R*-methoxy-*R*-(trifluoromethyl)-phenylacetyl chloride (MTPA chloride) and (*R*)-(-)-*R*-methoxy-*R*-(trifluoromethyl) phenylacetyl chloride reagent individually. The mixture was reacted at RT for 4 h. The completion of reaction was monitored by ^{1}H-NMR. Two derivatives **4.15a** and **4.15b** of compound **4.15** were obtained. The ^{1}H-NMR was collected in pyridine and the ^{1}H-^{1}H COSY spectrum was collected to help assign the proton.

4.3.9 S-MPTA ester of derivative (4.15a) of 4.15

^{1}H NMR (500 MHz, pyridine) δ = 6.12 - 6.36 (4H, m, H-3, H-4, H-5, H-6), 5.74 (1H, dd, *J* = 14.4 Hz, *J* = 7.1 Hz, H-2), 5.44 - 5.57 (2H, m, H-3, H-10), 3.11 (1H, d, *J* = 10.8 Hz, H-11), 2.79 (1H, t, *J* = 12.2 Hz, H-11), 2.20 - 2.34 (2H, m, H-8, H-13), 2.06 - 2.16 (1H, m, H-9),1.76 - 1.87 (1H, m, H-9), 1.69 (3H, d, *J* = 6.4 Hz, H-1), 1.06 (3H, d, *J* = 6.4 Hz, H-14).

4.3.10 R-MPTA ester of derivative (4.15b) of 4.15

^{1}H NMR (500MHz, pyridine) δ = 6.13 - 6.39 (4H, m, H-3, H-4, H-5, H-6), 5.69 - 5.80 (1H, m, H-2), 5.45 - 5.59 (2H, m, H-3, H-10), 3.04 (1H, ddd, *J* = 13.0 Hz, *J* = 5.1 Hz, *J* = 2.0 Hz, H-11), 2.65 (1H, t, *J* = 12.0 Hz, H-11), 2.32 (1H, dt, *J* = 12.2 Hz, *J* = 5.1 Hz, H-9), 2.25 (1H, dt, *J* = 12.1 Hz, *J* = 6.4 Hz, H-13), 2.13 (1H, tdd, *J* = 11.8 Hz, *J* = 8.7 Hz, *J* = 2.9 Hz, H-8), 1.86 - 1.96 (1H, m, H-9), 1.69 (3H, dd, *J* = 6.6 Hz, *J* = 1.2 Hz, H-1), 1.07 (3H, d, *J* = 6.4 Hz, H-14).

4.3.11 X-ray Crystal Structure Analysis.

X-ray diffraction data of **4.7** was collected on a Bruker APEX II CCD system equipped with a Cu ImuS micro-focus source with Quazar MX optics. A total of 67703 data were measured in the range $3.54 < \theta < 67.16°$ using and oscillation frames. The data were merged to form a set of 7859 independent data with R(int) = 0.0272 and a coverage of 97.6 %. A total of 635 parameters were refined against 21 restraints and 7859 data to give $wR(F^2) = 0.0845$ and S = 1.005 for weights of $w = 1/[\sigma^2 (F^2) + (0.0530\ P)^2 + 0.9000\ P]$, where $P = [Fo^2 + 2Fc^2] / 3$. The final R(F) was 0.0316 for the 7855 observed, [$F > 4\sigma(F)$]. The calculated minimum and maximum transmission coefficients (based on crystal size) are 0.6520 and 0.8418. The structure was solved by

direct methods and refined by full-matrix least-squares methods on F^2. The final anisotropic full-matrix least-squares refinement on F2 with 675 variables converged at R1 = 3.16%, for the observed data and wR2 = 8.45% for all data. The goodness-of-fit was 1.005. The largest shift/s.u. was 0.033 in the final refinement cycle. The final difference map had maxima and minima of 0.343 and -0.281 e/Å3. On the basis of the final model, the calculated density was 1.309 g/cm3 and F(000), 984 e-.

X-ray diffraction data of **4.15** was collected on a Bruker APEX ccd area detector and graphite-monochromated Mo K radiation (λ = 0.71073 Å). A total of 4287 data were measured in the range $2.36 < \theta < 22.99°$ using φ and ω oscillation frames, 1000 of which were independent R (int)=0.1127. The structure was solved by direct methods and refined by full-matrix least-squares methods on F2. Hydrogen atom positions were initially determined by geometry and refined by a riding model. Non-hydrogen atoms were refined with anisotropic displacement parameters.

4.3.12 Assay for Growth Inhibition and Biofilm Formation.

The effect of compounds on the growth of *C.albicans* DAY185 was tested using the method described in the guidelines of CLSI M27-A2 (NCCLS 2002). Biofilm assay was performed as described [89] with the following modifications. Strain *C. albicans* DAY185 were cultured in BHI medium (Brain Heart Infusion, Becton Dickinson and company, MD, USA) at 37 ℃ overnight and were washed with sterile PBS (phosphate-buffered saline, pH 7.4, EMD chemicals Inc., NJ, USA) and resuspended in RPMI 1640 medium (Sigma Chemical Corporation, MO, USA) buffered to pH 7.0 with MOPS (3-(N -morpholino) propanesulfonic acid, 0.165 M, Sigma). The compounds were prepared in DMSO (dimethyl sulfoxide, sigma) at a final concentration of 20 mM and were

serially diluted 2-fold from highest concentration of 200 μM with RPMI 1640 plus MOPS medium. Farnesol was used as positive control [90]. One hundred microliter of yeast suspension (2.5×103 cells/mL) containing the diluted compounds (from 200 μM to 6.25 μM) or DMSO (v/v 1%) was added in 96-well microplate (Costar 3370, Corning Incorporated, NY, USA). After 48 h of incubation at 37 °C, the viability of yeast was measured using the XTT (tetrazolium salt 2, 3-bis (2-methoxy-4-nitro-5-sulfophenyl)-5-(phenylamino)-carbonyl-2H-tetrazoliumhydroxide, Sigma) assay. In brief, yeast cells were treated with 0.1 mg/mL XTT at 37 °C for 1 h. The absorbance was taken at 490 nm using a microplate reader (Infinite M200, Tecan Group Ltd., Männedorf, Switzerland). The minimum inhibitory concentration (MIC) for growth was defined as the lowest antifungal concentrations that caused ≥80% reduction in the metabolic activity. To measure the biofilm formation, the medium was aspirated and wells were washed twice with sterile PBS to remove non-adherent cells, and 100 μL RPMI 1640 plus MOPS medium was added into each well. The prewashed biofilms were measured using XTT assay [91]. All experiments were performed in triplicate on three separate occasions. The 50% inhibitory concentration (IC_{50}) value for biofilm inhibition was calculated using GraphPad Prism software (GraphPad, La Jolla, CA, USA).

4.3.13 Hyphae Formation Assay.

C. albicans DAY185 was grown in BHI medium at 37 °C overnight. The cells were washed and suspended using PBS (pH 7.4, EMD). Cells were seeded in a 96-well plate at 1×106 cells/well and incubated at 37 °C for 1 h. Wells were washed twice with sterile PBS to remove non-adherent cells. μRPMI 1640 (Sigma) containing 2% glucose with compound **4.7** and **4.15**, farnesol, or DMSO (v/v 1%) was added into each well

and the plate were incubated at 37 ℃ for 24 h. Farnesol was used as positive control [90].The yeast cells were observed under a phase contrast microscope at 2.5, 6 and 24 h [89].

4.3.14 Time of addition assay.

Based on the biofilm formation assay, **4.7** (from 100 μM to 0.2 μM) was added before or at 0, 2, 4, 6, 8 and 24 h after seeding to *C. albicans* DAY185 culture in a 96-well microplate. At 48 h after seeding, the wells were washed by PBS twice and the amount of biofilm formation in the wells was determined using XTT assay [92]. The 50% inhibitory concentration (IC_{50}) value for biofilm inhibition was calculated using GraphPad Prism software (GraphPad, La Jolla, CA, USA). All experiments were performed in triplicate on three separate occasions.

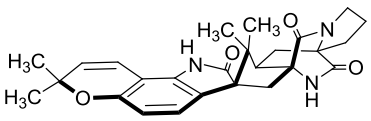

4.1

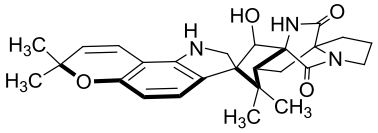

4.2

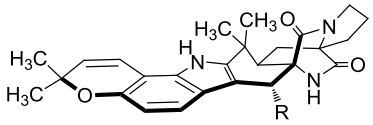

4.3 R = OCH_3
4.4 R = OH

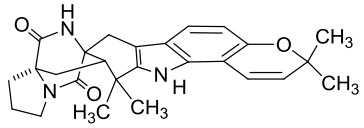

4.5

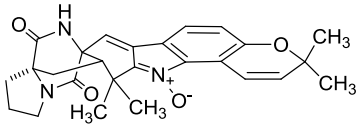

4.6

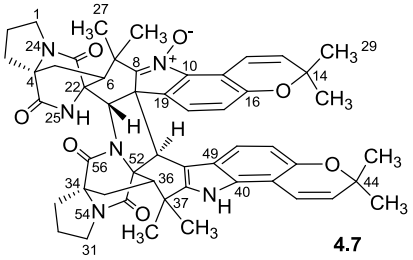

4.7

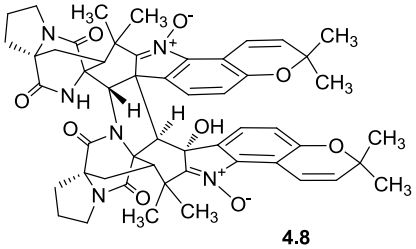

4.8

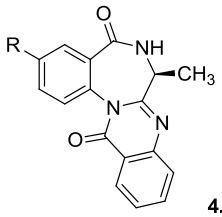

4.9 R = H
4.10 R = OH

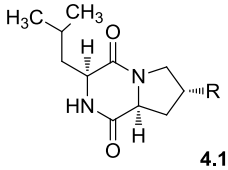

4.11 R = H
4.12 R = OH

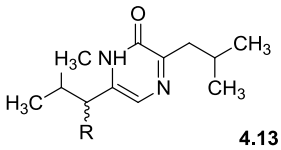

4.13 R = H
4.14 R = OH

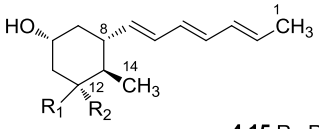

4.15 R_1, R_2 = O
4.16 R_1 = H R_2 = OH

Chapter 5 Fungal biofilm inhibitors from a human oral microbiome-derived bacterium

This chapter is adapted from publication that is currently submitted.

5.1 Introduction

An average adult human mouth has a surface area of only ~215 cm^2,[93] yet it is home to amazingly large and diversified assemblage of microbial species.[94] It is estimated that in excess of 1.9×10^4 bacterial phylotypes occupy the mouth[95] forming a complex community that is dominated by Firmicutes, Proteobacteria, Bacteroidetes, Actinobacteria, and Fusobacteria.[96] Certain fungi including *Candida* spp. are also resident members of the mouth, although these microbes tend to be numerically less abundant in healthy adults.[97]

Streptococcus mutans is one of the perennial members of the oral microbial community.[98] Substantial interest in this microbe has evolved due in part to its ubiquity, as well as evidence linking *S. mutans* to the development of dental caries.[99] However, recent studies using cultivation-dependent[100] and culture-independent[101] screening techniques of caries-associated microbial assemblages have called some of these assertions into question. Regardless, *S. mutans* is an important component of the oral microbial community due in part to its assorted interactions with other bacteria,[99c] fungi,[102] and mammalian cells.[103]

Although there is an abundance of published reports illustrating the extent to which bacteria and fungi are capable of interacting with other microorganisms within their vicinity,[104] the majority of biomolecules responsible for influencing these biological processes remain unknown. Small-molecule signals are thought to play vital

roles in the intraspecies and interspecies interactions involving microbiome bacteria and humans[105] and our group has taken an active role pursuing the identities of these chemical agents. We had previously reported that *S. mutans* UA159 generated the unique secondary metabolite mutanobactin A (**5.1**),[106] which inhibited the morphological switch of pathogenic *Candida albicans* from a yeast to a filamentous morphology.[107] Several questions emerged from that study that included 1) what is the absolute configuration of all the stereogenic centers in **5.1**, 2) what are the biosynthetic precursors that contribute to building this polyketide-non-ribosomal-peptide molecule, and 3) what are the structures of the analogues of **5.1**? In this study, we have addressed each of these issues, as well as examined the biological impact of mutanobactins on the ability of pathogenic *C. albicans* to form biofilms. The formation of biofilms by *Candida* spp. is a topic of significant medical relevance[108] because biofilms serve as reservoirs for antibiotic-resistant persister cells, which are key factors in the development of therapeutically-recalcitrant and life-threating yeast infections.[109]

5.2 Results and discussion

A sample taken from the ethyl-acetate-soluble material obtained from partitioning 40 L of *S. mutans* UA159 culture was analyzed by reversed-phase LC-ESIMS (positive mode). This revealed a group of three new peaks with retention times and mass-to-charge ratios similar to **5.1** (*m/z* 743 $[M + Na]^+$, t_R 24.6 min). The three compounds exhibited base peaks at *m/z* 757 $[M + Na]^+$ (t_R 25.8 min), 743 $[M + Na]^+$ (t_R 24.6 min), and 721 $[M + H]^+$ (t_R 24.9 min). In light of the substantial similarity between the LC-ESIMS properties of these compounds and **5.1**, we suspected that these peaks represented new mutanobactins. Subsequently, these metabolites were targeted for

purification and structure characterization (repeated HP20SS column chromatography by changing column size and elute gradient and reversed-phase HPLC).

HRESIMS analysis of mutanobactin B (**5.2**) provided a pseudomolecular ion with *m/z* 757.4298 that corresponded to a molecular formula of $C_{37}H_{62}N_6O_7SNa$ ($[M + Na]^+$, calcd 757.4298). Compared to **5.1**, this indicated that compound **5.2** possessed one additional carbon and two additional hydrogen atoms. Although the ^1H NMR data for **5.2** (Table 5.1) were nearly superimposable with those for **5.1**, we observed a subtle shift in the resonances appearing in the highfield region (~1.0 ppm) of the spectrum (*note:* upon further scrutiny, we have found it necessary to reassign some of the carbon and proton resonances in the hydrocarbon tail of **5.1**; refer to Table A4, for details of these changes). In addition, ^{13}C NMR (Table 5.1) revealed a new carbon resonance at δ_C 10.0 (C-18). Using ^1H-^1H COSY and ^1H-^1H TOCSY, we traced the spin system originating from the hydrogens (δ_H 0.78, H-18) attached to C-18 to a series of protons at δ_H 8.01 (N*H*-15) 3.75 (H-15), 2.19 (H-16), 0.79 (H-19), 1.35 (H-17a), and 1.02 (H-17b) that were deduced to be part of an Ile residue (Figure. 5.1). This was supported the ^1H-^{13}C HSQC and ^1H-^{13}C HMBC NMR data, which confirmed that the Val in **5.1** was replaced by an Ile in **5.2** (Figure. 5.1). Further examination revealed that all other portions of the planar structure of **5.2** remained unchanged relative to compound **5.1**.

Mutanobactin C (**5.3**) afforded a pseudomolecular ion at *m/z* 743.4138 that corresponded to a molecular formula of $C_{36}H_{60}N_6O_7SNa$ ($[M+Na]^+$, calcd 743.4142). In addition to sharing the same molecular formula as **5.1**, the ^{13}C NMR data for **5.1** and **5.3** (Table 5.1) were found to be remarkably similar. Analysis of the ^1H-^{13}C HSQC and ^1H-^{13}C HMBC data obtained for **5. 3** enabled us to determine that the new metabolite

possessed the same planar structure as **5.1**. But upon closer scrutiny, several subtle changes in chemical shifts for protons H-21a/b (Δ = -0.20 and 0.24 ppm), H-23a/b (Δ = -0.38 and -0.07 ppm), H-24 (Δ = -0.19 ppm), and H-25(Δ = -0.19 ppm) were observed (Table 5.1). Thus, it was concluded that **5.3** was a diastereomer of **5.1** with the configuration(s) of one or more stereogenic carbons having been altered in the vicinity of the aforementioned protons.

High resolution ESIMS of mutanobactin D (**5.4**) revealed that this metabolite possessed a molecular formula of $C_{37}H_{64}N_6O_8Na$ ($[M+Na]^+$, *m/z* of 743.4681, calcd 743.4683). The absence of the sulfur atom signified that the 1,4-thiazepan-5-one system in **5.1**-**5.3** was not present in **5.4**. The loss of this substructure was supported by analysis of the ^1H and ^{13}C NMR spectra (and later verified by 2D ^1H-^1H TOCSY, ^1H-^{13}C HSQC, and ^1H-^{13}C HMBC experiments), which showed that key resonances attributable to the Ile, Ala, Pro, and Val residues and hydrocarbon tail remained intact, but the 1,4-thiazepan-5-system was missing. Instead, a new spin set consisting of protons at δ_H 8.46 to 3.80, 1.52 and 0.85 was detected by TOCSY leading to the identification of an α-aminobutyric acid (Aaba) residue in **5.4**. A second spin set with protons at δ_H 2.65, 3.98, 3.38, and 4.70 (exchangeable) was identified that was attributed to a hydroxyglycine residue. HMBC data indicated that one of the hydroxyglycine carbons (δ_C 66.7, C-25) was attached to the C-26 methine (δ_C 61.7), which served as the junction between the C-27 (δ_C 166.3) and C-28 (δ_C 204.5) carbonyls (Figure. 5.1). Protons (δ_H 2.65, H-24a and 3.38, H-24b) attached to the other hydroxyglycine carbon (δ_C 42.1, C-24) exhibited $^3J_{H\text{-}C}$ coupling with the carbonyl of the adjacent Aaba residue (Figure. 5.1). In addition, the proton from the Aaba residue

methine (δ_H 3.80, H-20) coupled ($^3J_{H\text{-}C}$) with the Ala carbonyl (Figure. 5.1). Therefore, the planar structure of **5.4** was determined to comprise a new 20-membered macrocycle.

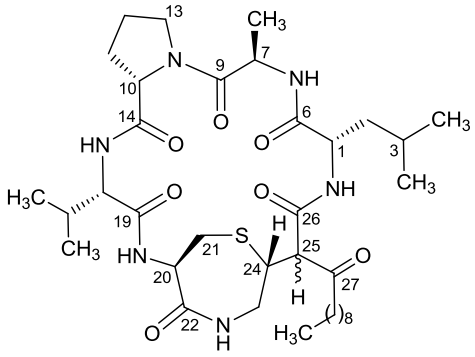

5.1 (25*R*)
5.3 (25*S*)

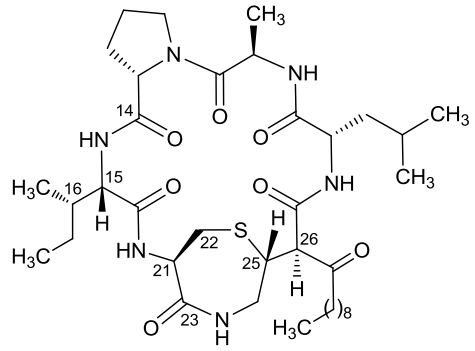

5.2

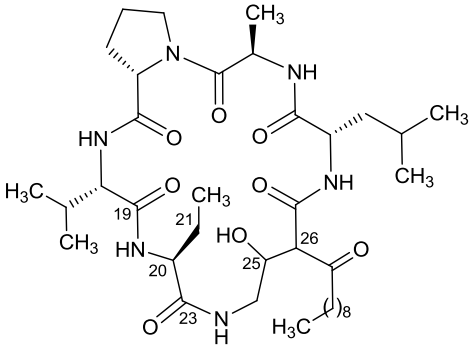

5.4

Table 5.1. ^{1}H and ^{13}C NMR data for **5.2-5.4** (500 and 100 MHz in DMSO-d_6)

position	5.2		5.3		5.4	
	δ_C	δ_H, mult. (*J* in Hz)	δ_C	δ_H, mult. (*J* in Hz)	δ_C	δ_H, mult. (*J* in Hz)
1	50.3, CH	4.43 ddd (3.6, 9.3, 11.0)	50.6, CH	4.43, m	52.3, CH	4.21, m
2a	40.4, CH_2	1.44, m	40.2, CH_2	1.59, m	40.5, CH_2	1.45, m
2b		1.82, ddd (3.6, 10.5, 13.9)		1.52, m		1.71
3	24.2, CH	1.60, m	24.4, CH	1.60, m	24.5, CH	1.43, m
4	20.8, CH_3	0.82, d (6.6)	21.1, CH_3	0.84, d (6.5)	21.6, CH_3	0.91, d (6.4)
5	23.5, CH_3	0.92, d (6.4)	23.1, CH_3	0.92,d (6.5)	23.6, CH_3	0.81, d (6.4)
6	170.5, C		170.2, C		172.0, C	
7	48.1, CH	4.51, q (6.7)	47.5, CH	4.46, m	47.5, CH	4.25, m
8	17.6, CH_3	1.17, d (6.7)	16.7, CH_3	1.20, d (6.8)	15.1, CH_3	1.20, d (6.9)
9	170.0, C		171.6, C		171.1, C	
10	61.2, CH	4.11, dd (3.4, 8.7)	61.2, CH	4.17, dd (3.7, 8.7)	60.0, CH	4.35, brd (7.0)
11a	29.6, CH_2	1.70, m	29.6, CH_2	1.87, m	29.4, CH_2	1.98, m
11b		2.13, m		2.12, m		2.06, m
12a	24.5, CH_2	1.90, m	24.2, CH_2	1.90, m; 1.78, m	23.6, CH_2	1.76, m
12b						1.98, m
13a	46.8, CH_2	3.42, m	47.2, CH_2	3.51, m	46.5, CH_2	3.54, m
13b		3.68, m		3.78, m		3.91, brt (8.9)
14	171.6, C		171.1, C		170.5, C	
15	56.7, CH	3.75, dd (8.7, 10.0)	58.8, CH	3.92, t (6.6, 7.0)	58.2, CH	4.05, brt (9.9)
16	31.5, CH	2.19, m	29.2, CH	2.21, m	29.5, CH	2.13, m
17a	21.4, CH_2	1.35, m	19.7, CH_3	0.92, d (6.7)	19.8, CH_3	0.90, d (6.5)
17b		1.02, m				
18	10.0, CH_3	0.78, m	18.5, CH_3	0.93, d (6.7)	19.4, CH_3	0.97, d (6.6)
19	16.2, CH_3	0.79, d (6.8)	170.1, C		172.0, C	
20	168.9, C		56.3, CH	4.46, m	56.4, CH	3.80, td (2.4, 7.4)
21a	52.3, CH	4.85, m	26.2, CH_2	2.43, m	23.8, CH_2	1.52, m
21b				2.95, dd (9.9, 15.3)		
22a	28.4, CH_2	2.21, brd 16.3	169.8, C		10.3, CH_3	0.85, t (7.4)
22b		3.19, dd (8.2, 16.3)				
23a	170.3, C		40.7, CH_2	3.17, m	172.5, C	
23b				3.35, m		
24a	43.8, CH_2	2.76, m	41.1, CH	3.44, m	42.1, CH_2	2.65, brd (13.7)
24b		3.28, m				3.38, m
25	40.9, CH	3.25, m	62.8, CH	4.06, d (8.9)	66.7, CH	4.18, m
26	61.7, CH	3.88, d (9.4)	166.3, C		61.7, CH	3.98, d (10.4)
27	167.7, C		202.7, C		166.3, C	
28a	203.8, C		40.8, CH_2	2.37, m	204.5, C	
28b				2.43, m		
29a	41.3, CH_2	2.33, m	23.0, CH_2	1.45, m	40.1, CH_2	2.23, m
29b		2.44, dd (8.4, 11.4)				2.35, m
30	23.0, CH_2	1.45, m	28.4, CH_2	1.17, m	22.5, CH_2	1.36, m
31	28.5, CH_2	1.20, m	28.7, CH_2	1.22, m	28.4, CH_2	1.16, m
32	28.6, CH_2	1.22, m	28.9, CH_2	1.22, m	28.6, CH_2	1.20, m
33	28.9, CH_2	1.22, m	28.7, CH_2	1.22, m	29.0, CH_2	1.21, m
34	28.7, CH_2	1.23, m	31.3, CH_2	1.22, m	28.7, CH_2	1.22, m
35	31.3, CH_2	1.23, m	22.1, CH_2	1.24, m	31.2, CH_2	1.22, m
36	22.1, CH_2	1.23, m	14.0, CH_3	0.85, t (6.8)	22.1, CH_2	1.22, m
37	14.0, CH_3	0.85, t (6.8)			13.9, CH_3	0.84, t (6.8)
1-NH		8.55, d (9.1)		8.70. brs		8.12, d (4.5)
7-NH		7.74, d (6.6)		7.91, d (4.9)		9.05, brs
15-NH		8.01, d (8.3)		7.35, brs		7.63, d (9.3)
20-NH				7.74, d (6.3)		8.46, d (2.6)
21-NH		7.20, d (7.6)				
23-NH				7.69, m		
24-NH		7.93, dd (6.2, 8.2)				7.81, dd (2.5, 14.1)
25-OH						4.70, brs

With the planar structures of metabolites **5.2**-**5.4** established, we proceeded to investigate the absolute configuration of each compound. Several approaches were used including biogenic consideration,[106] Marfey's method,[110] and ^{1}H-^{1}H NOESY. In addition, insights gained from our structure analyses of **5.2**-**5.4** provided a good opportunity to re-evaluate the yet undefined configuration of stereogenic centers C-20, C-24, and C-25 in **5.1**.[107] Numerous attempts to produce suitable crystals of **5.1**-**5.4** for X-ray analysis failed with gels or amorphous precipitates consistently formed.

Marfey's reagent, 1-fluoro-2,4-dinitrophenyl-5-L-alanine amide reacts with the optical isomers of amino acids to form diastereomers which can be separated by HPLC (Schme 5.1). The hydrolysates of **5.2**, **5.3**, and **5.4** were analyzed by HPLC and the products compared to derivatized amino acid standards for the D and L forms of Aaba, Ala, Ile, Leu, Pro, and Val. This enabled us to confirm that compound **5.2** contained L-Leu, D-Ala, L-Pro, and L-Ile residues; compound **5.3** contained L-Leu, D-Ala, L-Pro, and L-Val residues; and compound **5.4** contained L-Leu, D-Ala, L-Pro, L-Val, and L-Aaba residues.

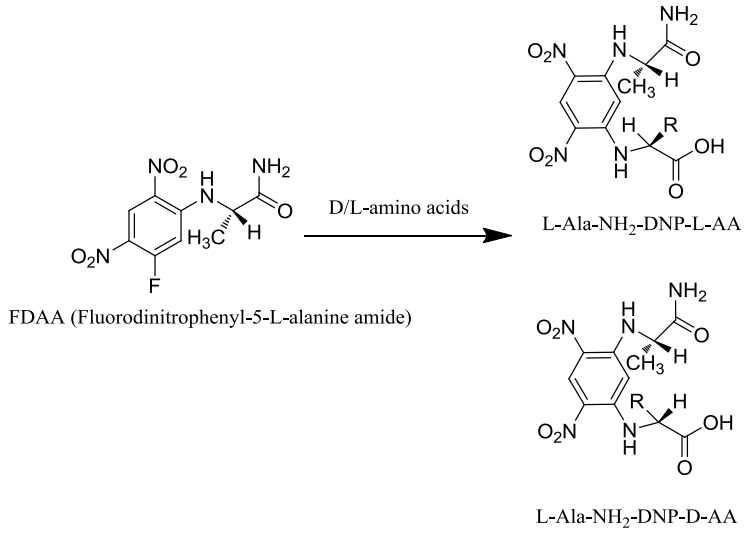

Scheme 5.1. Reaction of DL-amino acids with Marfey's reagent.

During our previous investigation of **5.1**, we had performed a 2D ^{1}H-^{1}H NOESY experiment and this had provided us with a substantial number of NOE cross peaks. However, the lack of additional mutanobactin congeners at that time prohibited us from confidently assigning the absolute configuration of C-22, C-24, and C-25. Now with diastereomer **5.3** in hand, determining the absolute configuration of each stereogenic carbon became relatively straightforward. We identified three key elements that made this analysis possible: first, both **5.1** and **5.3** exhibited large (*anti* configuration) vicinal couplings between H-24 and H-25 (J = 9.8 and J = 8.9 Hz, respectively); second, the *anti* relationships between H-24 and H-25 were further substantiated by the absence of NOE cross peaks between these protons in **5.1** and **5.3**; and third, compounds **5.1** and **5.3** exhibited dramatically different *trans*-annular NOE cross peaks between their respective 1,4-thiazepan-5-one rings and the amide protons of the D-Ala residues. In the case of compound **5.1**, both H-21a and H-21b exhibited *trans*-annular NOE cross peaks with the D-Ala N*H* (Figure. 5.2). In contrast, compound **5.3** H-23a and H-23b produced strong NOE correlations to the D-Ala N*H* (Figure. 2). These data provided compelling evidence that the 1,4-thiazepan-5-one system was rotated roughly 180 ^{o} in **5.3** relative **5.1**. Accordingly, we determined that **5.1** possessed a 24*R**,25*R** relative configuration and **3** has a 24*R**,25*S** relative configuration.

Further support for this hypothesis was obtained via computer-generated lowest energy calculations performed on **5.1** and **5.3** using a MM2 force field parameter set (Chembio 3D). In addition to delivering *in silico* validation of the configuration assignments, we observed striking differences in the predicted orientations of the Cys residue α-protons in **5.1** and **5.3** (Figure. 5.2). This was supported by spectroscopic data

in which Cys H-20 of **1** produced NOE cross peaks with the 1,4-thiazepan-5-one ring protons H-23 and H-25, as well as the L-Val H-17/H-18. In contrast, inversion of the 1,4-thiazepan-5-one ring in **3** resulted in Cys H-20 adopting a pseudoequitorial orientation (Figure. 5.2). This led to the absence of NOE cross peaks between Cys H-20 and H-23/H-25. Taking into account the configuration assignments for C-24/C-25, the NOE cross peaks involving the C-20 methine protons, NOESY data between protons within the 1,4-thiazepan-5-one ring and the surrounding amino acid residues, as well as the *trans*-annular NOE correlations (Figure. 5.2), we refined the absolute configuration of **5.1** as 1*S*,7*R*,10*S*,15*S*,20*R*, 24*R*,25*R* and its C-25 epimer **5.3** as 1*S*,7*R*,10*S*,15*S*,20*R*, 24*R*,25*S*.

Metabolite **5.2** provided 2D ^{1}H-^{1}H NOESY data that were nearly identical those afforded by **5.1**. In light of the significant similarities between these compounds, **5.2** was deduced as having a 1*S*,7*R*,10*S*,15*S*,16*S*,21*R*, 25*R*,26*R* absolute configuration. Data obtained from NOESY and long-range $^{2\text{-}3}J_{\text{H-C}}$ experiments with **5.4** proved inconclusive for discerning the absolute configuration of C-25 and C-26. However, results from the Marfey's experiment (*vide supra*) enabled us to deduce the absolute configuration of the other stereogenic carbons as 1*S*,7*R*,10*S*,15*S*,20*S*.

Previously, we had predicted that the mutanobactins were derived from a hybrid polyketide-nonribosomal-peptide-synthetase pathway.[106] Upon examination of the biosynthetic gene cluster, it was proposed that seven amino acids would be incorporated into the mutanobactins; however, evidence gathered from the chemical analysis of **5.1** revealed that only six amino acid residues were readily apparent.[107] We speculated that C-26 in **5.1** and carbon atoms in the immediate vicinity (i.e., C-24, C-25, and/or C-26)

may have been derived from the incorporation and subsequent rearrangement of Gly and Asp residues. In order to test this theory, feeding studies were performed utilizing ^{13}C and ^{15}N enriched (>98%) Gly and Asp. We observed that cultures dosed with [1,2-^{13}C,^{15}N]Gly showed significant isotope incorporation at N-23, C-23, and C24 (Table 5.2), whereas none of the atoms were labeled when [1,2,3,4-^{13}C,^{15}N]Asp was added (data not shown). These data indicated that Gly is fully integrated into the mutanobactin skeleton while Asp is either not incorporated or latter excised during the biosynthetic process (Figure. 5.3). Despite these new insights, the origins of C-25 and C-26 in **5.1** remained unknown. Suspecting that the polyketide synthase could contribute one or both of these carbon atoms, we conducted separate feeding experiments using [1-^{13}C]acetate and [2-^{13}C]acetate. Addition of [1-^{13}C]acetate to the culture medium resulted in substantial enhancement of the NMR signals for C-26, C-27, C-29, C-31, C-33, and C-35 in compound **5.1** (Table 5.2 and Figure.5.3). In contrast, incorporation of [2-^{13}C]acetate to the growth medium led to enhancement of the NMR resonances for C-25, C-28, C-30, C-32, and C-34 in compound **5.1** (Table 5.2 and Figure. 5.3). Therefore, head-to-tail condensation of six acetate units is believed to be responsible for generating these 12 carbon atoms in the mutanobactin skeleton. We propose that the mutanobactins are generated via the sequential addition of L-Leu, L-Ala (later epimerized), L-Pro, L-Val (or L-Ile), L-Cys (or L-Aaba), and L-Gly to the polyketide chain. In view of the structure of metabolite **5.4**, we suspect that closure of the 20-member macrocycle precedes formation of the 1,4-thiazepan-5-one ring. This process may occur by deprotonation of the β-keto amide methylene (C-25, pK_a ~10.8 based on ChemAxon pK_a predictor) to form an enolate anion, which would attack the

Gly thioester carbonyl and release the metabolite from the synthetase. Next, formation of the 1,4-thiazepan-5-one ring could proceed *via* either reduction of the C-24 carbonyl followed by nucleophilic attack of the thiol on the secondary alcohol or direct attack of the thiol on the C-24 carbonyl. While these mechanisms present certain challenges and should be regarded with caution, both help illustrate how inflection of the 1,4-thiazepan-5-one ring systems in **5.1** and **5.3** may arise.

Table 5.2. Enrichment ratios and ^{13}C-^{13}C, ^{15}N-^{13}C couplings (J(C, C)) for isotope feeding experiments with **5.1**

position	δ_C [a]	[1-^{13}C]acetate ER [b]	[2-^{13}C]acetate ER	[^{15}N,$^{13}C_2$]glycine ^1J (C-C, N-C) (Hz)
22	170.4	1.6	1.0	
23	43.7	1.5	1.8	**35.0, 9.5**
24	41.0	1.3	1.1	**35.0**
25	61.7	1.2	**25.6**	
26	167.7	**15.7** [c]	0.7	
27	203.8	**17.1**	0.7	
28	41.4	1.0	**20.2**	
29	23.1	**15.3**	1.0	
30	28.5	1.3	**21.5**	
31	28.7	**15.4**	1.0	
32	28.9	1.0	**19.6**	
33	28.8	**13.9**	0.8	
34	31.3	0.7	**15.6**	
35	22.1	**13.0**	0.7	
36	14.0	2.2	**50.4**	

[a] The DMSO signal (49.5ppm) was used as a reference
[b] Enrichment ratios (ER) were calculated by comparison to signals from the unlabeled compound
[c] Resonances in bold were determined as having been enriched

We had previously shown that the *S. mutans* mutant lacking the mutanobactin gene cluster was unable to block filament formation of pathogenic *Candida albicans* in a co-culture system.[107] Furthermore, addition of **5.1** to *C. albicans* under filament promoting conditions suppressed the formation of mycelia. Although the linkage between filament formation and pathogenesis is under debate,[111] it is well documented that it is one of several essential steps in biofilm formation.[112] In clinical settings, yeast

are often encountered in polymicrobial biofilm communities.[113] While ensconced in biofilms, pathogens such as *C. albicans* have diminished susceptibilities to antibiotics and are challenging targets for *in vivo* elimination.[114] We tested **5.1**-**5.4** in an assay designed to determine if the mutanobactins could inhibit *C. albicans* biofilm formation. Compound **5.4** was found to be the most potent inhibitor of biofilm formation with an IC_{50} value of 5.3 μM. In comparison, farnesol, a well-known and widely tested inhibitor of *C. albicans* biofilm formation,[115] had a much higher IC_{50} value of 1.4×10^2 μM. Compounds **5.1** and **5.2** showed reduced activities with IC_{50} values of 3.4×10 and 9.1×10 μM, respectively. Metabolite **3** showed no activity at concentrations up to 200 μM. This is rather remarkable since the only variation between compounds **5.1** and **5.3** is the substitution of a L-Ile residue in **5.3** for the L-Val in **5.1**. It is noteworthy that none of the compounds reduced the viability of *C. albicans* (tested over a range from 6.25 to 200 μM), which indicates that the mutanobactins may selectively exert their effects against a biofilm-formation-specific target (e.g., filament formation).

Table 5.3. Biofilm formation inhibition and MIC values of metabolites **1**-**4** and farnesol against *C.albicans* Day185

Compound	**Biofilm formation inhibition (IC_{50} ± SD in μM)[a]**	**Growth inhibition (MIC in μM)**
5.1	$3.4\times10\pm1.3$	>200
5.2	$9.1\times10\pm1.6$	>200
5.3	>200	>200
5.4	5.3 ± 0.9	>200
Farnesol	$1.4\times10^2\pm1.2$	>200

[a]IC_{50} expressed as the concentration of compound required to cause a 50% reduction in biofilm formation

5.3 Conclusions

The human microbiome contains an abundance of taxonomically diverse bacteria, a number of which have the potential to generate secondary metabolites. It is reasonable

to expect that many of these microbial-derived compounds will have evolved unique biological functions that make them important factors for maintaining our wellbeing. The mutanobactins provide a foretaste of the intriguing roles and potential therapeutic applications of compounds biosynthesized by bacteria living in and on the human body.

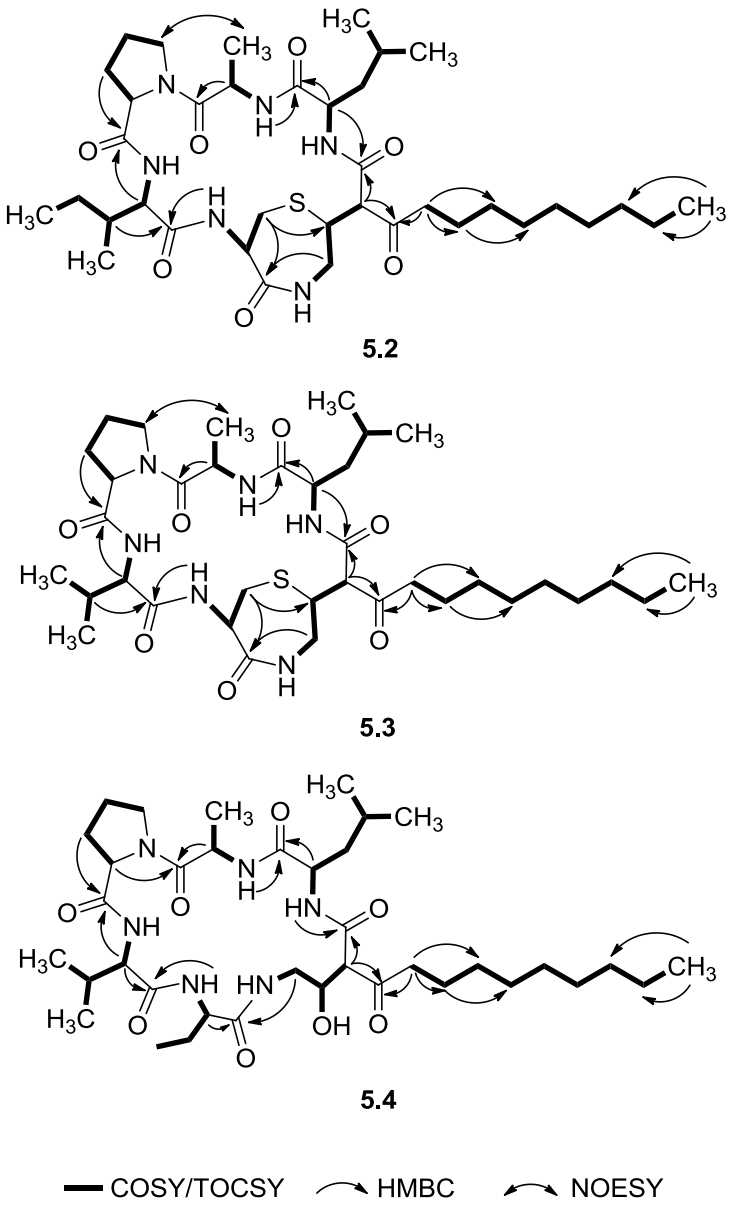

Figure 5.1. Important ^{1}H-^{1}H COSY, ^{1}H-^{1}H TOCSY, ^{1}H-^{13}C HMBC, and ^{1}H-^{1}H NOESY correlations used to deduce the structures of mutanobactin B-D (**5.2-5.4**).

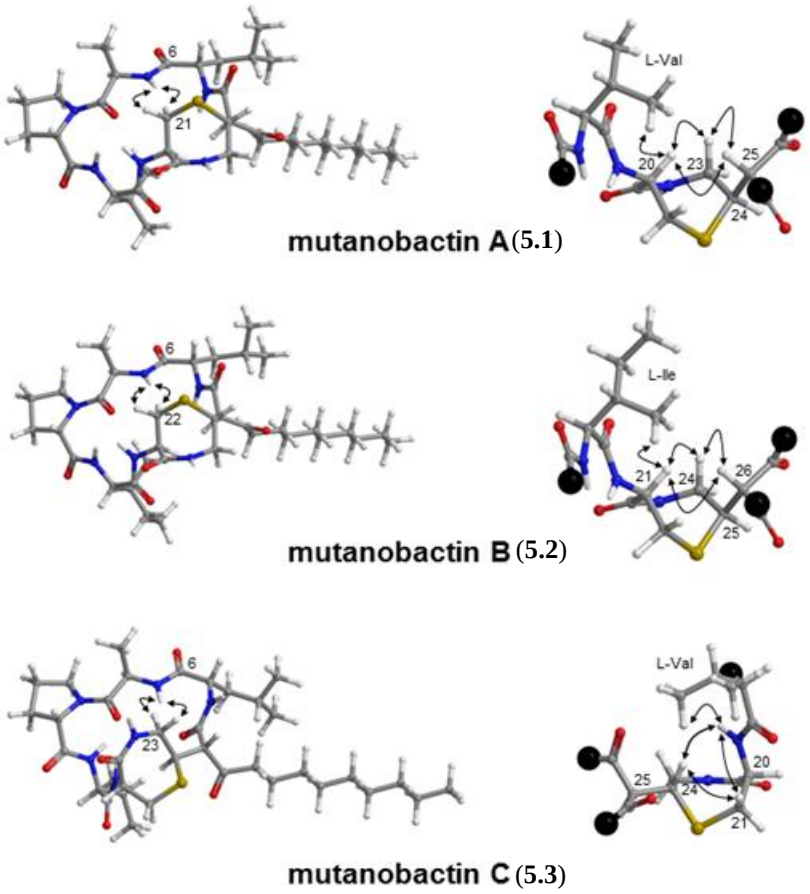

Figure 5.2. Key ^{1}H-^{1}H NOESY correlations observed for **5.1**-**5.3**. For each compound, *trans*-annular NOE correlations from the 1,4-thiazepan-5-one rings to the amid D-Ala 7-N*H* are shown on the left side of the figure. On the right, close-up views are shown of NOE correlations involving other 1,4-thiazepan-5-one ring protons. The black spheres represent places that the molecule was truncated for this figure.

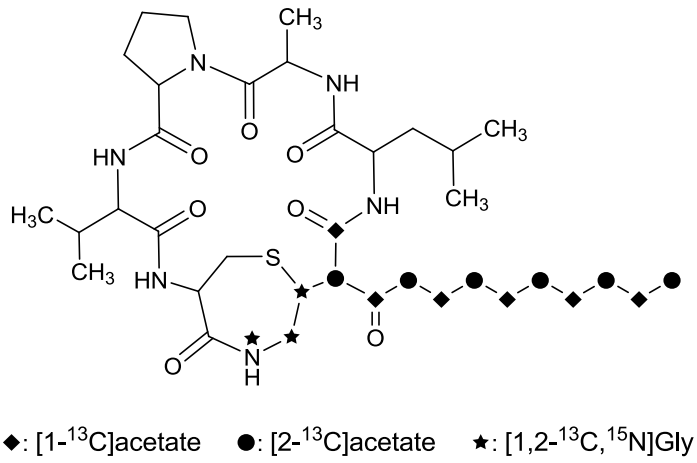

Figure 5.3. Incorporation of isotopically labeled [1-^{13}C]acetate, [2-^{13}C]acetate, and [1,2-^{13}C,^{15}N]glycine in mutanobactin A (**5.1**).

5.4 Experimental section

5.4.1 General experimental procedures

Optical rotations were measured on a Rudolph Research Autopol III automatic polarimeter. UV data were measured on Hewlett Packard 8452A diode array spectrophotometer, IR was measured on A2 Technology Nano FTIR. NMR data were obtained on Varian VNMR spectrometers (400 and 500 MHz for ^{1}H, 100 and 125 MHz for ^{13}C) with broad band and triple resonance probes at 20 ± 0.5 °C. LC-ESIMS data were collected using a Thermo-Finnigan Surveyor LC system and a Finnigan LCQ Deca mass analyzer. HRESIMS data were obtained by electrospray ionization employing an Agilent 6538 UHD Accurate-Mass Quadrupole TOF mass analyzer. Flash chromatography was performed on a Biotage Isolera One using a 50 g C18 column with a flow rate of 50 mL/min. HPLC separations were performed on a Shimadzu system using a SCL-10A VP system controller and Gemini 5 µm C_{18} column, (110Å, 250 x 21.2 mm) with flow rates of 1 to 10 mL/min. All solvents were of ACS grade or better.

5.4.2 Fermentation, extraction, and purification of mutanobactins

Streptococcus mutans UA159 was prepared by inoculating 40 L of brain-heart infusion broth with 100 mL of an overnight stationary *S. mutans* UA159 culture. The culture was incubated under microoxic conditions at 37 ℃ for 96 h. The culture was extracted three times with equal volumes of ethyl acetate, which was evaporated in vacuo to generate the *S. mutans* UA159 extract. The crude extract (35 g) was separated into five fractions by HP20SS column chromatography (step gradient of 30%, 50%, 70%, 90%, and 100% MeOH in H_2O). Fractions Fr.4 (824 mg) and Fr.5 (156 mg) were combined (named Fr.7) and further separated into seven subfractions by preparative reversed-phase HPLC (eluted with linear gradient of 20% to 100% MeOH in H_2O, 10.0 mL min-1). Subfraction Fr.7-5 was subjected to repeated semi-preparative reversed-phase HPLC (isocratic 85% MeOH in H_2O followed by 70% CH_3CN in H_2O, 4.0 mL/min) to provide **5.1** (52.7 mg, 0.15% yield), **5.2** (5.4 mg, 0.015% yield), **5.3** (34.6 mg, 0.098% yield), and **5.4** (2.4 mg, 0.0069% yield).

5.4.3 Biofilm and growth inhibition assays with *C. albicans*

The effects of mutanobactins on the growth of *C.albicans* DAY185 was tested using the methods prescribed in the CLSI guidelines.[116] The biofilm inhibition assay was performed as described by Chandra et al.[117] with the following modifications. Strain *C. albicans* DAY185 were cultured in BHI medium (Becton Dickinson, USA) at 37 ℃ overnight and were washed with sterile PBS buffer (pH 7.4, EMD Chemicals Inc., USA), and resuspended in RPMI 1640 medium (Sigma Chemical Corp., USA) buffered to pH 7.0 with MOPS (3-(*N*-morpholino)propanesulfonic acid, 0.165 M). Test compounds were prepared in DMSO at a final concentration of 20 mM and were serially diluted 2-fold from the highest concentration of 200 μM with RPMI 1640 plus

MOPS medium. Farnesol was used as positive control.[118] One hundred microliters of yeast suspension (2.5×10^3 cells/mL) containing the diluted compounds (from 200 μM to 6.25 μM) or DMSO (v/v 1%) were added to the wells of a 96-well microplate (Costar 3370, Corning Inc., USA), and the plate incubated at 37 ℃. After 48 h, the yeast viability was measured by XTT assay.[119] In brief, yeast cells were treated with 0.1mg/mL XTT at 37 ℃ for 1 h. The absorbance was taken at 490 nm using a microplate reader (Infinite M200, Tecan Group Ltd., Switzerland). The minimum inhibitory concentration (MIC) for growth was defined as the lowest concentration that caused ≥80% reduction in the metabolic activity of the yeast. After the XTT was completed, the spent medium was immediately aspirated from each well and the wells washed twice with sterile PBS to remove nonadherent cells. Aliquots consisting of 100 μL RPMI 1640 plus MOPS medium were then added to each well. The washed biofilms were again measured using the XTT assay. All experiments were performed in triplicate on three separate occasions. The 50% inhibitory concentration (IC_{50}) valuse for biofilm inhibition were calculated using GraphPad Prism software (GraphPad, USA).

5.4.4 Feeding experiments with isotopically labeled acetate and amino acids

For the isotope labeling experiments, 500 mg of [1-^{13}C] or [2-^{13}C] sodium acetate, or 100 mg [1,2-^{13}C,^{15}N]Gly or [1,2,3,4-^{13}C,^{15}N]Asp (Cambridge Isotope Laboratories, Inc., USA) was dissolved in water and filter sterilized. The isotopes were added separately to 6 L of sterile BHI medium and culture vessels inoculated with an overnight culture of *S. mutans*. Cultures were maintained at 37 ℃ for 86 h at which time they were extracted with equal volumes of EtOAc (3×). The extracts were each separated into three fractions over silica gel using an Isolera flash column (*vide supra*). The fractions containing mutanobactins were further purified by preparative-HPLC and

semi-preparative HPLC to give approximately 5 mg of labeled **1** from each of the three cultures. A ^{13}C NMR spectrum was obtained at 100 MHz for each of the labeled compounds under identical experimental conditions.

5.4.5 Mutanobactin B (5.2).

White amorphous powder, $[\alpha]^{21}_{D}$ 24.4 (*c* 0. 27, MeOH); UV (MeOH) λ_{max} (log ε) 204 (3.17) nm; IR ν_{max} 3300, 3250, 2960, 2920, 2850, 1640 cm^{-1}; ^{1}H and ^{13}C NMR data, see Table 5.1; HRESIMS *m*/*z* 757.4298 $[M + Na]^{+}$ (calcd for $C_{37}H_{62}N_6O_7SNa$,757.4298).

5.4.6 Mutanobactin C (5.3).

White amorphous powder, $[\alpha]^{21}_{D}$ –3.7 (*c* 0. 38, MeOH); UV (MeOH) λ_{max} (log ε) 204 (4.38) nm; IR ν_{max} 3280, 2960, 2920, 2850, 1640 cm^{-1}; ^{1}H and ^{13}C NMR data, see Table 5.1; HRESIMS *m*/*z* 743.4138 $[M + Na]^{+}$ (calcd for $C_{36}H_{60}N_6O_7SNa$, 743.4142).

5.4.7 Mutanobactin D (5.4).

White amorphous powder, $[\alpha]^{21}_{D}$ 18.3 (*c* 0. 12, MeOH); UV (MeOH) λ_{max} (log ε) 204 (4.29); IR ν_{max} 3290, 2960, 2920, 2850, 1640 cm^{-1}; ^{1}H and ^{13}C NMR data, see Table 5.1; HRESIMS *m*/*z* 743.4681 $[M + Na]^{+}$ (calcd for $C_{37}H_{64}N_6O_8Na$, 743.4683.

References

1. Baltz, R. H.; Davies, J. E.; Demain, A. L.; American Society for Microbiology., *Manual of industrial microbiology and biotechnology*. 3rd ed.; ASM Press: Washington, DC, **2010**; p xvii 766 p.

2. Cannell, R. J. P., *Natural products isolation*. Humana Press: Totowa, N.J., **1998**; p x, 473 p.

3. Harvey, A. L., Natural products in drug discovery. *Drug Discov Today* **2008,** *13* (19-20), 894-901.

4. (a) Li, J. W.; Vederas, J. C., Drug discovery and natural products: end of an era or an endless frontier? *Science* **2009,** *325* (5937), 161-5; (b) Sneader, W., *Drug prototypes and their exploitation*. Wiley: Chichester ; New York, 1996; p xii, 788 p.

5. Cragg, G. M.; Newman, D. J.; Snader, K. M., Natural products in drug discovery and development. *J Nat Prod* **1997,** *60* (1), 52-60.

6. Zhang, M. Q.; Wilkinson, B., Drug discovery beyond the 'rule-of-five'. *Curr Opin Biotechnol* **2007,** *18* (6), 478-488.

7. (a) Newman, D. J.; Cragg, G. M., Natural products as sources of new drugs over the last 25 years. *J Nat Prod* **2007,** *70* (3), 461-477; (b) Demain, A. L., Antibiotics: Natural Products Essential to Human Health. *Med Res Rev* **2009,** *29* (6), 821-842; (c) Zhang, M. Q.; Wilkinson, B., Drug discovery beyond the 'rule-of-five'. *Curr Opin Biotech* **2007,** *18* (6), 478-488.

8. (a) Walsh, C. T.; Clardy, J.; Fischbach, M. A., New antibiotics from bacterial natural products. *Nat Biotechnol* **2006,** *24* (12), 1541-1550; (b) Newman, D. J.; Cragg, G. M.; Snader, K. M., Natural products as sources of new drugs over the period 1981-2002. *J Nat Prod* **2003,** *66* (7), 1022-1037.

9. Tenover, F. C.; Hughes, J. M., The challenges of emerging infectious diseases. Development and spread of multiply-resistant bacterial pathogens. *JAMA* **1996,** *275* (4), 300-304.

10. Arias, C. A.; Murray, B. E., Antibiotic-Resistant Bugs in the 21st Century -- A Clinical Super-Challenge. *New Engl J Med* **2009,** *360* (5), 439-443.

11. Demain, A. L., Antibiotics: Natural Products Essential to Human Health. *Med Res Rev* **2009,** *29* (6), 821-842.

12. (a) Brakhage, A. A.; Schroeckh, V., Fungal secondary metabolites - Strategies to activate silent gene clusters. *Fungal Genet Biol* **2011,** *48* (1), 15-22; (b) Nierman, W. C.; Losada, L.; Ajayi, O.; Frisvad, J. C.; Yu, J. J., Effect of competition on the production and activity of secondary metabolites in Aspergillus species. *Med Mycol* **2009,** *47*, S88-S96.

13. Keller, N. P.; Turner, G.; Bennett, J. W., Fungal secondary metabolism - From biochemistry to genomics. *Nature Reviews Microbiology* **2005,** *3* (12), 937-947.

14. Fisch, K. M.; Gillaspy, A. F.; Gipson, M.; Henrikson, J. C.; Hoover, A. R.; Jackson, L.; Najar, F. Z.; Wagele, H.; Cichewicz, R. H., Chemical induction of silent

biosynthetic pathway transcription in Aspergillus niger. *J Ind Microbiol Biotechnol* **2009,** *36* (9), 1199-1213.

15. (a) Wilkinson, B.; Micklefield, J., Mining and engineering natural-product biosynthetic pathways. *Nat Chem Biol* **2007,** *3* (7), 379-386; (b) Omura, S.; Ikeda, H.; Ishikawa, J.; Hanamoto, A.; Takahashi, C.; Shinose, M.; Takahashi, Y.; Horikawa, H.; Nakazawa, H.; Osonoe, T.; Kikuchi, H.; Shiba, T.; Sakaki, Y.; Hattori, M., Genome sequence of an industrial microorganism Streptomyces avermitilis: Deducing the ability of producing secondary metabolites. *P Natl Acad Sci USA* **2001,** *98* (21), 12215-12220; (c) Galagan, J. E.; Calvo, S. E.; Cuomo, C.; Ma, L. J.; Wortman, J. R.; Batzoglou, S.; Lee, S. I.; Basturkmen, M.; Spevak, C. C.; Clutterbuck, J.; Kapitonov, V.; Jurka, J.; Scazzocchio, C.; Farman, M.; Butler, J.; Purcell, S.; Harris, S.; Braus, G. H.; Draht, O.; Busch, S.; D'Enfert, C.; Bouchier, C.; Goldman, G. H.; Bell-Pedersen, D.; Griffiths-Jones, S.; Doonan, J. H.; Yu, J.; Vienken, K.; Pain, A.; Freitag, M.; Selker, E. U.; Archer, D. B.; Penalva, M. A.; Oakley, B. R.; Momany, M.; Tanaka, T.; Kumagai, T.; Asai, K.; Machida, M.; Nierman, W. C.; Denning, D. W.; Caddick, M.; Hynes, M.; Paoletti, M.; Fischer, R.; Miller, B.; Dyer, P.; Sachs, M. S.; Osmani, S. A.; Birren, B. W., Sequencing of Aspergillus nidulans and comparative analysis with A-fumigatus and A-oryzae. *Nature* **2005,** *438* (7071), 1105-1115; (d) Challis, G. L.; Corre, C., New natural product biosynthetic chemistry discovered by genome mining. *Nat Prod Rep* **2009,** *26* (8), 977-986; (e) Walsh, C. T.; Fischbach, M. A., Natural Products Version 2.0: Connecting Genes to Molecules. *J Am Chem Soc* **2010,** *132* (8), 2469-2493.

16. Bode, H. B.; Bethe, B.; Höfs, R.; Zeeck, A., Big effects from small changes: possible ways to explore nature's chemical diversity. *ChemBioChem* **2002,** *3* (7), 619-627.

17. Fuchser, J.; Zeeck, A., Secondary metabolites by chemical screening. 34. Aspinolides and aspinonene/aspyrone co-metabolites, new pentaketides produced by *Aspergillus ochraceus*. *Liebigs Annalen-Recueil* **1997,** (1), 87-95.

18. Paranagama, P. A.; Wijeratne, E. M. K.; Gunatilaka, A. A. L., Uncovering biosynthetic potential of plant-associated fungi: effect of culture conditions on metabolite production by *Paraphaeosphaeria quadriseptata* and *Chaetomium chiversii*. *Journal of Natural Products* **2007,** *70* (12), 1939-1945.

19. Amagata, T.; Tanaka, M.; Yamada, T.; Doi, M.; Minoura, K.; Ohishi, H.; Yamori, T.; Numata, A., Variation in Cytostatic Constituents of a Sponge-Derived Gymnascella dankaliensis by Manipulating the Carbon Source. *Journal of Natural Products* **2007,** *70* (11), 1731-1740.

20. Christian, O. E.; Compton, J.; Christian, K. R.; Mooberry, S. L.; Valeriote, F. A.; Crews, P., Using jasplakinolide to turn on pathways that enable the isolation of new chaetoglobosins from *Phomospis asparagi*. *Journal of Natural Products* **2005,** *68* (11), 1592-1597.

21. Bode, H. B.; Walker, M.; Zeeck, A., Secondary metabolites by chemical screening, 42 - Cladospirones B to I from *Sphaeropsidales* sp F-24'707 by variation of culture conditions. *European Journal of Organic Chemistry* **2000,** (18), 3185-3193.

22. Bode, H. B.; Zeeck, A., Sphaerolone and dihydrosphaerolone, two bisnaphthyl-pigments from the fungus *Sphaeropsidales* sp. F-24'707. *Phytochemistry* **2000,** *54*, 597-601.

23. Lin, Z.; Zhu, T.; Wei, H.; Zhang, G.; Wang, H.; Gu, Q., Spicochalasin A and new aspochalasins from the marine-derived fungus *Spicaria elegans*. *European Journal of Organic Chemistry* **2009,** *2009* (18), 3045-3051.

24. Shao, H.-J.; Qin, X.-D.; Dong, Z.-J.; Zhang, H.-B.; Liu, J.-K., Induced daldinin A, B, C with a new skeleton from cultures of the ascomycete *Daldinia concentrica*. *The Journal of Antibiotics* **2008,** *61* (3), 115-119.

25. Seibert, S. F.; Krick, A.; Eguereva, E.; Kehraus, S.; Konig, G. M., Ascospiroketals A and B, unprecedented cycloethers from the marine-derived fungus *Ascochyta salicorniae*. *Organic Letters* **2007,** *9* (2), 239-242.

26. Amagata, T.; Tanaka, M.; Yamada, T.; Doi, M.; Minoura, K.; Ohishi, H.; Yamori, T.; Numata, A., Variation in cytostatic constituents of a sponge-derived *Gymnascella dankaliensis* by manipulating the carbon source. *Journal of Natural Products* **2007,** *70* (11), 1731-1740.

27. Gloer, J. B., Applications of Fungal Ecology in the Search for New Bioactive Natural Products In *The Mycote*, Kubicek, C. P.; Druzhinina, I. S., Eds. Springer: Berlin, 2007; pp 257-283.

28. Burgess, J. G.; Jordan, E. M.; Bregu, M.; Mearns-Spragg, A.; Boyd, K. G., Microbial antagonism: a neglected avenue of natural products research. *Journal of Biotechnology* **1999,** *70* (1-3), 27-32.

29. Cueto, M.; Jensen, P. R.; Kauffman, C.; Fenical, W.; Lobkovsky, E.; Clardy, J., Pestalone, a new antibiotic produced by a marine fungus in response to bacterial challenge. *J Nat Prod* **2001,** *64* (11), 1444-1446.

30. Oh, D.-C.; Jensen, P. R.; Kauffman, C. A.; Fenical, W., Libertellenones A-D: Induction of cytotoxic diterpenoid biosynthesis by marine microbial competition. *Bioorganic & Medicinal Chemistry* **2005,** *13* (17), 5267-5273.

31. Oh, D. C.; Kauffman, C. A.; Jensen, P. R.; Fenical, W., Induced production of emericellamides A and B from the marine-derived fungus *Emericella* sp. in competing co-culture. *Journal of Natural Products* **2007,** *70* (4), 515-520.

32. Angell, S.; Bench, B. J.; Williams, H.; Watanabe, C. M. H., Pyocyanin isolated from a marine microbial population: synergistic production between two distinct bacterial species and mode of action. *Chemistry & Biology* **2006,** *13* (12), 1349-1359.

33. (a) Brakhage, A. A.; Schroeckh, V., Fungal secondary metabolites - Strategies to activate silent gene clusters. *Fungal Genet Biol* **2011,** *48* (1), 15-22; (b) Hoffmeister, D.; Schneider, P.; Misiek, M., In vivo and in vitro production options for fungal secondary metabolites. *Mol Pharm* **2008,** *5* (2), 234-242; (c) Hertweck, C.; Winter, J. M.; Behnken, S., Genomics-inspired discovery of natural products. *Curr Opin Chem Biol* **2011,** *15* (1), 22-31.

34. Gross, F.; Luniak, N.; Perlova, O.; Gaitatzis, N.; Jenke-Kodama, H.; Gerth, K.; Gottschalk, D.; Dittmann, E.; Müller, R., Bacterial type III polyketide synthases: phylogenetic analysis and potential for the production of novel secondary metabolites by heterologous expression in pseudomonads. *Archives of Microbiology* **2006,** *185* (1), 28-38.

35. Palmu, K.; Ishida, K.; Mantsala, P.; Hertweck, C.; Metsa-Ketela, M., Artificial reconstruction of two cryptic angucycline antibiotic biosynthetic pathways. *Chembiochem* **2007,** *8* (13), 1577-84.

36. Palmu, K.; Ishida, K.; Mäntsälä, P.; Hertweck, C.; Mikko Metsä-Ketelä, Artificial reconstruction of two cryptic angucycline antibiotic biosynthetic pathways. *ChemBioChem* **2007,** *8* (13), 1577-1584.

37. Kennedy, J.; Turner, G., delta-(L-alpha-aminoadipyl)-L-cysteinyl-D-valine synthetase is a rate limiting enzyme for penicillin production in Aspergillus nidulans. *Mol Gen Genet* **1996,** *253* (1-2), 189-197.

38. Chiang, Y.-M.; Szewczyk, E.; Davidson, A. D.; Keller, N.; Oakley, B. R.; Wang, C. C. C., A gene cluster containing two fungal polyketide synthases encodes the biosynthetic pathway for a polyketide, asperfuranone, in *Aspergillus nidulans*. *Journal of the American Chemical Society* **2009,** *131* (8), 2965-2970.

39. Gross, H.; Stockwell, V. O.; Henkels, M. D.; Nowak-Thompson, B.; Loper, J. E.; Gerwick, W. H., The genomisotopic approach: a systematic method to isolate products of orphan biosynthetic gene clusters. *Chemistry & Biology* **2007,** *14* (1), 53-63.

40. Ballestar, E., An Introduction to Epigenetics. *Epigenetic Contributions in Autoimmune Disease* **2011,** *711*, 1-11.

41. (a) Esteller, M., Cancer epigenomics: DNA methylomes and histone-modification maps. *Nature Reviews Genetics* **2007,** *8* (4), 286-298; (b) Felsenfeld, G.; Groudine, M., Controlling the double helix. *Nature* **2003,** *421* (6921), 448-453.

42. (a) Suzuki, M. M.; Bird, A., DNA methylation landscapes: provocative insights from epigenomics. *Nat Rev Genet* **2008,** *9* (6), 465-76; (b) Strauss, J.; Reyes-Dominguez, Y., Regulation of secondary metabolism by chromatin structure and epigenetic codes. *Fungal Genet Biol* **2011,** *48* (1), 62-69.

43. Rountree, M. R.; Selker, E. U., DNA methylation inhibits elongation but not initiation of transcription in Neurospora crassa. *Genes Dev* **1997,** *11* (18), 2383-2395.

44. (a) Tamaru, H.; Zhang, X.; McMillen, D.; Singh, P. B.; Nakayama, J.; Grewal, S. I.; Allis, C. D.; Cheng, X.; Selker, E. U., Trimethylated lysine 9 of histone H3 is a mark for DNA methylation in Neurospora crassa. *Nat Genet* **2003,** *34* (1), 75-9; (b) Tamaru, H.; Selker, E. U., A histone H3 methyltransferase controls DNA methylation in Neurospora crassa. *Nature* **2001,** *414* (6861), 277-283.

45. Fisch, K. M.; Gillaspy, A. F.; Gipson, M.; Henrikson, J. C.; Hoover, A. R.; Jackson, L.; Najar, F. Z.; Wagele, H.; Cichewicz, R. H., Chemical induction of silent biosynthetic pathway transcription in Aspergillus niger. *J Ind Microbiol Biot* **2009,** *36* (9), 1199-1213.

46. Williams, R. B.; Henrikson, J. C.; Hoover, A. R.; Lee, A. E.; Cichewicz, R. H., Epigenetic remodeling of the fungal secondary metabolome. *Org Biomol Chem* **2008,** *6* (11), 1895-1897.

47. Wang, X. R.; Sena, J. G.; Hoover, A. R.; King, J. B.; Ellis, T. K.; Powell, D. R.; Cichewicz, R. H., Chemical Epigenetics Alters the Secondary Metabolite Composition of Guttate Excreted by an Atlantic-Forest-Soil-Derived Penicillium citreonigrum. *J Nat Prod* **2010,** *73* (5), 942-948.

48. Xie, Z. J.; Okinaga, T.; Niu, G. Q.; Qi, F. X.; Merritt, J., Identification of a novel bacteriocin regulatory system in Streptococcus mutans. *Mol Microbiol* **2010,** *78* (6), 1431-1447.

49. Joyner, P. M.; Liu, J.; Zhang, Z.; Merritt, J.; Qi, F.; Cichewicz, R. H., Mutanobactin A from the human oral pathogen Streptococcus mutans is a cross-kingdom regulator of the yeast-mycelium transition. *Org Biomol Chem* **2010,** *8* (24), 5486-5489.

50. Wang, X. R.; Sena, J. G.; Hoover, A. R.; King, J. B.; Ellis, T. K.; Powell, D. R.; Cichewicz, R. H., Chemical Epigenetics Alters the Secondary Metabolite Composition of Guttate Excreted by an Atlantic-Forest-Soil-Derived Penicillium citreonigrum. *J Nat Prod* **2010,** *73* (5), 942-948.

51. Cichewicz, R. H., Epigenome manipulation as a pathway to new natural product scaffolds and their congeners. *Nat. Prod. Rep.* **2010,** *27* (1), 11-22.

52. Fisch, K. M.; Gillaspy, A. F.; Gipson, M.; Henrikson, J. C.; Hoover, A. R.; Jackson, L.; Najar, F. Z.; Waegele, H.; Cichewicz, R. H., Chemical induction of silent biosynthetic pathway transcription in Aspergillus niger. *J. Ind. Microbiol. Biotechnol.* **2009,** *36* (9), 1199-1213.

53. (a) Henrikson, J. C.; Hoover, A. R.; Joyner, P. M.; Cichewicz, R. H., A chemical epigenetics approach for engineering the in situ biosynthesis of a cryptic natural product from Aspergillus niger. *Org. Biomol. Chem.* **2009,** *7* (3), 435-438; (b) Williams, R. B.; Henrikson, J. C.; Hoover, A. R.; Lee, A. E.; Cichewicz, R. H., Epigenetic remodeling of the fungal secondary metabolome. *Org. Biomol. Chem.* **2008,** *6* (11), 1895-1897.

54. (a) Morellato, L. P. C.; Haddad, C. F. B., Introduction: The Brazilian Atlantic Forest¹. *Biotropica* **2000,** *32* (4b), 786-792; (b) Carnaval, A. C.; Hickerson, M. J.; Haddad, C. F. B.; Rodrigues, M. T.; Moritz, C., Stability Predicts Genetic Diversity in the Brazilian Atlantic Forest Hotspot. *Science* **2009,** *323* (5915), 785-789.

55. (a) Hutwimmer, S.; Wang, H.; Strasser, H.; Burgstaller, W., Formation of exudate droplets by *Metarhizium anisopliae* and the presence of destruxins. *Mycologia* **2009**, 09-079; (b) Colotelo, N.; Sumner, J. L.; Voegelin, W. S., Chemical studies on the exudate and developing sclerotia of *Sclerotinia sclerotiorum* (Lib.) DeBary. *Canadian Journal of Microbiology* **1971,** *17* (9), 1189-1194; (c) Colotelo, N., Physiological and biochemical properties of the exudate associated with developing sclerotia of *Sclerotinia sclerotiorum* (Lib.) DeBary. *Canadian Journal of Microbiology* **1973,** *19* (1), 73-79; (d) Colotelo, N., Fungal exudates. *Canadian Journal of Microbiology* **1978,** *24* (10), 1173-1181; (e) Gareis, M.; Gareis, E.-M., Guttation droplets of Penicillium

nordicum and Penicillium verrucosum contain high concentrations of the mycotoxins ochratoxin A and B. *Mycopathologia* **2007,** *163* (4), 207-214.

56. Jennings, D. H., The role of droplets in helping to maintain a constant growth rate of aerial hyphae. *Mycological Research* **1991,** *95* (7), 883-884.

57. (a) McPhee, W. J.; Colotelo, N., Fungal exudates. I. Characteristics of hyphal exudates in *Fusarium culmorum*. *Canadian Journal of Botany* **1977,** *55* (3), 358-365; (b) Willmann, G.; Fakoussa, R., Extracellular oxidative enzymes of coal-attacking fungi. *Fuel Processing Technology* **1997,** *52* (1-3), 27-41.

58. (a) Singh, T.; Arora, D. K., Motility and chemotactic response of Pseudomonas fluorescens toward chemoattractants present in the exudate of Macrophomina phaseolina. *Microbiological Research* **2001,** *156* (4), 343-351; (b) Sun, Y.-P.; Unestam, T.; Lucas, S. D.; Johanson, K. J.; Kenne, L.; Finlay, R., Exudation-reabsorption in a mycorrhizal fungus, the dynamic interface for interaction with soil and soil microorganisms. *Mycorrhiza* **1999,** *9* (3), 137-144; (c) de Boer, W.; Folman, L. B.; Summerbell, R. C.; Boddy, L., Living in a fungal world: impact of fungi on soil bacterial niche development. *FEMS Microbiology Reviews* **2005,** *29* (4), 795-811.

59. Powell, A. D. G.; Robertson, A.; Whalley, W. B., *Chem. Soc. Spec. Publ.* **1956,** (5), 27.

60. (a) Whalley, W. B.; Ferguson, G.; Marsh, W. C.; Restivo, R. J., The chemistry of fungi. Part LXVIII. The absolute configuration of (+)-sclerotiorin and the azaphilones. *J. Chem. Soc., Perkin Trans. 1* **1976,** (13), 1366-9; (b) Pairet, L.; Wrigley, S. K.; Chetland, I.; Reynolds, E. E.; Hayes, M. A.; Holloway, J.; Ainsworth, A. M.; Katzer, W.; Cheng, X.-M.; Hupe, D. J.; Charlton, P.; Doherty, A. M., Azaphilones with endothelin receptor binding activity produced by *Penicillium sclerotiorum*: taxonomy, fermentation, isolation, structure elucidation and biological activity. *Journal of Antibiotics* **1995,** *48* (9), 913-23.

61. Seto, H.; Tanabe, M., Utilization of ^{13}C-^{13}C coupling in structural and biosynthetic studies. III. Ochrephilone - a new fungal metabolite. *Tetrahedron Letters* **1974,** *15* (8), 651-654.

62. Matsuzaki, K.; Tahara, H.; Inokoshi, J.; Tanaka, H.; Masuma, R.; Omura, S., New brominated and halogen-less derivatives and structure-activity relationship of azaphilones inhibiting gp120-CD4 binding. *Journal of Antibiotics* **1998,** *51* (11), 1004-1011.

63. Eade, R. A.; Page, H.; Robertson, A.; Turner, K.; Whalley, W. B., The chemistry of fungi. Part XXVII. Sclerotiorin and its hydrogenation products. *Journal of the Chemical Society* **1957**, 4913-4924.

64. (a) Birch, A. J.; Cassera, A.; Fitton, P.; Holker, J. S. E.; Smith, H.; Thompson, G. A.; Whalley, W. B., Studies in relation to biosynthesis. Part XXX. Rotiorin, monascin, and rubropunctatin. *Journal of the Chemical Society* **1962**, 3583 - 3586; (b) Birch, A. J.; Fitton, P.; Pride, E.; Ryan, A. J.; Smith, H.; Whalley, W. B., Studies in relation to biosynthesis. Part XVII. Sclerotiorin, citrinin, and citromycetin. *Journal of the Chemical Society* **1958**, 4576 - 4581.

65. Chiang, Y.-M.; Szewczyk, E.; Davidson, A. D.; Keller, N.; Oakley, B. R.; Wang, C. C. C., A Gene Cluster Containing Two Fungal Polyketide Synthases Encodes the Biosynthetic Pathway for a Polyketide, Asperfuranone, in Aspergillus nidulans. *Journal of the American Chemical Society* **2009,** *131* (8), 2965-2970.

66. (a) Wei, W.-G.; Yao, Z.-J., Synthesis Studies toward Chloroazaphilone and Vinylogous Î¾Pyridones: Two Common Natural Product Core Structures. *The Journal of Organic Chemistry* **2005,** *70* (12), 4585-4590; (b) Arai, N.; Shiomi, K.; Tomoda, H.; Tabata, N.; Yang, D. J.; Masuma, R.; Kawakubo, T.; Omura, S., Isochromophilones III-VI, inhibitors of acyl-CoA:cholesterol acyltransferase produced by Penicillium multicolor FO-3216. *Journal of Antibiotics* **1995,** *48* (7), 696-702.

67. Whalley, W. B., The sclerotiorin group of fungal metabolites: their structure and biosynthesis. *Pure and Applied Chemistry* **1963,** *7* (4), 565-588.

68. Birkinshaw, J. H.; Kalyanpur, M. G.; Stickings, C. E., Studies in the biochemistry of micro-organisms. 113. Pencolide, a nitrogen-containing metabolite of Penicillium multicolor Grigorieva-Manilova and Poradielova. *Biochem J* **1963,** *86*, 237-243.

69. (a) Takahashi, J. A.; Castro, M. C. M. d.; Souza, G. G.; Lucas, E. M. F.; Bracarense, A. A. P.; Abreu, L. M.; Marriel, I. E.; Oliveira, M. S.; Floreano, M. B.; Oliveira, T. S., Isolation and screening of fungal species isolated from Brazilian cerrado soil for antibacterial activity against Escherichia coli, Staphylococcus aureus, Salmonella typhimurium, Streptococcus pyogenes and Listeria monocytogenes. *Journal de Mycologie Médicale / Journal of Medical Mycology* **2008,** *18* (4), 198-204; (b) Lucas, E. M. F.; Castro, M. C. M. d.; Takahashi, J. A., Antimicrobial properties of sclerotiorin, isochromophilone VI, and pencolide, metabolites from a Brazilian cerrado isolate of *Penicillium sclerotiorum* van Beyma. *Brazilian Journal of Microbiology* **2007,** *38*, 785-789.

70. (a) Sutherland, J. K., The proton-magnetic-resonance spectrum of pencolide. *Biochem J* **1963,** *86*, 243; (b) Strunz, G. M.; Ren, W.-Y., Synthesis of pencolide and corroboration of its revised stereochemistry. *Can. J. Chem.* **1976,** *54* (18), 2862-4; (c) Srinivasan, A.; Richards, K. D.; Olsen, R. K., Comments on assignment of stereochemistry to 2-acylaminocrotonates. *Tetrahedron Letters* **1976,** (12), 891-894.

71. Shiomi, K.; Uchida, R.; Inokoshi, J.; Tanaka, H.; Iwai, Y.; Omura, S., Andrastins A~C, new protein farnesyltransferase inhibitors, produced by Penicillium sp. FO-3929. *Tetrahedron Letters* **1996,** *37* (8), 1265-1268.

72. Kosemura, S., Meroterpenoids from Penicillium citreo-viride B. IFO 4692 and 6200 hybrid. *Tetrahedron* **2003,** *59* (27), 5055-5072.

73. Geris, R.; Simpson, T. J., Meroterpenoids produced by fungi. *Nat. Prod. Rep.* **2009,** *26*, 1063–1094.

74. (a) Quang, D. N.; Hashimoto, T.; Stadler, M.; Radulovic, N.; Asakawa, Y., Antimicrobial azaphilones from the fungus Hypoxylon multiforme. *Planta Medica* **2005,** *71* (11), 1058-1062; (b) Quang, D. N.; Hashimoto, T.; Fournier, J.; Stadler, M.; Radulovic, N.; Asakawa, Y., Sassafrins A-D, new antimicrobial azaphilones from the fungus Creosphaeria sassafras. *Tetrahedron* **2005,** *61* (7), 1743-1748; (c) Stadler, M.;

Quang, D. N.; Tomita, A.; Hashimoto, T.; Asakawa, Y., Changes in secondary metabolism during stromatal ontogeny of Hypoxylon fragiforme. *Mycological Research* **2006,** *110* (7), 811-820.

75. (a) Wang, X. R.; Sena, J. G.; Hoover, A. R.; King, J. B.; Ellis, T. K.; Powell, D. R.; Cichewicz, R. H., Chemical Epigenetics Alters the Secondary Metabolite Composition of Guttate Excreted by an Atlantic-Forest-Soil-Derived Penicillium citreonigrum. *Journal of Natural Products* **2010,** *73* (5), 942-948; (b) Williams, R. B.; Henrikson, J. C.; Hoover, A. R.; Lee, A. E.; Cichewicz, R. H., Epigenetic remodeling of the fungal secondary metabolome. *Organic & Biomolecular Chemistry* **2008,** *6* (11), 1895-1897.

76. Whyte, A. C.; Gloer, J. B.; Wicklow, D. T.; Dowd, P. F., Sclerotiamide: A new member of the paraherquamide class with potent antiinsectan activity from the sclerotia of Aspergillus sclerotiorum. *Journal of Natural Products* **1996,** *59* (11), 1093-1095.

77. (a) Barrows, B. R.; Azimzadeh, A. M.; McCulle, S. L.; Vives-Rodriguez, G.; Stark, W. N., Jr.; Ambulos, N.; Yin, J.; Chen, H.; Balke, C. W.; Moravec, C. S.; Pierson, R. N., 3rd; Gottlieb, S. S.; Bond, M.; Johnson, F. L., Robust gene expression with amplified RNA from biopsy-sized human heart tissue. *J Mol Cell Cardiol* **2007,** *42* (1), 260-4; (b) Tsukamoto, S.; Kato, H.; Samizo, M.; Nojiri, Y.; Onuki, H.; Hirota, H.; Ohta, T., Notoamides F-K, Prenylated Indole Alkaloids Isolated from a Marine-Derived Aspergillus sp. *Journal of Natural Products* **2008,** *71* (12), 2064-2067.

78. Tsukamoto, S.; Umaoka, H.; Yoshikawa, K.; Ikeda, T.; Hirota, H., Notoamide O, a Structurally Unprecedented Prenylated Indole Alkaloid, and Notoamides P-R from a Marine-Derived Fungus, Aspergillus sp. *J Nat Prod* **2010,** *73* (8), 1438-1440.

79. Qian-Cutrone, J. F.; Huang, S.; Shu, Y. Z.; Vyas, D.; Fairchild, C.; Menendez, A.; Krampitz, K.; Dalterio, R.; Klohr, S. E.; Gao, Q., Stephacidin A and B: Two structurally novel, selective inhibitors of the testosterone-dependent prostate LNCaP cells. *Journal of the American Chemical Society* **2002,** *124* (49), 14556-14557.

80. Sugie, Y.; Hirai, H.; Inagaki, T.; Ishiguro, M.; Kim, Y. J.; Kojima, Y.; Sakakibara, T.; Sakemi, S.; Sugiura, A.; Suzuki, Y.; Brennan, L.; Duignan, J.; Huang, L. H.; Sutcliffe, J.; Kojima, N., A new antibiotic CJ-17,665 from Aspergillus ochraceus. *Journal of Antibiotics* **2001,** *54* (11), 911-916.

81. Qian-Cutrone, J.; Huang, S.; Shu, Y. Z.; Vyas, D.; Fairchild, C.; Menendez, A.; Krampitz, K.; Dalterio, R.; Klohr, S. E.; Gao, Q., Stephacidin A and B: two structurally novel, selective inhibitors of the testosterone-dependent prostate LNCaP cells. *J Am Chem Soc* **2002,** *124* (49), 14556-14557.

82. Rahbaek, L.; Breinholt, J., Circumdatins D, E, and F: Further fungal benzodiazepine analogues from Aspergillus ochraceus. *Journal of Natural Products* **1999,** *62* (6), 904-905.

83. Rahbaek, L.; Breinholt, J.; Frisvad, J. C.; Christophersen, C., Circumdatin A, B, and C: Three new benzodiazepine alkaloids isolated from a culture of the fungus Aspergillus ochraceus. *Journal of Organic Chemistry* **1999,** *64* (5), 1689-1692.

84. Furtado, N. A. J. C.; Pupo, M. T.; Carvalho, I.; Campo, V. L.; Duarte, M. C. T.; Bastos, J. K., Diketopiperazines produced by an Aspergillus fumigatus Brazilian strain. *J Brazil Chem Soc* **2005,** *16* (6B), 1448-1453.

85. Dunn, G.; Newbold, G. T.; Spring, F. S., Synthesis of Flavacol, a Metabolic Product of Aspergillus-Flavus. *Journal of the Chemical Society* **1949,** (Oct), 2586-2587.

86. Li, H. J.; Cai, Y. T.; Chen, Y. Y.; Lam, C. K.; Lan, W. J., Metabolites of Marine Fungus Aspergillus sp Collected from Soft Coral Sarcophyton tortuosum. *Chem Res Chinese U* **2010,** *26* (3), 415-419.

87. (a) Ohtani, I.; Kusumi, T.; Kashman, Y.; Kakisawa, H., A New Aspect of the High-Field Nmr Application of Mosher Method - the Absolute-Configuration of Marine Triterpene Sipholenol-A. *Journal of Organic Chemistry* **1991,** *56* (3), 1296-1298; (b) Hoye, T. R.; Jeffrey, C. S.; Shao, F., Mosher ester analysis for the determination of absolute configuration of stereogenic (chiral) carbinol carbons. *Nat Protoc* **2007,** *2* (10), 2451-2458.

88. Ramage, G.; Saville, S. P.; Wickes, B. L.; Lopez-Ribot, J. L., Inhibition of Candida albicans Biofilm Formation by Farnesol, a Quorum-Sensing Molecule. *Appl. Environ. Microbiol.* **2002,** *68* (11), 5459-5463.

89. Chandra, J.; Mukherjee, P. K.; Ghannoum, M. A., In vitro growth and analysis of Candida biofilms. *Nat Protoc* **2008,** *3* (12), 1909-1924.

90. Deveau, A.; Hogan, D. A., Linking quorum sensing regulation and biofilm formation by Candida albicans. *Methods Mol Biol* **2011,** *692*, 219-233.

91. Nett, J. E.; Cain, M. T.; Crawford, K.; Andes, D. R., Optimizing a Candida biofilm microtiter plate model for measurement of antifungal susceptibility by XTT assay. *J. Clin. Microbiol.* **2011**, JCM.02273-10.

92. Zhang, Y.; Cai, C.; Yang, Y.; Weng, L.; Wang, L., Blocking Candida albicans Biofilm Formation by BDSF and trans-BDSF. *Journal of medical microbiology* **2011**.

93. Collins, L. M. C.; Dawes, C., The Surface Area of the Adult Human Mouth and Thickness of the Salivary Film Covering the Teeth and Oral Mucosa. *Journal of Dental Research* **1987,** *66* (8), 1300-1302.

94. (a) Xie, G.; Chain, P. S. G.; Lo, C. C.; Liu, K. L.; Gans, J.; Merritt, J.; Qi, F., Community and gene composition of a human dental plaque microbiota obtained by metagenomic sequencing. *Molecular Oral Microbiology* **2010,** *25* (6), 391-405; (b) Zaura, E.; Keijser, B.; Huse, S.; Crielaard, W., Defining the healthy "core microbiome" of oral microbial communities. *BMC Microbiology* **2009,** *9* (1), 259; (c) Nasidze, I.; Li, J.; Quinque, D.; Tang, K.; Stoneking, M., Global diversity in the human salivary microbiome. *Genome Research* **2009,** *19* (4), 636-643; (d) Lazarevic, V.; Whiteson, K.; Hernandez, D.; Francois, P.; Schrenzel, J., Study of inter- and intra-individual variations in the salivary microbiota. *BMC Genomics* **2010,** *11* (1), 523; (e) Dewhirst, F. E.; Chen, T.; Izard, J.; Paster, B. J.; Tanner, A. C. R.; Yu, W.-H.; Lakshmanan, A.; Wade, W. G., The Human Oral Microbiome. *J. Bacteriol.* **2010,** *192* (19), 5002-5017.

95. Keijser, B. J. F.; Zaura, E.; Huse, S. M.; van der Vossen, J. M. B. M.; Schuren, F. H. J.; Montijn, R. C.; ten Cate, J. M.; Crielaard, W., Pyrosequencing analysis of the Oral Microflora of healthy adults. *Journal of Dental Research* **2008,** *87* (11), 1016-1020.

96. Ahn, J.; Yang, L.; Paster, B. J.; Ganly, I.; Morris, L.; Pei, Z.; Hayes, R. B., Oral Microbiome Profiles: 16S rRNA Pyrosequencing and Microarray Assay Comparison. *PLoS ONE* **2011,** *6* (7), e22788.

97. Ghannoum, M. A.; Jurevic, R. J.; Mukherjee, P. K.; Cui, F.; Sikaroodi, M.; Naqvi, A.; Gillevet, P. M., Characterization of the Oral Fungal Microbiome (Mycobiome) in Healthy Individuals. *PLoS Pathog* **2010,** *6* (1), e1000713.

98. (a) Maruyama, F.; Kobata, M.; Kurokawa, K.; Nishida, K.; Sakurai, A.; Nakano, K.; Nomura, R.; Kawabata, S.; Ooshima, T.; Nakai, K.; Hattori, M.; Hamada, S.; Nakagawa, I., Comparative genomic analyses of Streptococcus mutans provide insights into chromosomal shuffling and species-specific content. *BMC Genomics* **2009,** *10* (1), 358; (b) Ajdić, D.; McShan, W. M.; McLaughlin, R. E.; Savić, G.; Chang, J.; Carson, M. B.; Primeaux, C.; Tian, R.; Kenton, S.; Jia, H.; Lin, S.; Qian, Y.; Li, S.; Zhu, H.; Najar, F.; Lai, H.; White, J.; Roe, B. A.; Ferretti, J. J., Genome sequence of Streptococcus mutans UA159, a cariogenic dental pathogen. *Proceedings of the National Academy of Sciences* **2002,** *99* (22), 14434-14439.

99. (a) Kreth, J.; Merritt, J.; Qi, F., Bacterial and host interactions of oral streptococci. *DNA Cell Biol* **2009,** *28* (8), 397-403; (b) Lemos, J. A.; Burne, R. A., A model of efficiency: stress tolerance by Streptococcus mutans. *Microbiology* **2008,** *154* (11), 3247-3255; (c) Kuramitsu, H. K.; He, X.; Lux, R.; Anderson, M. H.; Shi, W., Interspecies Interactions within Oral Microbial Communities. *Microbiol. Mol. Biol. Rev.* **2007,** *71* (4), 653-670.

100. Aas, J. A.; Griffen, A. L.; Dardis, S. R.; Lee, A. M.; Olsen, I.; Dewhirst, F. E.; Leys, E. J.; Paster, B. J., Bacteria of Dental Caries in Primary and Permanent Teeth in Children and Young Adults. *J. Clin. Microbiol.* **2008,** *46* (4), 1407-1417.

101. Belda-Ferre, P.; Alcaraz, L. D.; Cabrera-Rubio, R.; Romero, H.; Simon-Soro, A.; Pignatelli, M.; Mira, A., The oral metagenome in health and disease. *ISME J* **2011**.

102. (a) Pereira-Cenci, T.; Deng, D. M.; Kraneveld, E. A.; Manders, E. M. M.; Del Bel Cury, A. A.; ten Cate, J. M.; Crielaard, W., The effect of Streptococcus mutans and Candida glabrata on Candida albicans biofilms formed on different surfaces. *Archives of oral biology* **2008,** *53* (8), 755-764; (b) V Íchez, R.; Lemme, A.; Ballhausen, B.; Thiel, V.; Schulz, S.; Jansen, R.; Sztajer, H.; Wagner-D öbler, I., Streptococcus mutans Inhibits Candida albicans Hyphal Formation by the Fatty Acid Signaling Molecule trans-2-Decenoic Acid (SDSF). *ChemBioChem* **2010,** *11* (11), 1552-1562.

103. (a) Zeisel, M. B.; Druet, V. A.; Sibilia, J.; Klein, J.-P.; Quesniaux, V.; Wachsmann, D., Cross Talk between MyD88 and Focal Adhesion Kinase Pathways. *The Journal of Immunology* **2005,** *174* (11), 7393-7397; (b) Berlutti, F.; Catizone, A.; Ricci, G.; Frioni, A.; Natalizi, T.; Valenti, P.; Polimeni, A., Streptococcus mutans and Streptococcus sobrinus are able to adhere and invade human gingival fibroblast cell line. *Int J Immunopathol Pharmacol* **2010,** *23* (4), 1253-1260.

104. (a) Crawford, J. M.; Clardy, J., Bacterial symbionts and natural products. *Chemical Communications* **2011,** *47* (27), 7559-7566; (b) Kolenbrander, P. E.; Palmer, R. J.; Periasamy, S.; Jakubovics, N. S., Oral multispecies biofilm development and the key role of cell–cell distance. *Nat Rev Micro* **2010,** *8* (7), 471-480; (c) Jakubovics, N. S., Talk of the town: interspecies communication in oral biofilms. *Molecular Oral Microbiology* **2010,** *25* (1), 4-14.

105. (a) Yang, J. Y.; Karr, J. R.; Watrous, J. D.; Dorrestein, P. C., Integrating '-omics' and natural product discovery platforms to investigate metabolic exchange in microbiomes. *Current Opinion in Chemical Biology* **2011,** *15* (1), 79-87; (b) Sonnenburg, J. L.; Fischbach, M. A., Community Health Care: Therapeutic Opportunities in the Human Microbiome. *Science Translational Medicine* **2011,** *3* (78), 78ps12; (c) Zimmermann, M.; Fischbach, M. A., A Family of Pyrazinone Natural Products from a Conserved Nonribosomal Peptide Synthetase in Staphylococcus aureus. *Chemistry & biology* **2010,** *17* (9), 925-930.

106. Wu, C.; Cichewicz, R.; Li, Y.; Liu, J.; Roe, B.; Ferretti, J.; Merritt, J.; Qi, F., Genomic Island TnSmu2 of Streptococcus mutans Harbors a Nonribosomal Peptide Synthetase-Polyketide Synthase Gene Cluster Responsible for the Biosynthesis of Pigments Involved in Oxygen and H2O2 Tolerance. *Appl. Environ. Microbiol.* **2010,** *76* (17), 5815-5826.

107. Joyner, P. M.; Liu, J.; Zhang, Z.; Merritt, J.; Qi, F.; Cichewicz, R. H., Mutanobactin A from the human oral pathogen Streptococcus mutans is a cross-kingdom regulator of the yeast-mycelium transition. *Organic & Biomolecular Chemistry* **2010,** *8* (24), 5486-5489.

108. Williams, D. W.; Kuriyama, T.; Silva, S.; Malic, S.; Lewis, M. A. O., Candida biofilms and oral candidosis: treatment and prevention. *Periodontology 2000* **2011,** *55* (1), 250-265.

109. (a) LaFleur, M. D.; Qi, Q.; Lewis, K., Patients with Long-Term Oral Carriage Harbor High-Persister Mutants of Candida albicans. *Antimicrob. Agents Chemother.* **2010,** *54* (1), 39-44; (b) LaFleur, M. D.; Kumamoto, C. A.; Lewis, K., Candida albicans Biofilms Produce Antifungal-Tolerant Persister Cells. *Antimicrob. Agents Chemother.* **2006,** *50* (11), 3839-3846.

110. Bhushan, R.; Brückner, H., Marfey's reagent for chiral amino acid analysis: A review. *Amino Acids* **2004,** *27* (3), 231-247.

111. (a) Noble, S. M.; French, S.; Kohn, L. A.; Chen, V.; Johnson, A. D., Systematic screens of a Candida albicans homozygous deletion library decouple morphogenetic switching and pathogenicity. *Nat Genet* **2010,** *42* (7), 590-598; (b) Carlisle, P. L.; Banerjee, M.; Lazzell, A.; Monteagudo, C.; López-Ribot, J. L.; Kadosh, D., Expression levels of a filament-specific transcriptional regulator are sufficient to determine Candida albicans morphology and virulence. *Proceedings of the National Academy of Sciences* **2009,** *106* (2), 599-604.

112. (a) Fuchs, B. B.; Eby, J.; Nobile, C. J.; El Khoury, J. B.; Mitchell, A. P.; Mylonakis, E., Role of filamentation in Galleria mellonella killing by Candida albicans. *Microbes and Infection* **2010,** *12* (6), 488-496; (b) Ramage, G.; VandeWalle, K.; López-

Ribot, J. L.; Wickes, B. L., The filamentation pathway controlled by the Efg1 regulator protein is required for normal biofilm formation and development in Candida albicans. *FEMS Microbiology Letters* **2002,** *214* (1), 95-100.

113. (a) Peleg, A. Y.; Hogan, D. A.; Mylonakis, E., Medically important bacterial–fungal interactions. *Nat Rev Micro* **2010,** *8* (5), 340-349; (b) Shirtliff, M. E.; Peters, B. M.; Jabra-Rizk, M. A., Cross-kingdom interactions: Candida albicans and bacteria. *FEMS Microbiology Letters* **2009,** *299* (1), 1-8.

114. (a) Seneviratne, C. J.; Jin, L. J.; Samaranayake, Y. H.; Samaranayake, L. P., Cell Density and Cell Aging as Factors Modulating Antifungal Resistance of Candida albicans Biofilms. *Antimicrob. Agents Chemother.* **2008,** *52* (9), 3259-3266; (b) Mukherjee, P. K.; Chandra, J., Candida biofilm resistance. *Drug Resistance Updates 7* (4-5), 301-309.

115. (a) Nickerson, K. W.; Atkin, A. L.; Hornby, J. M., Quorum Sensing in Dimorphic Fungi: Farnesol and Beyond. *Appl. Environ. Microbiol.* **2006,** *72* (6), 3805-3813; (b) Ramage, G.; Saville, S. P.; Wickes, B. L.; Lopez-Ribot, J. L., Inhibition of Candida albicans Biofilm Formation by Farnesol, a Quorum-Sensing Molecule. *Appl. Environ. Microbiol.* **2002,** *68* (11), 5459-5463; (c) Weber, K.; Schulz, B.; Ruhnke, M., The quorum-sensing molecule E,E-farnesol—its variable secretion and its impact on the growth and metabolism of Candida species. *Yeast* **2010,** *27* (9), 727-739.

116. Clinical and Laboratory Standards Institute, Reference Method for Broth Dilution Antifungal Susceptibility Testing of Yeasts - Approved Standard (CLSI document M27-A3). 3rd ed.; 2008.

117. Chandra, J.; Mukherjee, P. K.; Ghannoum, M. A., In vitro growth and analysis of Candida biofilms. *Nat. Protocols* **2008,** *3* (12), 1909-1924.

118. Deveau, A.; Hogan, D. A., Linking Quorum Sensing Regulation and Biofilm Formation by *Candida albicans*. In *Quorum Sensing Methods and Protocols. Part II. Determining the Function of Autoinducers In vivo*, Rumbaugh, K. P., Ed. Humana Press (Springer): New York, 2011; Vol. 692, pp 219-233.

119. Nett, J. E.; Cain, M. T.; Crawford, K.; Andes, D. R., Optimizing a Candida Biofilm Microtiter Plate Model for Measurement of Antifungal Susceptibility by Tetrazolium Salt Assay. *J. Clin. Microbiol.* **2011,** *49* (4), 1426-1433.

120. Kato H., Yoshida T., Tokue T., Nojiri Y., Hirota H., Ohta T., Williams R. M., and Tsukamoto S. Notoamides A-D: new prenylated indole alkaloids isolated from a marine-derived fungus, *Aspergillus* sp. Angew Chem Int Ed Engl. 2007, 46, 2254-2256.

Appendix

Appendix Table of Contents

Table A1. Crystal data and structure refinement for atlantinone A (**3.9**)

Empirical formula	$(C_{26}H_{34}O_6)$ (CH_4O)
	$C_{27}H_{38}O_7$
Formula weight	474.57
Crystal system	Orthorhombic
Space group	P212121
Unit cell dimensions	a = 12.0199(6) Å = 90 °
	b = 13.7713(6) Å = 90 °
	c = 14.8276(8) Å = 90 °
Volume	2454.4[97] Å3
Z, Z'	4, 1
Density (calculated)	1.284 Mg/m3
Wavelength	1.54178 Å
Temperature	100[97] K
F(000)	1024
Absorption coefficient	0.746 mm-1
Absorption correction	Semi-empirical from
equivalents	
Max. and min. transmission	0.832 and 0.694
Theta range for data collection	4.38 to 69.53 °
Reflections collected	26979
Independent reflections	4555 [R(int) = 0.0476]
Data / restraints / parameters	4555 / 0 / 314
wR(F2 all data)	wR2 = 0.0802
R(F obsd data)	R1 = 0.0327
Goodness-of-fit on	F2 1.001
Observed data	[I > 2(I)] 4244
Absolute structure parameter	0.01(14)
Extinction coefficient	0.0040[97]
Largest and mean shift / s.u.	0.000and 0.000
Largest diff. peak and hole	0.216 and -0.201 e/Å3

Table A2. Crystal data and structure refinement for waikialoid A (**4.7**)

Empirical formula	$(C_{52}\ H_{54}\ N_6O_7) \cdot (H_2\ O) \cdot (C\ H_4\ O)$
	$C_{53}\ H_{60}\ N_6\ O_9$
Formula weight	925.07
Crystal system	Monoclinic
Space group	$P2_1$
Unit cell dimensions	a = 10.6276(4) Å α= 90°
	b = 17.6706(6) Å β= 104.187(2) °
	c = 12.8917(4) Å γ= 90°
Volume	2347.17(14) $Å^3$
Z, Z'	2, 1
Density (calculated)	1.309 Mg/m^3
Wavelength	1.54178 Å
Temperature	100(2) K
F(000)	984
Absorption coefficient	0.731 mm^{-1}
Absorption correction	Semi-empirical from equivalents
Max. and min. transmission	0.8418 and 0.6520
Theta range for data collection	3.54 to 67.16 °
Reflections collected	67703
Independent reflections	7859 [R(int) = 0.0272]
Data / restraints / parameters	7859 / 21 / 635
wR (F^2 all data)	$wR2$ = 0.0845
R(F obsd data)	$R1$ = 0.0316
Goodness-of-fit on F^2	1.005
Observed data [I > 2σ(I)]	7855
Absolute structure parameter	0.05(11)
Largest and mean shift / s.u.	0.033 and 0.001
Largest diff. peak and hole	0.343 and -0.281 e/$Å^3$

Table A3. Crystal data and structure refinement for asperonol A (**4.15**)

Empirical formula	$C_{14}\ H_{20}\ O_2$
Formula weight	220.30
Crystal system	Monoclinic
Space group	$P2_1$
Unit cell dimensions	a = 7.274(8) Å α= 90°
	b = 5.066(6) Å β= 98.53[99] °
	c = 17.43[97] Å γ= 90°
Volume	635.2(13) Å3
Z, Z'	2,1
Density (calculated)	1.152 Mg/m^3
Wavelength	0.71073 Å
Temperature	100[97] K
F(000)	240
Absorption coefficient	0.075 mm^{-1}
Absorption correction	Semi-empirical from equivalents
Max. and min. transmission	0.9970 and 0.9613
Theta range for data collection	2.36 to 22.99 °
Reflections collected	4287
Independent reflections	1000 [R (int) = 0.1127]
Data / restraints / parameters	1000 / 1 / 150
wR(F^2 all data)	wR2 = 0.1720
R(*F* obsd data)	R1 = 0.0710
Goodness-of-fit on F^2	1.051
Observed data [I > 2σ(I)]	730
Absolute structure parameter	-3(5)
Largest and mean shift / s.u.	0.000and 0.000
Largest diff. peak and hole	0.227 and -0.257 e/Å3
Empirical formula	$C_{14}\ H_{20}\ O_2$
Formula weight	220.30
Crystal system	Monoclinic
Space group	$P2_1$

Table A4. Revised ^{1}H-NMR and ^{13}C-NMR NMR data for mutanobactin A (**5.1**) (500 and 100 MHz, DMSO-d_6) – Shifts shown in red have been revised.

position	Mutanobactin A (5.1) (original)		Mutanobactin A (5.1) (revised)	
	δ_C	**δ_H mult. (*J* in Hz)**	**δ_C**	**δ_H mult. (*J* in Hz)**
1	50.4, CH	4.43 ddd (3.7, 9.0, 11.0)	50.4, CH	4.43 ddd (3.7, 9.0, 11.0)
2a	40.4, CH_2	1.44, m	40.4, CH_2	1.44, m
2b		1.81, ddd (3.9, 10.5, 13.8)		1.81, ddd (3.9, 10.5, 13.8)
3	24.2, CH	1.59, m	24.2, CH	1.59, m
4	20.9, CH_3	0.82, d (6.6)	20.9, CH_3	0.82, d (6.6)
5	23.5, CH_3	0.92, d (6.7)	23.5, CH_3	0.92, d (6.7)
6	170.5, C		170.5, C	
7	48.0, CH	4.52, q (6.8)	48.0, CH	4.52, q (6.8)
8	17.7, CH_3	1.17, d (6.7)	17.7, CH_3	1.17, d (6.7)
9	169.7, C		169.7, C	
10	61.0, CH	4.12, dd (3.7, 8.9)	61.0, CH	4.12, dd (3.7, 8.9)
11a	29.6, CH_2	1.72, m	29.6, CH_2	1.72, m
11b		2.13, m		2.13, m
12	24.5, CH_2	1.90, m	24.5, CH_2	1.90, m
13a	46.8, CH_2	3.43, m	46.8, CH_2	3.43, m
13b		3.65, ddd (4.5, 7.5, 9.8)		3.65, ddd (4.5, 7.5, 9.8)
14	171.6, C		171.6, C	
15	58.8, CH	3.57, dd (8.3, 10.0)	58.8, CH	3.57, dd (8.3, 10.0)
16	26.2, CH	2.33, m	26.2, CH	2.33, m
17	20.4, CH_3	0.84, d (6.6)	20.4, CH_3	0.84, d (6.6)
18	18.8, CH_3	0.77, d (6.8)	18.8, CH_3	0.77, d (6.8)
19	168.8, C		168.8, C	
20	52.2, CH	4.87 ddd (2.6, 8.0, 9.0)	52.2, CH	4.87 ddd (2.6, 8.0, 9.0)
21a	28.5, CH_2	2.23, dd (2.6, 16.0)	28.4, CH_2	2.23, dd (2.6, 16.0)
21b		3.19, dd (9.0, 16.0)		3.19, dd (9.0, 16.0)
22	170.4, C		170.4, C	
23a	43.7, CH_2	2.79, m	43.7, CH_2	2.79, m
23b		3.28, m		3.28, m
24	41.0, CH	3.25, m	41.0, CH	3.25, m
25	61.7, CH	3.87, d (9.8)	61.7, CH	3.87, d (9.8)
26	167.7, C		167.7, C	
27	203.8, C		203.8, C	
28a	41.4, CH_2	2.33, m	41.4, CH_2	2.33, m
28b		2.44, dd (6.0, 16.6)		2.44, dd (6.0, 16.6)
29	23.1, CH_2	1.44, m	23.1, CH_2	1.44, m
30	28.7, CH_2	1.20, m	28.5, CH_2	1.20, m
31	22.1, CH_2	1.25, m	28.7, CH_2	1.25, m
32	28.8, CH_2	1.23, m	28.9, CH_2	1.27, m
33	22.1, CH_2	1.25, m	28.8, CH_2	1.23, m
34	31.3, CH_2	1.23, m	31.3, CH_2	1.23, m
35	28.9, CH_2	1.27, m	22.1, CH_2	1.25, m
36	14.0, CH_3	0.85, t (6.8)	14.0, CH_3	0.85, t (6.8)
C1-NH		8.59, d (9.0)		8.59, d (9.0)
C7-NH		7.77, d (6.5)		7.77, d (6.5)
C15-NH		8.05, d (8.5)		8.05, d (8.5)
C20-NH		7.23, d (8.0)		7.23, d (8.0)
C23-NH		7.90, dd (5.3, 9.0)		7.90, dd (5.3, 9.0)

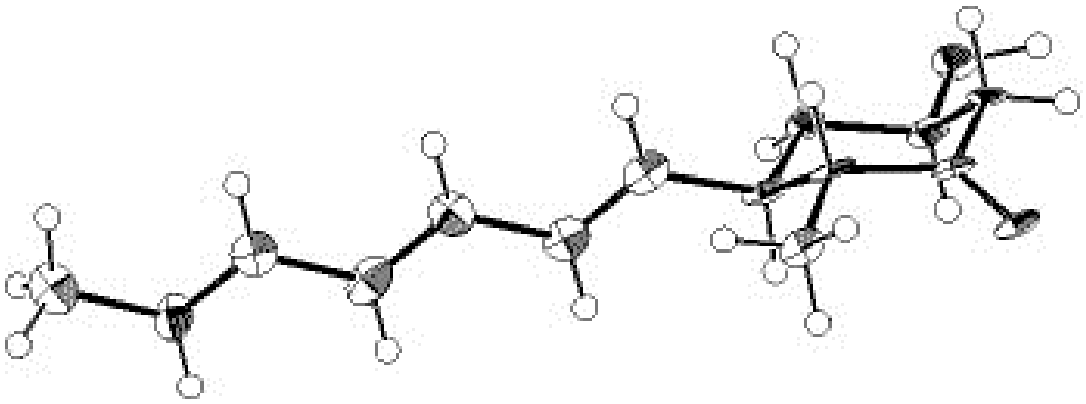

Figure A1. ORTEP structure for **4.15** generated from the X-ray diffraction data

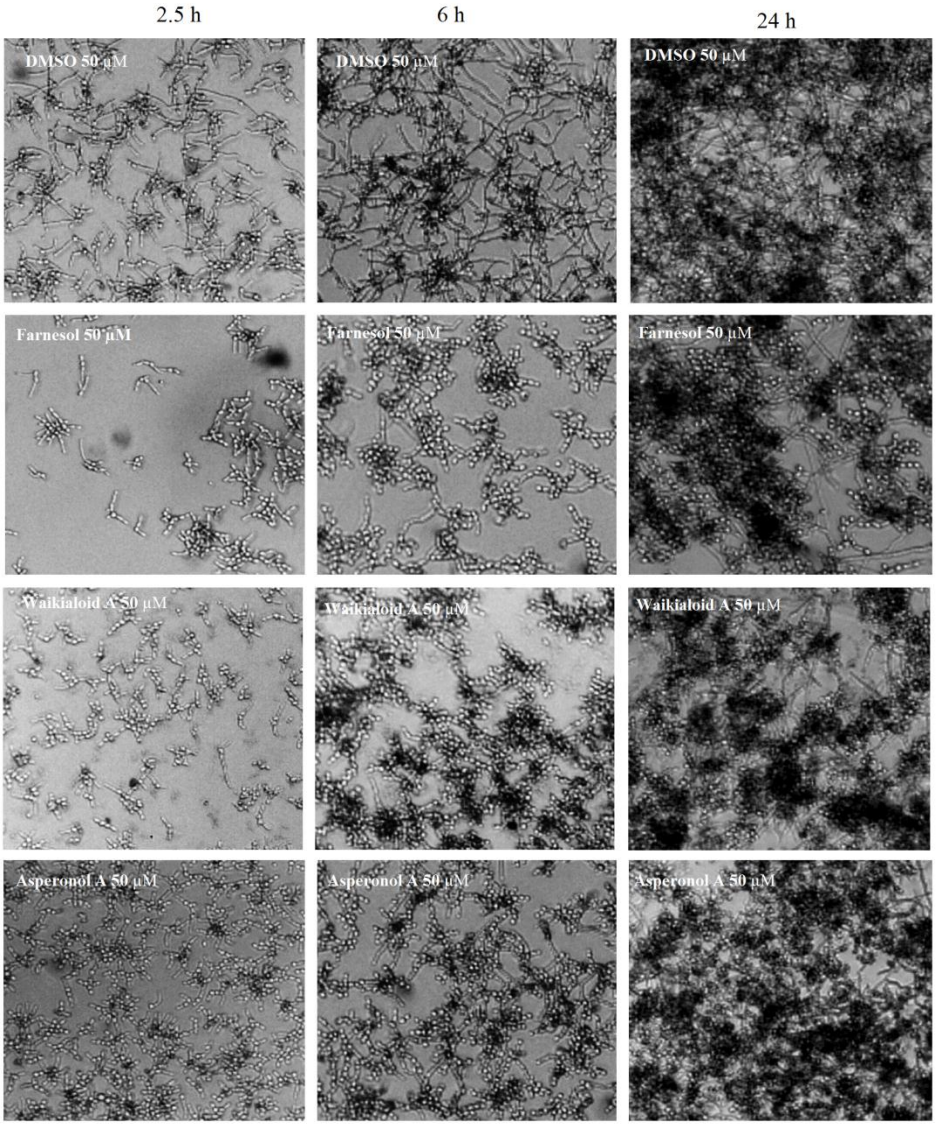

Figure A2. Effects of compounds **4.7** and **4.15** on Candida albicans hyphae formation. *C.albicans* DAY185 cells were treated with DMSO as negative control, farnesol as positive control, compound **4.7** and **4.15** for 6 h. Cell morphology was visualized at 2.5, 6 and 24 h using a phase contrast microscope (magnification, ×200).

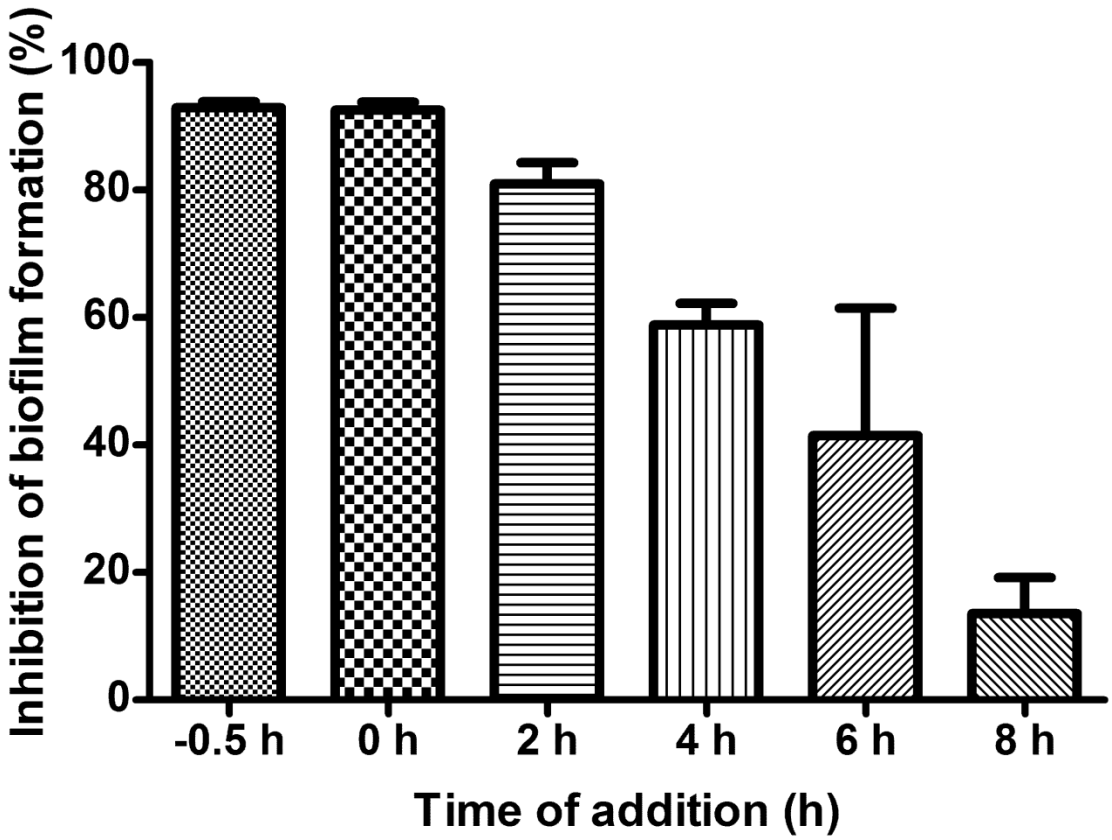

Figure A3. Time of addition assay of compound **4.7.** Compound **4.7** (25 μM) was added before (-0.5 h) or at 0, 2, 4, 6, 8 and 24 h after seeding to *C. albicans* DAY185 culture in a 96-well microplate. At 48 h after seeding, the wells were washed by PBS twice and the amount of biofilm formation in the wells was determined using XTT assay. All experiments were performed in triplicate on three separate occasions.

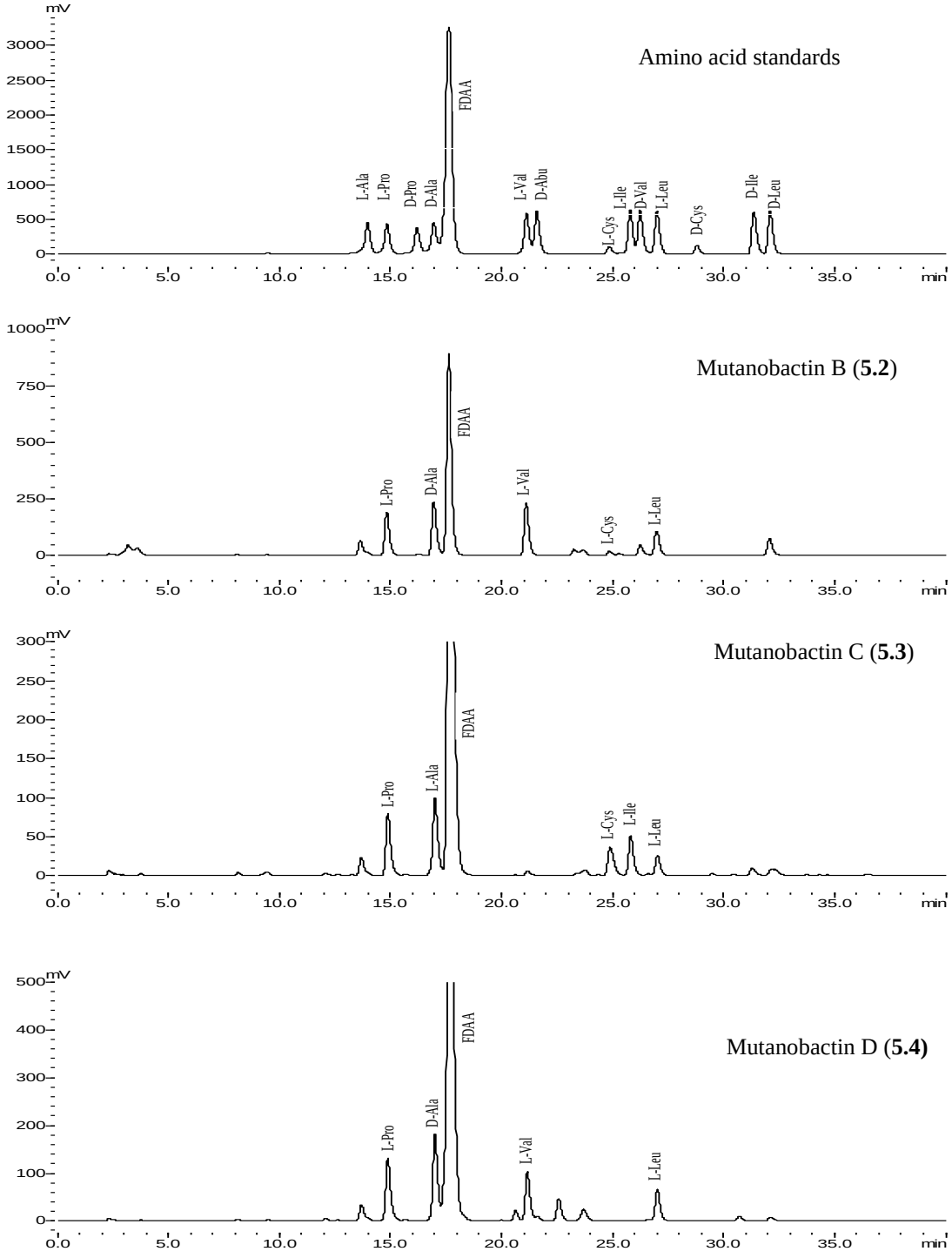

Figure A4. HPLC analysis of FDAA derivatized hydrolysate mutanobactin B-D (5.2-5.4) and amino acid standards. (Gradient elution: 30-60% MeCN, 40mins)

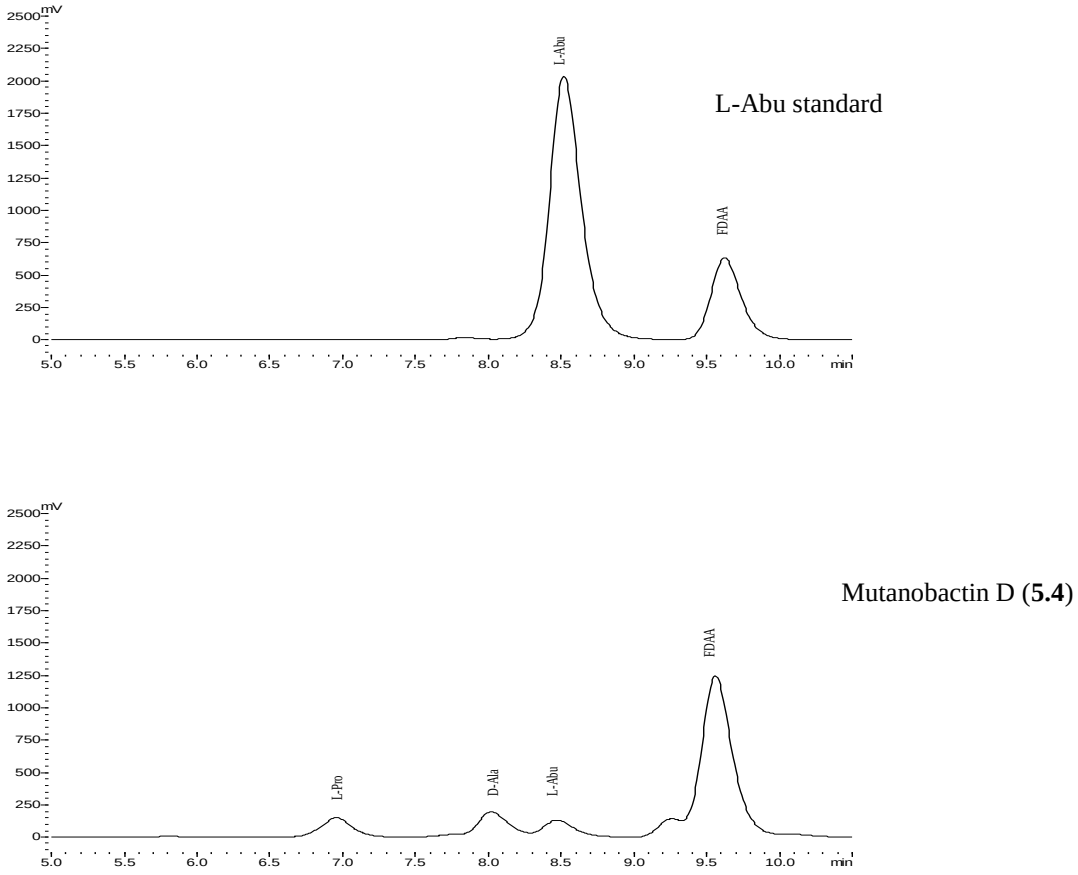

Figure A5. HPLC analysis of FDAA derivatized hydrolysate mutanobactin D and α -aminobutyric acid standard. (Isocratic elution: 40% MeCN)

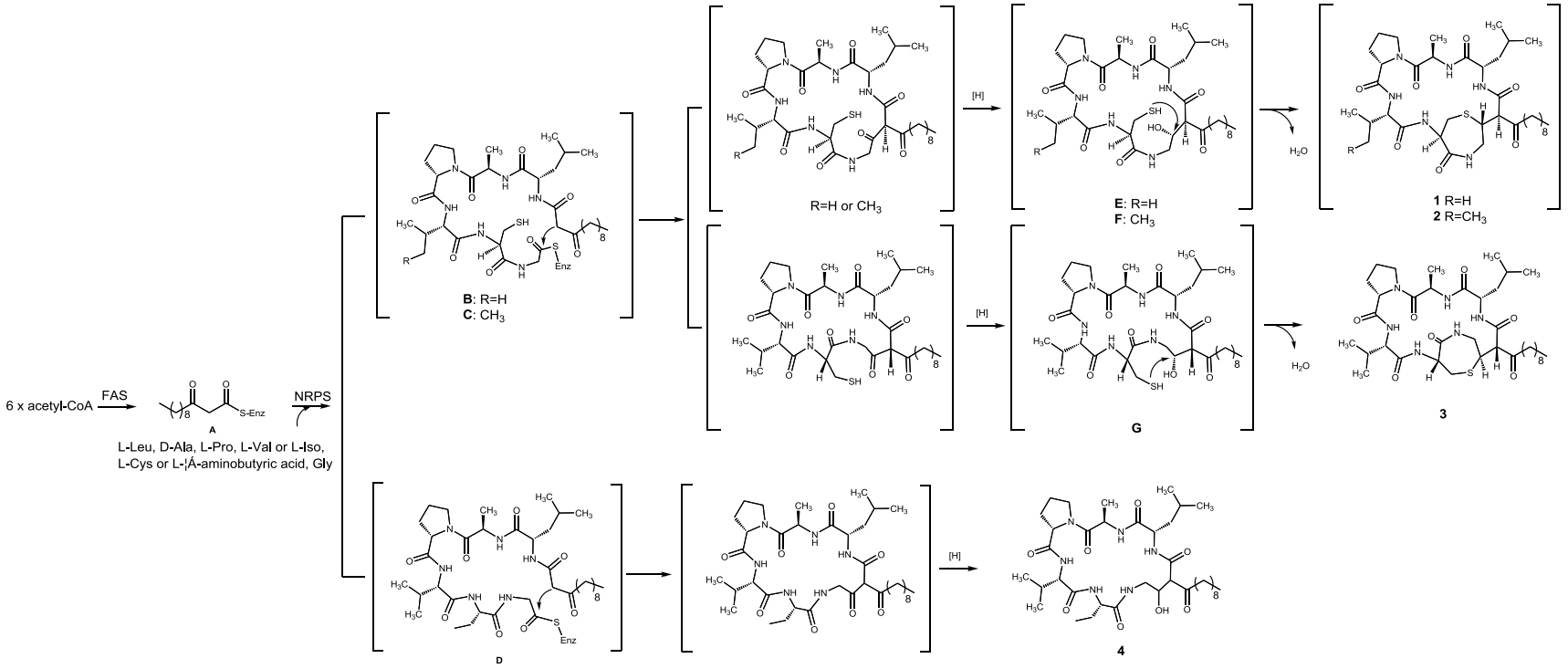

Fig. A6. Proposed biosynthetic pathways for the mutanobactins

^{1}H-NMR spectrum (500 MHz, $CDCl_3$) of atlantinone A (**3.9b**)

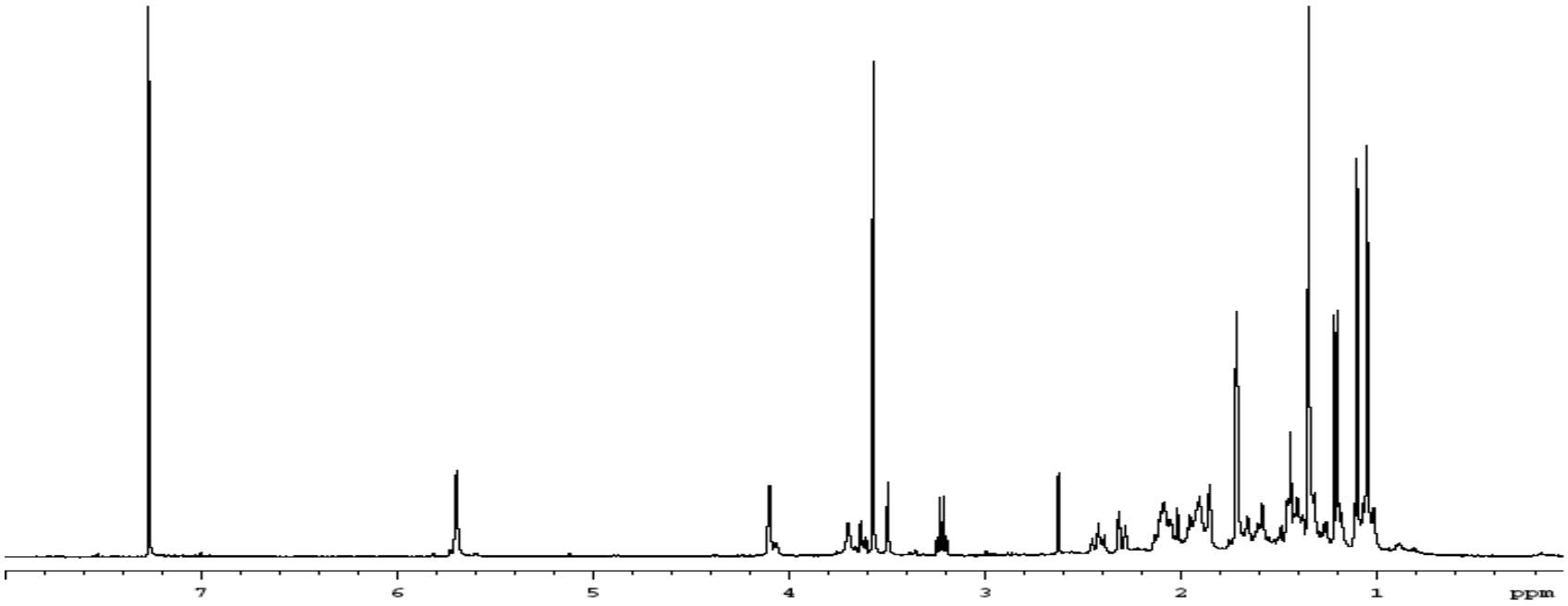

^{13}C-NMR spectrum (125 MHz, $CDCl_3$) of atlantinone A (**3.9b**)

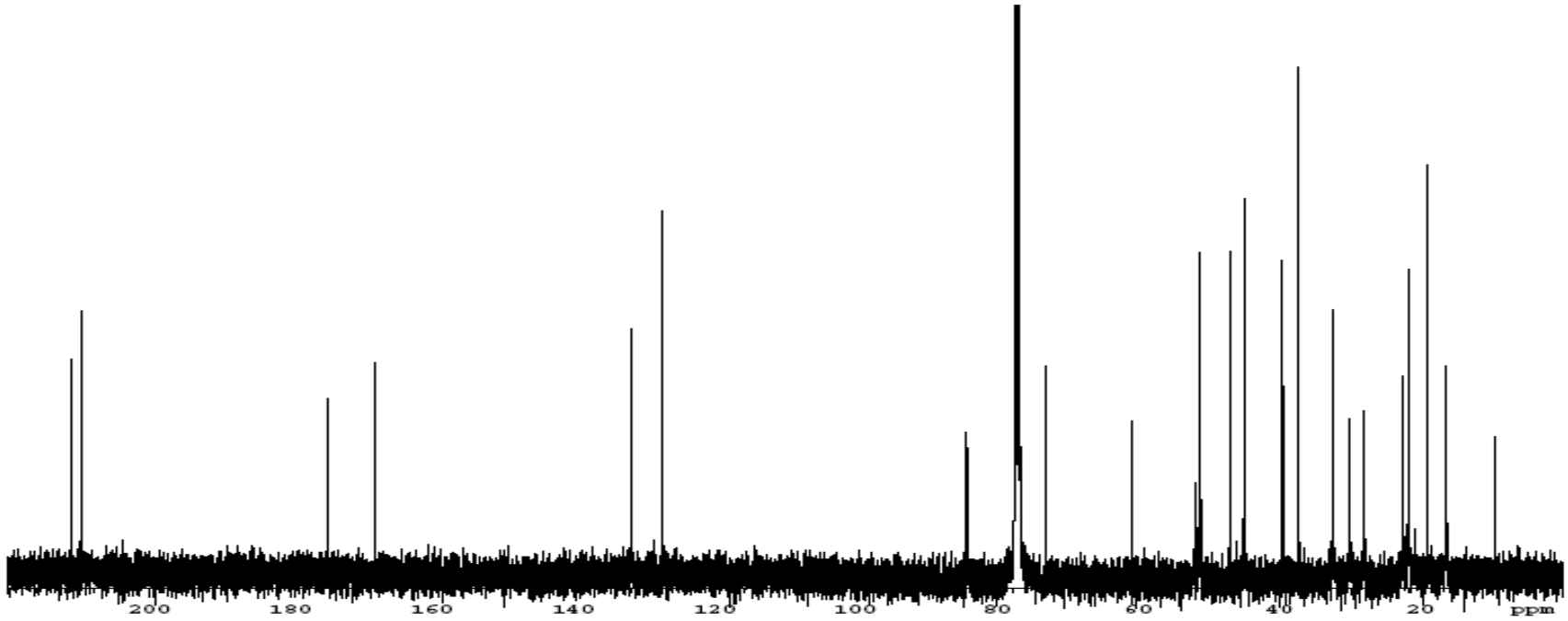

HSQC-NMR spectrum (500 MHz, $CDCl_3$) of atlantinone A (**3.9b**)

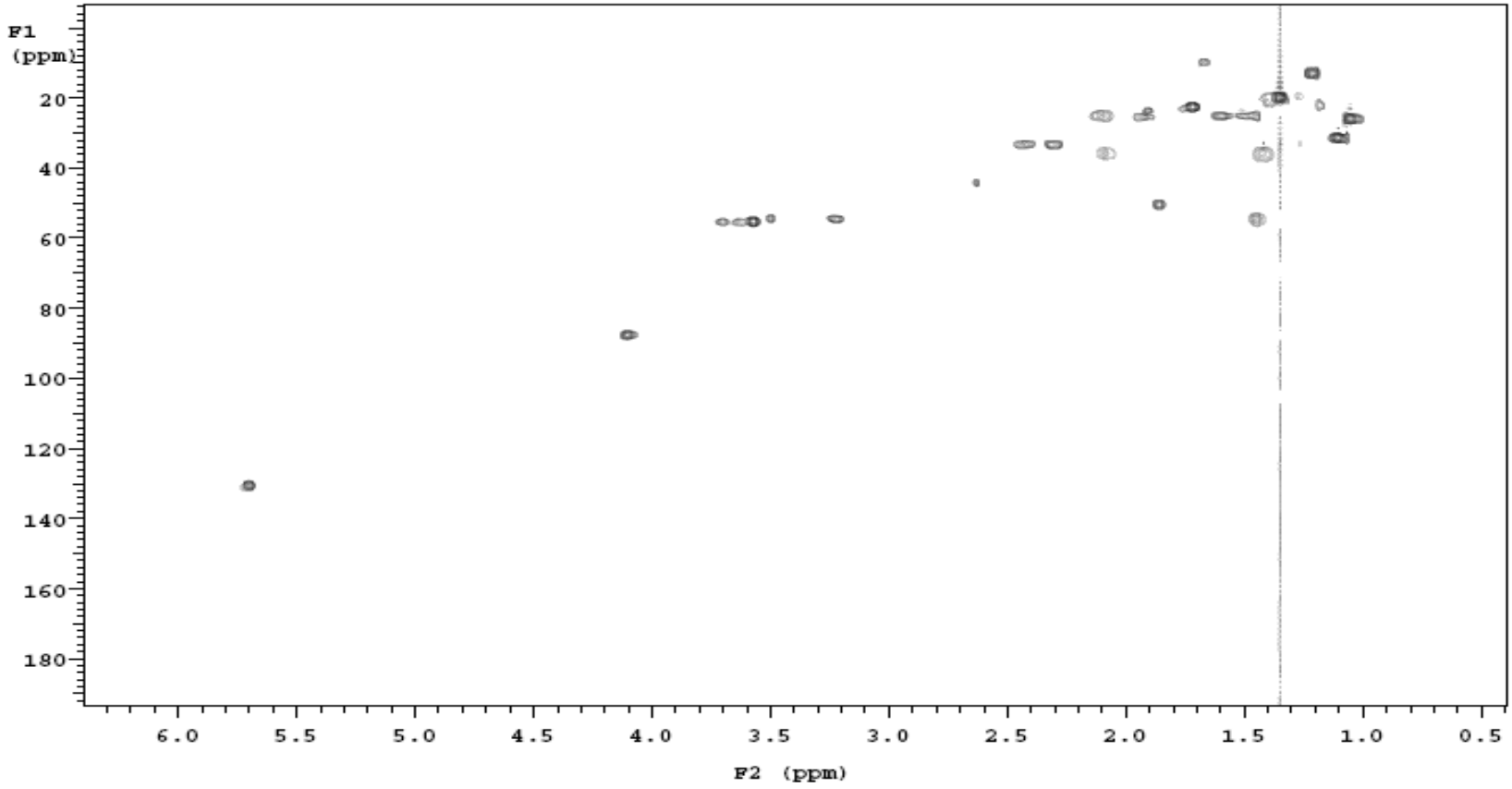

HMBC-NMR spectrum (500 MHz, $CDCl_3$) of atlantinone A (**3.9b**)

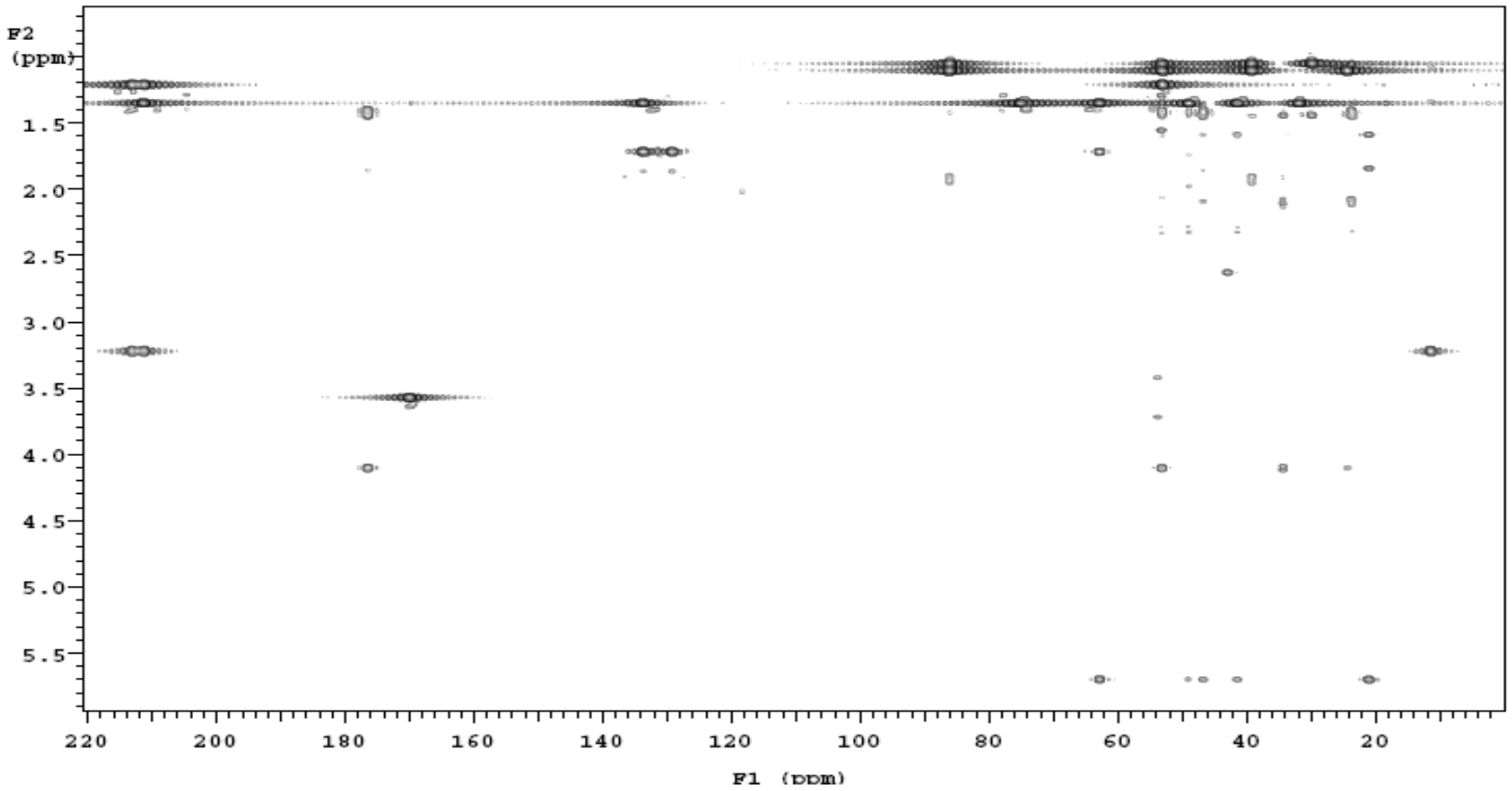

COSY-NMR spectrum (500 MHz, $CDCl_3$) of atlantinone A (**3.9b**)

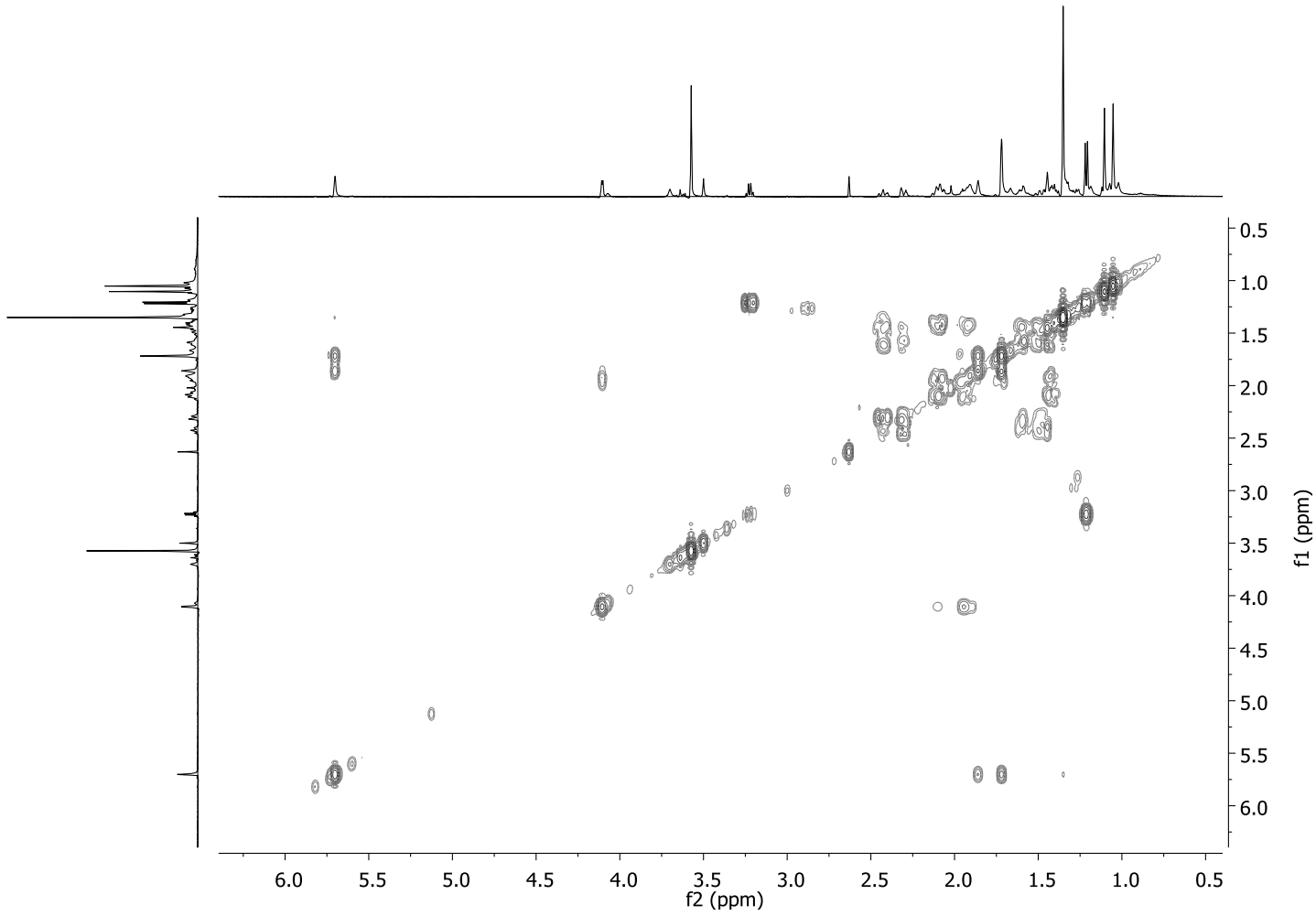

ROESY-NMR spectrum (400 MHz, $CDCl_3$) of atlantinone A (**3.9b**)

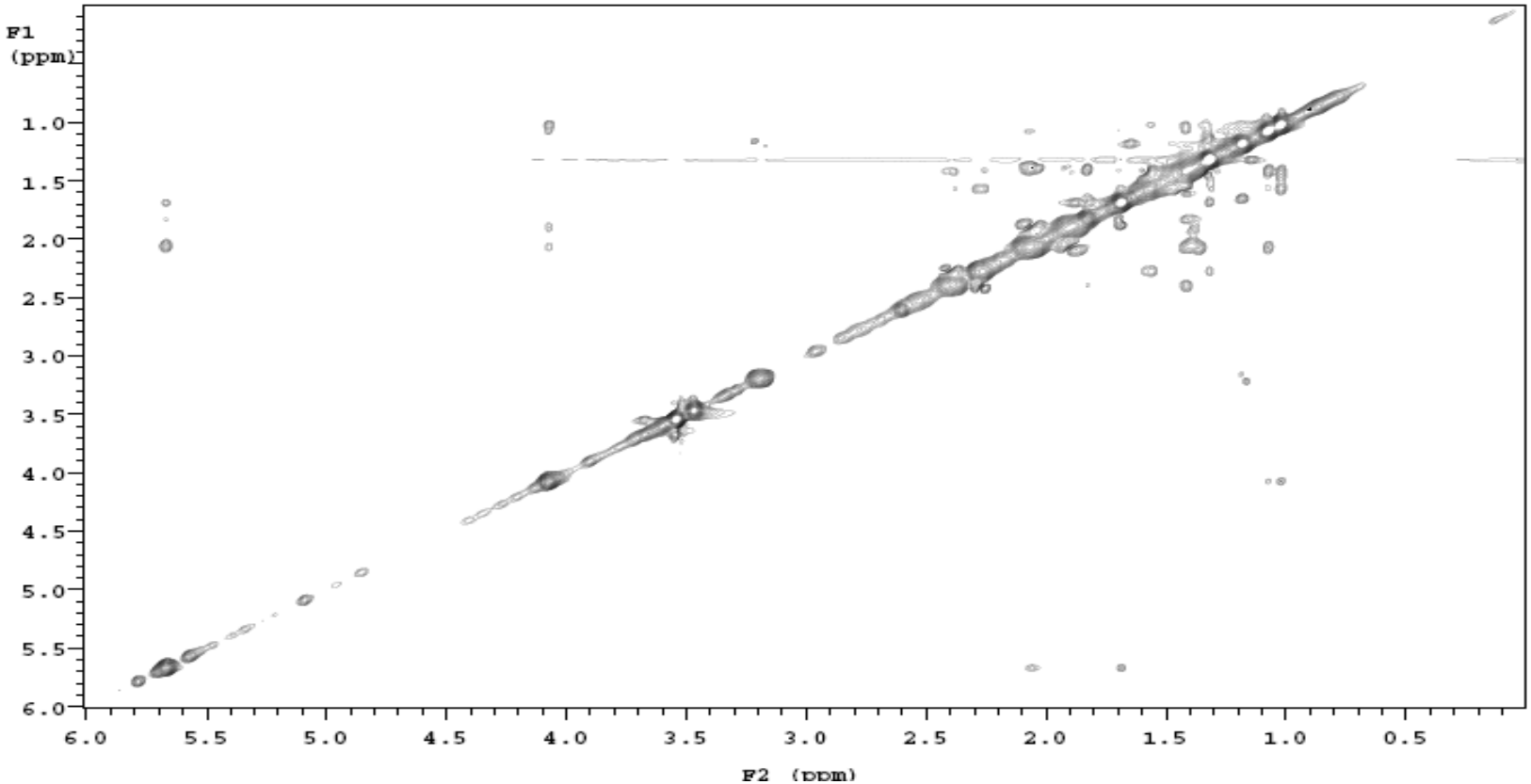

^{1}H-NMR spectrum (500 MHz, CD_3OD) of atlantinone A (**3.9a**)

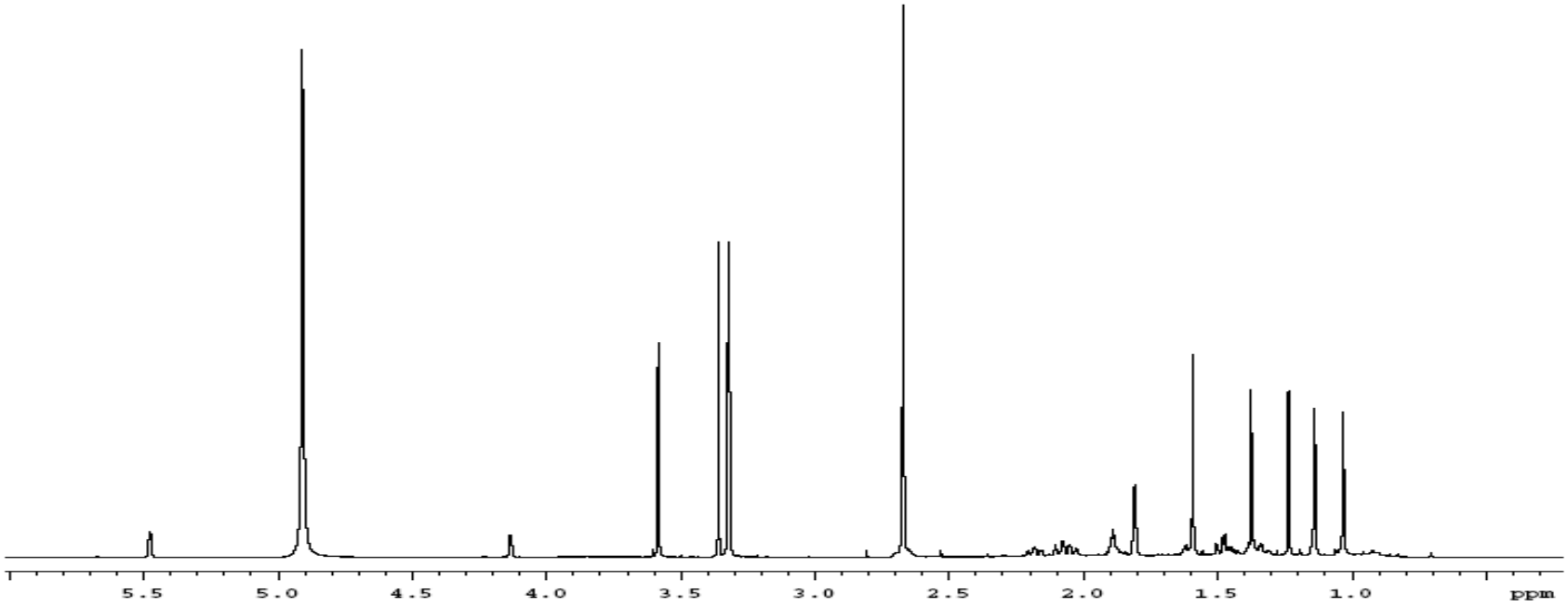

^{13}C-NMR spectrum (125 MHz, CD_3OD) of atlantinone A (**3.9a**)

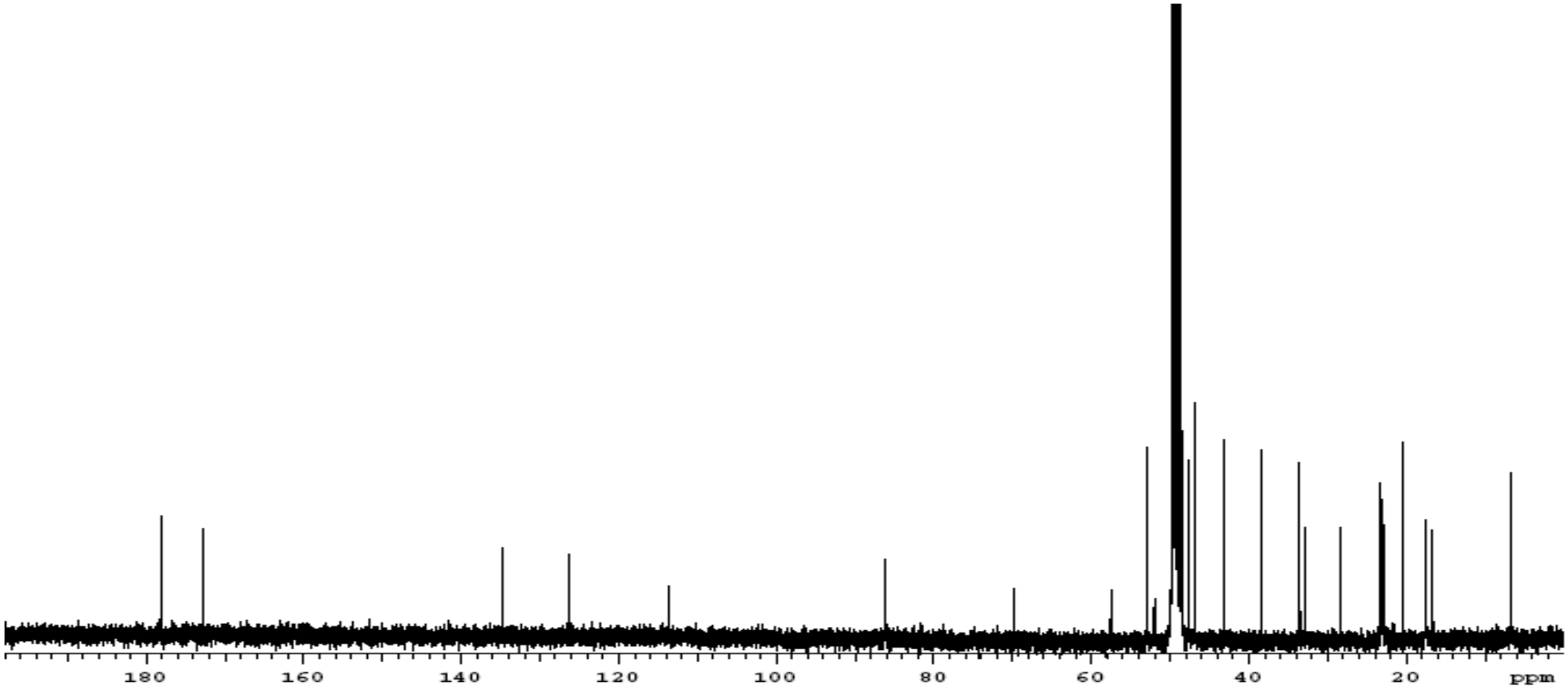

HSQC-NMR spectrum (500 MHz, CD_3OD) of atlantinone A (**3.9a**)

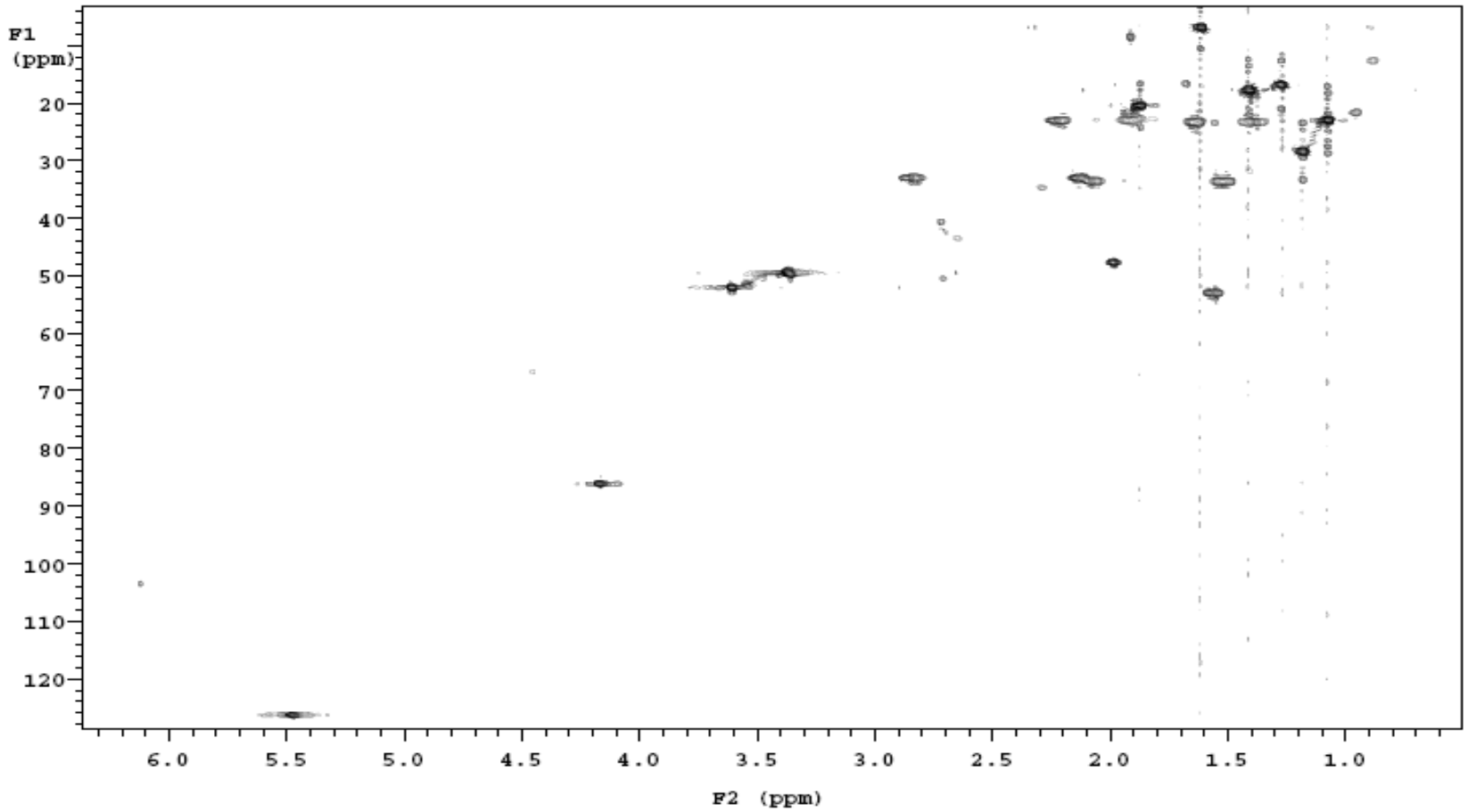

HMBC-NMR spectrum (500 MHz, CD_3OD) of atlantinone A (**3.9a**)

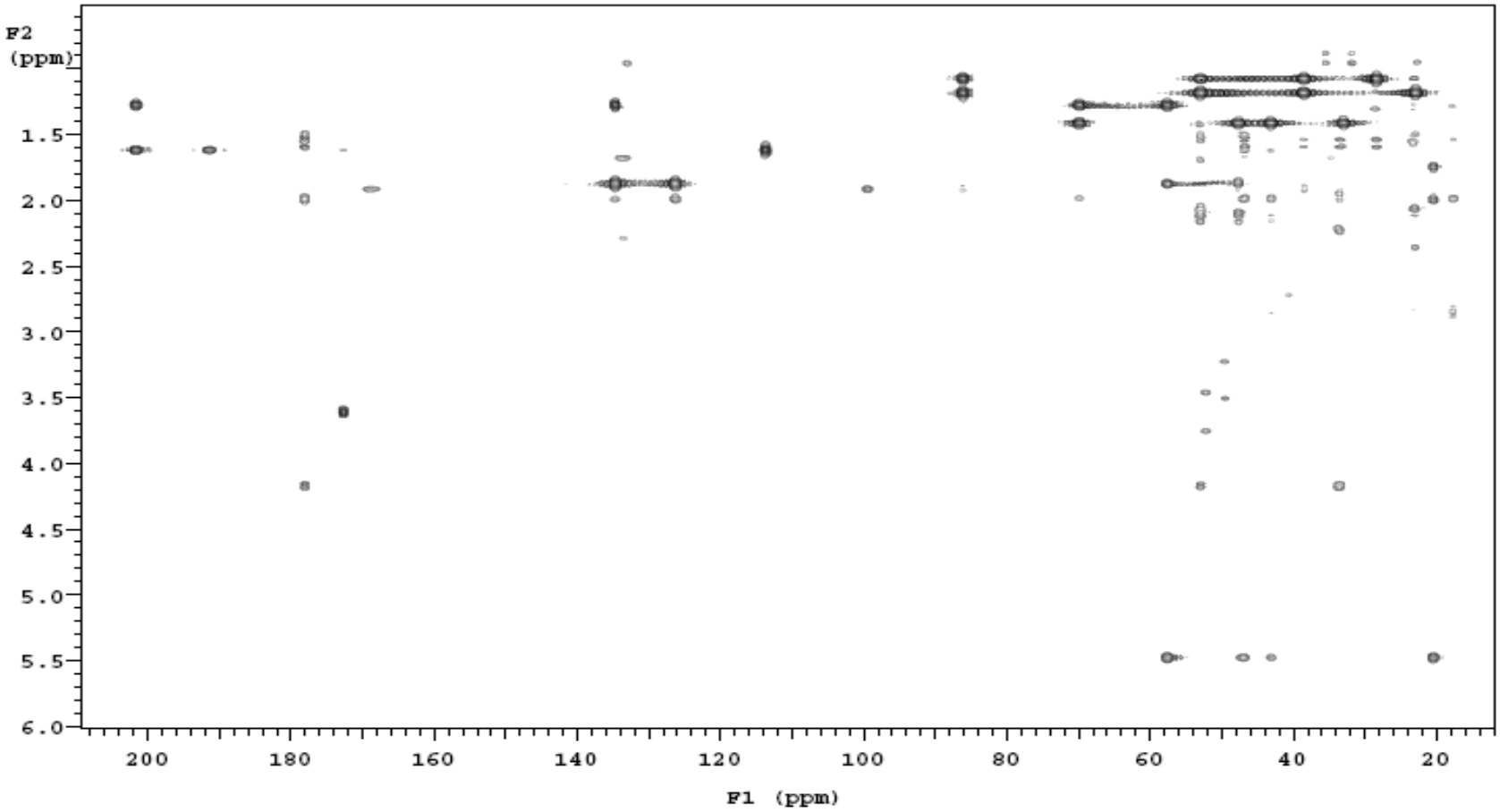

ROESY-NMR spectrum (500 MHz, CD_3OD) of atlantinone A (**3.9a**)

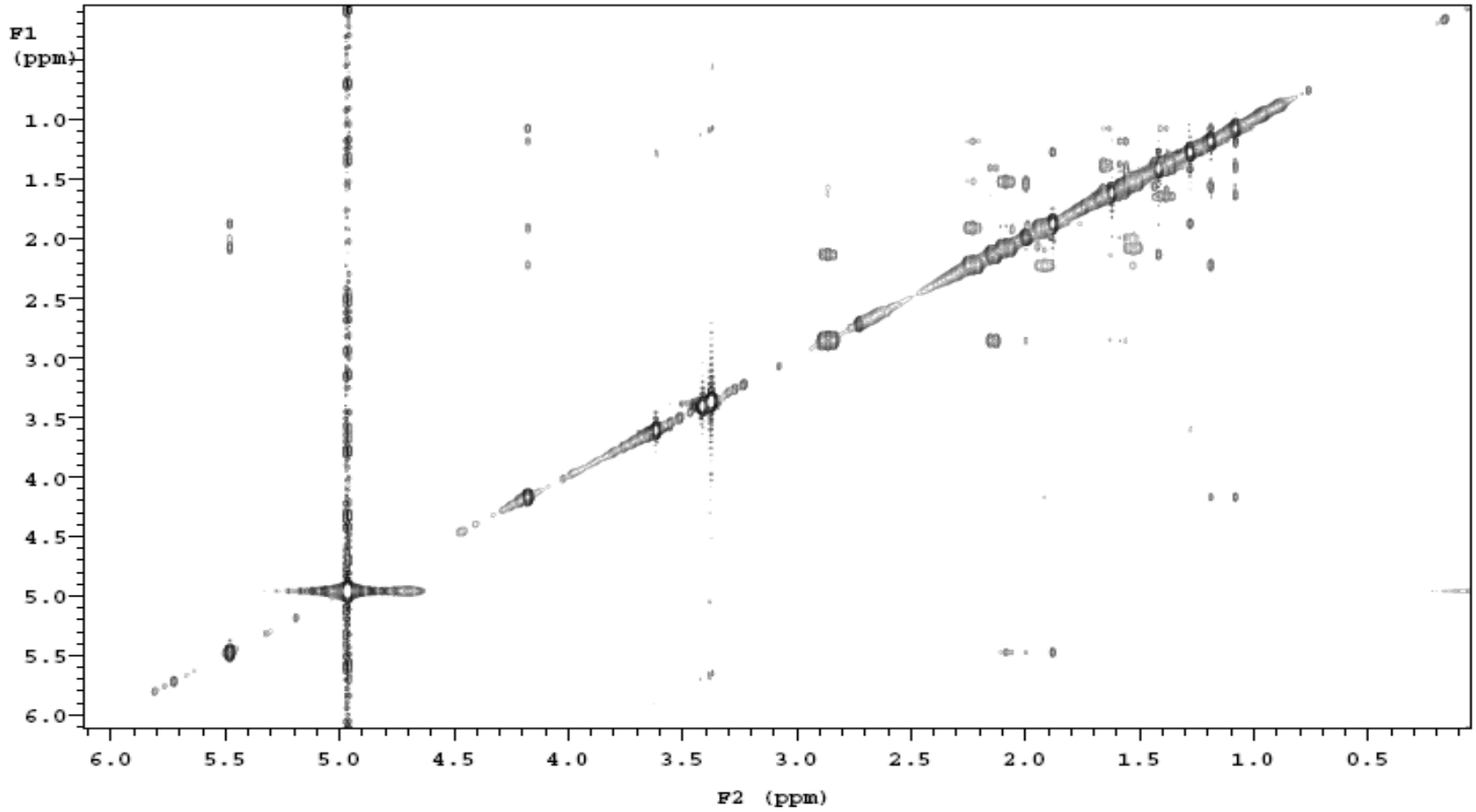

^{1}H-NMR spectrum (500 MHz, $CDCl_3$) of atlantinone B (**3.10**)

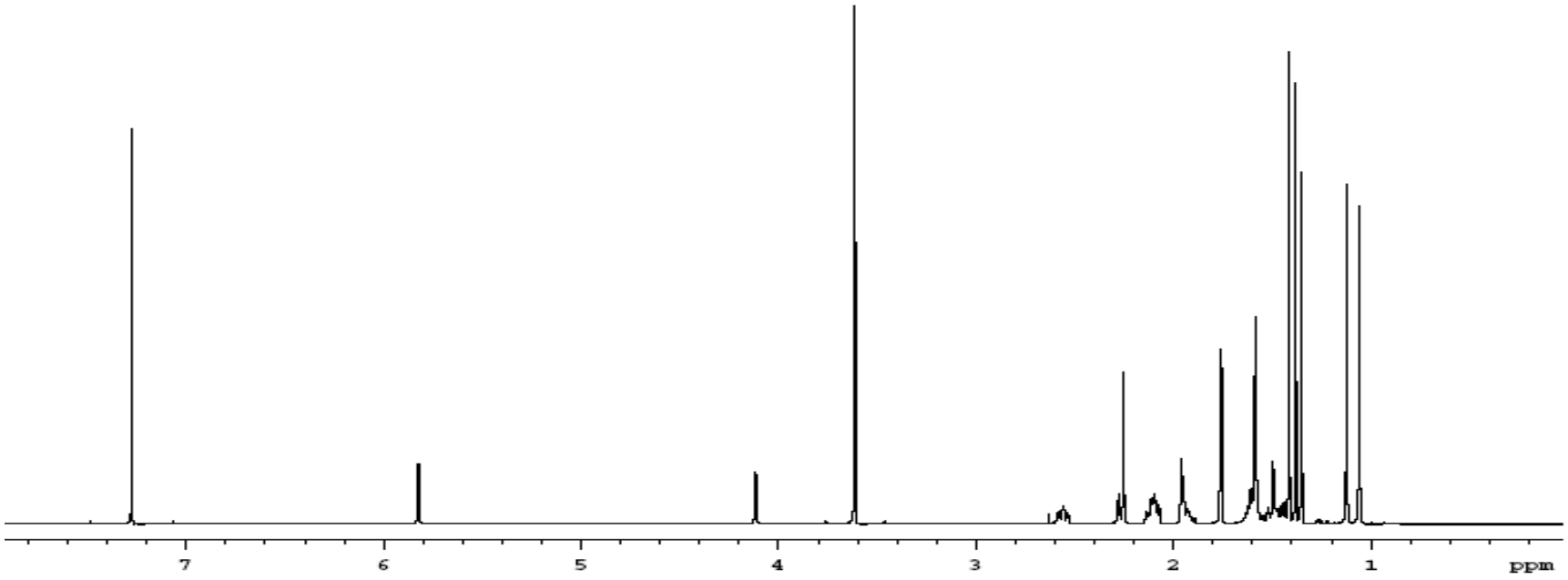

^{13}C-NMR (125 MHz, $CDCl_3$) of atlantinone B (**3.10**)

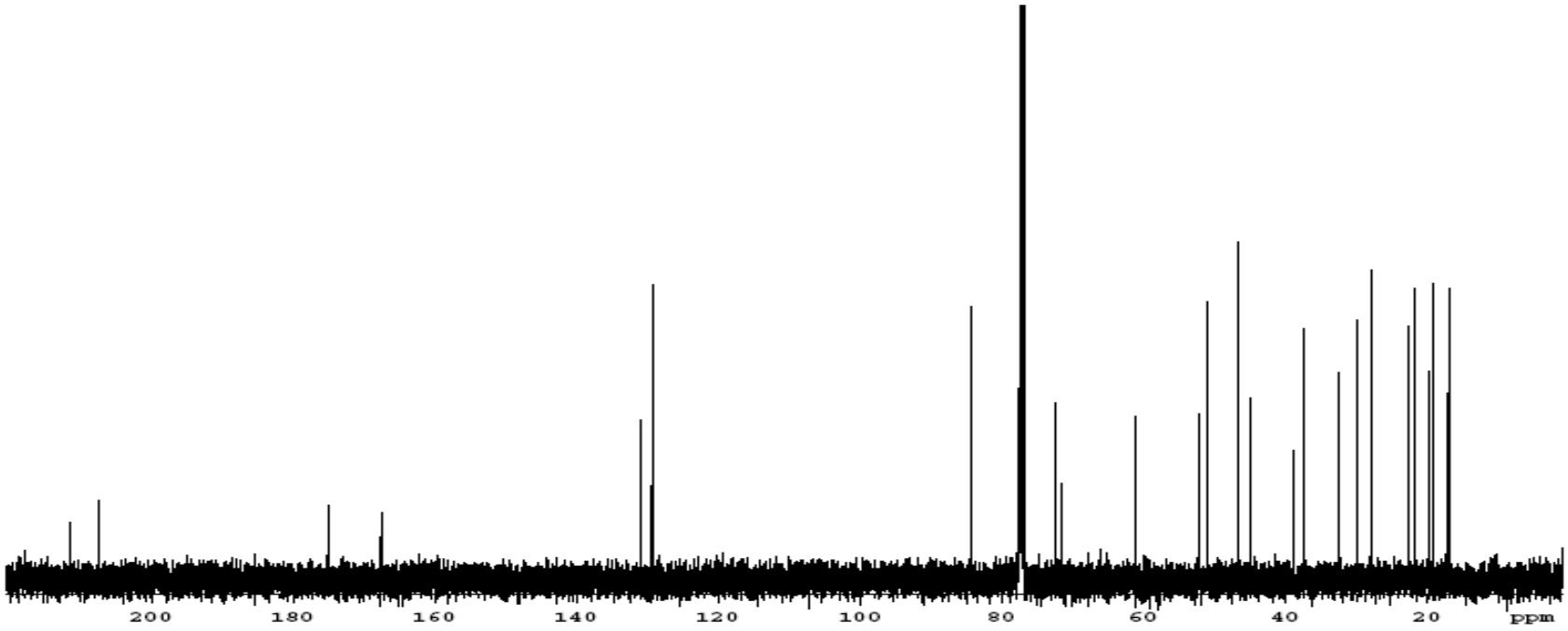

HSQC-NMR spectrum (500 MHz, $CDCl_3$) of atlantinone B (**3.10**)

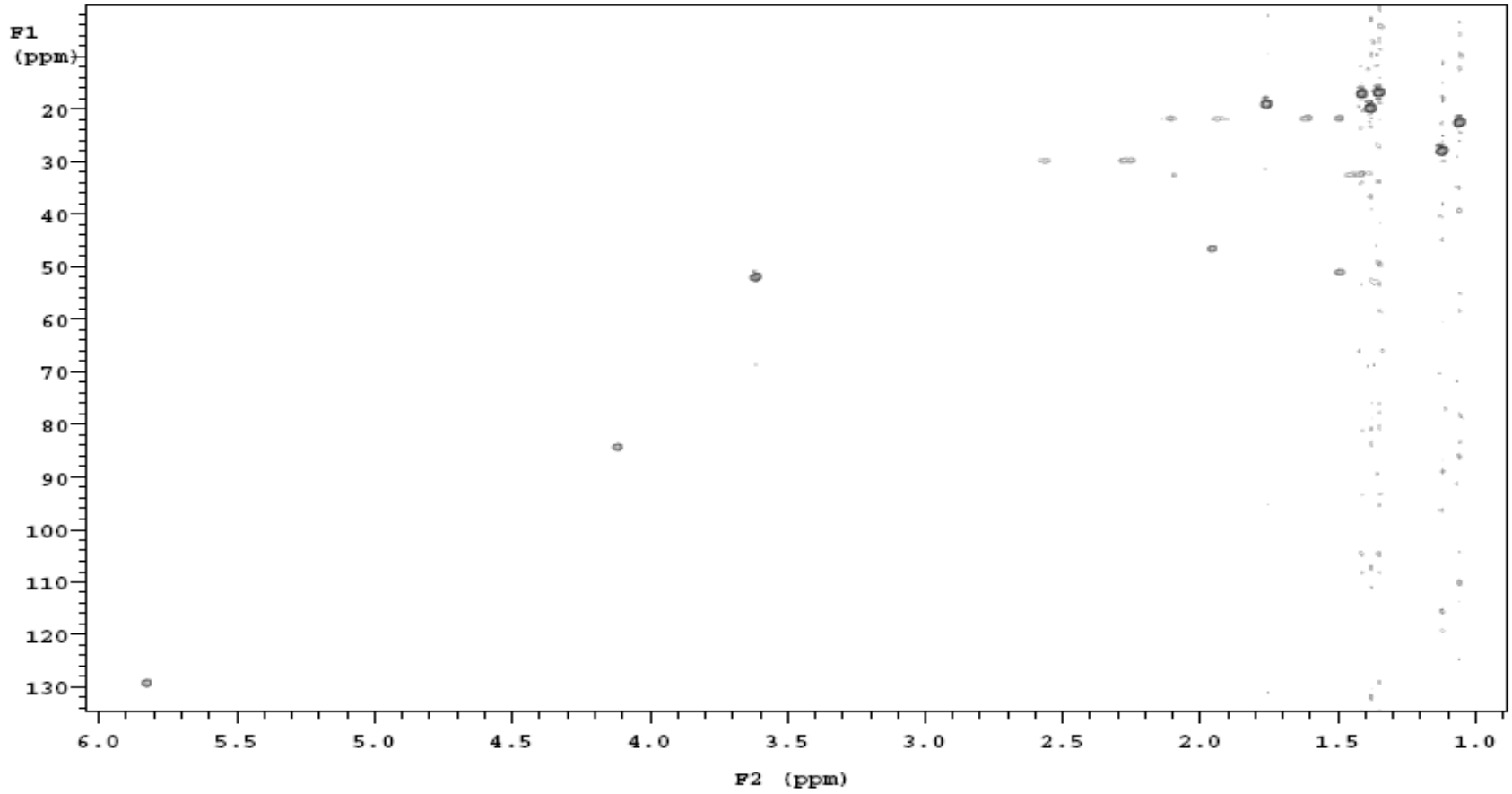

HMBC-NMR spectrum (500 MHz, $CDCl_3$) of atlantinone B (**3.10**)

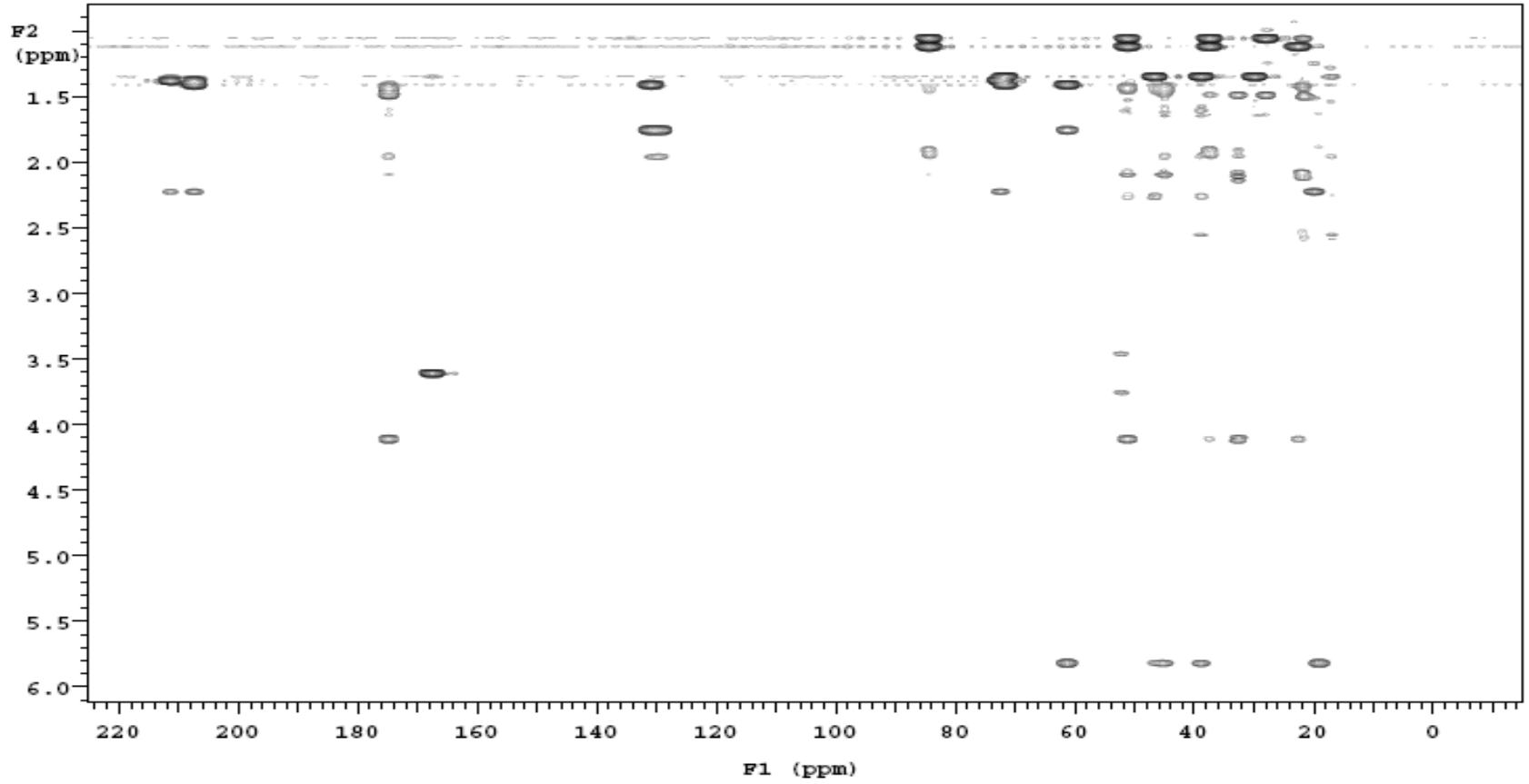

ROESY-NMR spectrum (500 MHz, $CDCl_3$) of atlantinone B (**3.10**)

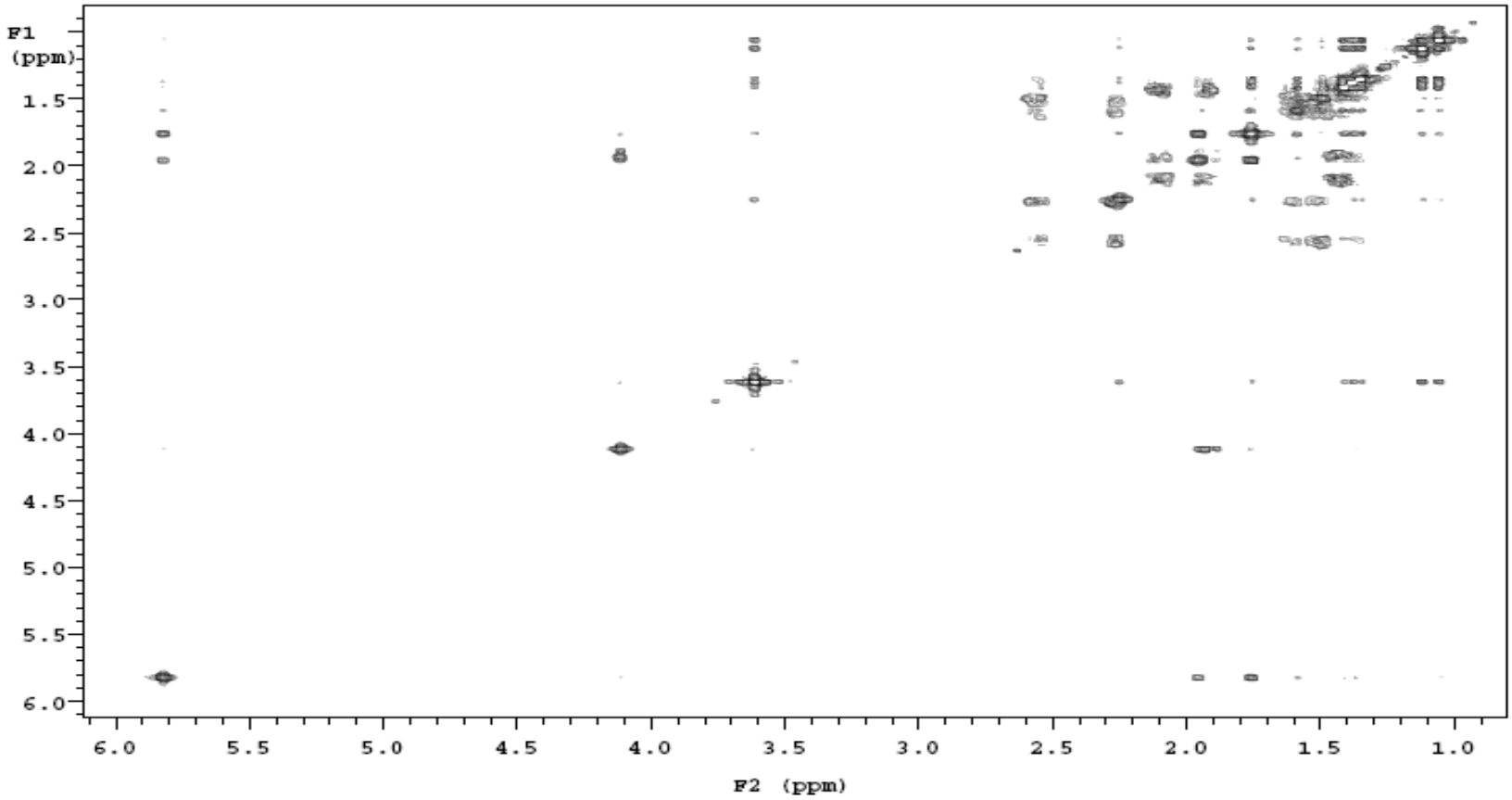

^{1}H-NMR (400 MHz, $CDCl_3$) of sclerotioramine (**3.6**)

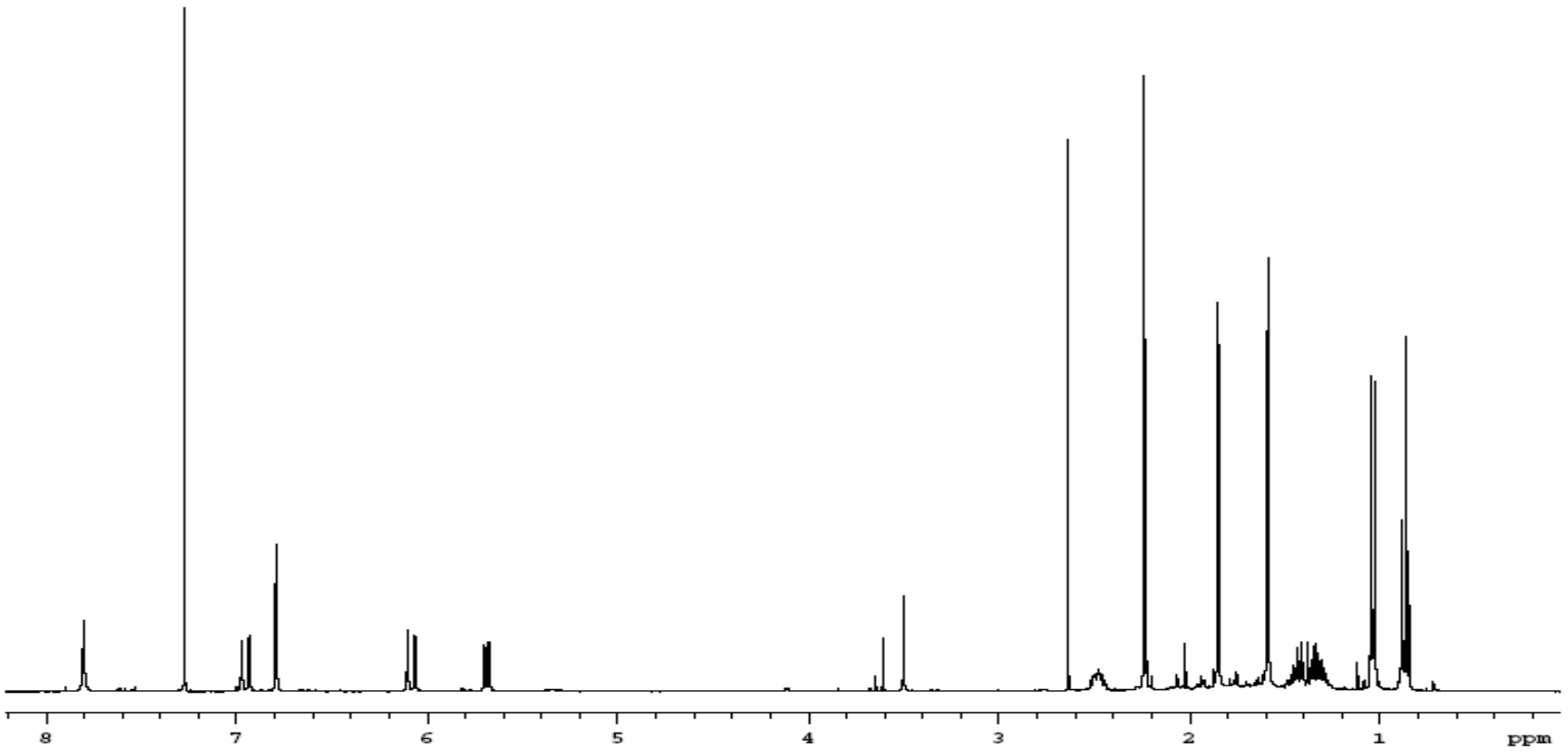

^{13}C-NMR (100 MHz, $CDCl_3$) of sclerotioramine (**3.6**)

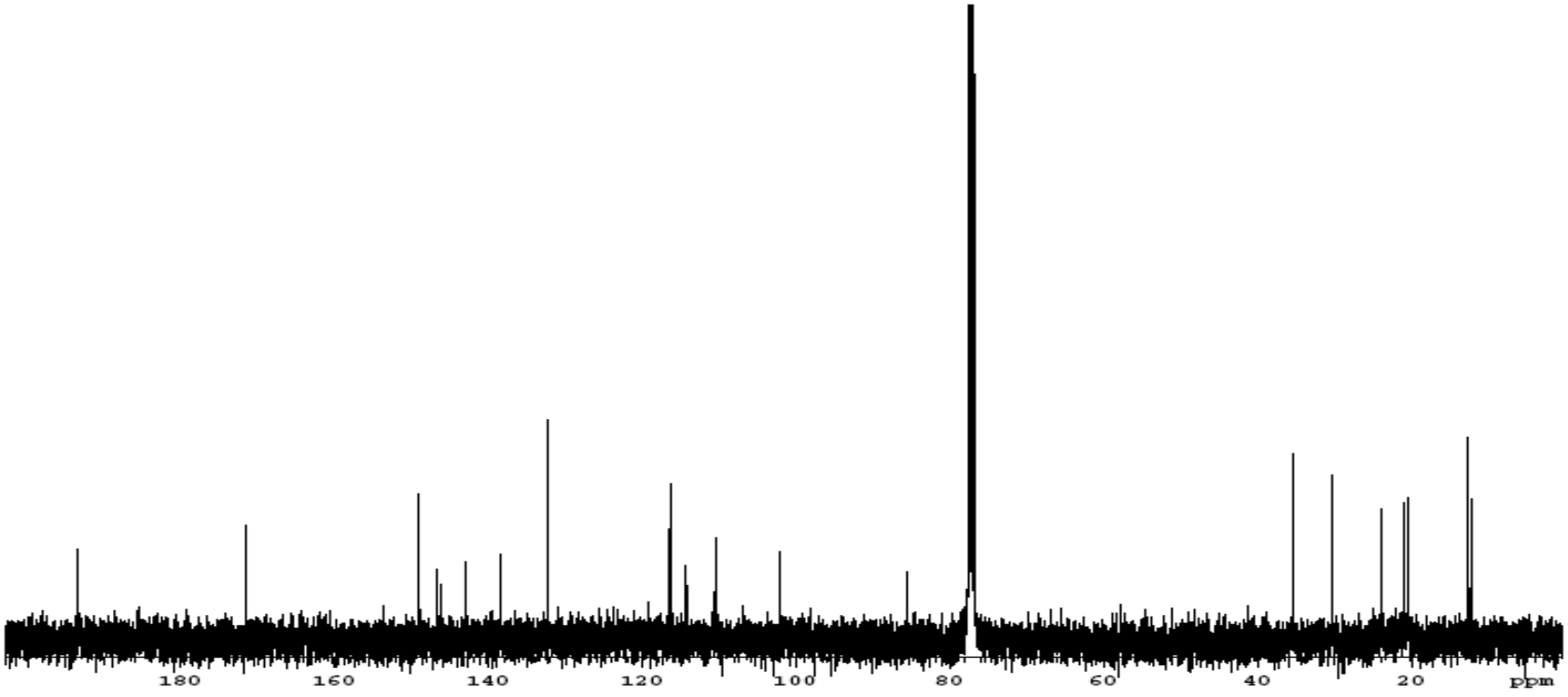

HSQC-NMR (500 MHz, $CDCl_3$) of sclerotioramine (**3.6**)

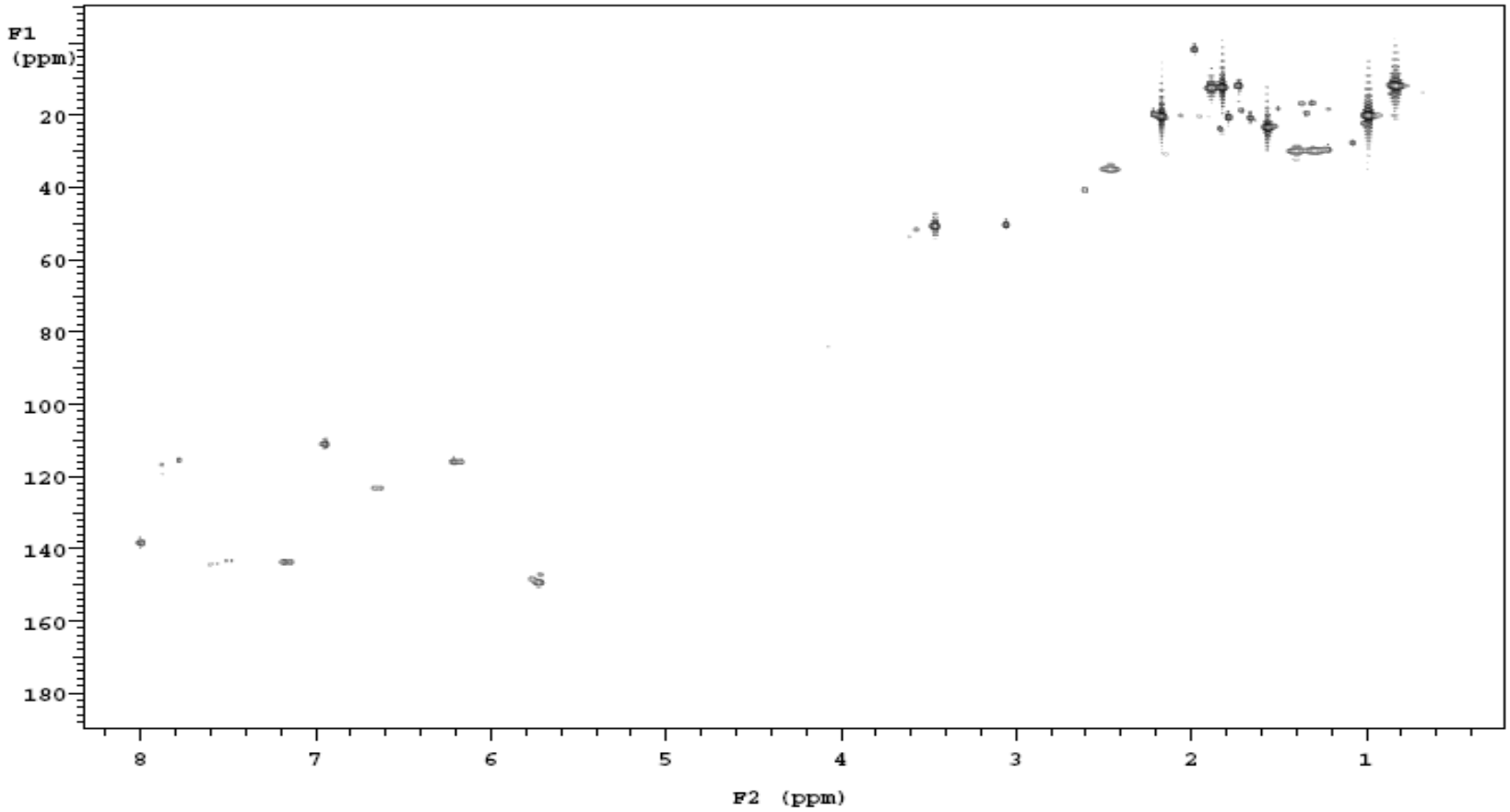

HMBC-NMR (500 MHz, $CDCl_3$) of sclerotioramine (**3.6**)

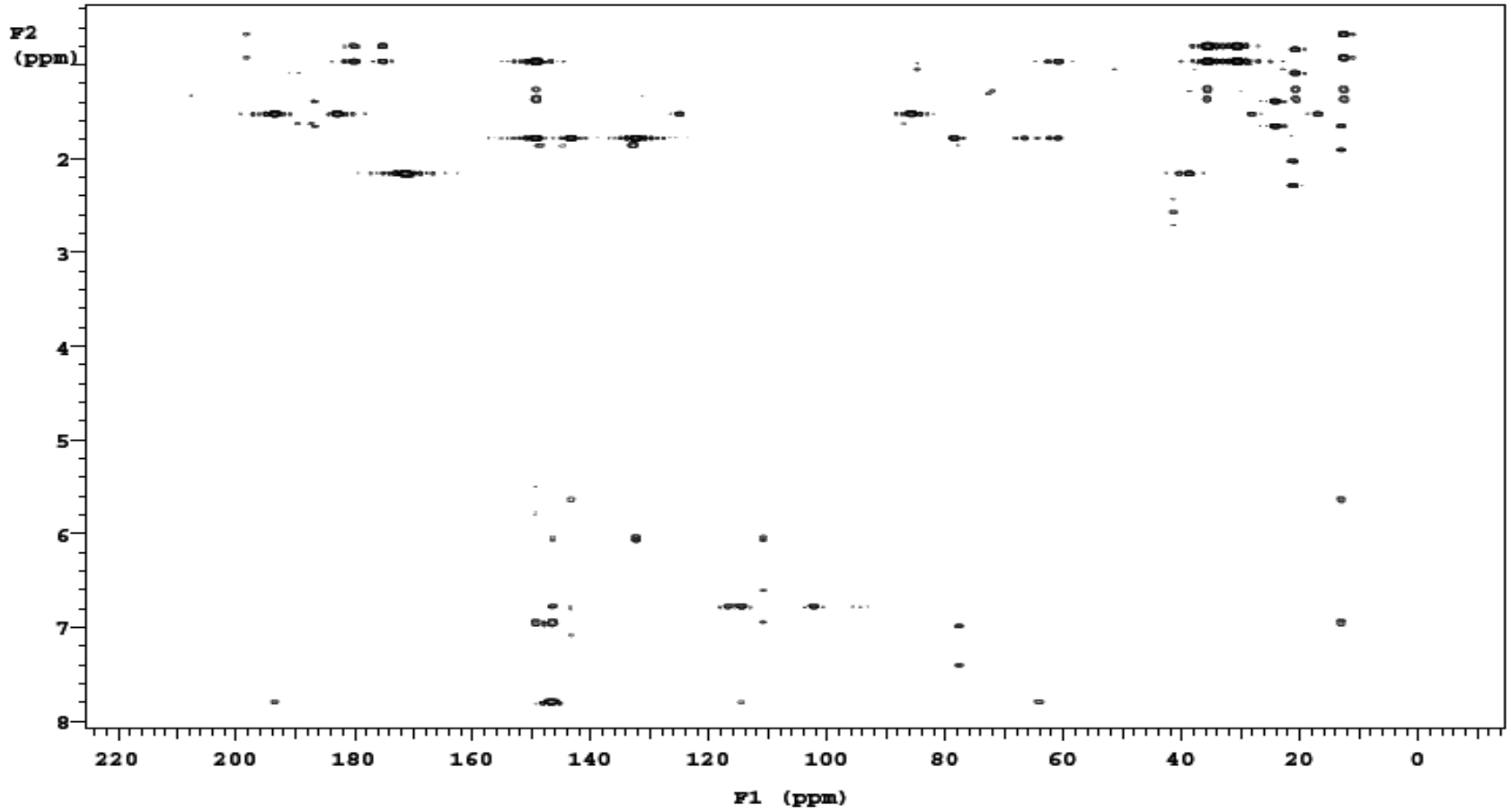

COSY-NMR (400 MHz, $CDCl_3$) of sclerotioramine (**3.6**)

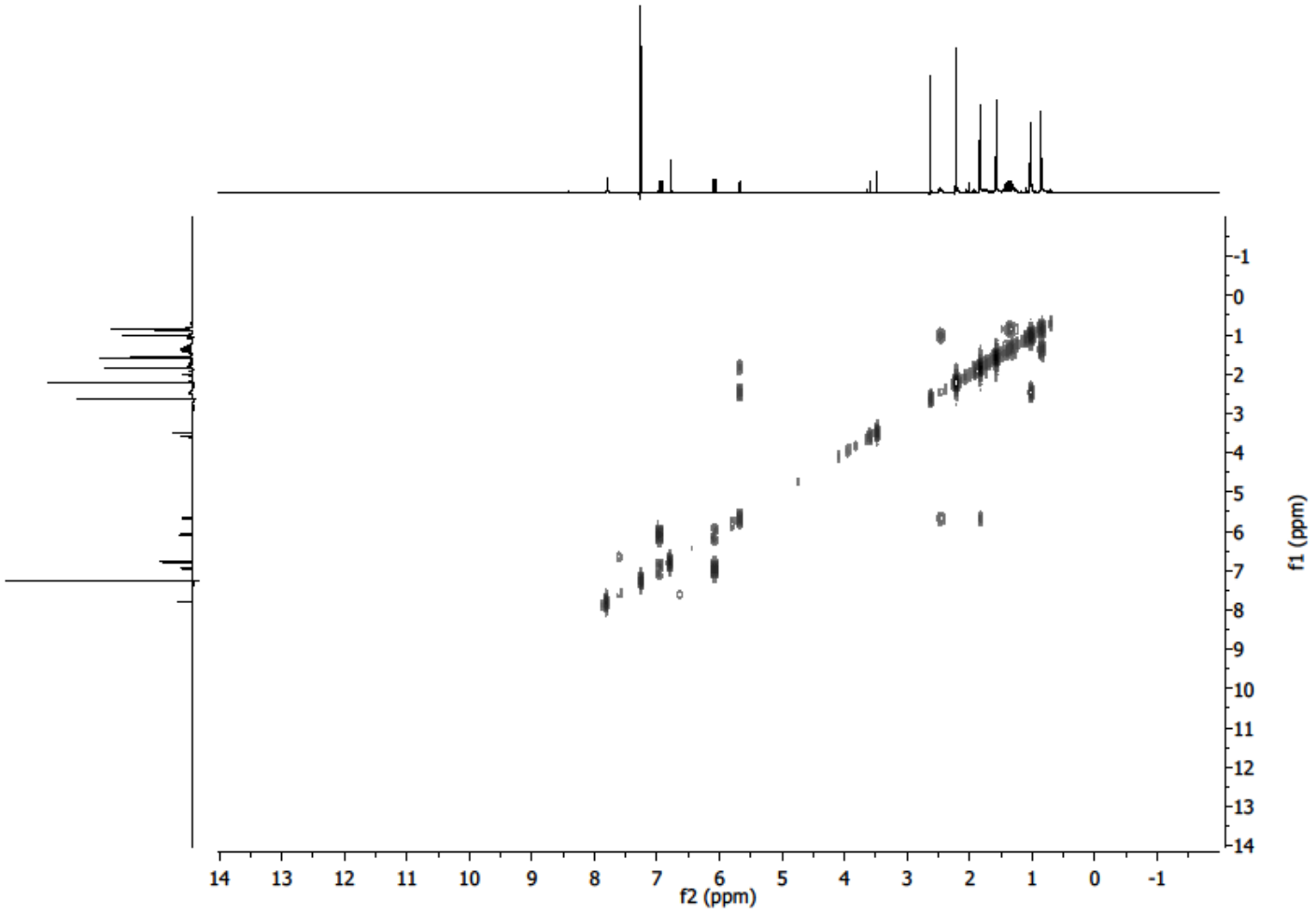

^{1}H-NMR (500 MHz, $CDCl_3$) of pencolide (**3.7**)

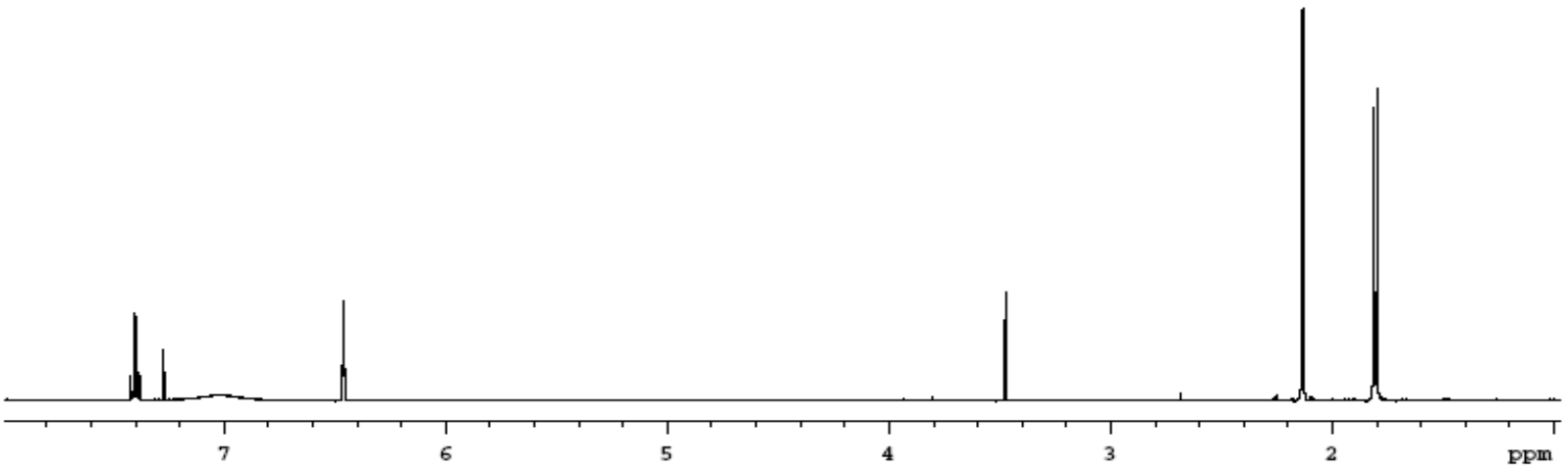

^{13}C-NMR (125 MHz, $CDCl_3$) of pencolide (**3.7**)

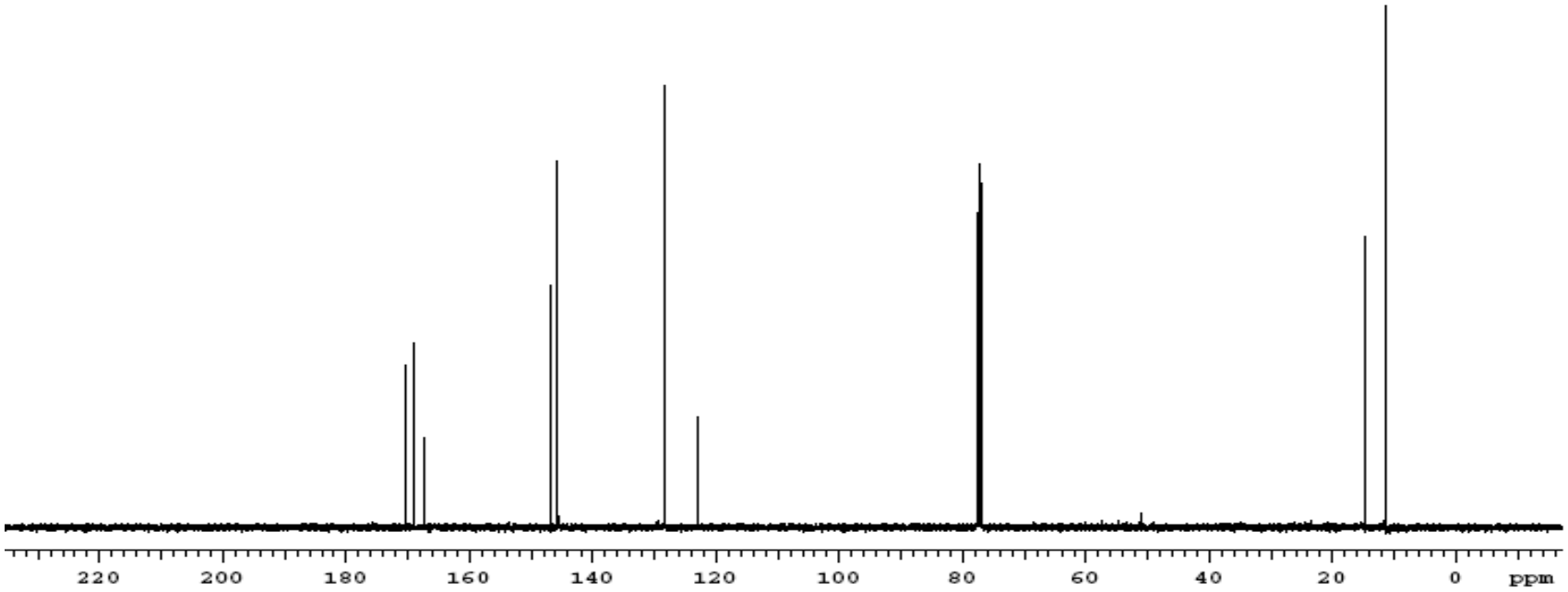

HSQC-NMR (500 MHz, $CDCl_3$) of pencolide (**3.7**)

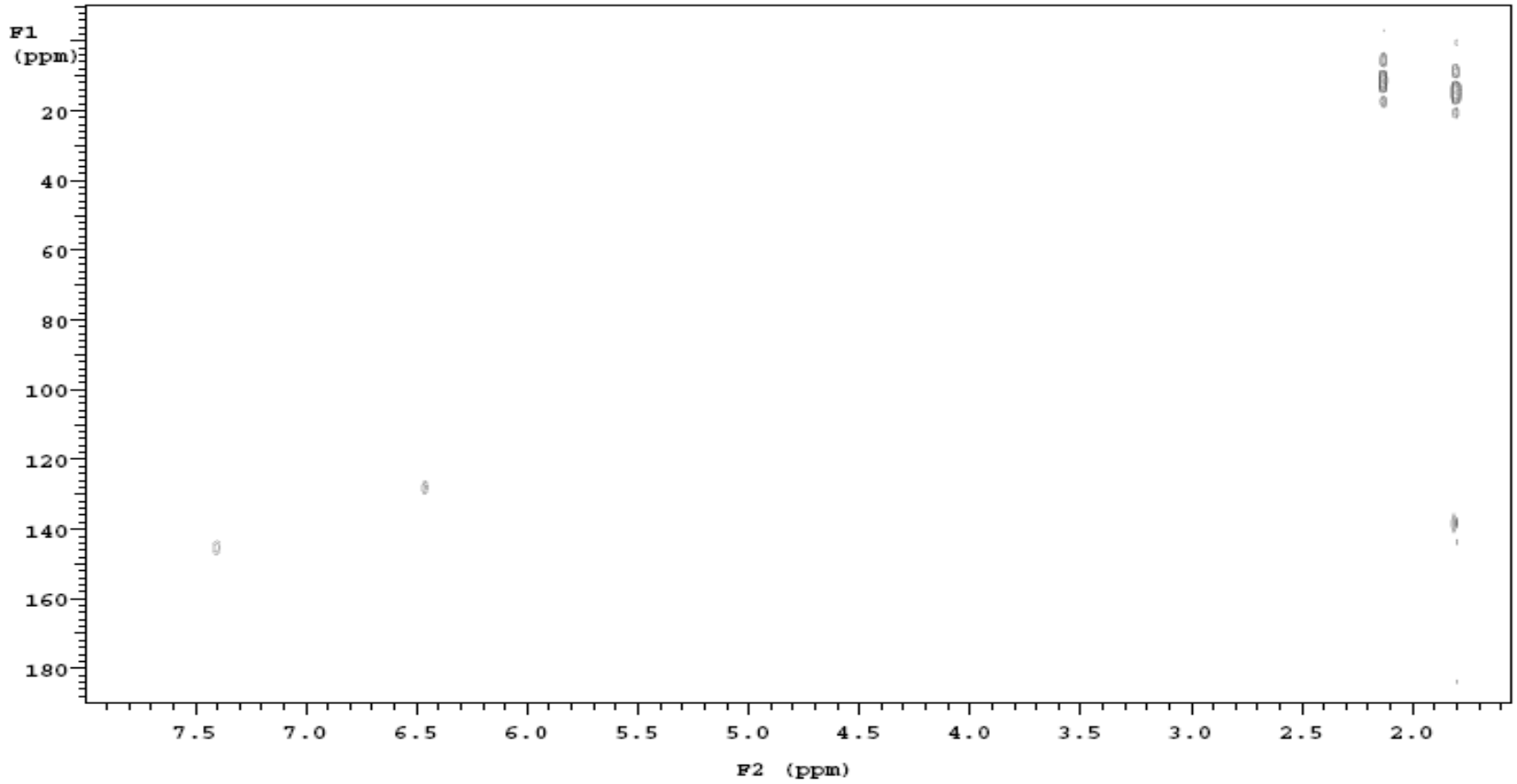

HMBC-NMR (500 MHz, $CDCl_3$) of pencolide (**3.7**)

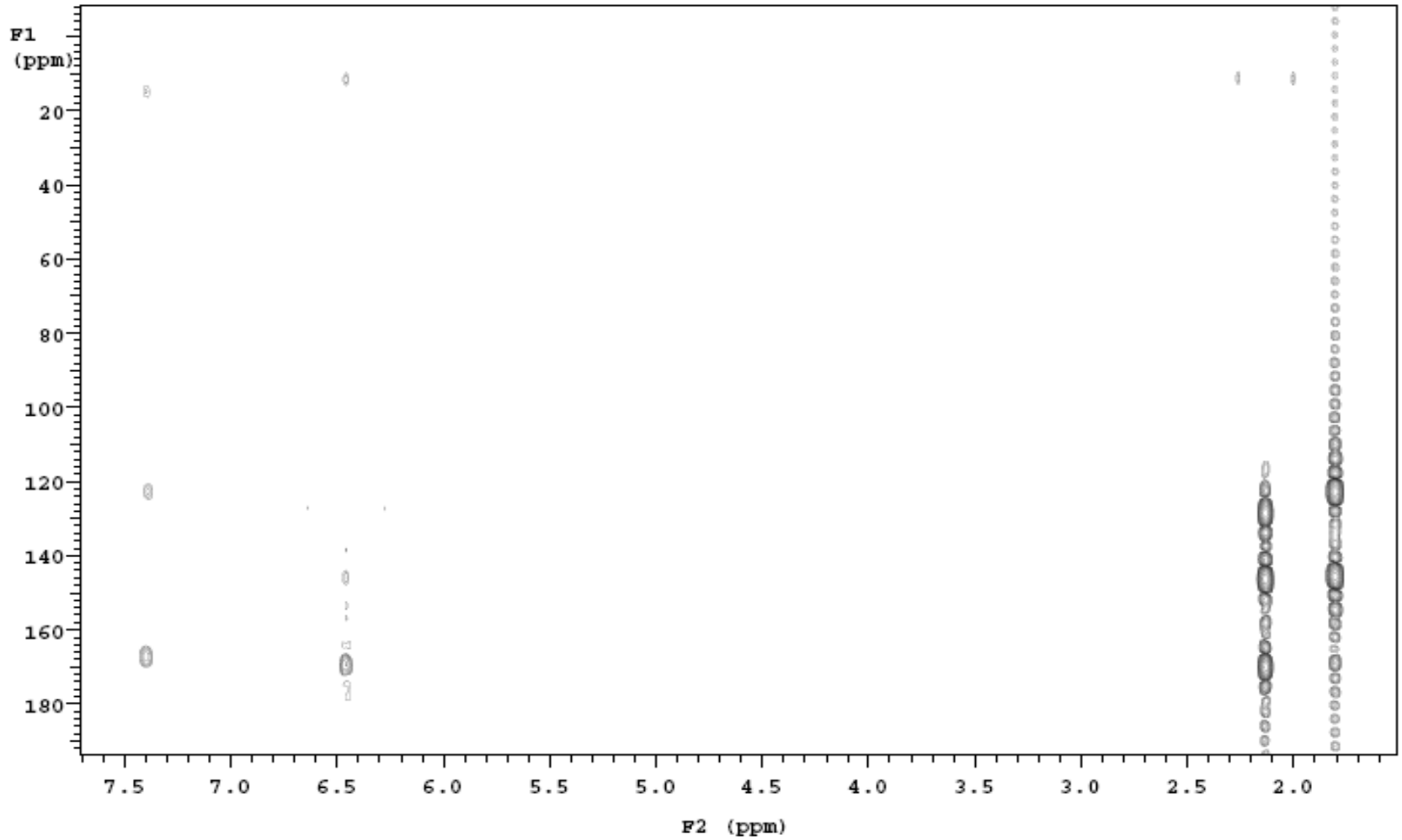

^{1}H-NMR (500 MHz, CD_3OD) of pencolide methyl ester (**3.8**)

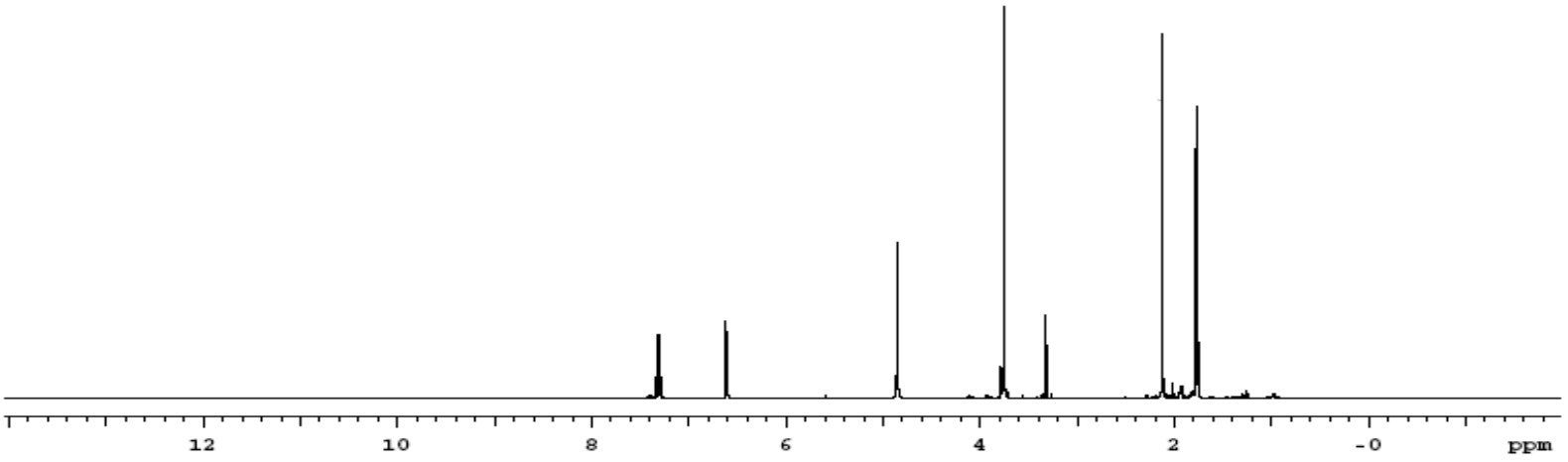

1D difference NOE-NMR (500 MHz, $CDCl_3$) of pencolide methyl ester (**3.8**)

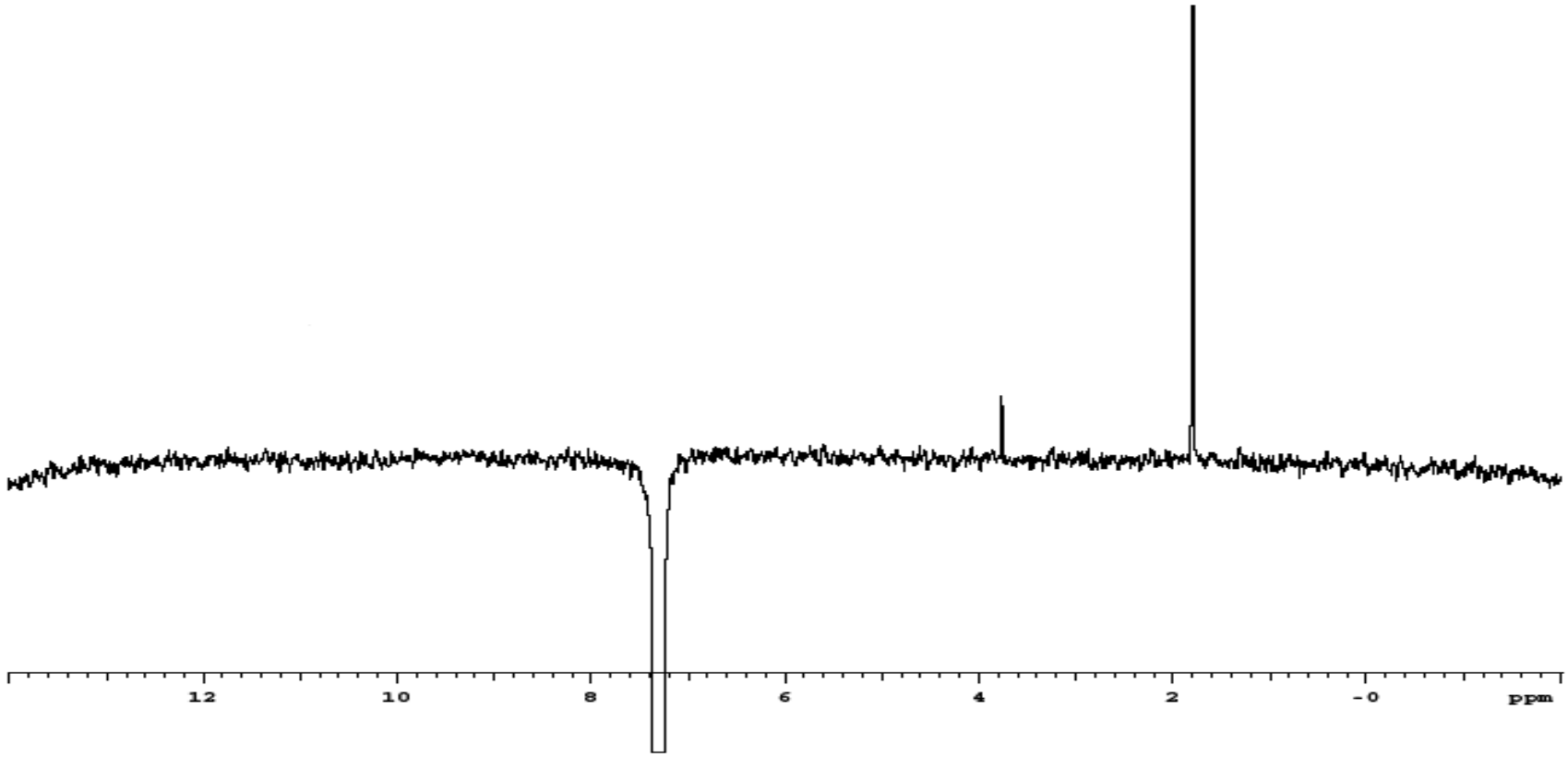

^{1}H-NMR spectrum (500 MHz, $CDCl_3$) of waikialoid A (**4.7**)

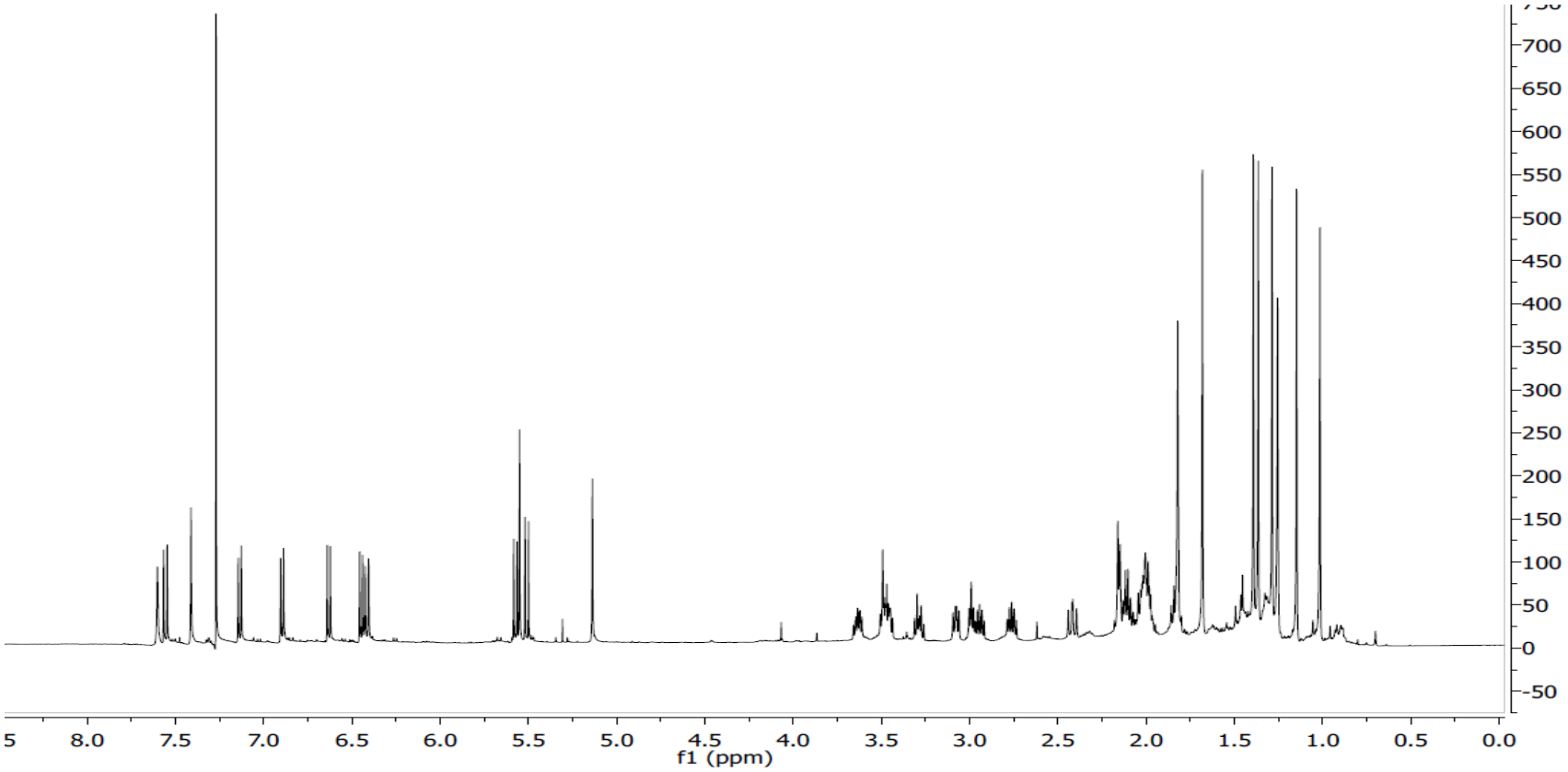

^{13}C-NMR spectrum (100 MHz, $CDCl_3$) of waikialoid A (**4.7**)

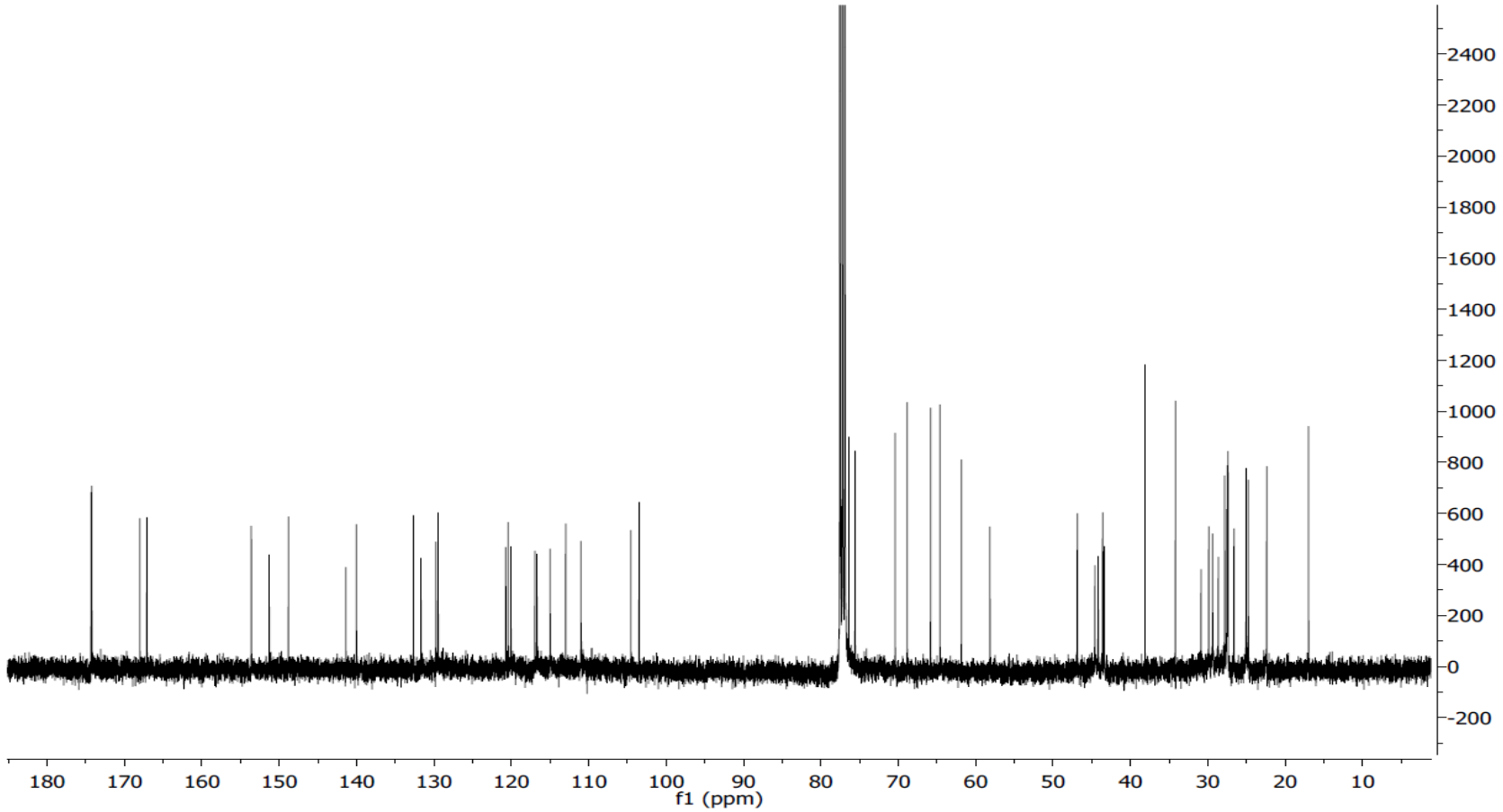

HSQC-NMR spectrum (500 MHz, $CDCl_3$) of waikialoid A (**4.7**)

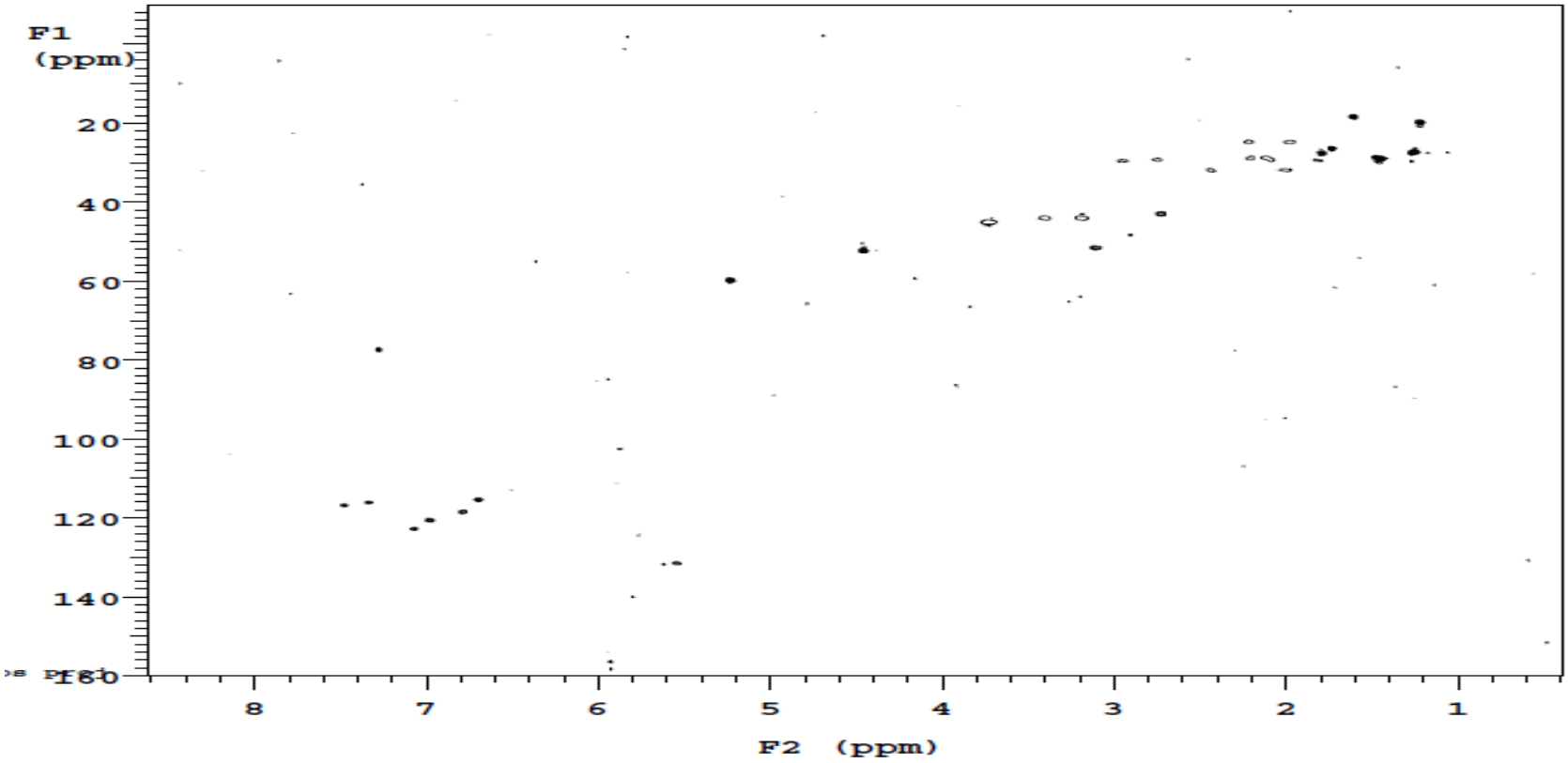

HMBC-NMR spectrum (500 MHz, $CDCl_3$) of waikialoid A (**4.7**)

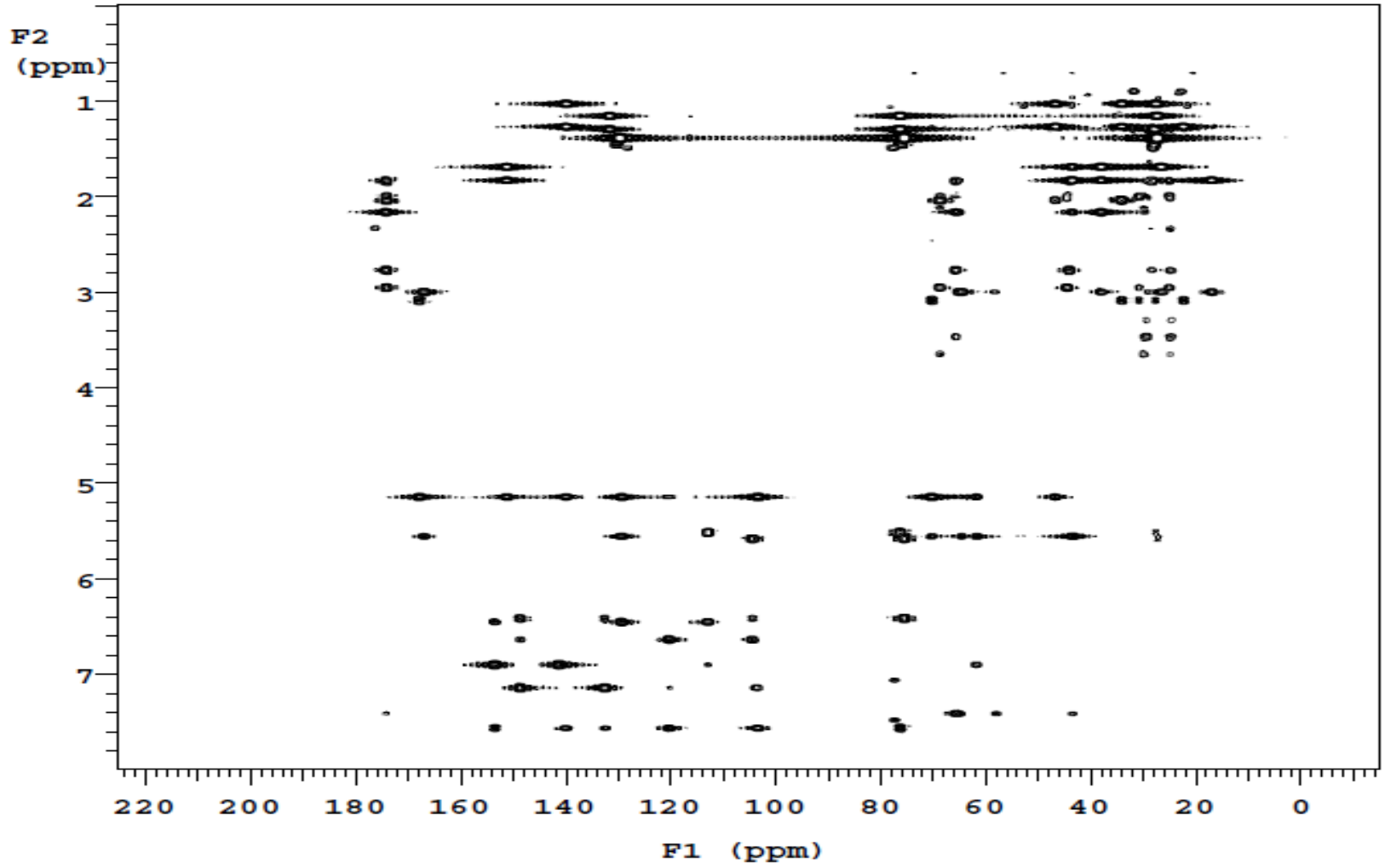

COSY-NMR spectrum (500 MHz, $CDCl_3$) of waikialoid A (**4.7**)

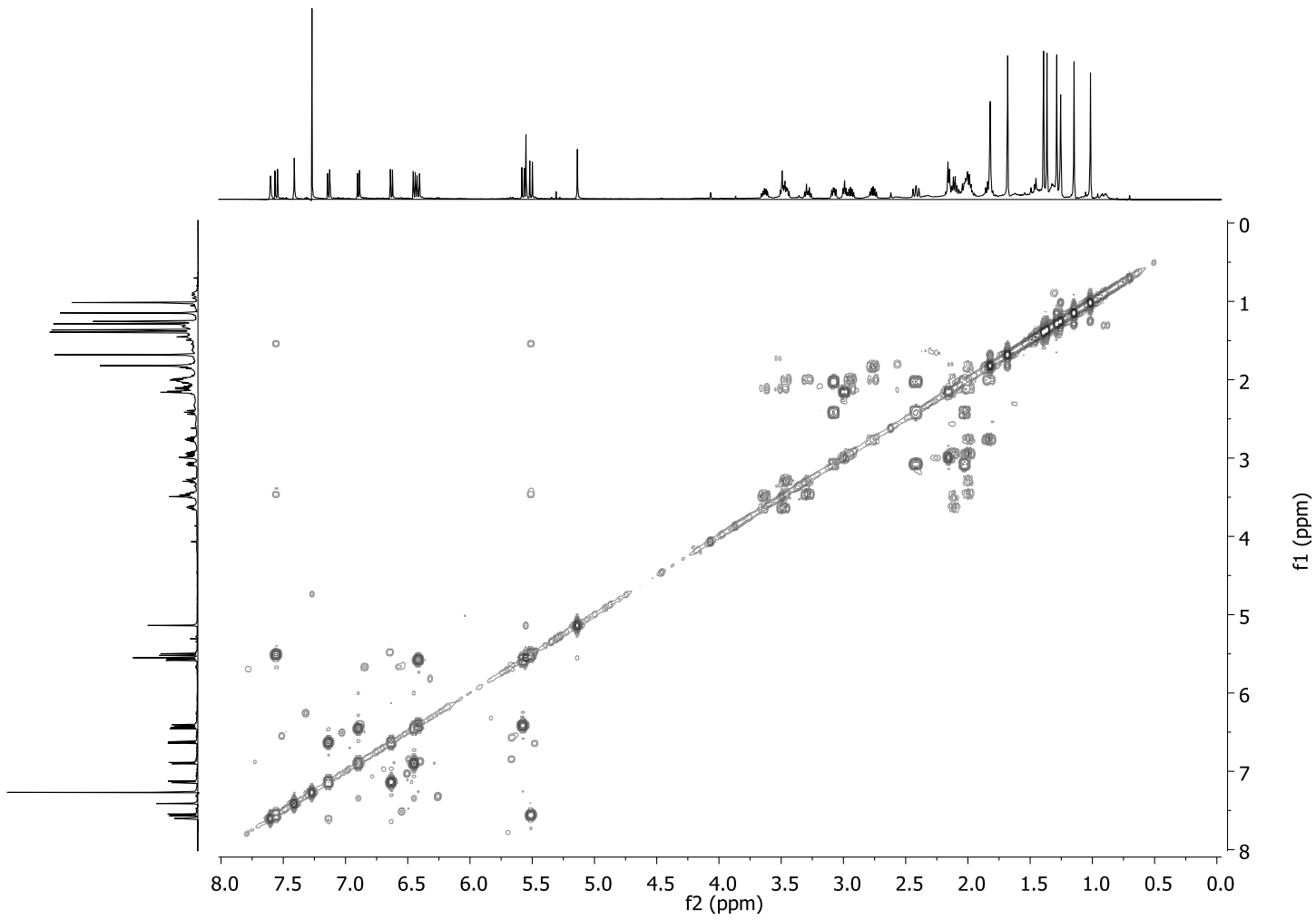

NOESY-NMR spectrum (400 MHz, $CDCl_3$) of waikialoid A (**4.7**)

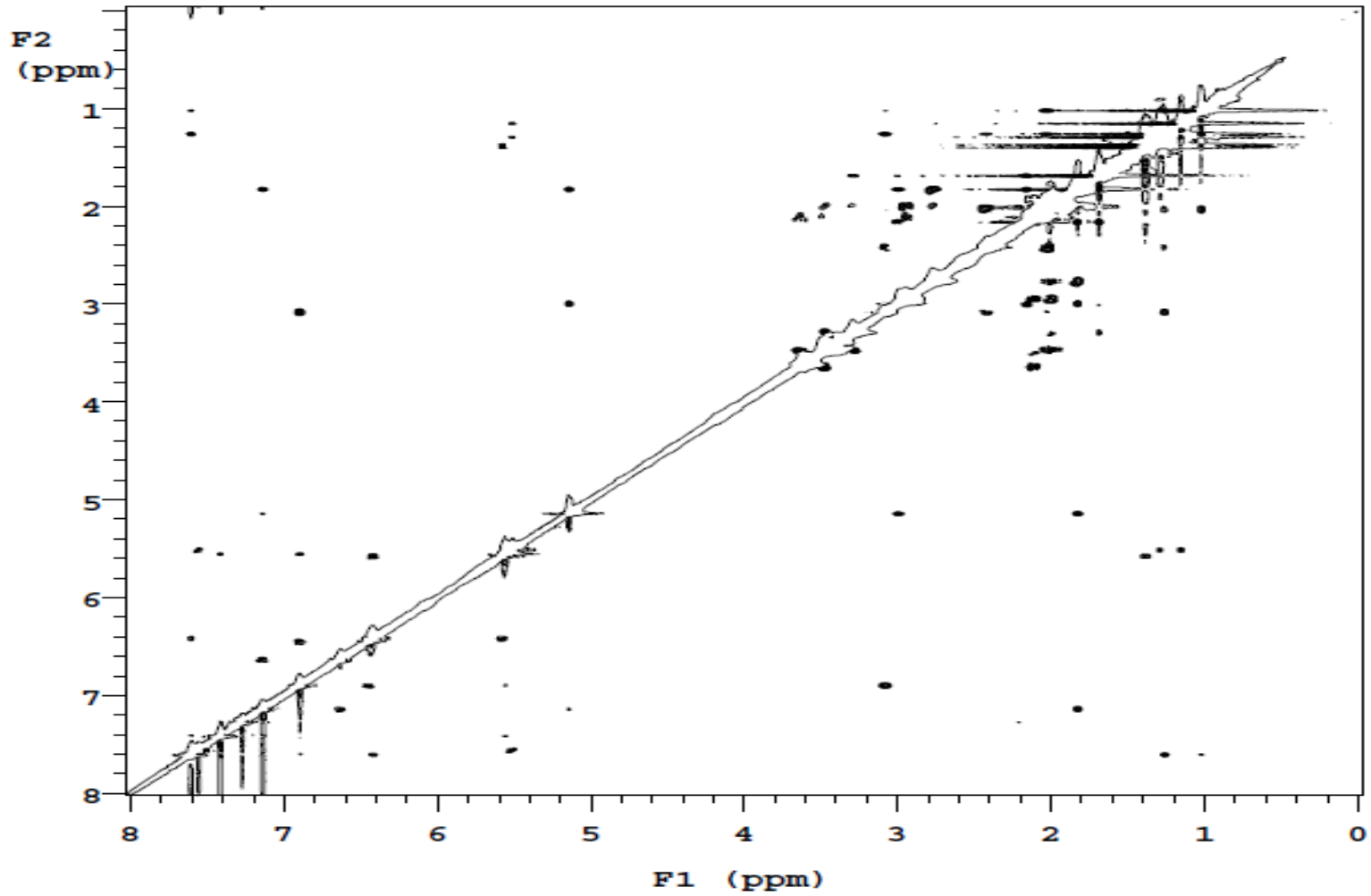

CD spectrum of waikialoid A **(4.7)**

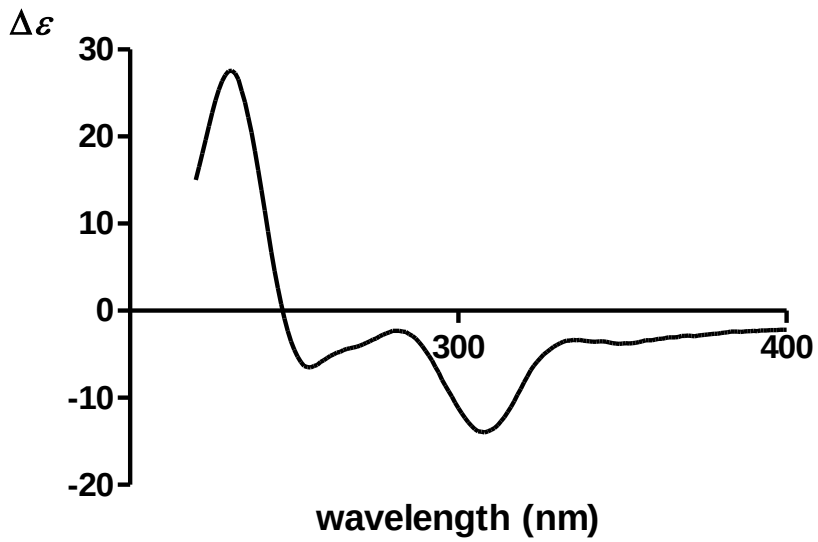

^{1}H-NMR spectrum (500 MHz, $CDCl_3$) of waikialoid B (**4.8**)

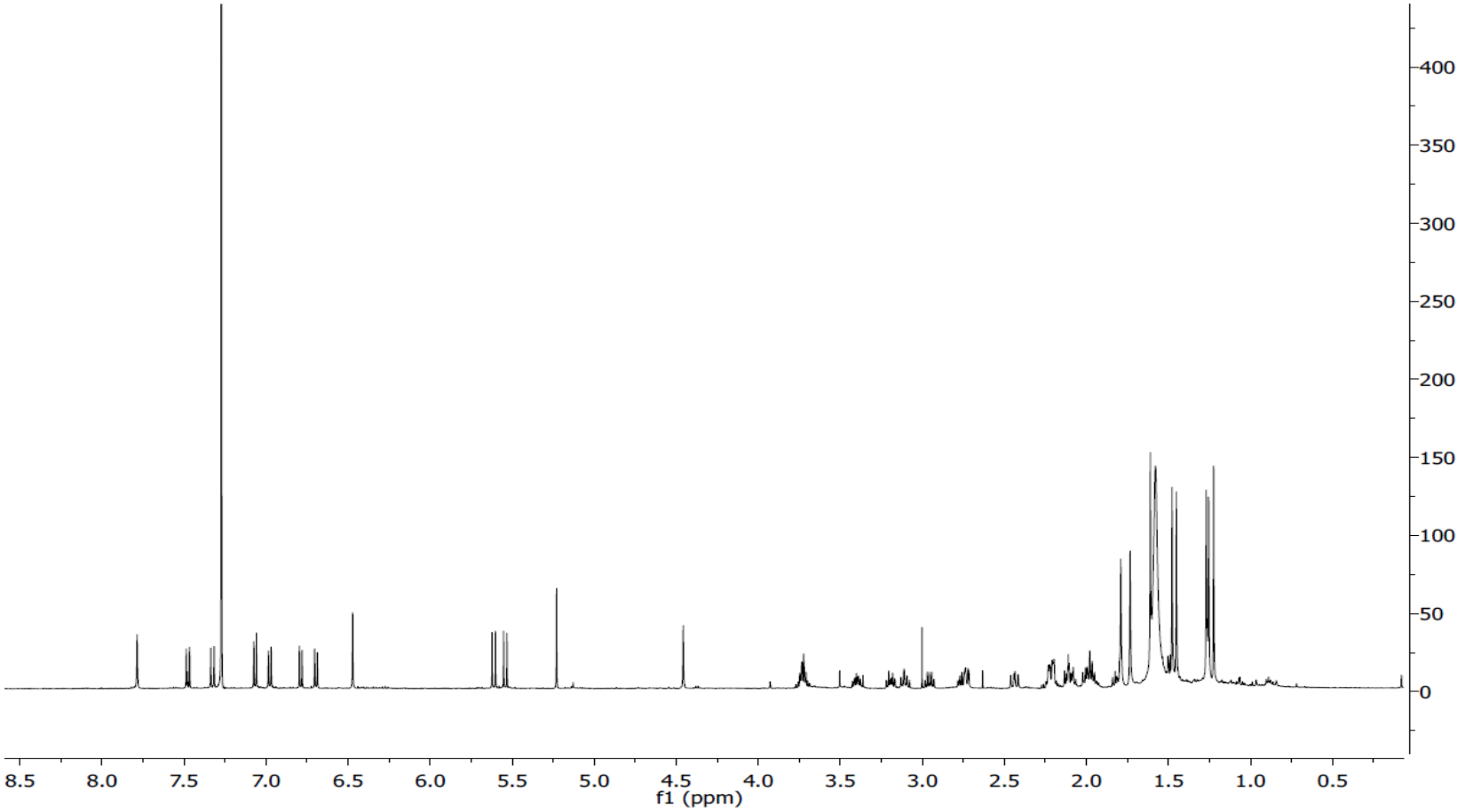

HSQC-NMR spectrum (500 MHz, $CDCl_3$) of waikialoid B (**4.8**)

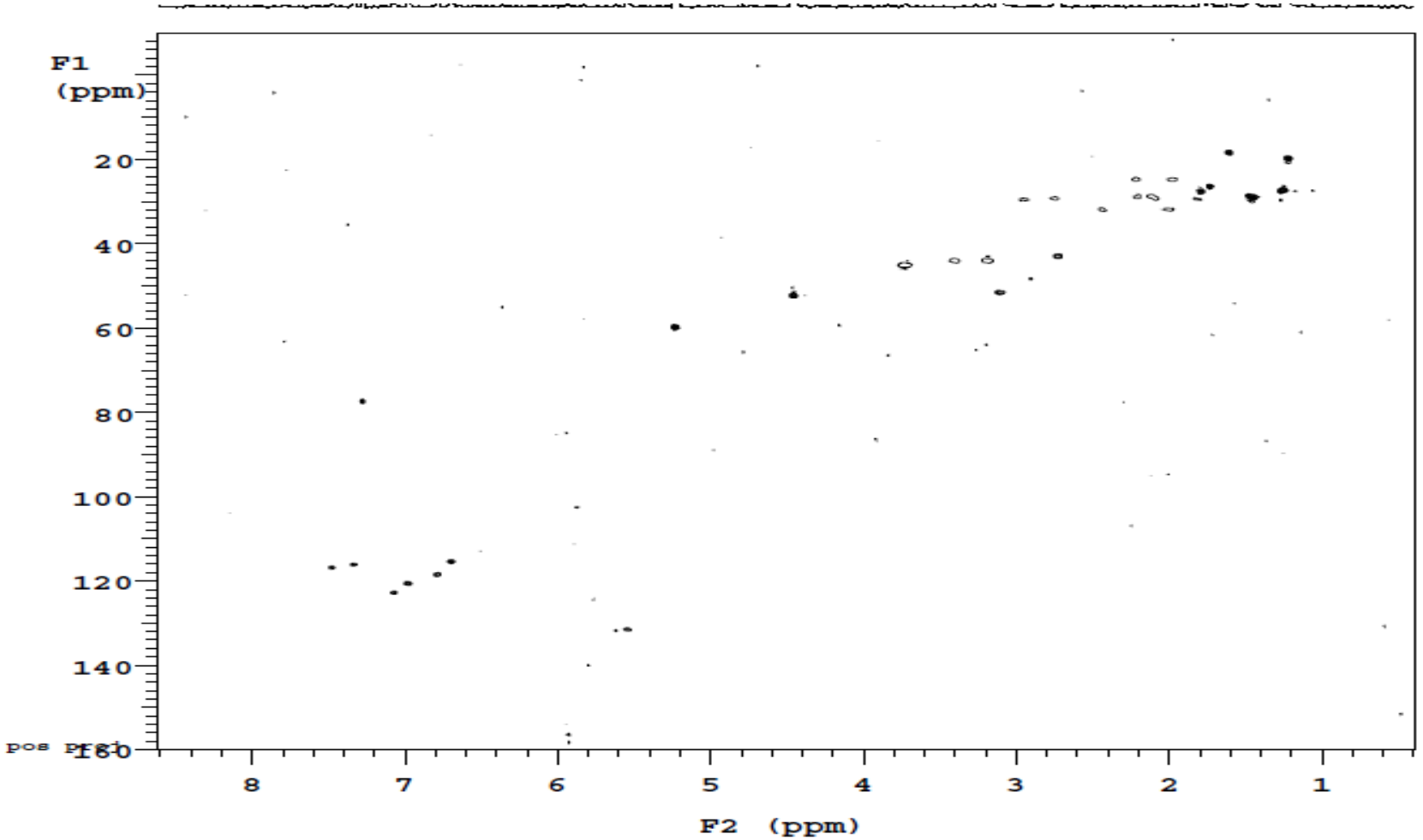

HMBC-NMR spectrum (500 MHz, $CDCl_3$) of waikialoid B (**4.8**)

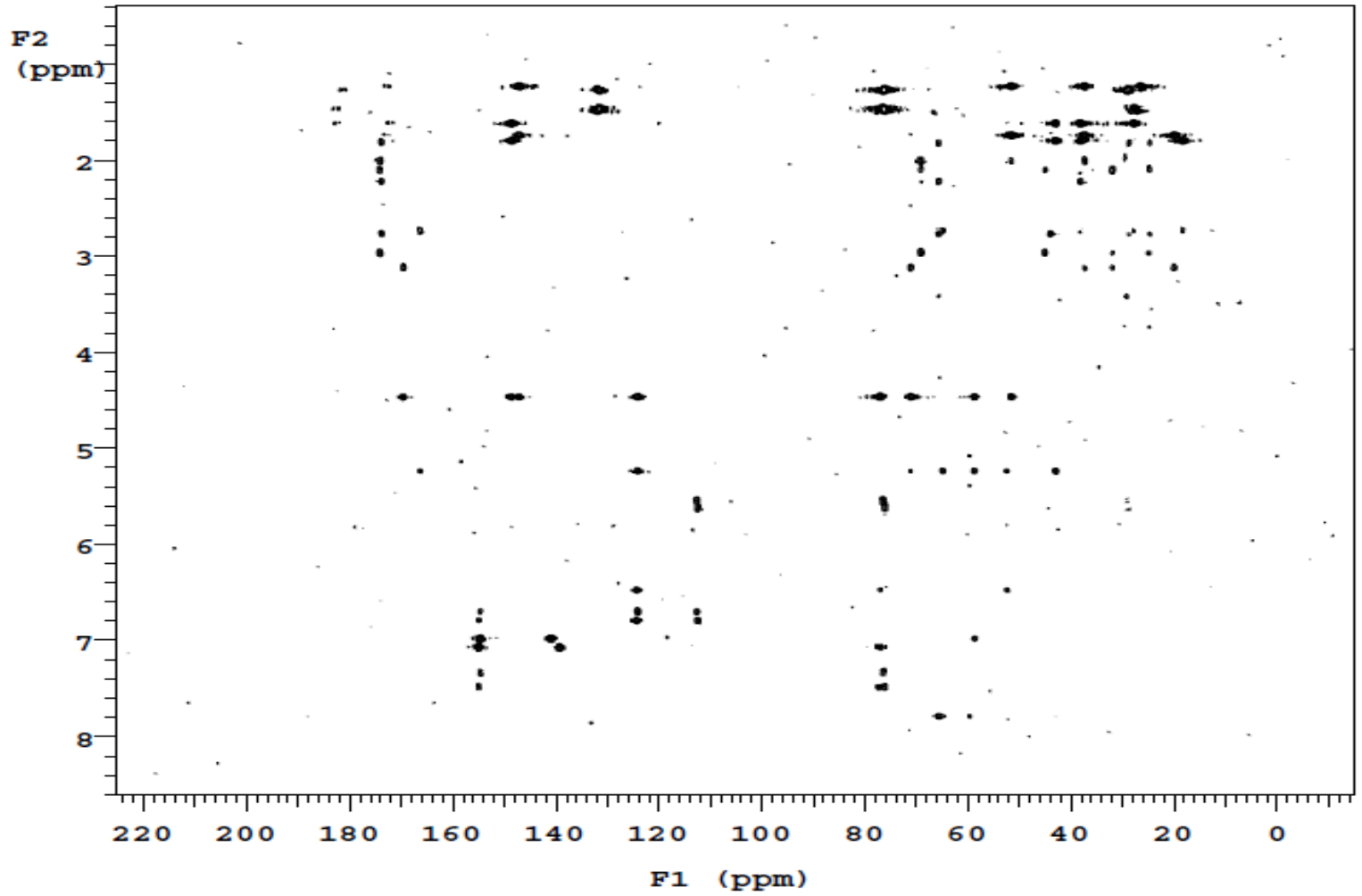

COSY-NMR spectrum (500 MHz, $CDCl_3$) of waikialoid B (**4.8**)

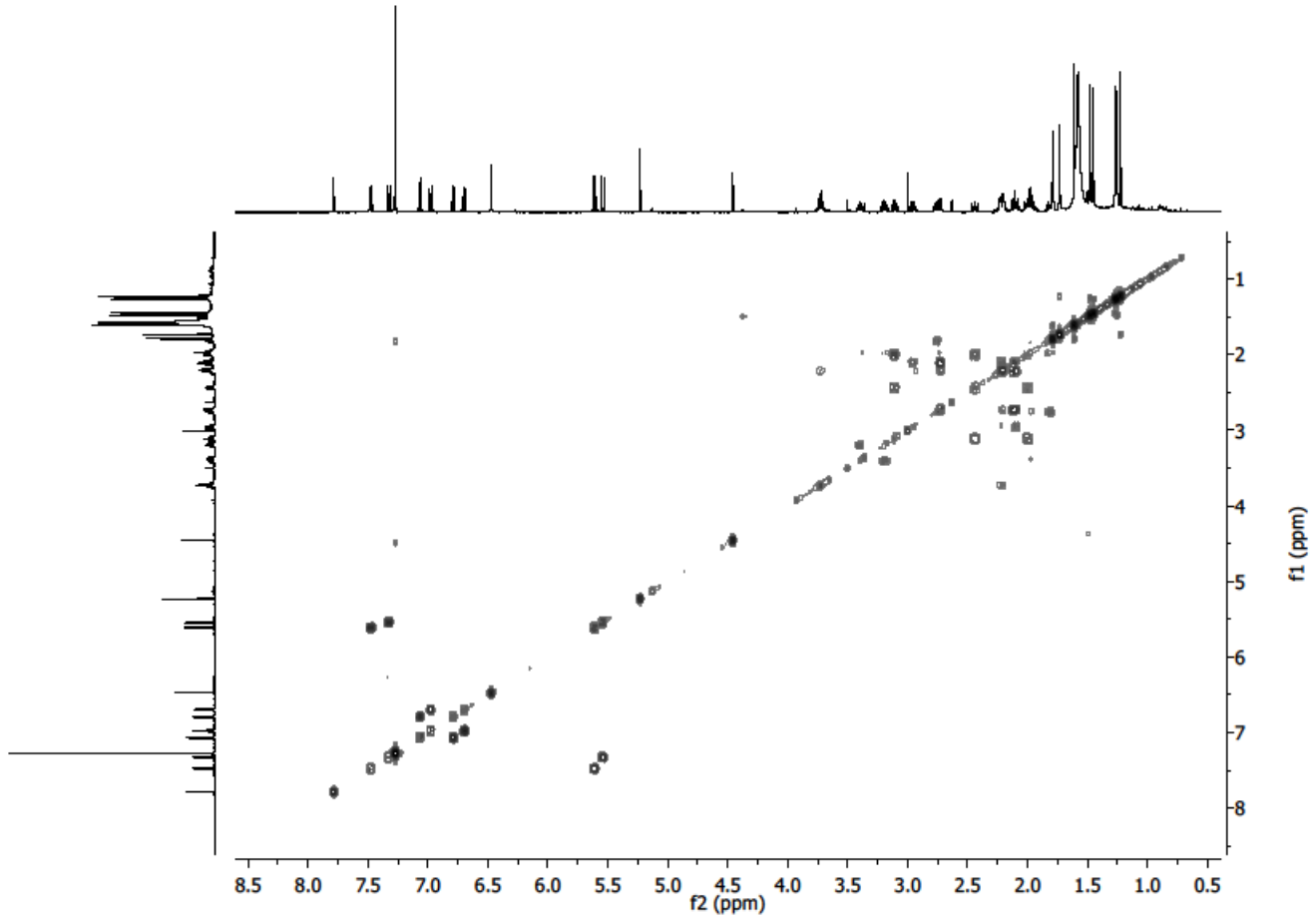

ROESY-NMR spectrum (400 MHz, $CDCl_3$) of waikialoid B (**4.8**)

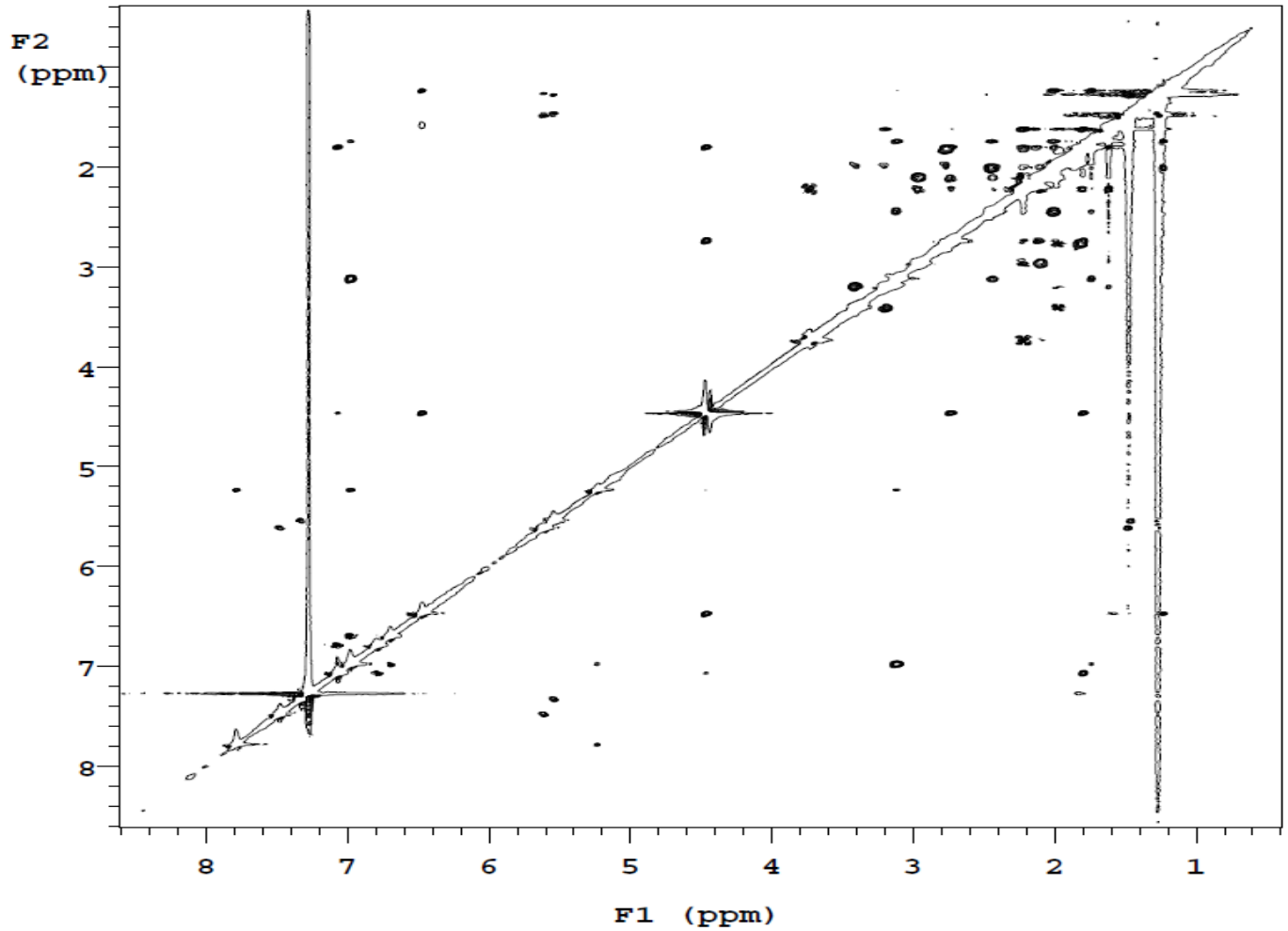

CD spectrum of waikialoid B (**4.8**)

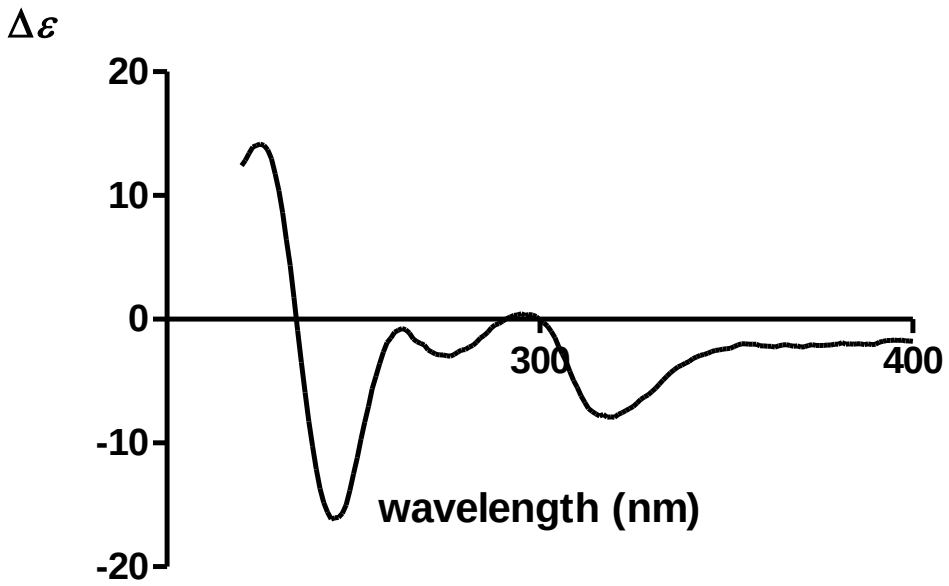

^{1}H-NMR (400 MHz, $CDCl_3$) of asperonol A (**4.15**)

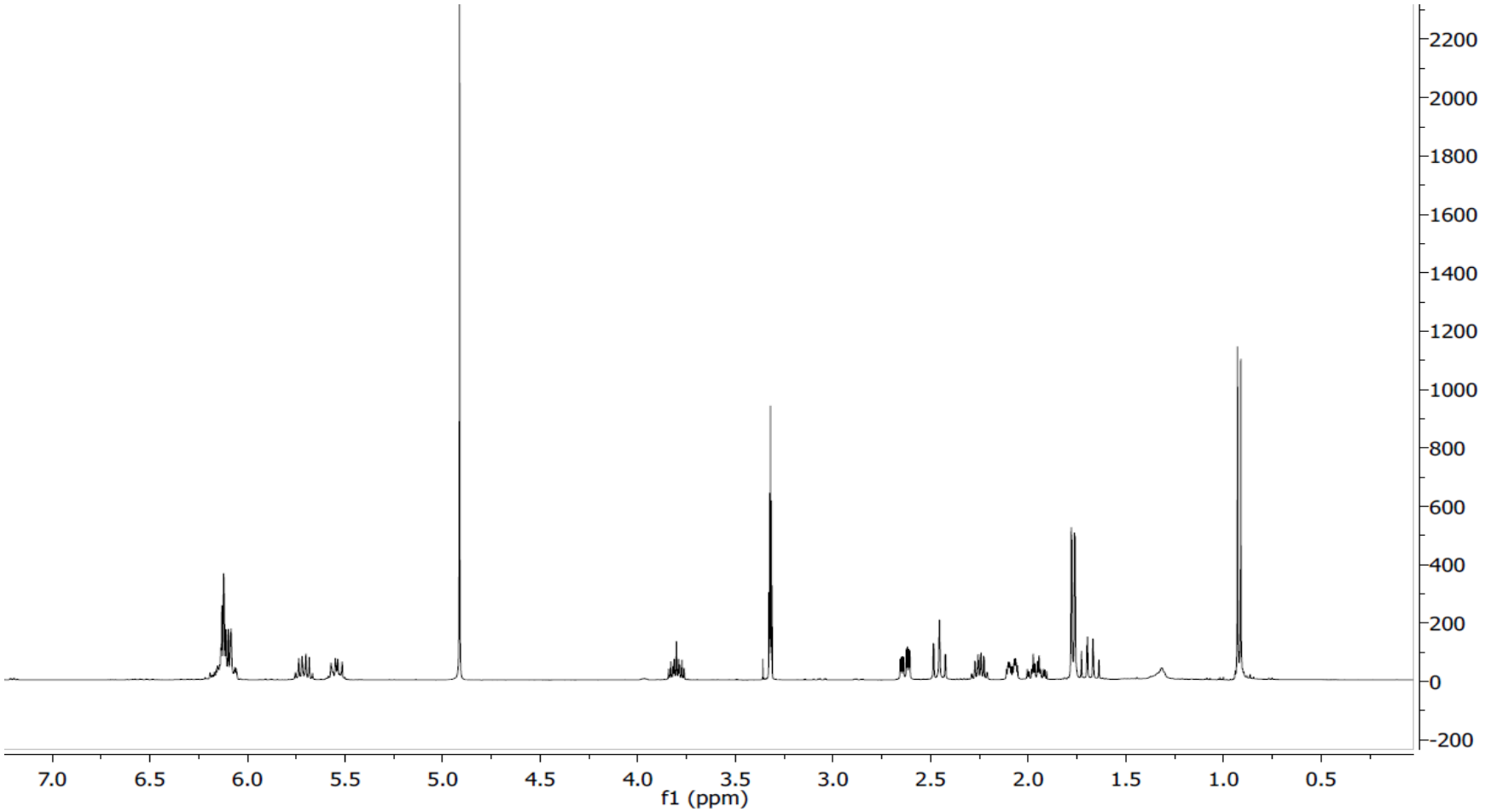

^{13}C-NMR (100 MHz, $CDCl_3$) of asperonol A (**4.15**)

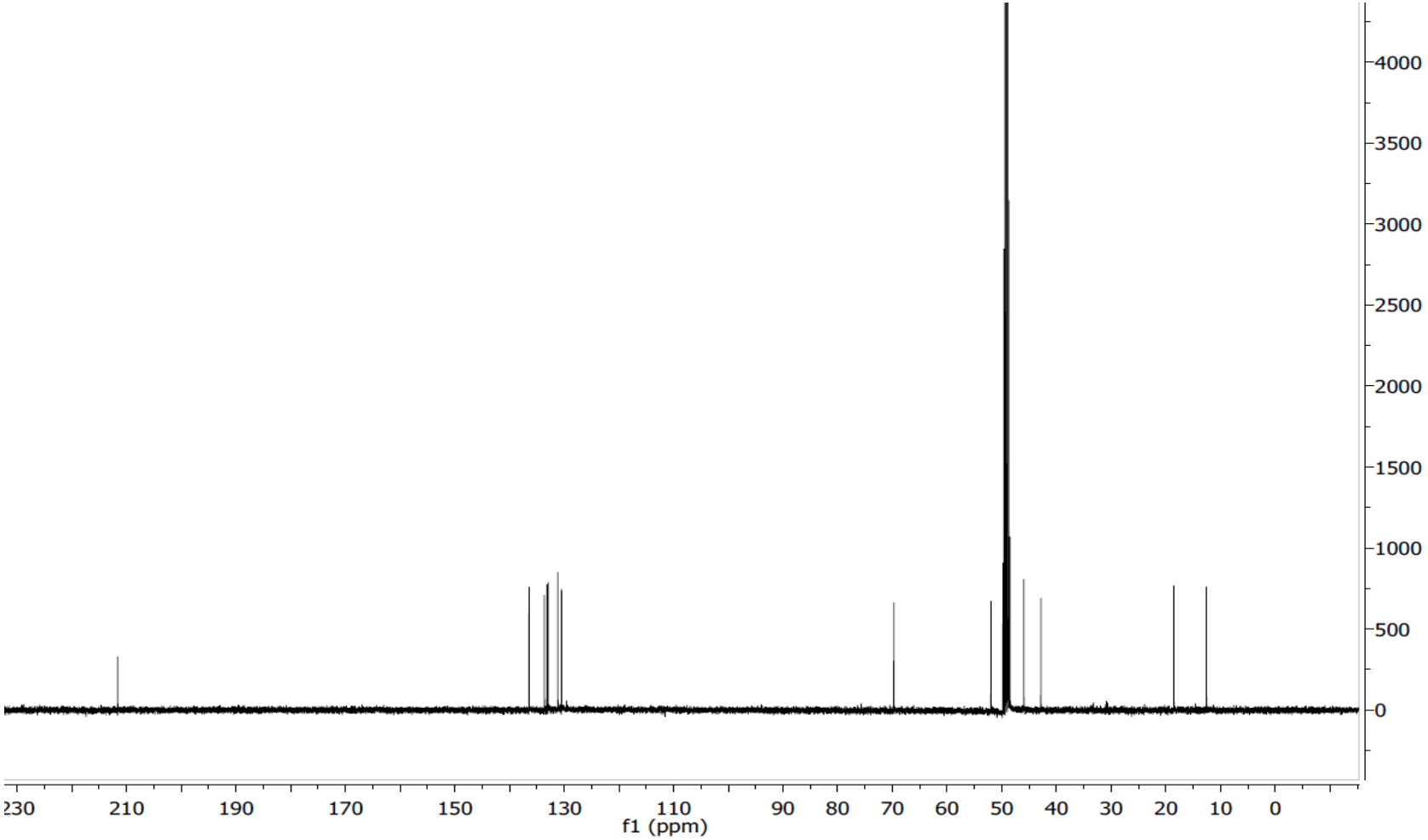

HSQC-NMR (400 MHz, CDCl3) of asperonol A (**4.15**)

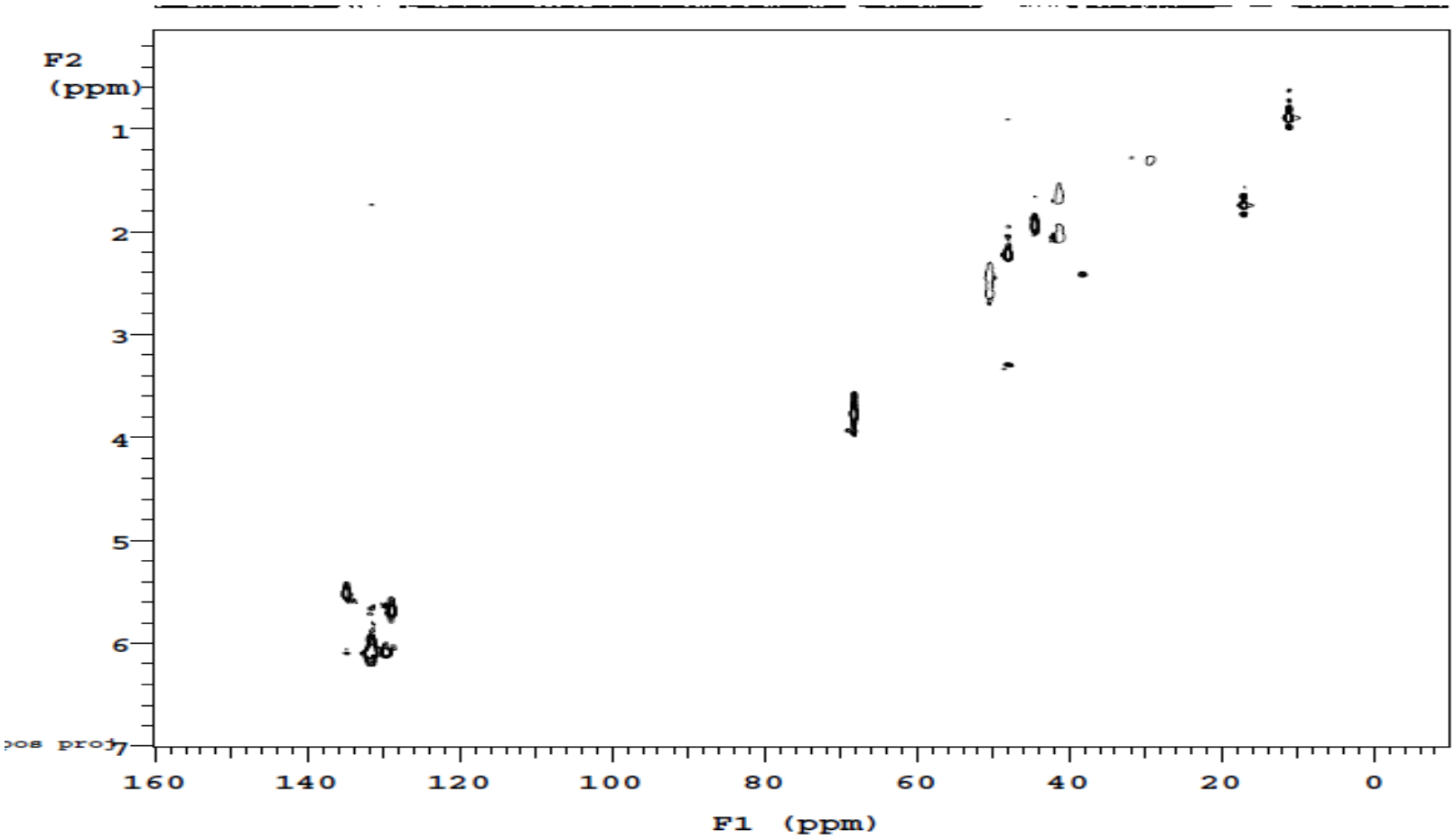

HMBC-NMR (400 MHz, $CDCl_3$) of asperonol A (**4.15**)

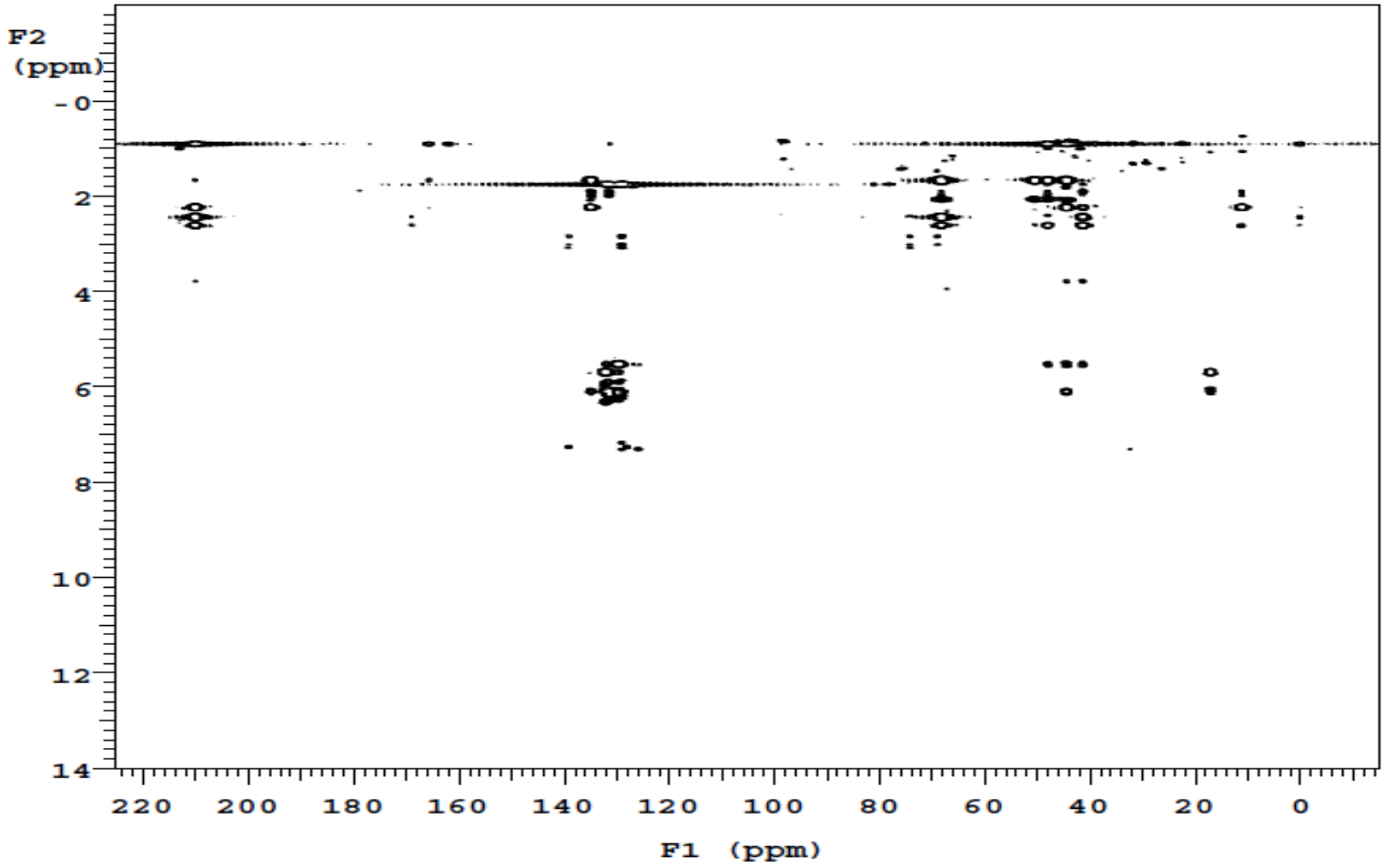

COSY-NMR (400 MHz, $CDCl_3$) of asperonol A (**4.15**)

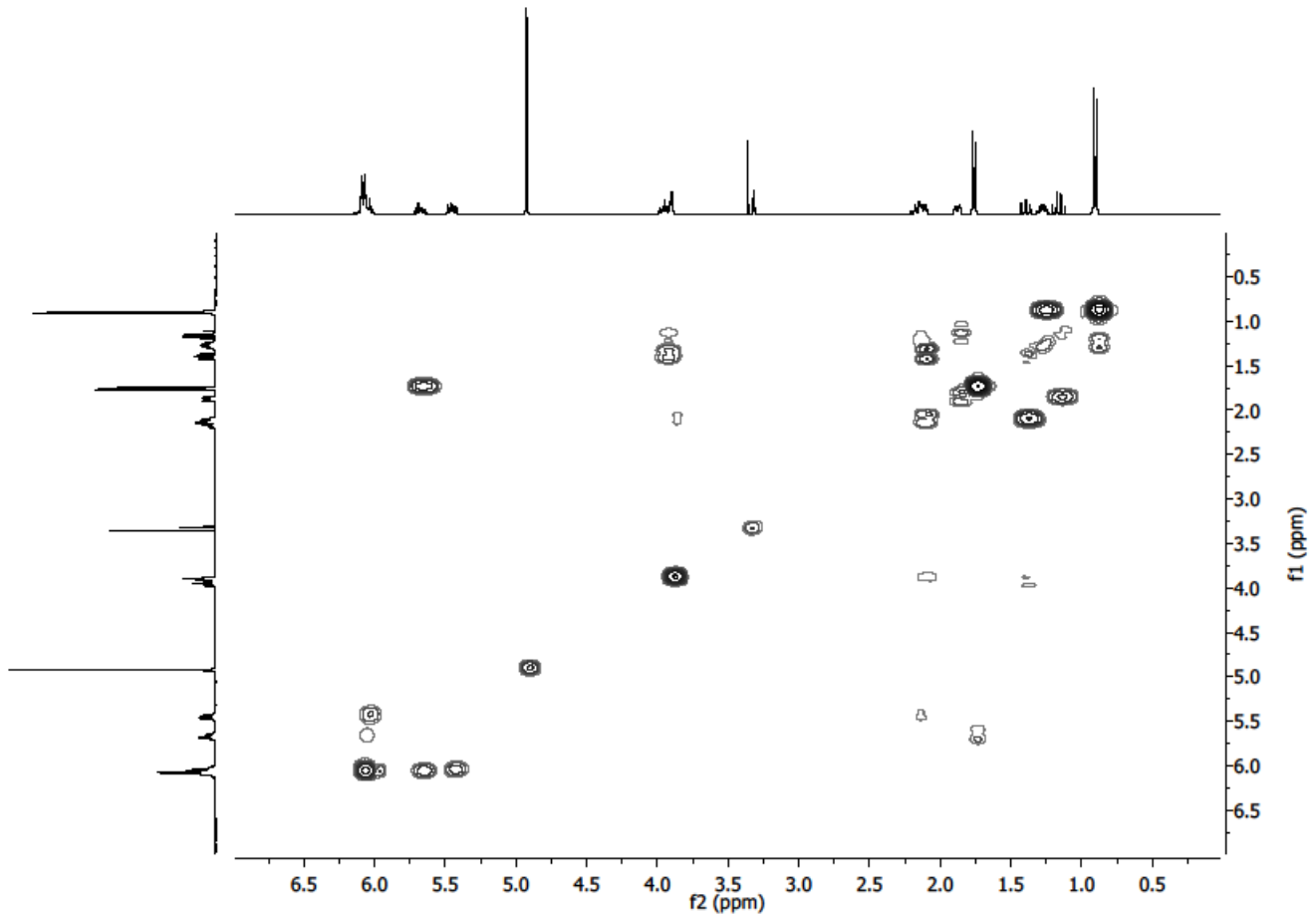

NOESY-NMR spectrum (400 MHz, CD_3OD) of asperonol A (**4.15**)

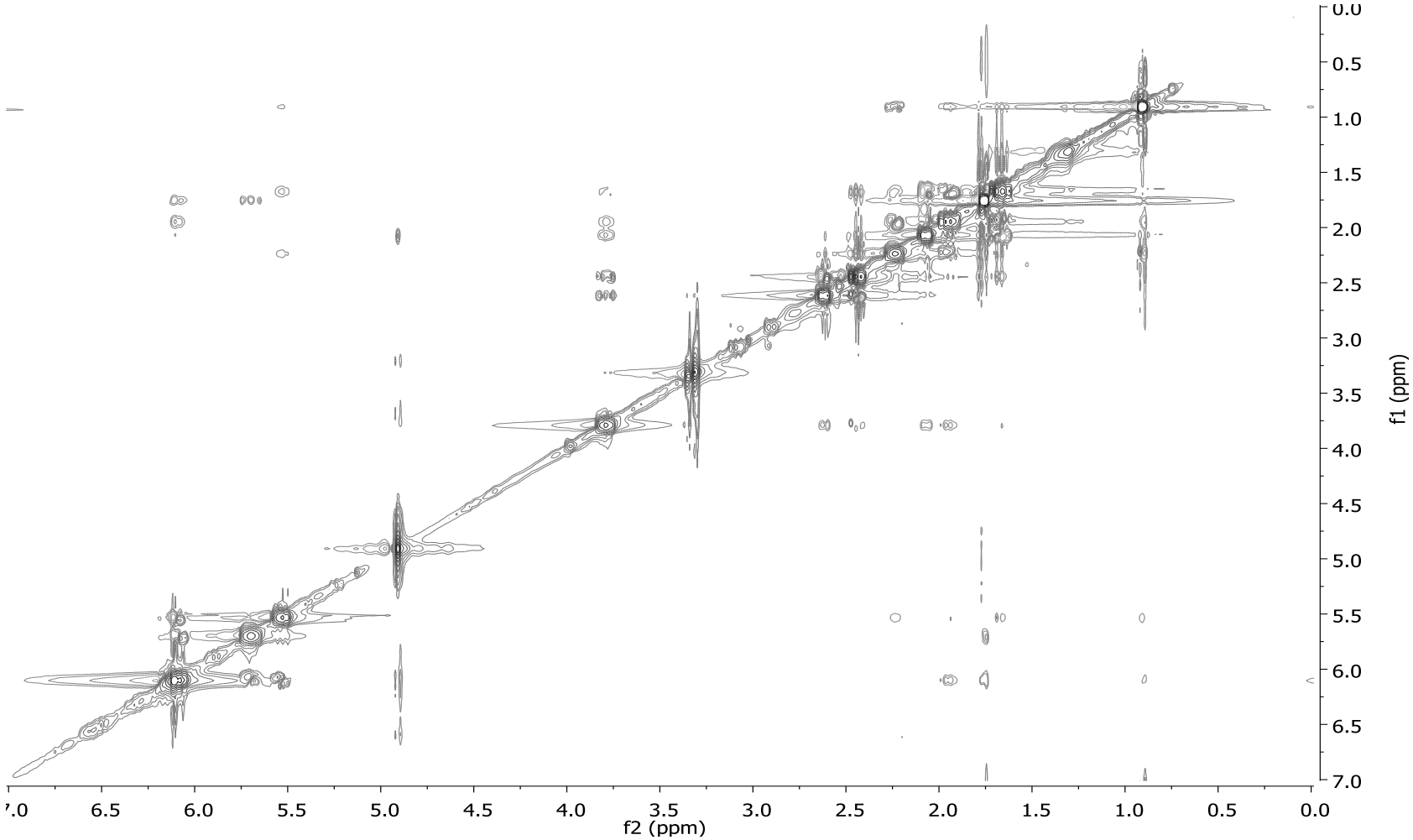

^{1}H -NMR (500 MHz, pyrindine-d_5) of derivative of asperonol A (**4.15a**)

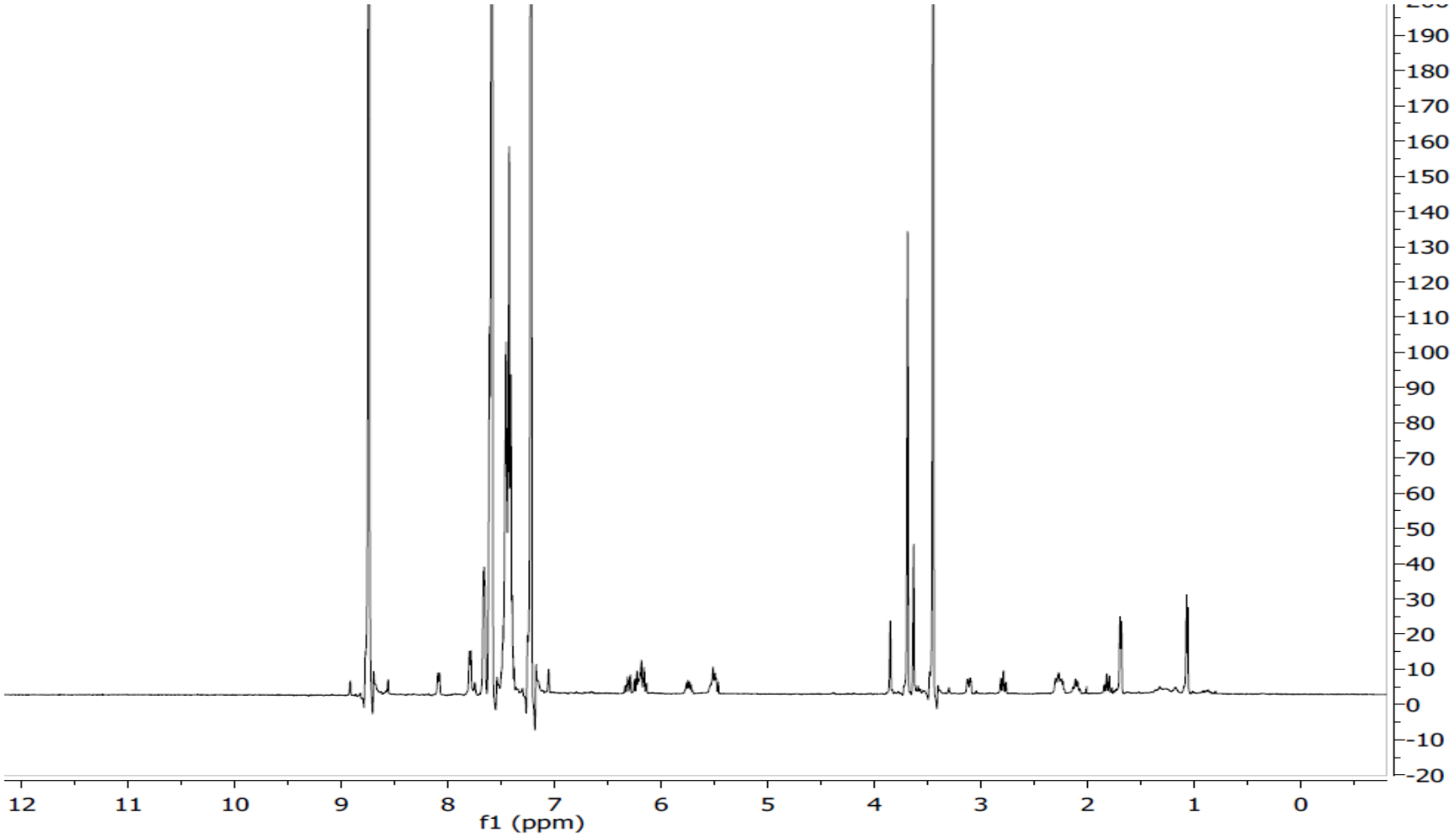

^{1}H -NMR (500 MHz, pyrindine-d_5) of derivative of asperonol A (**4.15b**)

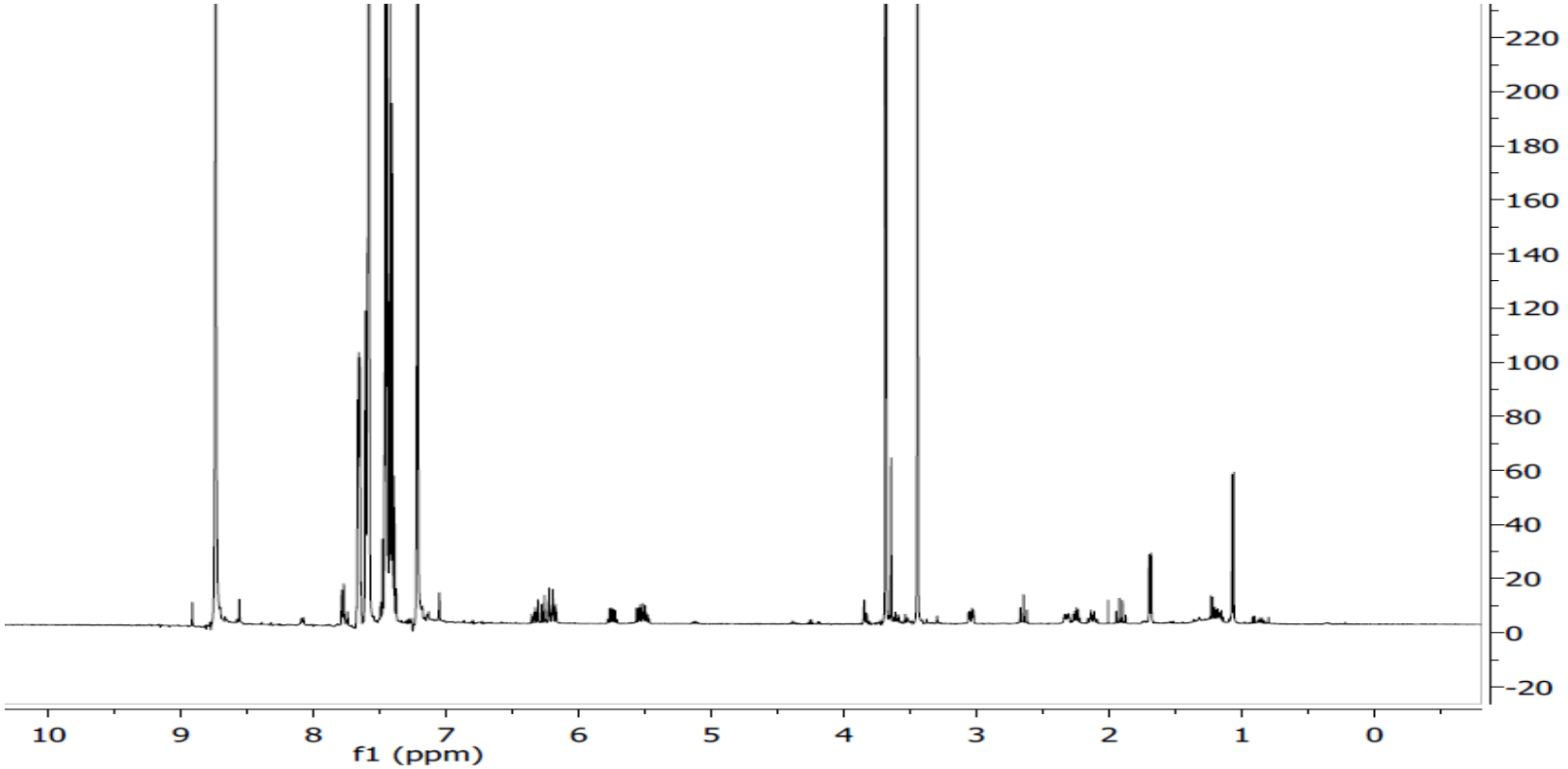

CD spectrum of asperonol A **(4.15)**

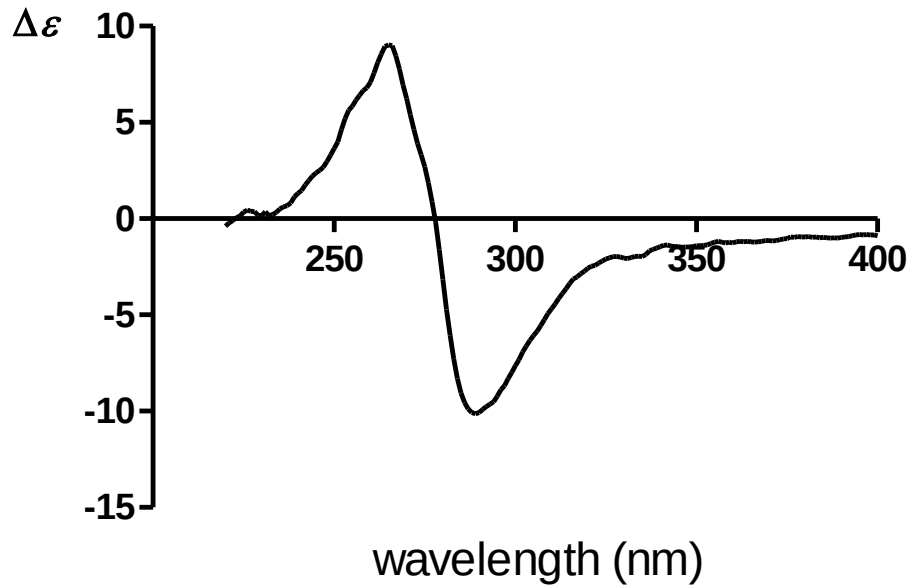

1H-NMR (400 MHz, CDCl3) of asperonol B (**4.16**)

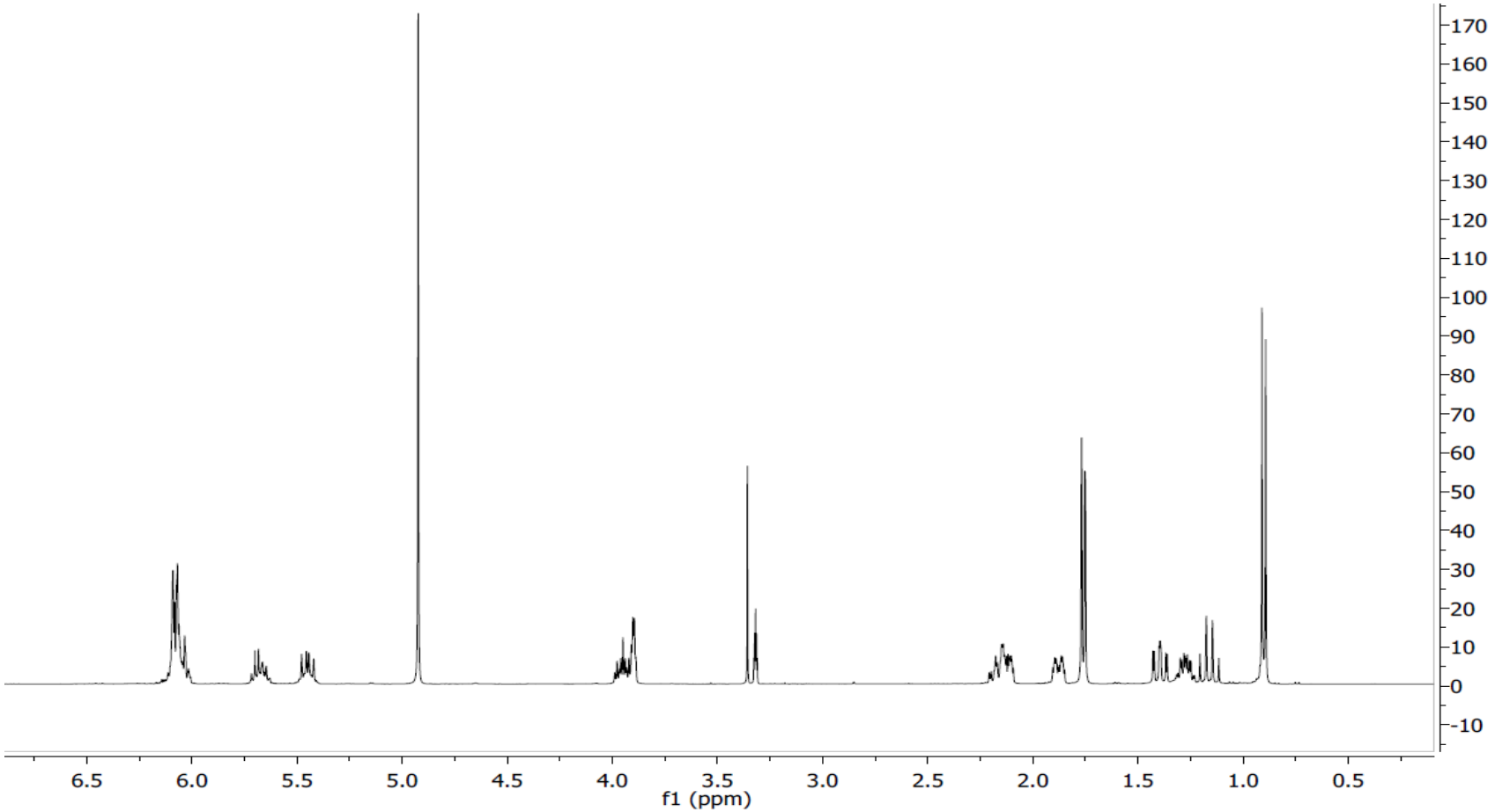

^{13}C-NMR spectrum (100 MHz, CD_3OD) asperonol B (**4.16**)

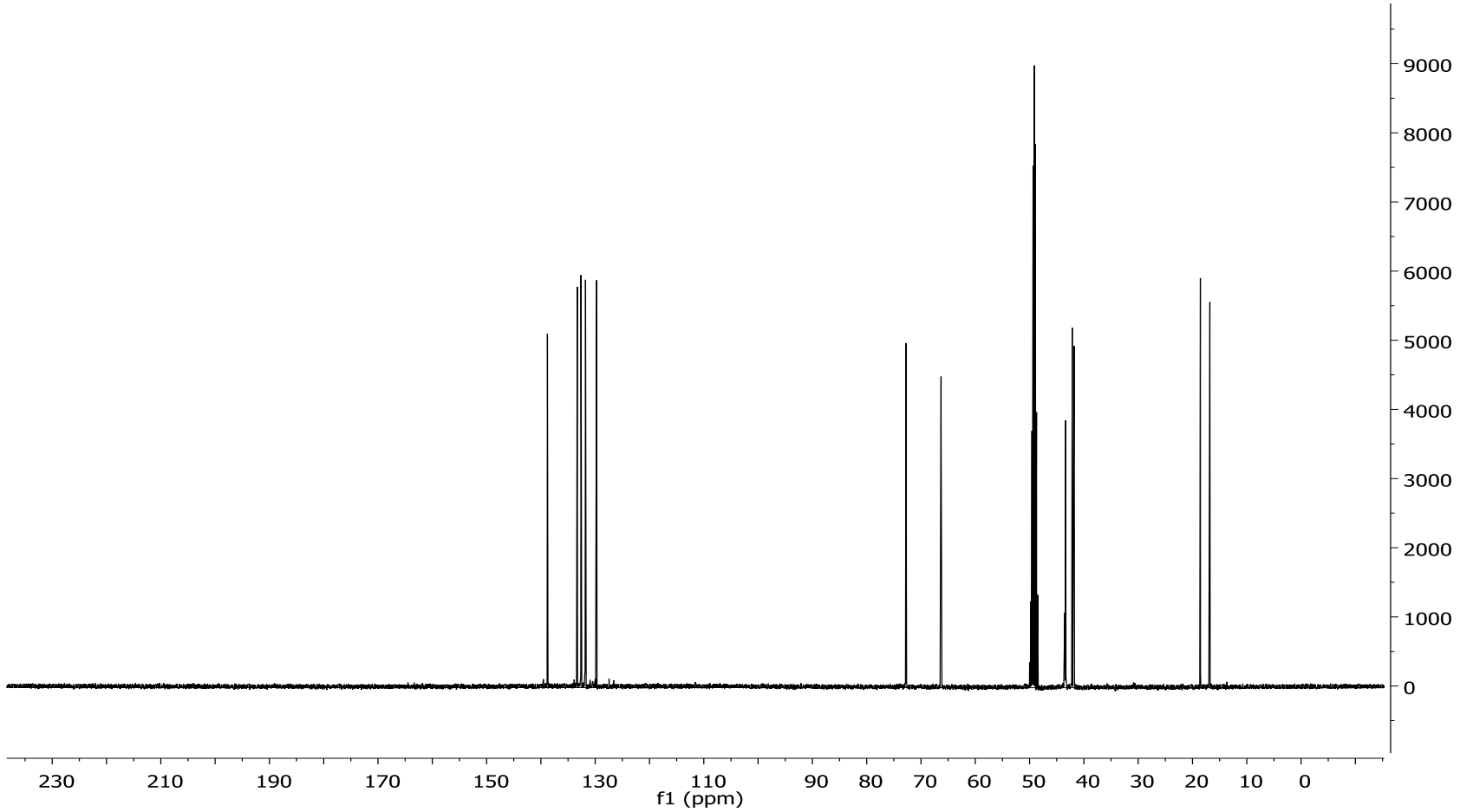

HSQC-NMR (400 MHz, $CDCl_3$) of asperonol B (**4.16**)

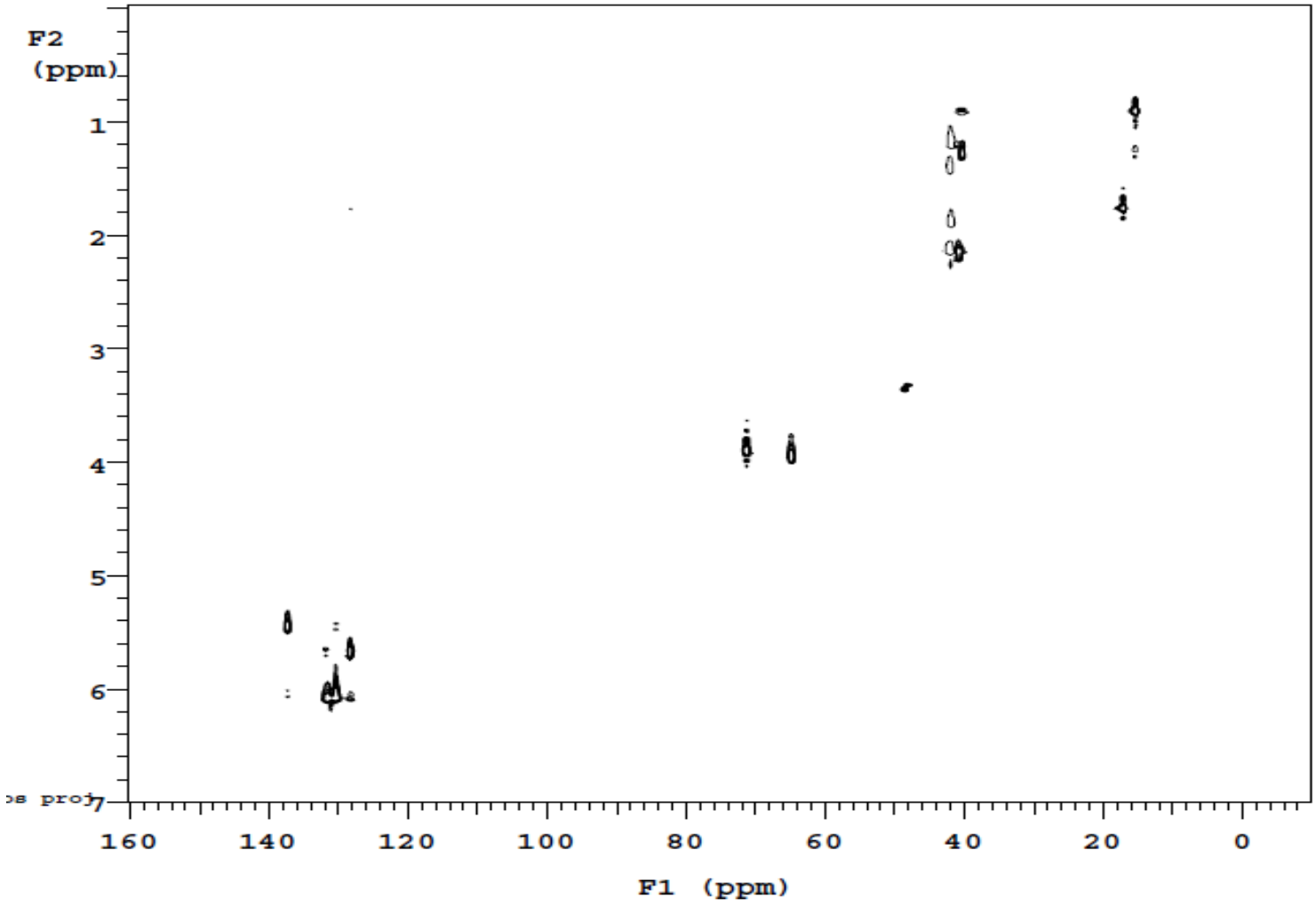

HMBC-NMR (400 MHz, $CDCl_3$) of asperonol B (**4.16**)

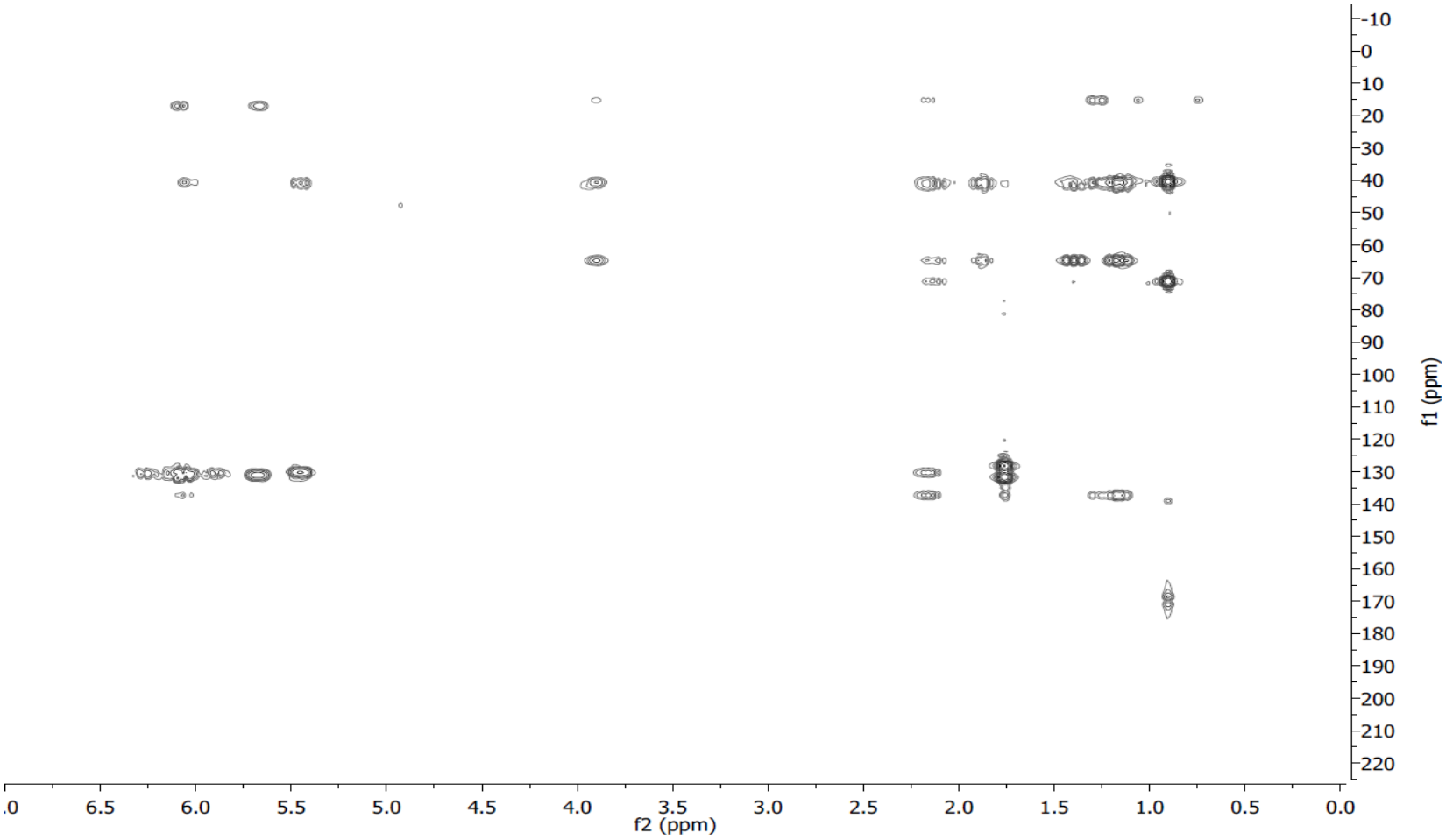

COSY-NMR spectrum (400 MHz, $CDCl_3$) of asperonol B (**4.16**)

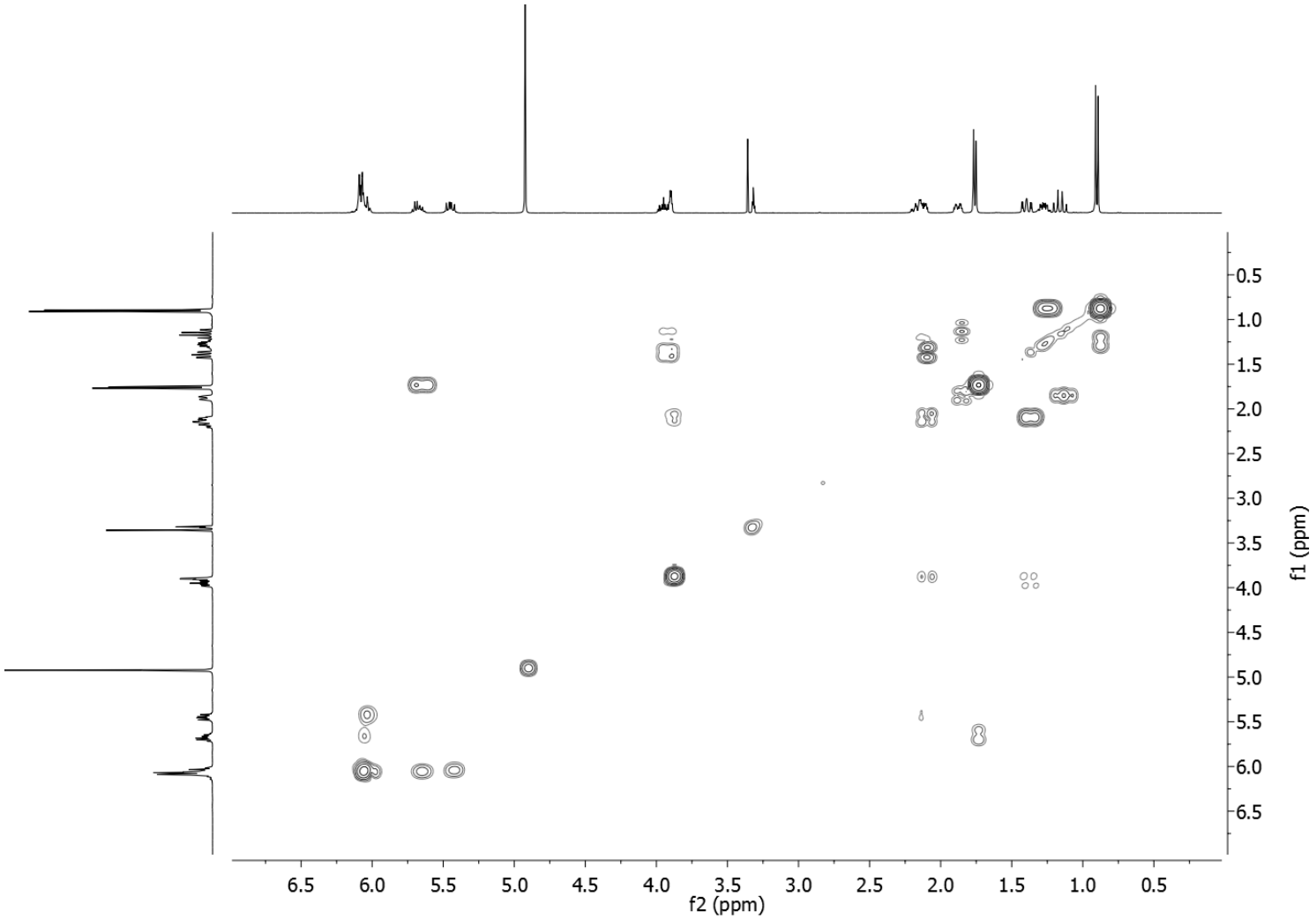

NOESY-NMR spectrum (400 MHz, $CDCl_3$) of asperonol B (**4.16**)

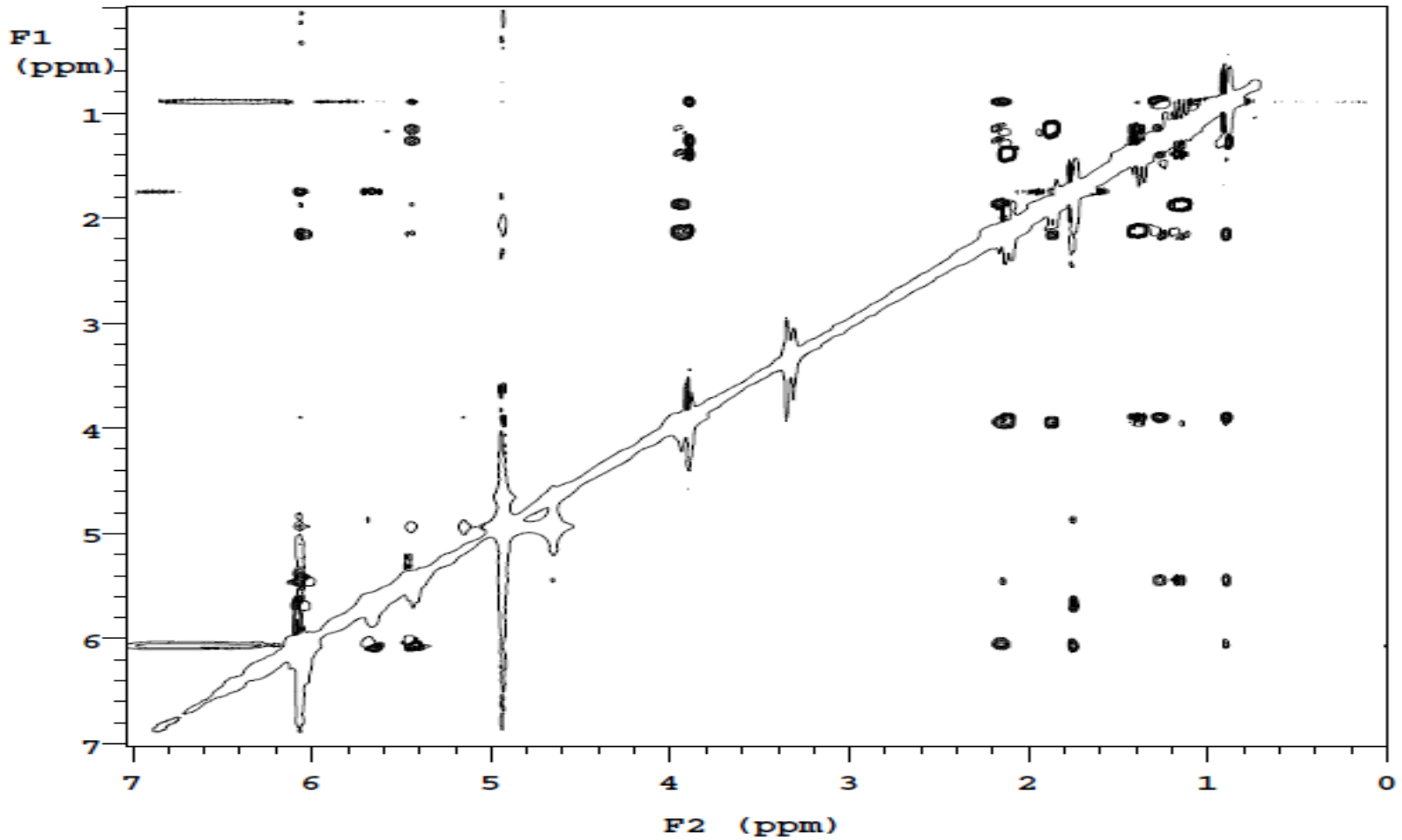

^{1}H-NMR spectrum (500 MHz, DMSO-d_6) of mutanobactin B **(5.2)**

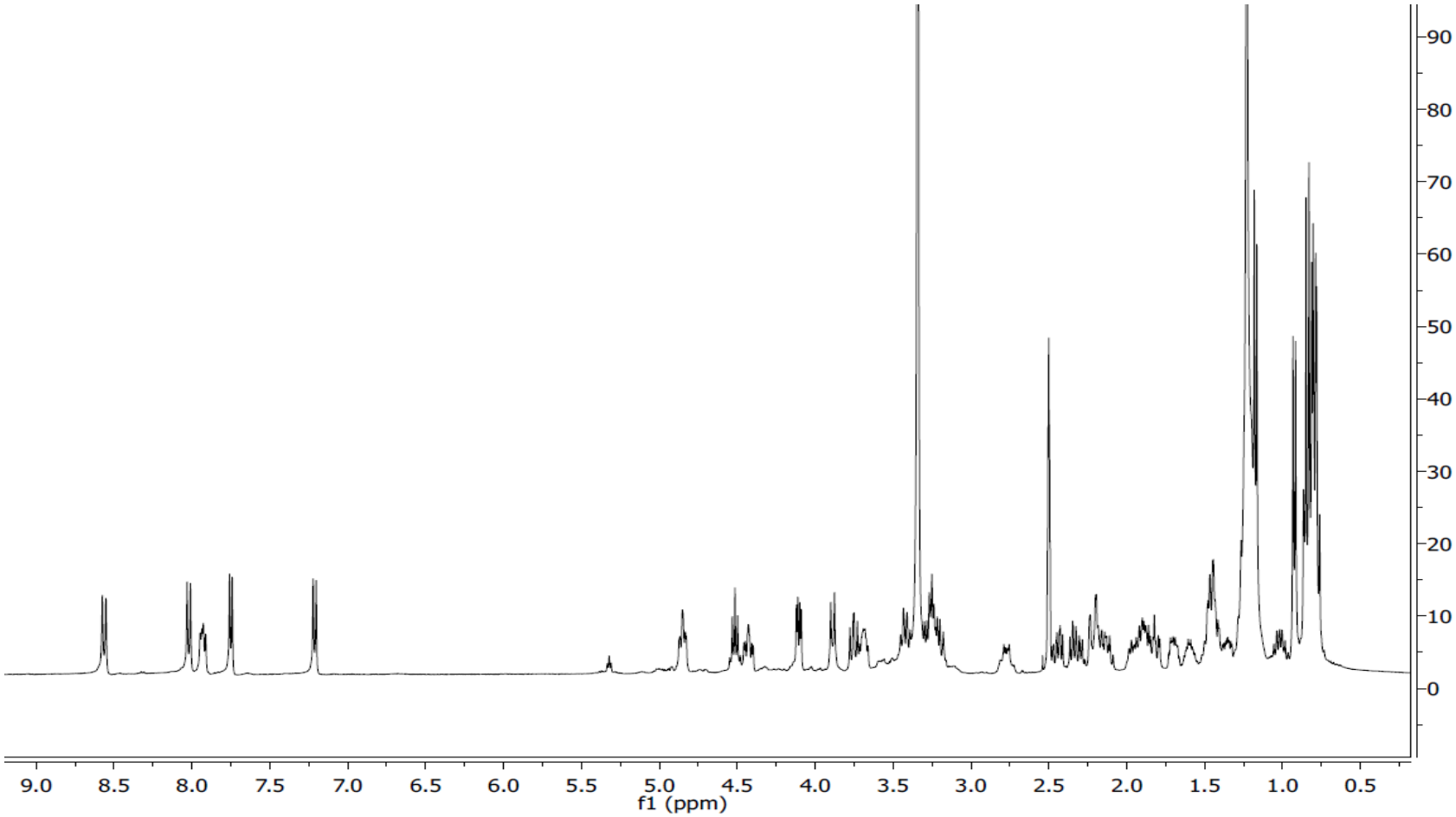

^{13}C-NMR spectrum (100 MHz, DMSO-d_6) of mutanobactin B (**5.2**)

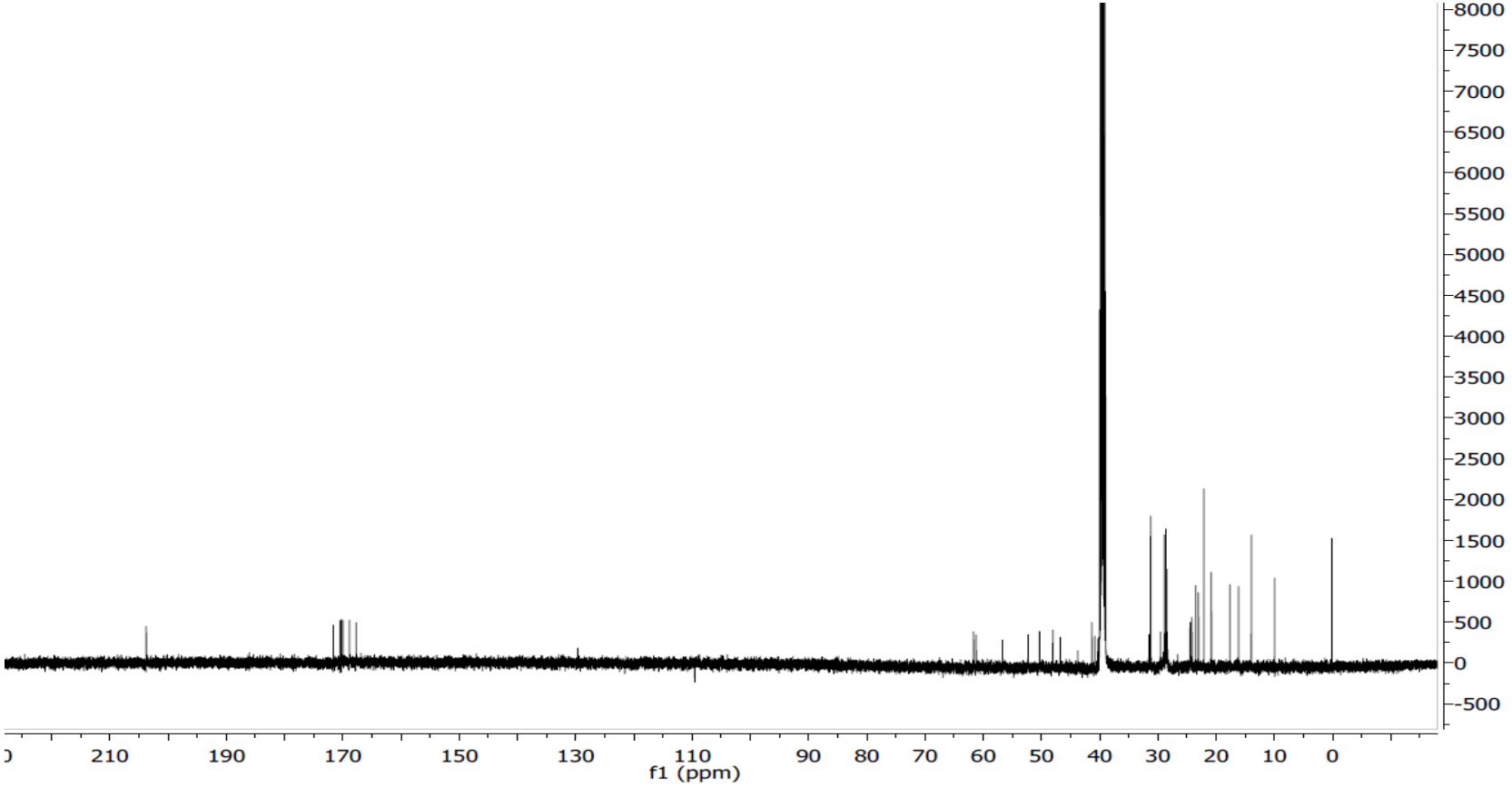

HSQC-NMR spectrum (500 MHz, DMSO-d_6) of mutanobactin B (**5.2**)

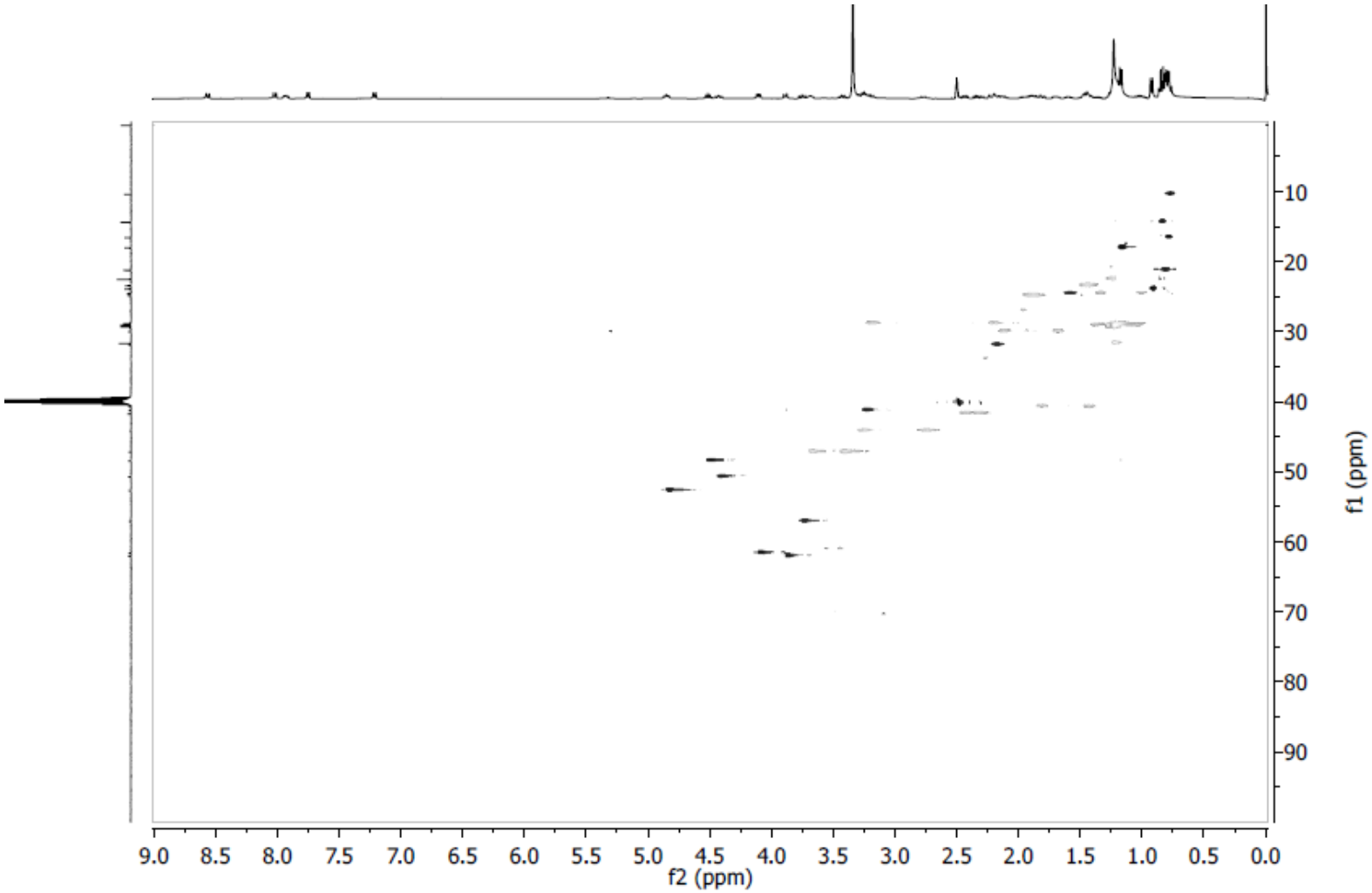

HMBC-NMR spectrum (500 MHz, DMSO-d_6) of mutanobactin B (**5.2**)

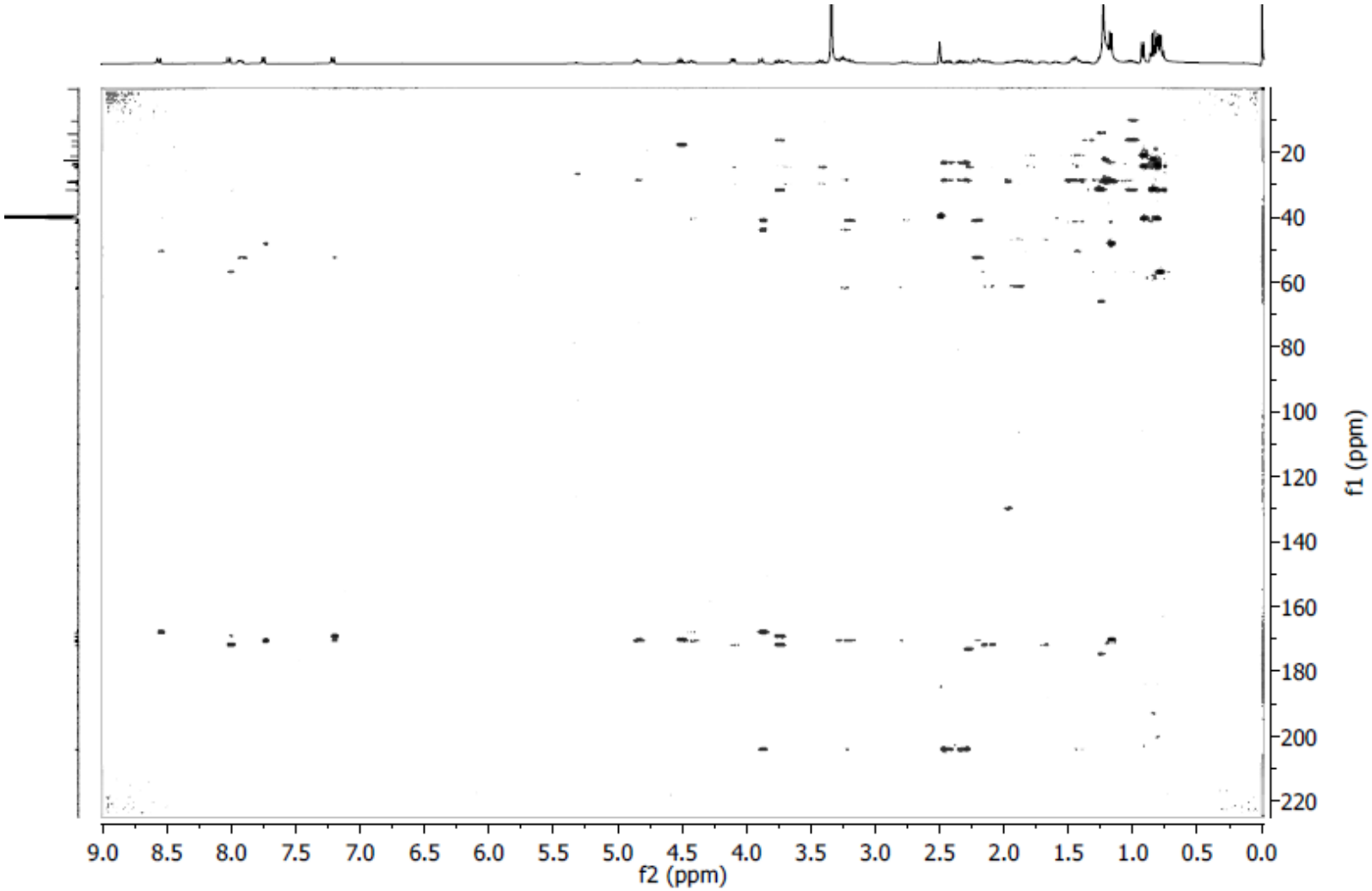

COSY-NMR spectrum (500 MHz, DMSO-d_6) of mutanobactin B (**5.2**)

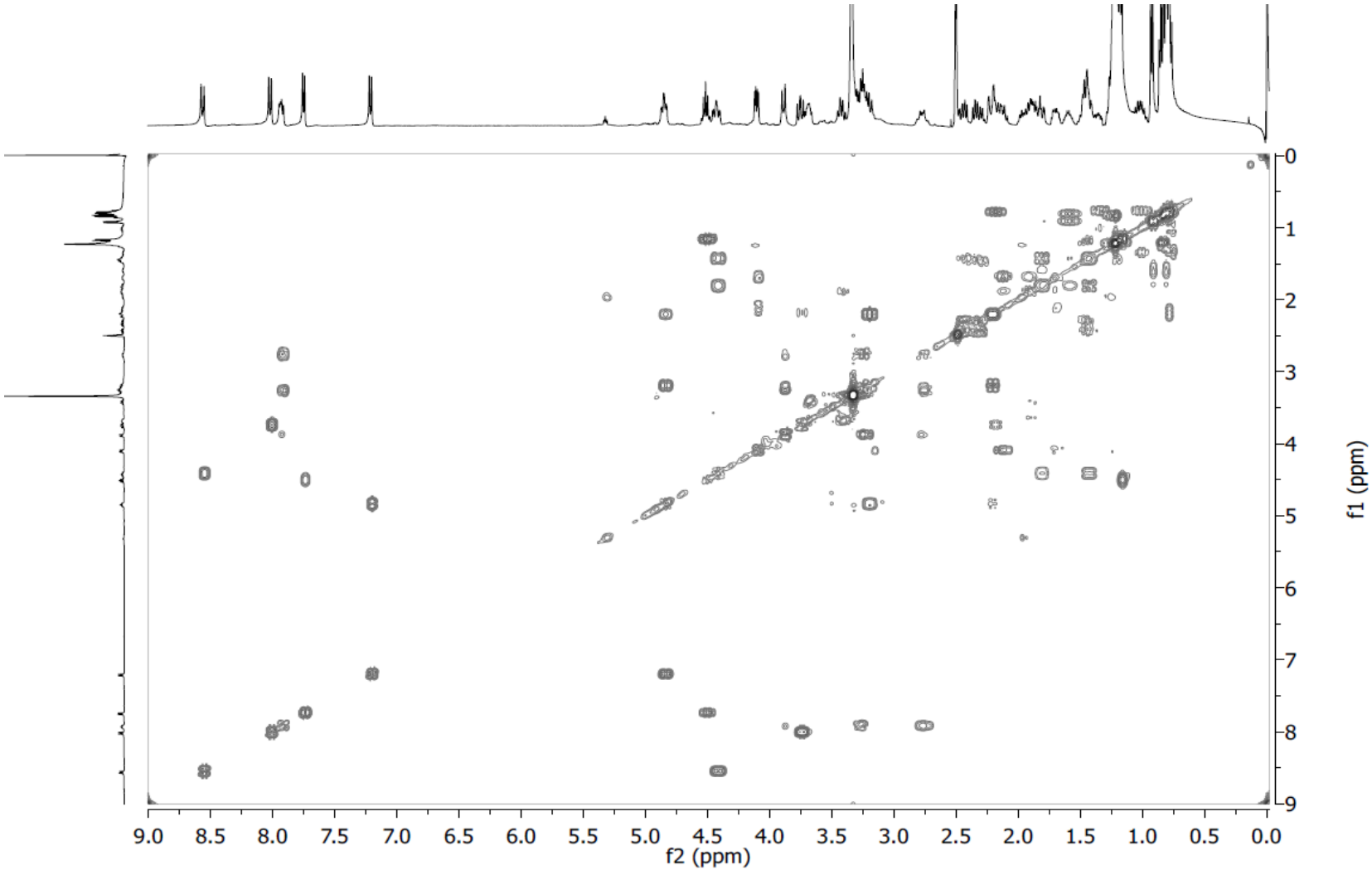

NOESY-NMR spectrum (500 MHz, DMSO-d_6) of mutanobactin B (**5.2**)

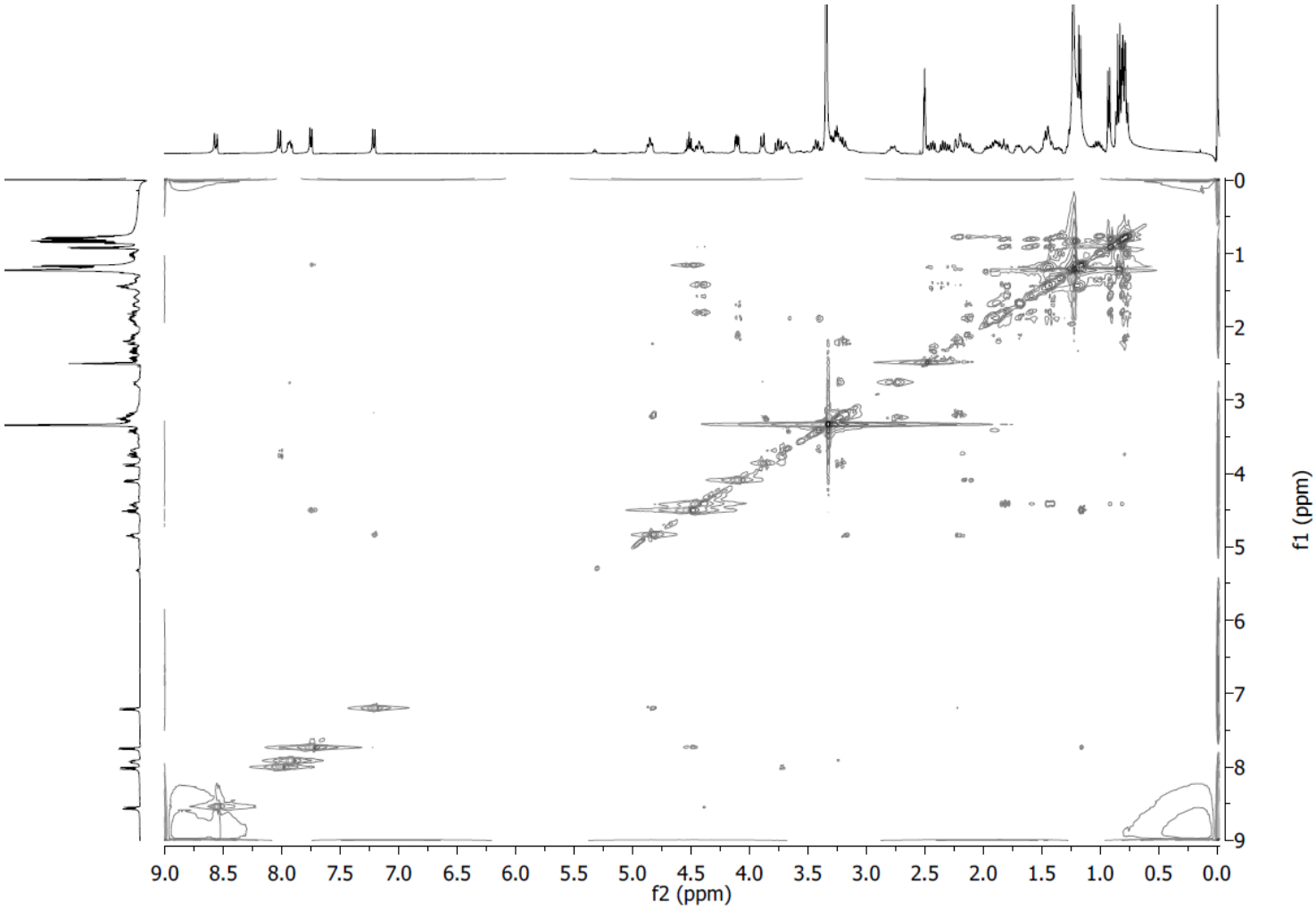

^{1}H-NMR spectrum (500 MHz, DMSO-d_6) of mutanobactin C (**5.3**)

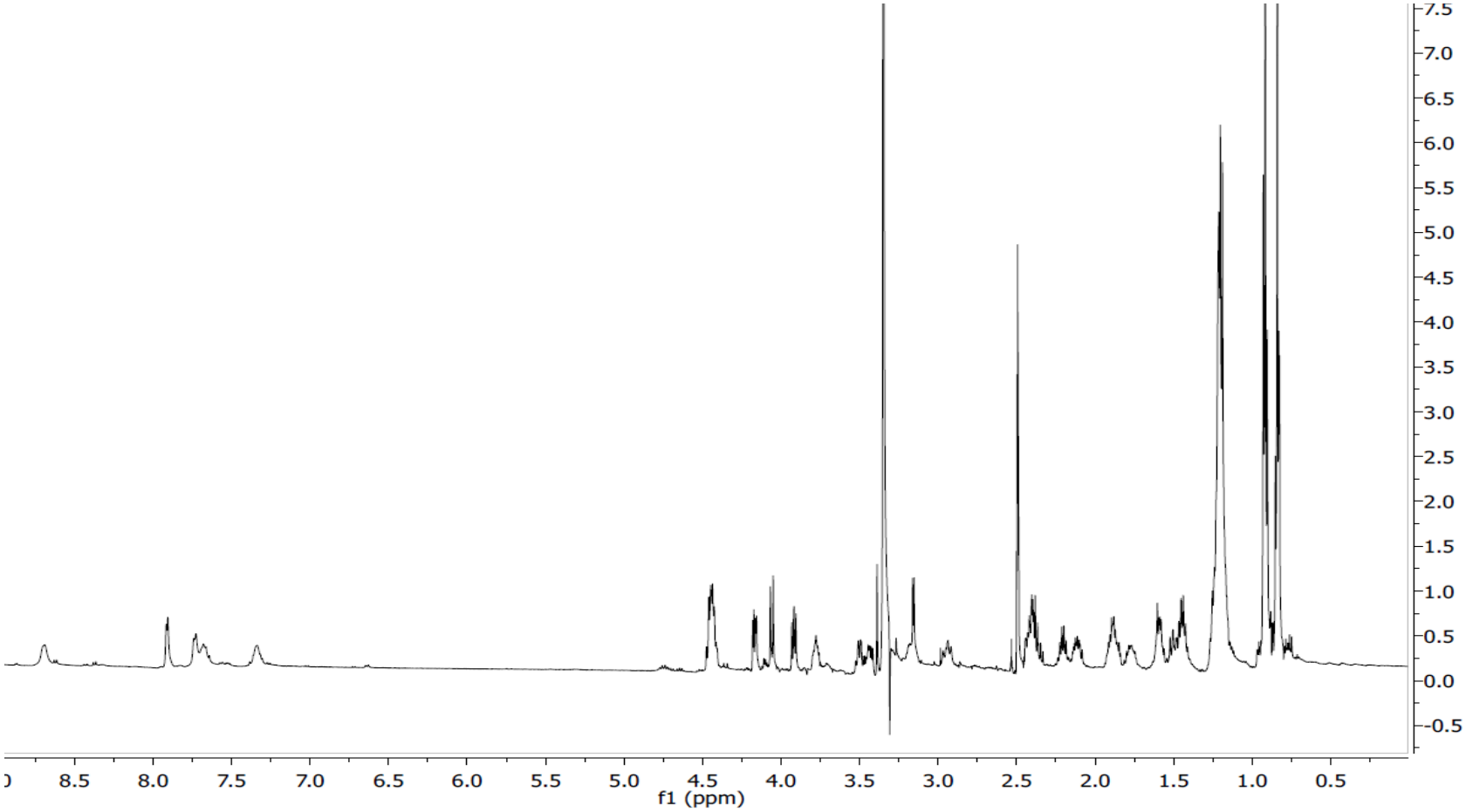

^{13}C-NMR spectrum (100 MHz, DMSO-d_6) of mutanobactin C (**5.3**)

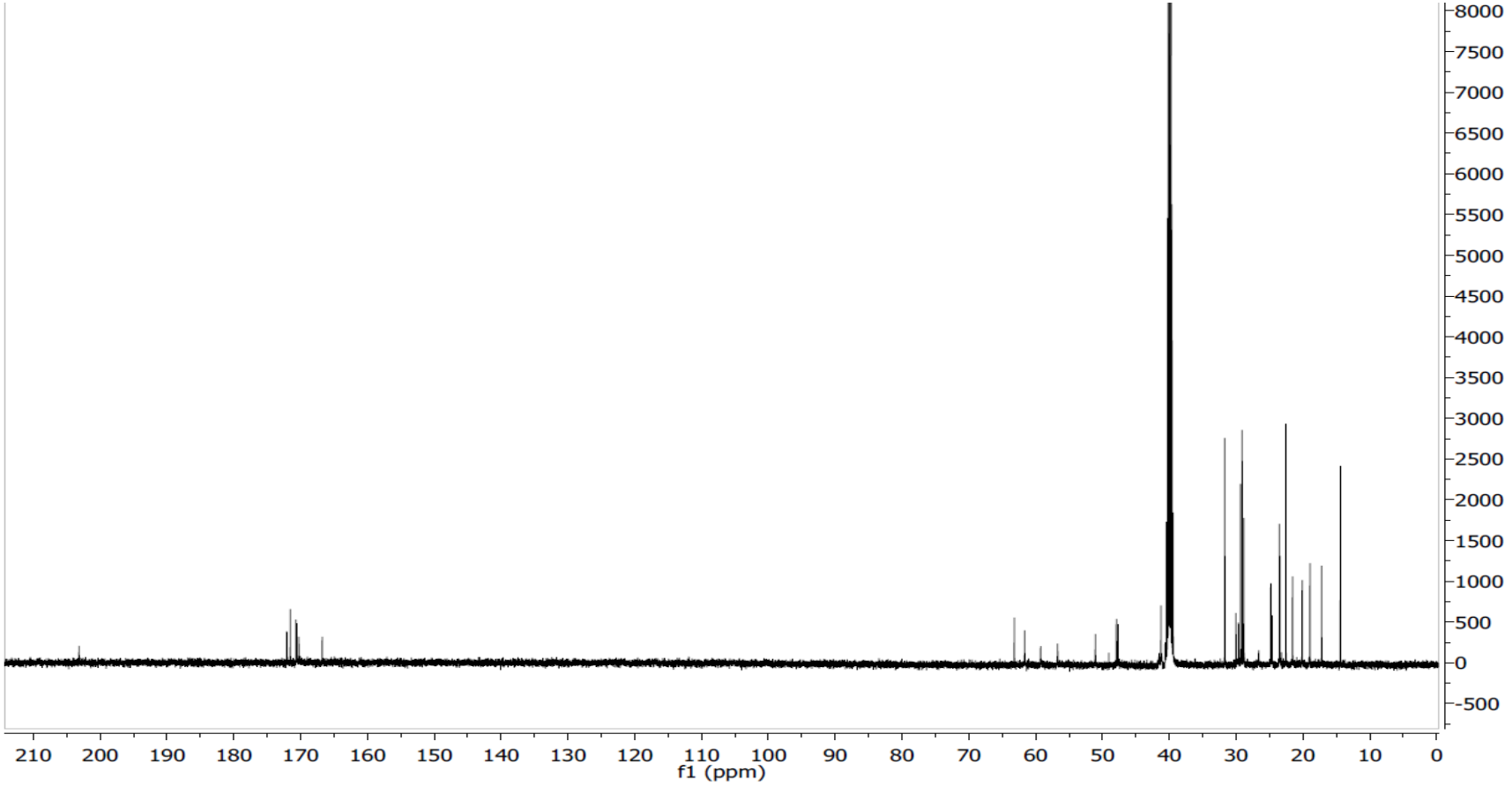

HSQC-NMR spectrum (500 MHz, DMSO-d_6) of mutanobactin C (**5.3**)

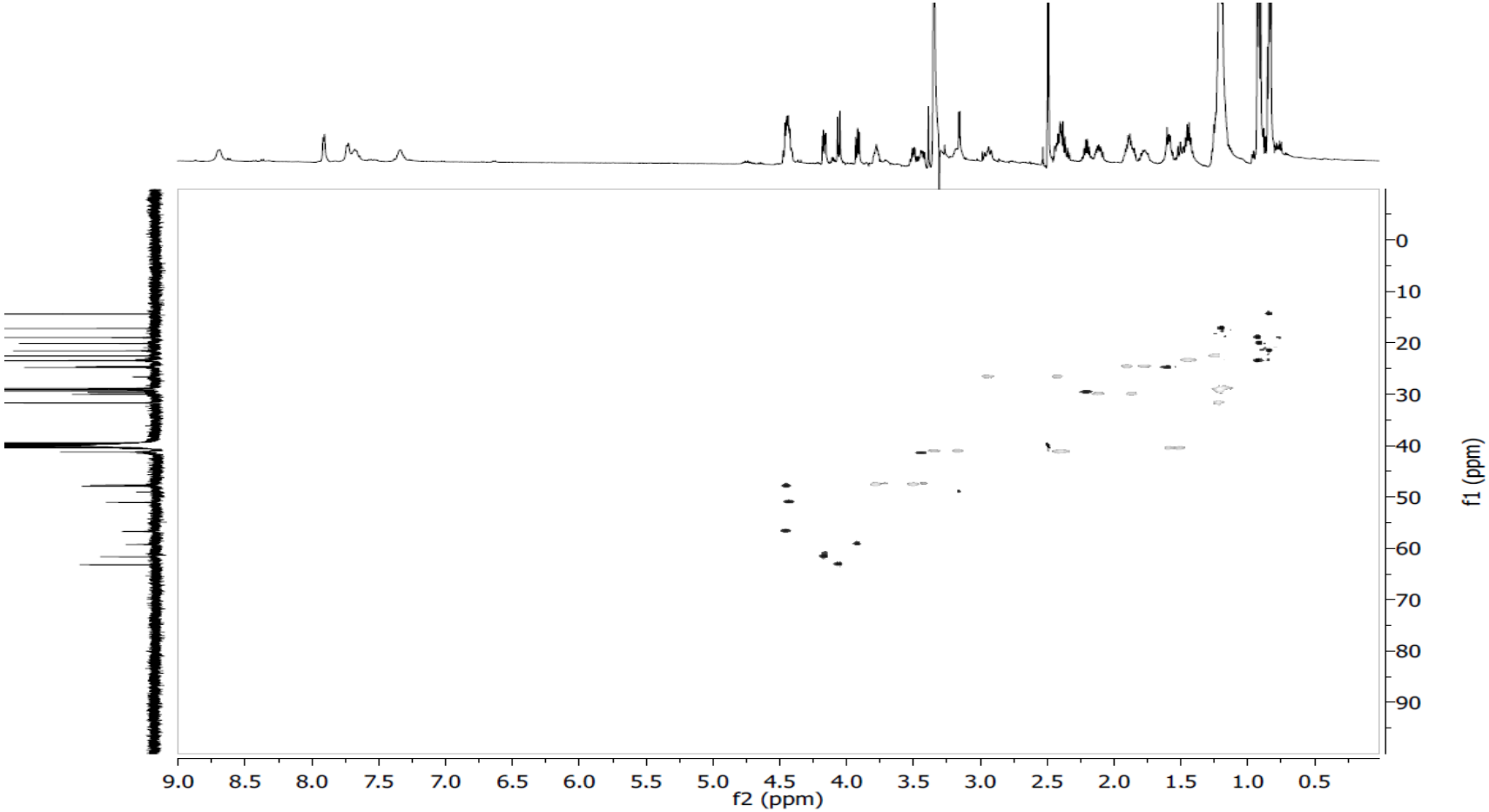

HMBC-NMR spectrum (500 MHz, DMSO-d_6) of mutanobactin C (**5.3**)

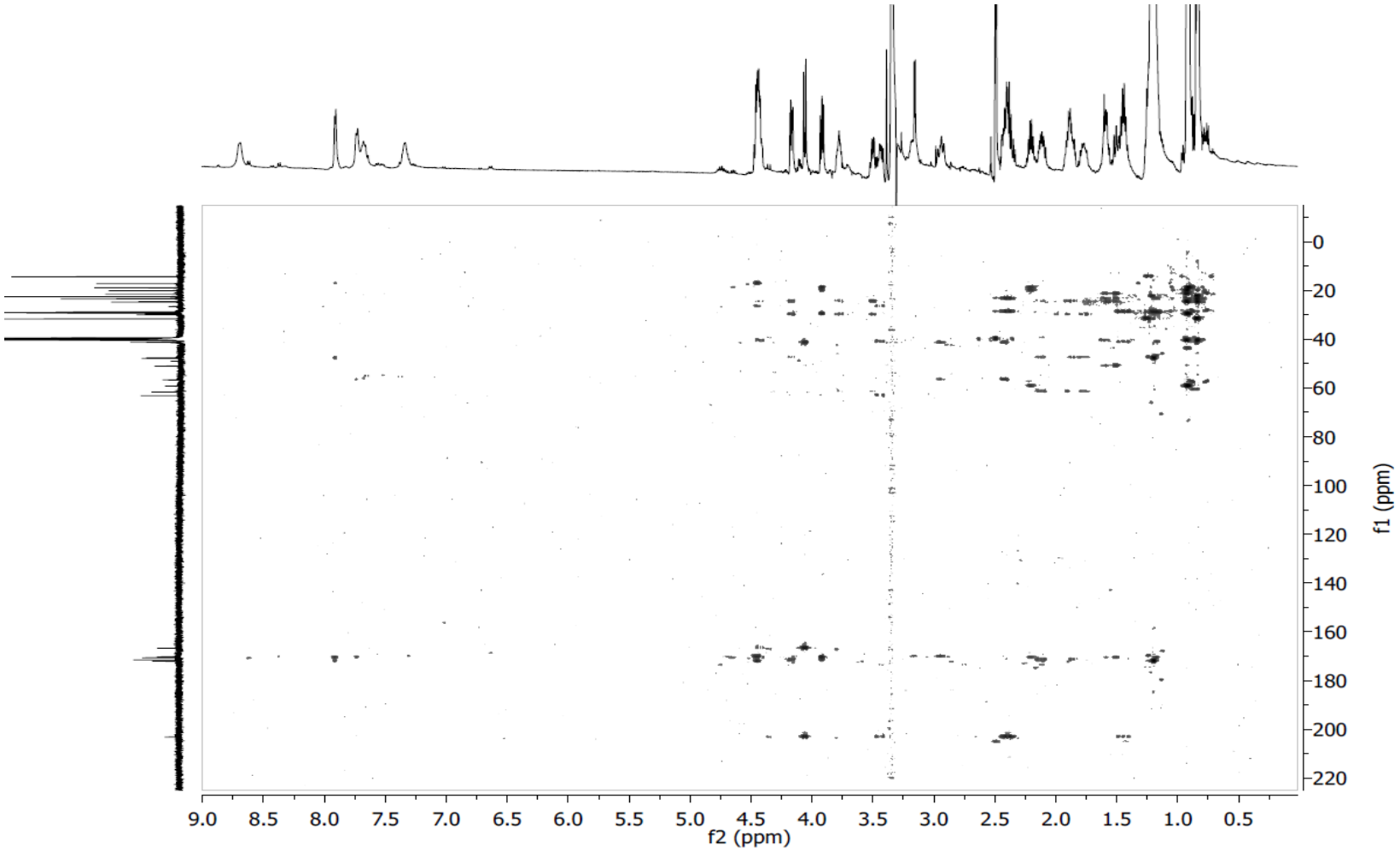

COSY-NMR spectrum (500 MHz, DMSO-d_6) of mutanobactin C (**5.3**)

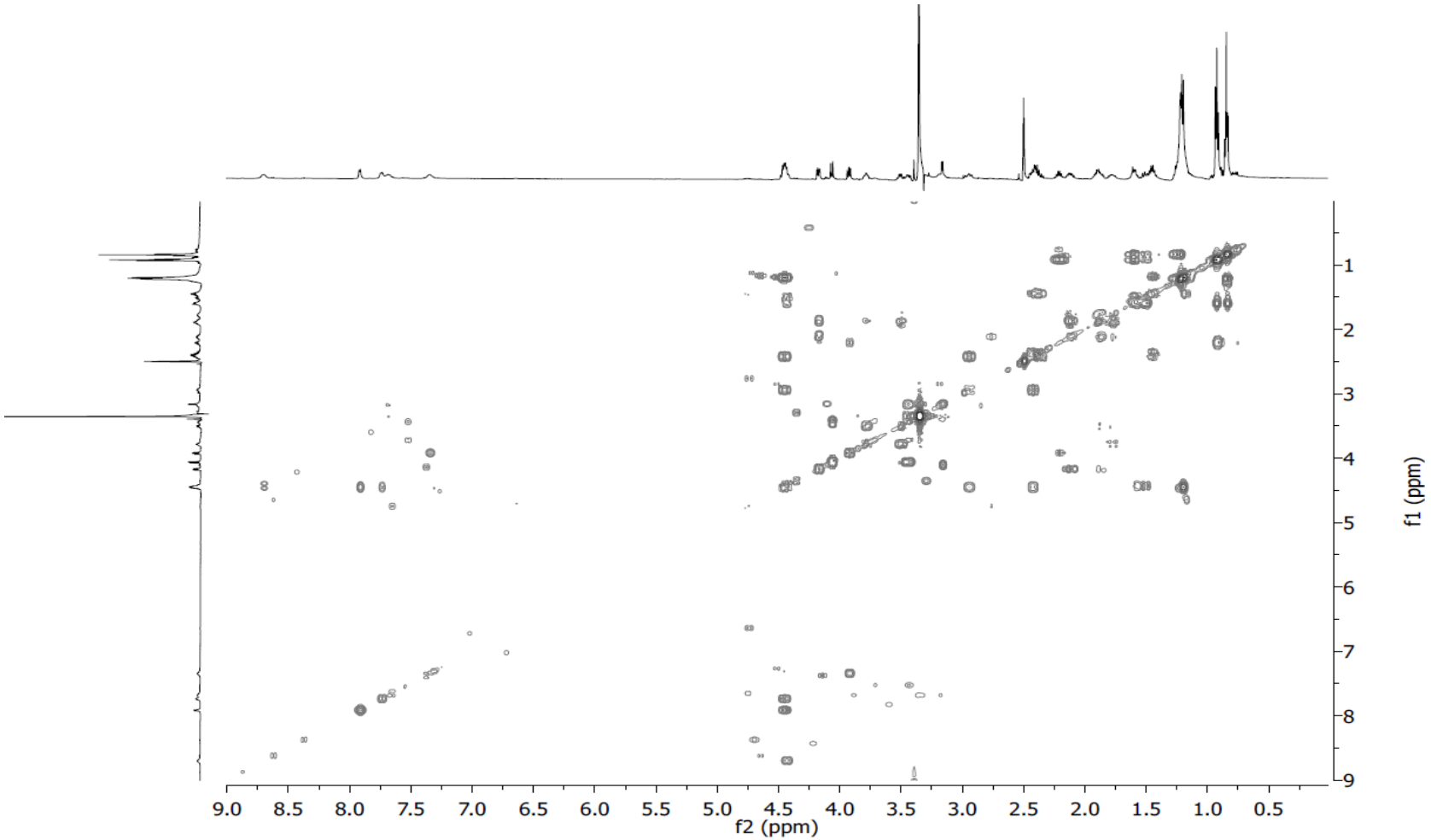

TOCSY-NMR spectrum (500 MHz, DMSO-d_6) of mutanobactin C (**5.3**)

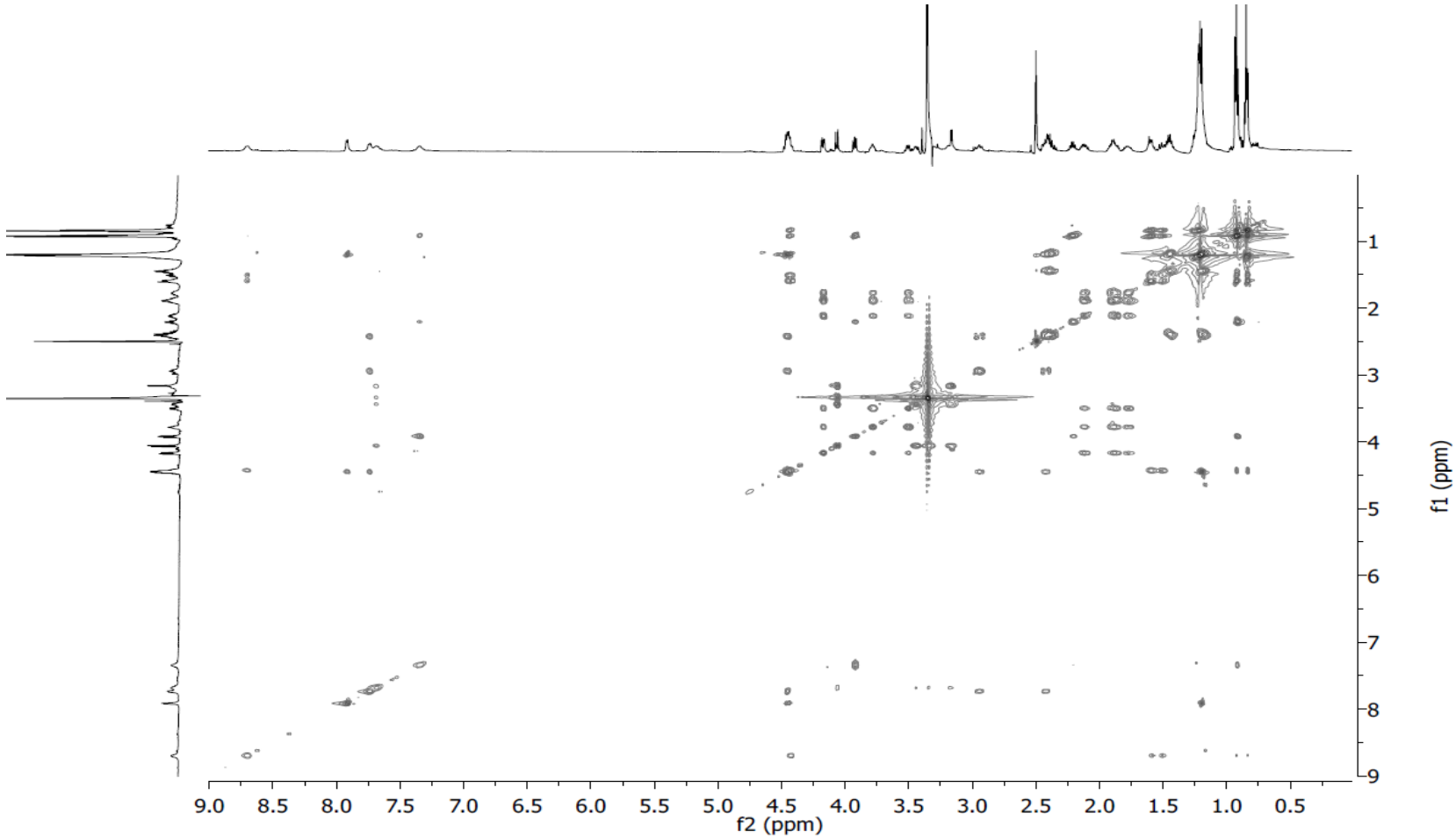

NOESY-NMR spectrum (500 MHz, DMSO-d_6) of mutanobactin C (**5.3**)

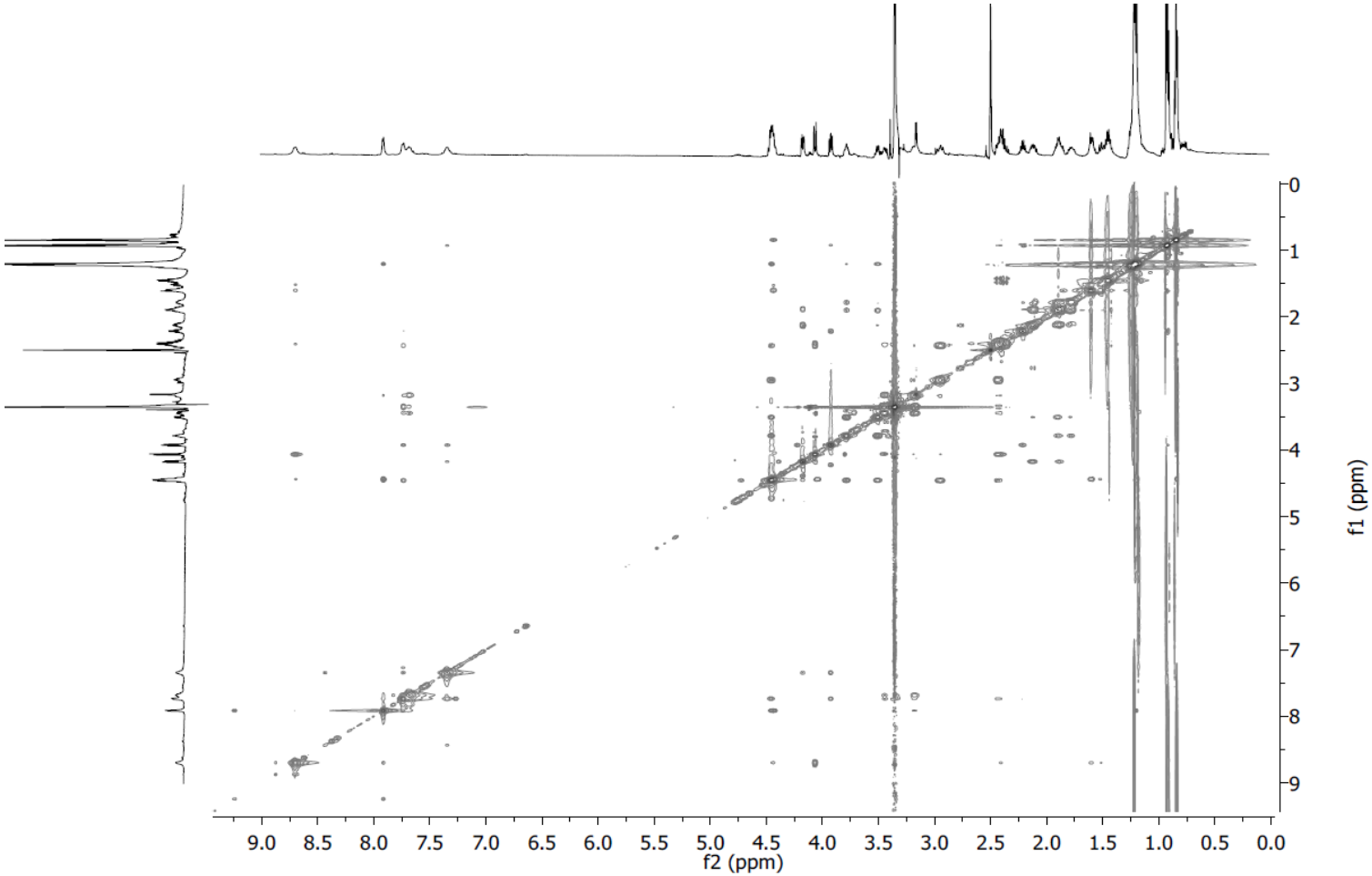

^{1}H-NMR spectrum (500 MHz, DMSO-d_6) of mutanobactin D (**5.4**)

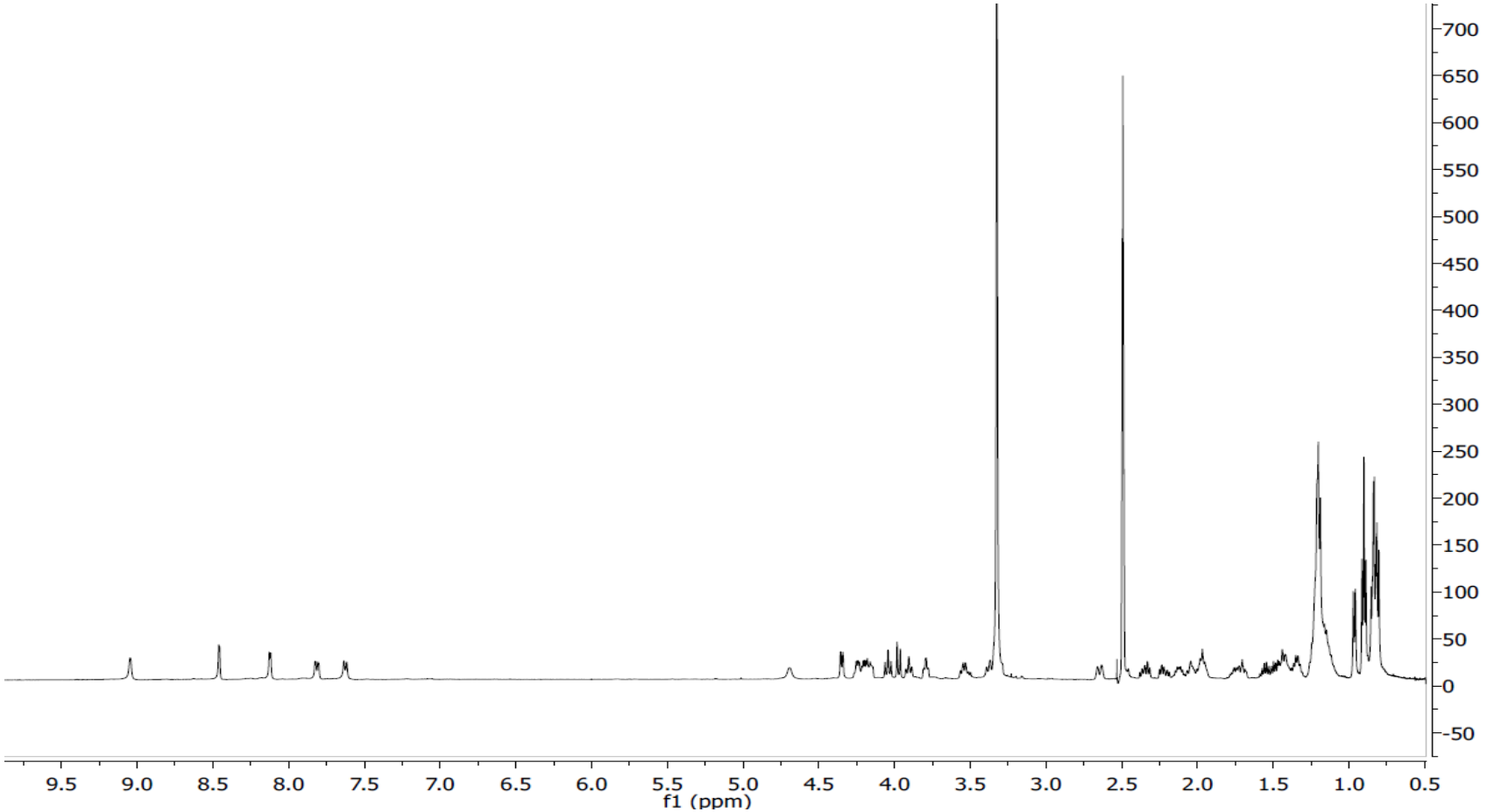

^{13}C-NMR spectrum (100 MHz, DMSO-d_6) of mutanobactin D (**5.4**)

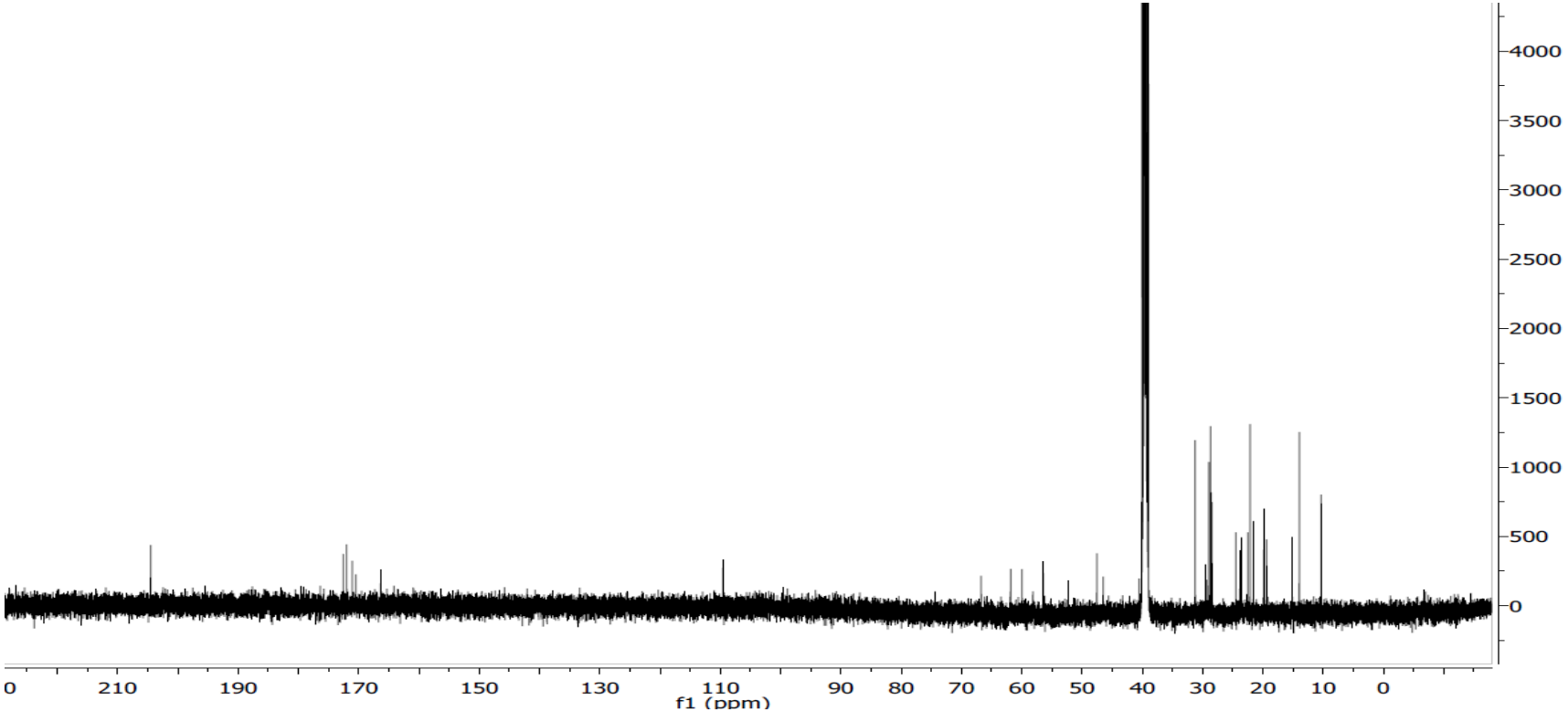

HSQC-NMR spectrum (500 MHz, DMSO-d_6) of mutanobactin D (**5.4**)

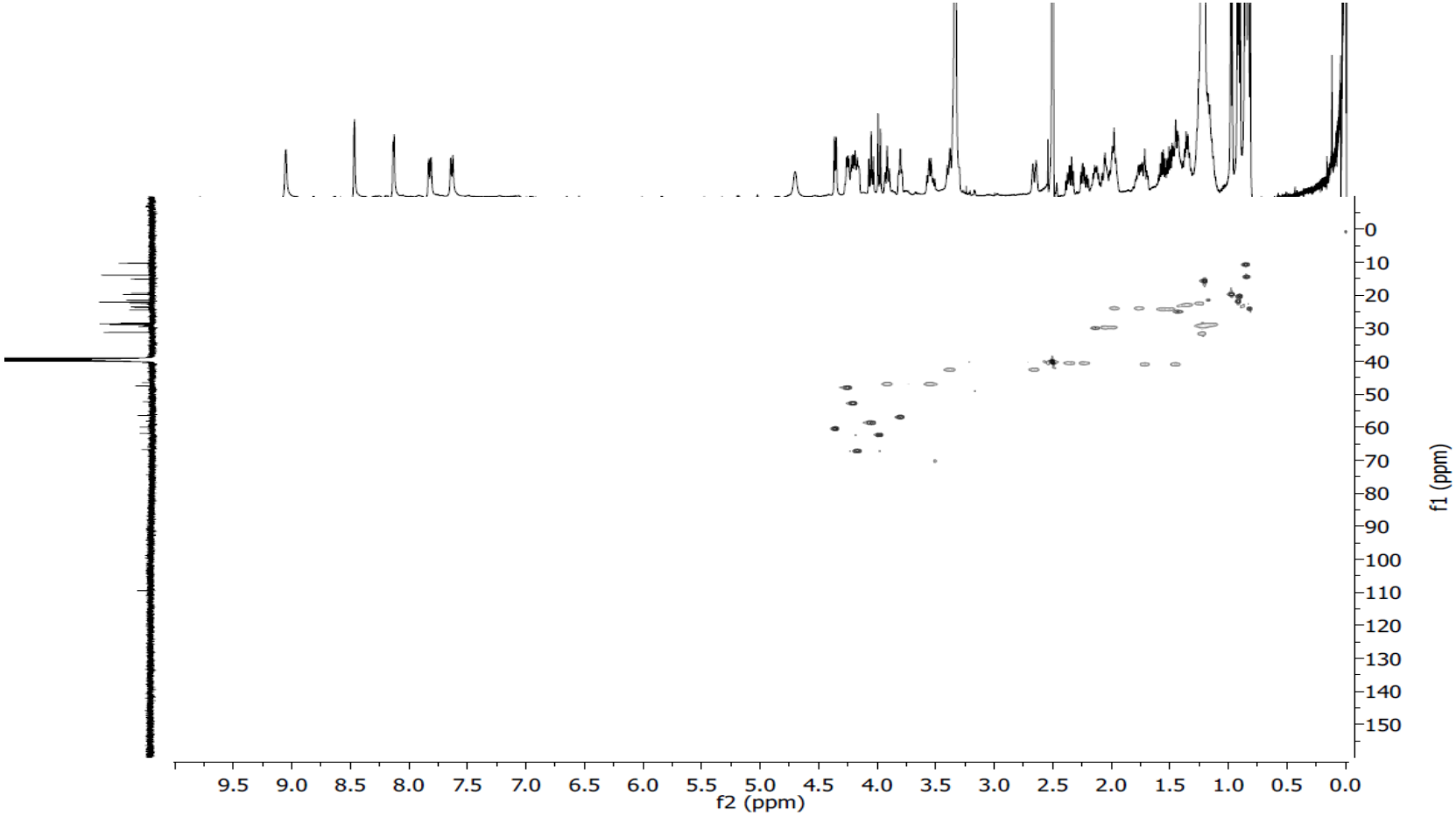

HMBC-NMR spectrum (500 MHz, DMSO-d_6) of mutanobactin D (**5.4**)

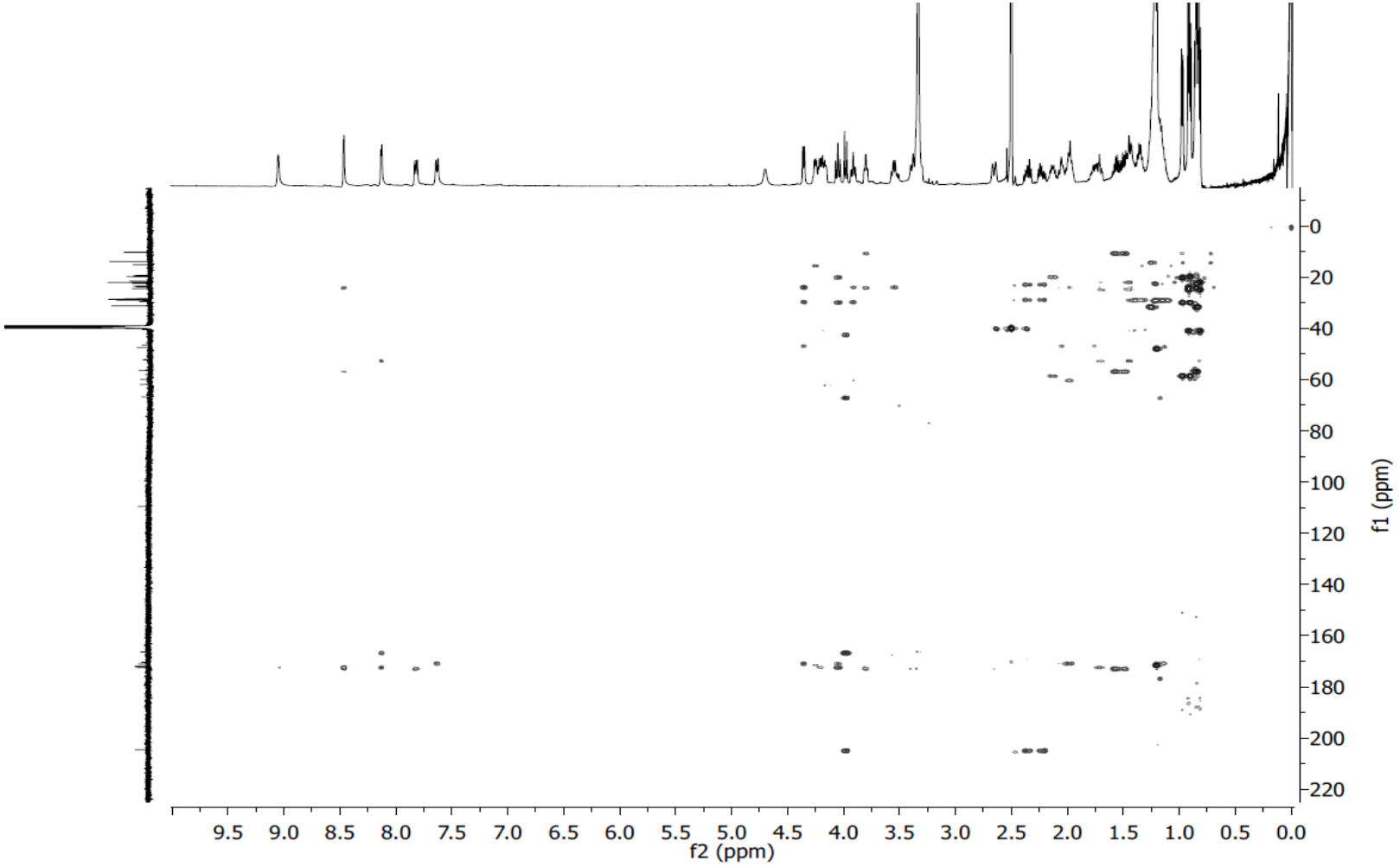

COSY-NMR spectrum (500 MHz, DMSO-d_6) of mutanobactin D (**5.4**)

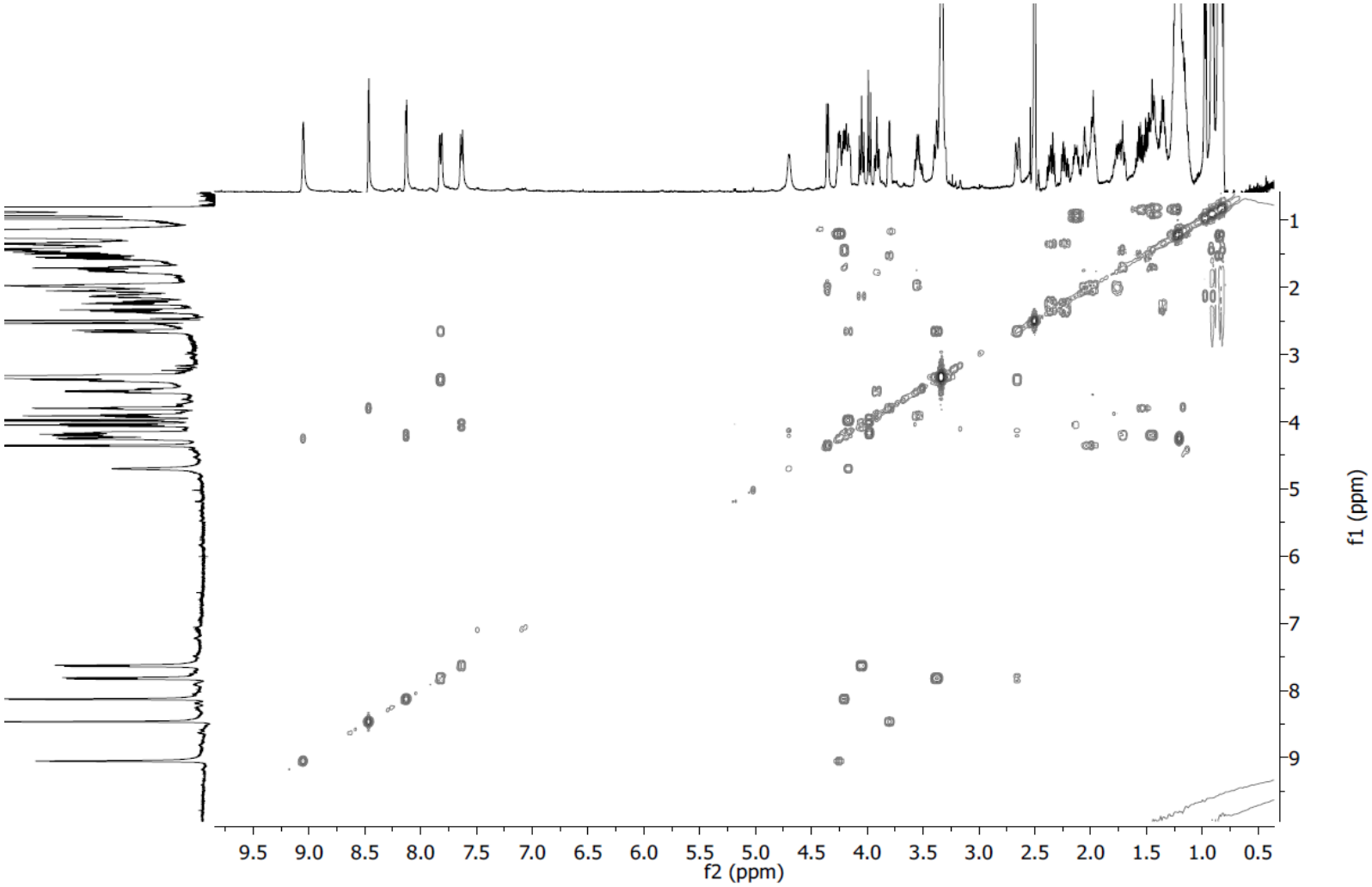

NOESY-NMR spectrum (500 MHz, DMSO-d6) of mutanobactin D (**5.4**)

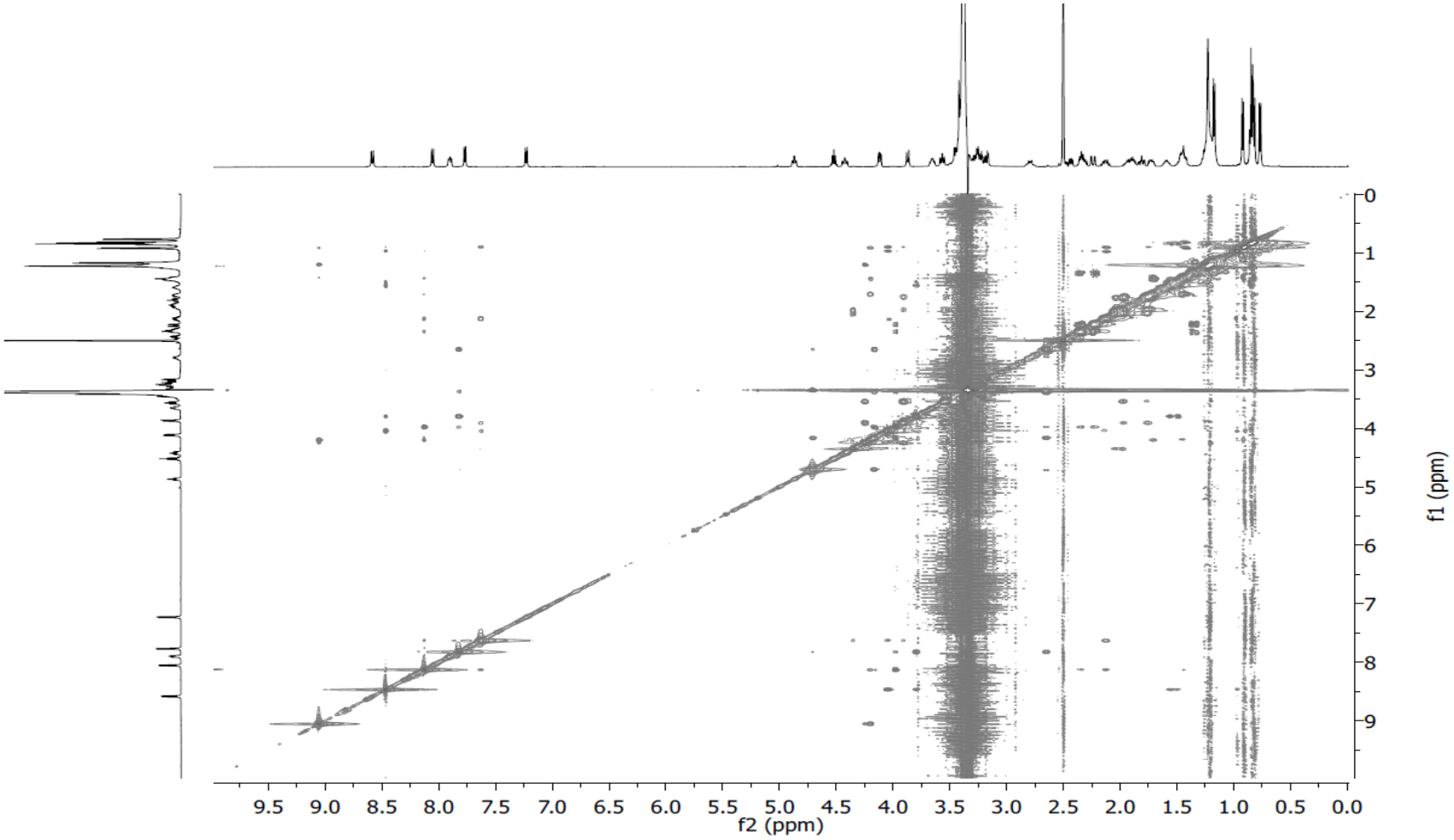

^{13}C-NMR spectrum (100 MHz, DMSO-d_6) of mutanobactin A-[1-^{13}C] Acetate labeled

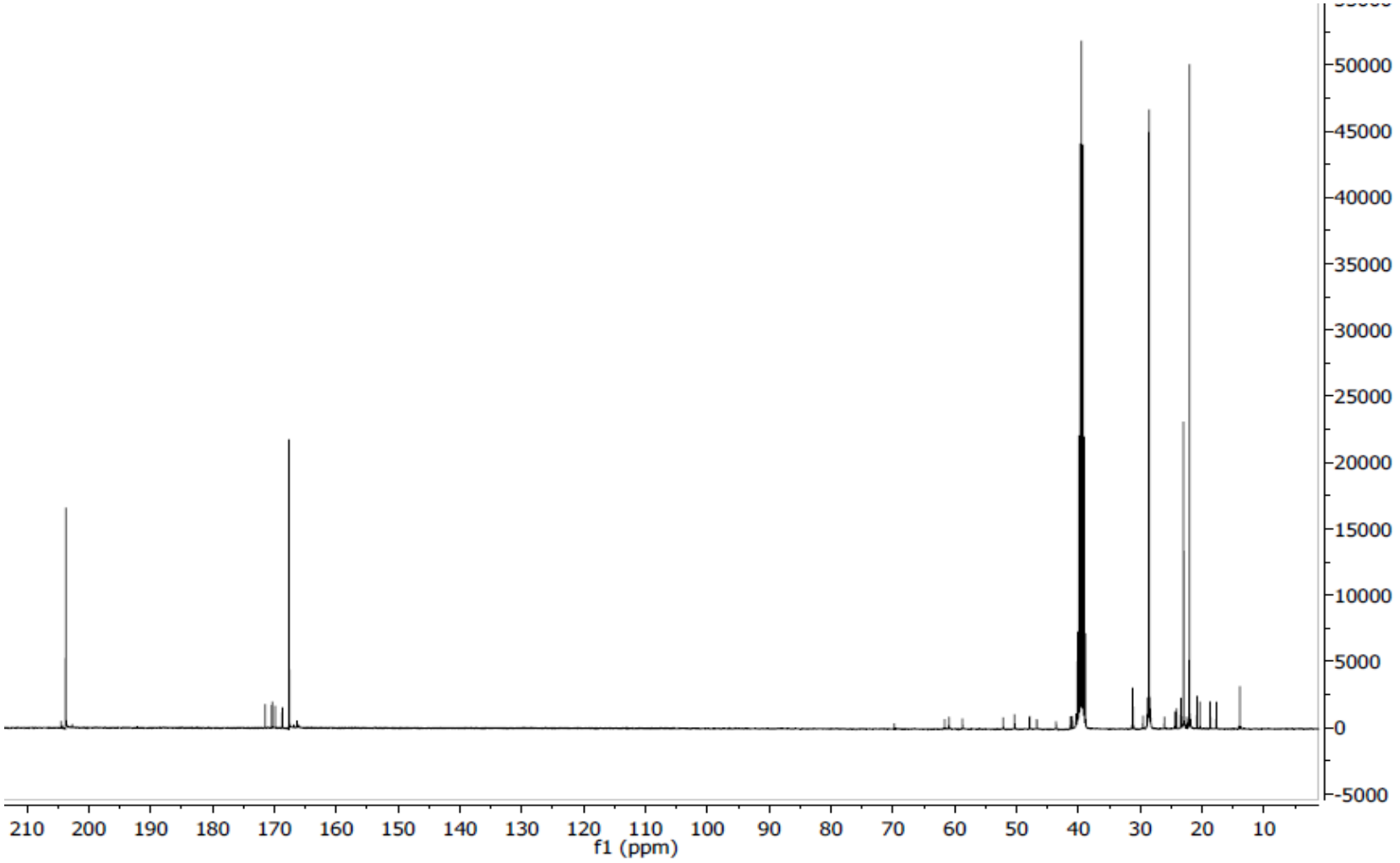

^{13}C-NMR spectrum (100 MHz, DMSO-d6) of mutanobactin A-[2-13C] Acetate labeled

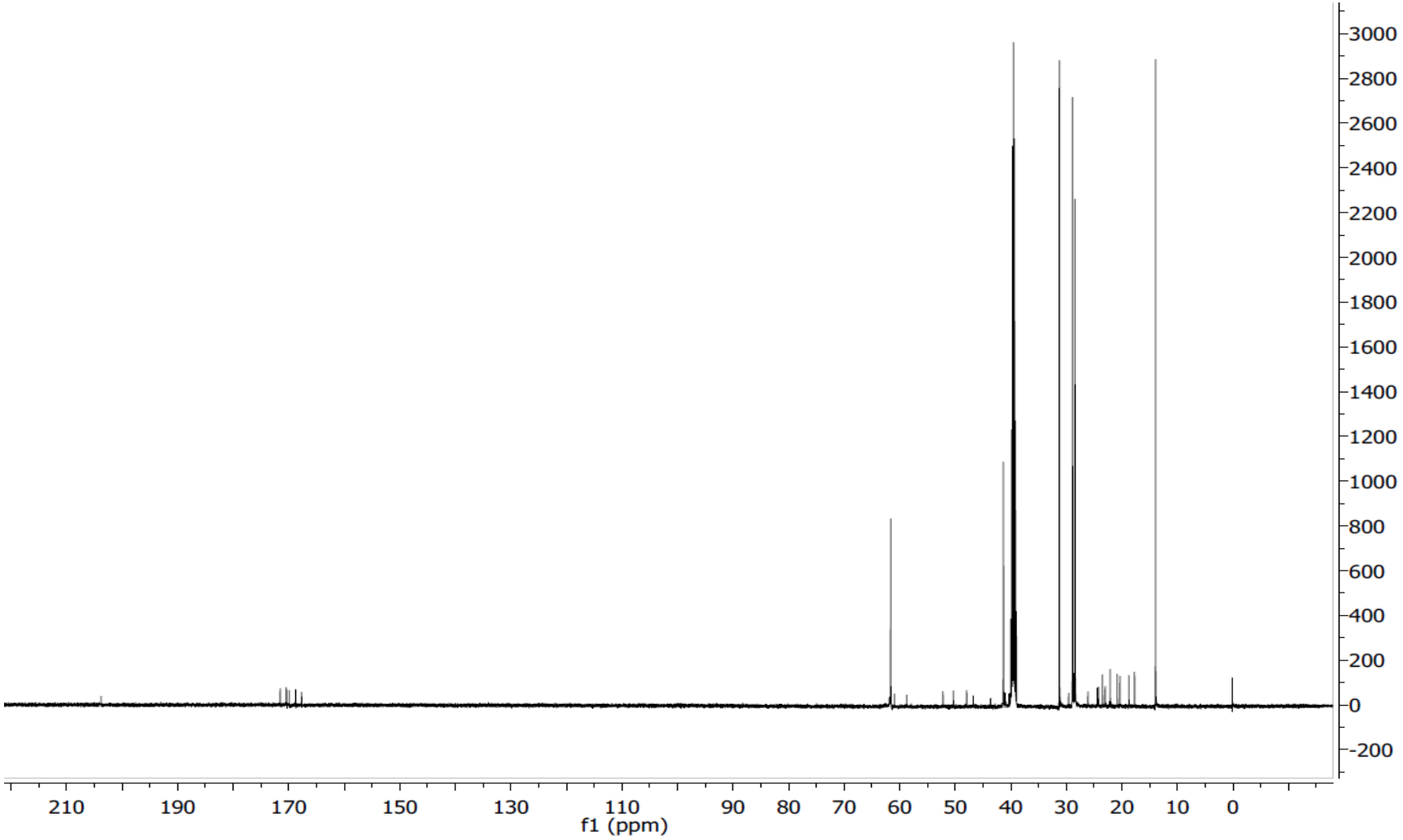

^{13}C-NMR spectrum (100 MHz, DMSO-d6) of mutanobactin A-[^{15}N,^{13}C2] Glycine labeled

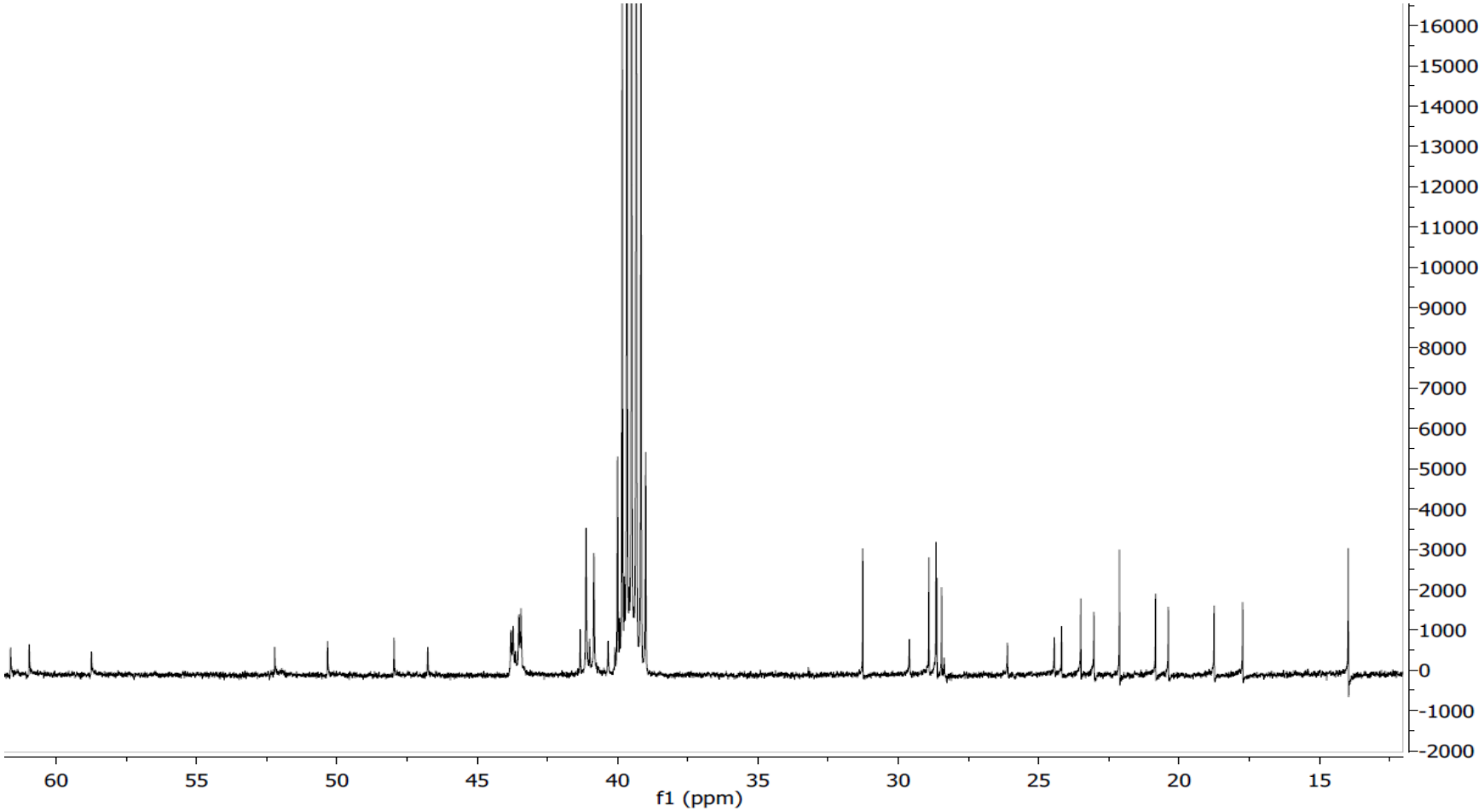

^{1}H-NMR spectrum (500 MHz, DMSO-d_6) of mutanobactin A (**5.1**)

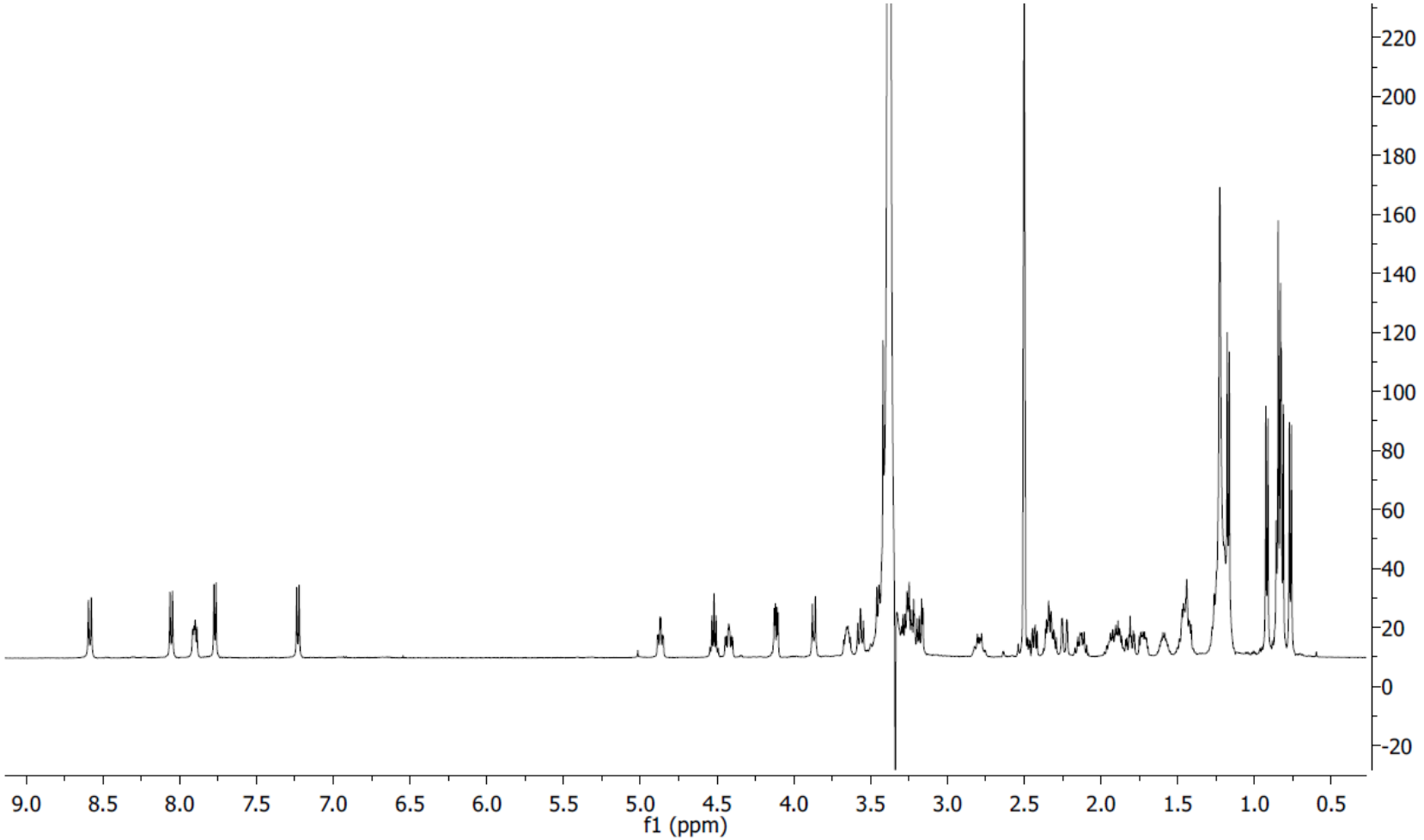

NOESY-NMR spectrum (500 MHz, DMSO-d6) of mutanobactin A (**5.1**)